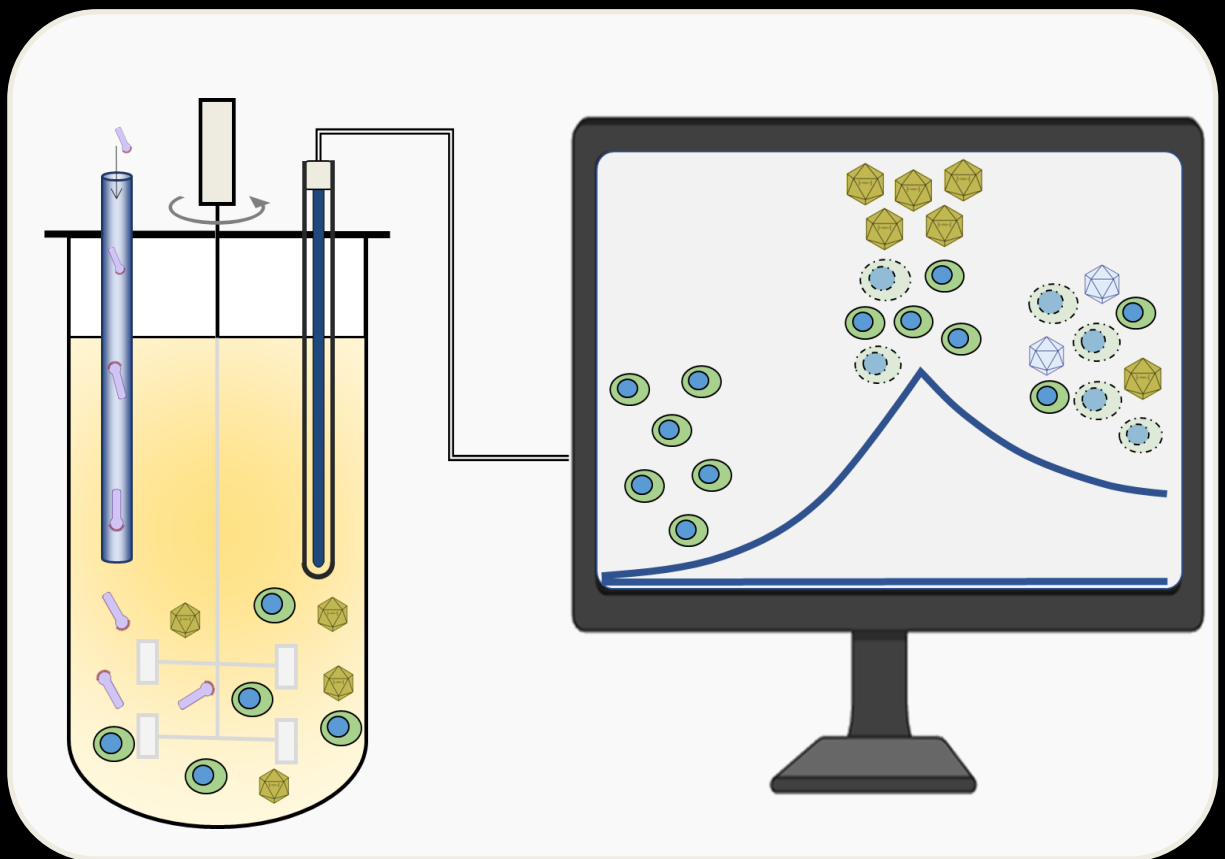


Development of advanced monitoring and control tools for rAAV production in the insect cell system

Daniel Alexandre Marques Pais



Dissertation presented to obtain the Ph.D degree in Bioengineering
Instituto de Tecnologia Química e Biológica António Xavier | Universidade Nova de Lisboa

Oeiras,
April, 2020

Development of advanced monitoring and control tools for rAAV production in the insect cell system

Daniel Alexandre Marques Pais

Dissertation presented to obtain the Ph.D degree in Bioengineering (MIT-Portugal)

Instituto de Tecnologia Química e Biológica António Xavier | Universidade Nova de Lisboa

Oeiras, April, 2020

Development of advanced monitoring and control tools for rAAV production in the insect cell system

Daniel Alexandre Marques Pais

The work developed in this thesis was supervised by:

Professor Paula Alves, Instituto de Biologia Experimental e Tecnológica (iBET) and Instituto de Tecnologia Química e Biológica António Xavier, Universidade Nova de Lisboa (ITQB-NOVA) (supervisor)

Doctor Inês Isidro, Instituto de Biologia Experimental e Tecnológica (iBET) and Instituto de Tecnologia Química e Biológica António Xavier, Universidade Nova de Lisboa (ITQB-NOVA) (co-supervisor)

Development of advanced monitoring and control tools for rAAV production in the insect cell system

By Daniel Pais

Cover: Representation of the time-course profile of rAAV production in insect cells using the baculovirus expression vector system; depiction of the translation of the probe measurements into process data. Initial design by Hugo Soares and Carolina Figueira (iBET).

ITQB-NOVA and iBET - Animal Cell Technology Unit

Instituto de Tecnologia Química e Biológica António Xavier / Instituto de Biologia Experimental e Tecnológica

Av. da República EAN, 2780-157 Oeiras, Portugal

<http://www.itqb.unl.pt>

<http://www.ibet.pt>

Copyright© 2020 by Daniel Alexandre Marques Pais

All rights reserved

Printed in Portugal



From left to right and top to bottom: Dr Cristina Silva Pereira; Dr João Paulo Crespo; Dr Duarte Miguel Prazeres; Dr Cecília Calado; Dr Paula Alves; Dr Emma Petiot; Dr Inês Isidro; Dr Daniel Pais

Supervisors:

Professor Paula Alves, Instituto de Biologia Experimental e Tecnológica (iBET) and Instituto de Tecnologia Química e Biológica António Xavier, Universidade Nova de Lisboa (ITQB-NOVA), Oeiras, Portugal

Doctor Inês Isidro, Instituto de Biologia Experimental e Tecnológica (iBET) and Instituto de Tecnologia Química e Biológica António Xavier, Universidade Nova de Lisboa (ITQB-NOVA), Oeiras, Portugal

President of the Jury:

Professor Cristina Silva Pereira, Principal Investigator at Instituto de Tecnologia Química e Biológica António Xavier, Universidade Nova de Lisboa (ITQB-NOVA), Oeiras, Portugal

Jury:

Professor Emma Petiot, Associate Professor at CPE-Lyon Engineer school, Lyon, France

Professor João Paulo Crespo, Full Professor, Chemistry Department, Universidade Nova de Lisboa, Portugal

Professor Cecília Calado, Adjunct Professor in Biomedical Engineering, Instituto Politécnico de Lisboa - Instituto Superior de Engenharia de Lisboa, Lisboa, Portugal

Professor Duarte Miguel Prazeres, Full Professor, Department of Bioengineering, Instituto Superior Técnico, Universidade de Lisboa, Portugal

Financial support from:

Fundação para a Ciência e Tecnologia (FCT)

PhD Grant PD/BD/105873/2014

iNOVA4Health Research Unit
(LISBOA-01-0145-FEDER-007344), which is cofunded by
FCT/ Ministério da Ciência e do Ensino Superior, through
national funds, and by FEDER under the PT2020
Partnership Agreement

iNOVA4Health



FCT

Fundação para a Ciência e a Tecnologia
MINISTÉRIO DA EDUCAÇÃO E CIÊNCIA

MIT Portugal

Foreword

The MIT-Portugal PhD program in Bioengineering Systems comprises four years. The first one consists in a six-month period of class attendance in four Portuguese universities, followed by two lab rotations of 9 weeks each. The remaining three years are dedicated to the PhD project. The present thesis dissertation is the result of three years of research at the Animal Cell Technology Unit of ITQB–NOVA / iBET (Oeiras, Portugal) under the supervision of Prof. Paula Alves and Dr. Inês Isidro. The work presented in Chapter IV results from a one-year co-op in the Upstream Process Development group at Voyager Therapeutics, under the supervision of Dr. Peter Slade. Voyager Therapeutics is a gene therapy company developing treatments for central nervous system diseases based in Cambridge, MA (USA).

Acknowledgments

During this 5-year PhD journey, I had the opportunity to meet and work with fantastic people, who contributed directly or indirectly for this thesis to be completed. This thesis is dedicated to everyone who supported me throughout the years.

To my supervisor, Professor Paula Alves, for accepting me as her PhD student, for being able see my potential, for believing in me and pushing me so that I could improve myself as a scientist. For the example of leadership, for sharing her knowledge and scientific vision, for all the opportunities to share my work to the scientific community. This work would not be possible without her guidance and the unmatched resources and working conditions at iBET. Thank you for teaching me how to be a scientist, how to zoom out and see the bigger picture.

To my co-supervisor, Dr. Inês Isidro, for always finding a time to help me and advise me, to show me the bright side of being a scientist and lifting my spirit every time I crashed into the “researcher wall”. For sharing so much of her modeling expertise and showing me new ways to face the problems. I feel I grew a lot as a scientist thanks to you.

To Professor José Cardoso Menezes and Otto Merten, my Thesis Committee members, for the fruitful discussions of my work and the useful comments for improvement. A special thank you to Professor José Menezes, because it is thanks to you I started growing my interest in Chemometrics.

To Professor Manuel Carrondo, for being an inspiration and a role model in his vision for founding iBET, for being a true entrepreneur, for motivating me, trusting in me and encouraging me to be big. Thank you for being a visionary

leader, for your professional advices, and for inspiring me with an example of excellence and hard work.

To all my colleagues at the Animal Cell Technology Unit. For all the help provided, for the opportunity to work in such an amazing environment, for great scientific discussions and crazy ideas, for sharing your work and teaching me so much. A special thanks to the insect cells team, Ricardo, Bárbara, Alexandre, Ana, Sofia, Daniela and Paulo, without a doubt the best team to work in a lab, for all the good moments doing MTT assays together and the overall happy environment.

To António and Marcos, for the help with the design of experiments and STB assembly and for sharing their knowledge with me.

To Paulo, it was a pleasure to teach you and watch you grow as a scientist. I felt better knowing the AAV project keeps going. Thank you for the help in my experiments and for being an awesome lab mate.

To Hugo, for being a role model of a scientist, for all your ideas and pleasure teaching me about everything, for all the great advice you gave me during these years.

To Bernardo, Maria João and Sofia, for being the perfect roommates. We had great times together in the “consultório”. Thank you Bernardo and Maria João for being the best bullies and confidants I could ask for, and all your support in the hardest moments of this journey.

To all my friends, the “miguxos”, who know me for so many years and still like to hang around with me. Thank you for all your encouragement and for all the good laughs we shared during these 12 years.

To all my Voyager friends: thanks for being such an amazing team. My year in Boston was so much better thanks to you. Thank you for sharing your knowledge and making me feel at home, and the great moments we shared together. A special thanks to Peter, for being a brilliant scientist and the best boss possible, and to Luís, for providing me this opportunity and teaching me so much.

À minha família, que estão e sempre estarão comigo. Por todo o apoio que me dão, pelas belas jantaradas e os cafés e outras coisas à conta. Que não sabem muito bem o que eu faço, mas sabem que tem a ver com insetos e doenças genéticas, o que é uma melhoria em relação à fase das bactérias. Que ficaram espantados por haver empresas em Boston a trabalhar no mesmo (se calhar isto afinal é importante!) e me encorajaram a ir e a ficar longe deles se isso fosse o melhor para mim. Um beijinho especial à minha prima Inês, que via em mim um modelo a seguir, mas que felizmente não seguiu cegamente. E aos meus avós, pelo amor e por serem um verdadeiro exemplo de avós. Aos meus pais e irmão, um agradecimento muito especial por estarem a meu lado incondicionalmente e me apoiarem e ajudarem a chegar onde cheguei.

À Susana, a minha maior amiga, confidente e quem mais me encoraja a ser ainda melhor. Obrigado pelo teu apoio, por me fazeres rir diariamente, por estares sempre lá para mim para os bons e os maus momentos, tornando os bons melhores e os maus menos maus, e tornando esta jornada muito menos solitária.

À minha família e à Susana

Abstract

Since the first publication introducing the concept in 1972, gene therapy has had a series of success stories and setbacks. However, the recent rise of awareness, public interest, promising results in clinical trials and recent market approvals indicate that gene therapy has come to stay. Currently there is a growing interest from the biopharmaceutical industry in gene and cell therapy, mostly using viral vectors.

Adeno-associated virus (AAV) are one of the most used vectors in gene therapy clinical trials, already culminating in three recent approvals of AAV-based gene therapies: Glybera in 2012, the first approved gene therapy in Europe, and Luxturna and Zolgensma in the US in 2017 and 2019, respectively. Their attractiveness stems from their apparent lack of pathogenicity; sustainable episomal gene expression; ability to transduce both quiescent and dividing cells from a myriad of tissues; and physical resistance to withstand the manufacturing process.

To cope with the actual high vector dose requirements, there is a high demand for efficient and scalable recombinant AAV (rAAV) manufacturing platforms, from which the insect cell - baculovirus expression vector system (IC-BEVS) stands out. The IC-BEVS combines the high recombinant protein expression capabilities of the baculovirus vector with the GMP-amenable characteristics of insect cells: suspension growth to high cell densities with well-defined culture media without the need of serum supplementation. This combination resulted in multiple products already approved for human and veterinary use. However, being a lytic system, recombinant AAV production comes to an end when the baculovirus induces host cell lysis, which also contributes to the release of intracellular proteases to the culture media, which can severely impact the quality of the produced vectors. Altogether,

this makes **the time of harvest one of the most important process parameters**, followed by the variables related with the infection step, the multiplicity of infection and the cell concentration at seeding and at infection. Consequently, the bioprocess with insect cell-baculovirus system can inherently benefit from the implementation of real-time monitoring tools to accurately estimate the best infection and harvest timing.

This thesis aimed at developing and implementing real-time monitoring tools for critical process variables in the insect cell-baculovirus system, specifically for rAAV production. Furthermore, the possibility to detect in real-time rAAV production kinetics was also investigated.

In **Chapter I** these topics are introduced, and a revision of the most important achievements published in the literature is discussed.

In **Chapter II**, the use of fluorescence spectroscopy as a soft sensor for monitoring rAAV production, cell concentration and viability is assessed. Artificial neural network models were developed, complemented with a genetic algorithm-based approach for spectra pre-treatment which significantly increased fluorescence spectra signal-to-noise ratio and positively impacted prediction models. Fluorescence spectroscopy proved to be a powerful tool for bioprocess monitoring, due to its straightforward implementation and the substantial information it provides from rapid culture medium measurements.

In **Chapter III**, the objective was to detect rAAV-associated changes in cultured insect cells, using digital holographic imaging. A commercially available online automatic sampling system (iLine F, Ovizio Imaging Systems) was applied to insect cell culture, in growth and production batches, in order to clearly isolate image attributes associated with rAAV production. Model interpretability and robustness was assured by combining multiple

linear regression with parameter selection using forward stepwise regression, resulting in the identification of cell attributes associated with rAAV production, cell concentration and culture viability. This approach confirms the feasibility of digital holographic imaging to trace the biological state of the cell at each infection stage, and for real-time monitoring of rAAV titer and overall culture progression in lytic systems, making it a valuable tool to support the time of harvest decision.

In **Chapter IV** the influence of rAAV production and baculovirus replication in the dielectric potential of the cell was investigated using dielectric spectroscopy. Due to the high amount of intracellular activity in the cell during the viral vector production process, a highly variable range of different culture conditions was covered in order to build a robust monitoring platform. With that aim, the system was challenged with purposely low rAAV-titer batches and transgene-devoid baculoviruses. Models for in-process prediction of cell concentration, viability and specific rAAV production were developed. Moreover, dielectric spectroscopy applicability as a process analytical tool was demonstrated, by accurately predicting infection time more than 24 hours in advance using the continuously monitored permittivity of the culture. The work presented in this chapter was performed in Voyager Therapeutics, a Boston-based gene therapy company focused on central nervous system disorders.

The main drive behind the work performed in **Chapters II to IV** was the Process Analytical Technology (PAT) initiative, a guidance for the pharmaceutical manufacturing industry with three main pillars: product analysis, monitoring and control. The first pillar, product analysis, is heavily focused in de-risking the manufacturing process by increasing process understanding, identifying the product critical quality attributes (CQAs) and the critical process parameters (CPPs) affecting it. The second pillar stems

from the need to monitor in real-time the identified quality-related characteristics. The focus of this thesis was in these two first pillars. **Chapter V** addresses the third pillar: the implementation of a control strategy to correct product quality deviations. An overview of the most used bioprocessing control strategies is provided, encompassing both classic and advanced control strategies.

In **Chapter VI**, the main achievements obtained in the previous chapters are discussed in a broad context, and future perspectives are addressed.

Overall, this thesis explores the suitability of three different spectroscopic techniques or image-based tools for quantitative real-time monitoring of rAAV production and viable cell concentration in the insect cell – baculovirus system. The quantitative models developed allow the monitoring of critical process variables, decision of the harvest time and are applicable to the establishment of controlled feeding strategies. The tools and methodologies presented in this thesis can be applied for real-time monitoring of other rAAV serotypes, other biopharmaceuticals produced in the IC-BEVS and potentially for other viral vector production processes. Consequently, in the scope of the PAT initiative, we envision this thesis significantly contributes for increasing rAAV production process understanding and towards implementation of real-time monitoring tools for monitoring rAAV production in insect cells.

Resumo

Desde a primeira publicação científica que introduziu o conceito de terapia génica, em 1972, que esta tem tido sucessivas histórias de sucessos e de insucessos. No entanto, o aumento recente da sua notoriedade, os avanços em ensaios clínicos com resultados promissores, o aumento do interesse público e do número de produtos aprovados parecem indicar que a terapia génica veio para ficar. Atualmente, há um interesse crescente por parte da comunidade científica e de empresas em terapias génicas e celulares, usando, na grande maioria dos casos, vetores virais.

O Vírus Adeno-Associado (VAA) tem sido cada vez mais usado para ensaios clínicos de terapia génica, o que culminou com a aprovação de três terapias baseados neste vírus: Glybera, em 2012, a primeira aprovada na Europa, e Luxturna e Zolgensma, aprovados nos Estados Unidos da América em 2017 e 2019, respetivamente. As principais vantagens destes vetores são a sua aparente não-patogenicidade; a sua capacidade de induzir uma expressão genética duradoura e de transduzir tanto células quiescentes como células em divisão celular, e isto numa enorme variedade de tecidos; e a sua resistência física, que lhes permite resistir ao processo de produção e purificação.

O número crescente de ensaios clínicos de terapia génica resultou numa demanda alta por plataformas de produção de VAA eficientes e escaláveis, das quais se destaca o sistema de expressão baculovirus-célula de inseto (SEB-CI). Este sistema combina a alta capacidade de expressão de proteínas recombinantes do baculovirus com as características adequadas às Boas Práticas de Fabrico (BPF) das células de inseto: estas são capazes de crescer em suspensão, atingindo concentrações celulares elevadas sem o uso excessivo de recursos para o seu crescimento e sem a necessidade

de suplementação de soro. Esta combinação resultou em diversos produtos aprovados para uso humano e veterinário. No entanto, sendo um sistema lítico, a produção de VAA recombinante acaba quando o baculovirus induz apoptose na célula infetada. A lise celular induzida pelo baculovirus contribui ainda para a libertação de proteases intracelulares para o sobrenadante da cultura celular, que podem afetar a qualidade dos vetores virais produzidos. Assim, o momento em que se termina a cultura para recolha dos vetores virais produzidos é uma das mais importantes variáveis neste processo, assim como a altura da infeção, a multiplicidade de infeção e a concentração celular ao inocular e infetar a cultura. Por este motivo, o sistema de expressão baculovirus-célula de inseto claramente beneficia da implementação de ferramentas de monitorização em tempo real para estimar com precisão a melhor altura para infetar e recolher a cultura celular.

O objetivo principal desta tese é desenvolver e implementar ferramentas de monitorização em tempo real para variáveis críticas do bioprocessamento no sistema de expressão baculovirus-célula de inseto, especificamente para a produção de VAA. Para além disso, também foi estudada a possibilidade de detetar em tempo real a cinética de produção do VAA.

No **capítulo I**, são apresentados estes tópicos e é feita uma revisão dos trabalhos mais importantes já publicados na literatura

No **capítulo II**, foi avaliado o uso de espectroscopia de fluorescência como um sensor indireto para monitorizar o título de VAA, concentração celular e viabilidade. Foram desenvolvidas redes neuronais artificiais, complementadas com uma abordagem baseada num algoritmo genético para o pré-processamento dos espectros de fluorescência. A abordagem desenvolvida para o pré-processamento aumentou significativamente o rácio sinal/ruído e teve um impacto positivo nos modelos de previsão. A

espectroscopia de fluorescência provou ser uma ferramenta poderosa para monitorização de bioprocessos, devido à sua fácil implementação e à quantidade substancial de informação que providencia a partir de medições rápidas do sobrenadante da cultura celular.

No **capítulo III**, o objetivo foi detetar, nas células de inseto em cultura, alterações morfológicas associadas à produção de VAA, usando microscopia holográfica digital. Foi aplicado um sistema comercial de amostragem automática (*iLine F, Ovizio imaging systems*) a culturas em reator de células de inseto infetadas e não infetadas, para isolar características da imagem associadas à produção de VAA. As características associadas às variáveis a monitorizar foram determinadas usando regressão gradual para a frente combinada com regressão linear múltipla, culminando com a identificação das características da célula associadas à produção de VAA, concentração celular e viabilidade da cultura. Esta abordagem confirma que é possível usar microscopia holográfica digital para a deteção do estado biológico da célula a cada fase da infeção, e para monitorização em tempo real do título de VAA e da progressão da cultura em sistemas léticos. Assim, esta é uma ferramenta valiosa para determinar o tempo de recolha da cultura celular.

No **capítulo IV**, foi investigada a influência da produção de VAA e da replicação do baculovirus no potencial dielétrico da célula, utilizando espectroscopia dielétrica. Devido à elevada atividade intracelular da célula durante o processo de produção, e de modo a construir uma plataforma de monitorização robusta, incluímos diferentes condições de cultura, adicionando culturas de reatores com títulos de VAA proposadamente baixos e com infeção por baculovirus sem transgene. Com esta estratégia, foram desenvolvidos modelos para prever, durante o processo, a concentração celular, viabilidade e produção de VAA por célula. Foi também demonstrada a aplicabilidade da espectroscopia dielétrica como Tecnologia
xx

Análítica de Processo (TAP), com previsões precisas do tempo de infecção mais de 24 horas antes, usando as medições contínuas da permitividade da cultura. O trabalho apresentado neste capítulo foi realizado na *Voyager Therapeutics*, uma empresa de terapia génica sediada em Boston focada no tratamento de doenças do sistema nervoso central.

A principal motivação por detrás do trabalho desenvolvido nos **capítulos II a IV** foi a iniciativa Tecnologia Analítica de Processo (TAP), um guia criado pela *Food and Drug Administration* (FDA) dos Estados Unidos da América (EUA) para a indústria farmacêutica, assente em três pilares principais: análise, monitorização e controlo do produto. A análise do produto foca-se em diminuir o risco do processo de produção através do aumento de conhecimento sobre o processo, identificando os Atributos Críticos da Qualidade (ACQ) do produto assim como os Parâmetros Críticos do Processo (PCC) que os afetam. O segundo pilar tem origem na necessidade de monitorizar em tempo real as características do produto identificadas como relacionadas com a qualidade deste. O trabalho desenvolvido nesta tese incidiu sobretudo nestes dois primeiros pilares.

O **capítulo V** aborda o terceiro pilar referido: a implementação de uma estratégia de controlo para corrigir desvios ao perfil de qualidade do produto. É apresentada uma visão geral das estratégias de controlo mais usadas para bioprocessos que inclui abordagens clássicas e avançadas.

No **capítulo VI**, são discutidos de modo geral os principais resultados obtidos nos capítulos anteriores. É também feita uma reflexão sobre as perspetivas futuras nesta área.

Assim, esta tese explora o uso de três métodos diferentes, baseadas em espectroscopia ou em análise de imagem, para a quantificação em tempo-real da produção de VAA e da concentração de células viáveis no

sistema de expressão baculovirus-célula de inseto. Os modelos quantitativos desenvolvidos permitem monitorizar os Parâmetros Críticos do Processo e decidir o momento de recolha da cultura celular, e são aplicáveis para estabelecer estratégias controladas de suplementação de nutrientes. As ferramentas e metodologias apresentadas podem ser aplicadas na monitorização em tempo real de outros serotipos de VAA, outros biofarmacêuticos produzidos no SEB-CI e, potencialmente, outros processos de produção de vetores virais. Deste modo, e no âmbito da iniciativa TAP, acreditamos estar a contribuir significativamente para aumentar o conhecimento do processo de produção do VAA e para a implementação de ferramentas de monitorização em tempo real da produção de VAA nas células de inseto.

Thesis Publications

Pais, D.A.M., Portela, R.M.C., Carrondo, M.J.T., Isidro, I.A., & Alves, P.M. (2019). "Enabling PAT in insect cell bioprocesses: in-situ monitoring of recombinant adeno-associated virus production by fluorescence spectroscopy". *Biotechnol. Bioeng.* bit.27117. <https://doi.org/10.1002/bit.27117>

Pais, D.A.M., Galvão, P., Kryzhanska A., Isidro, I.A., Alves, P.M., "Online holographic imaging of insect cell cultures: monitoring viable cell concentration and adeno-associated virus production", (*in preparation*)

Pais, D.A.M., Brown, C., Grewal, H., Isidro, I.A.; Alves, P.M.; Slade, P.G., "Dielectric Spectroscopy as PAT tool in the IC-BEVS system: Optimization of infection timing and robustness in AAV manufacturing" (*in preparation*).

Book chapters

Isidro, I.A.; **Pais, D.A.M.**; Alves, P.M.; Carrondo, M.J.T. "Online Control Strategies" In *Comprehensive Biotechnology*, Vol. 2, Moo-Young, M., Ed., Elsevier: Pergamon, 2019; pp 943–951. <https://dx.doi.org/10.1016/B978-0-444-64046-8.00112-9>.

Additional publications on the scope of real-time monitoring

Daniel AM Pais, Manuel JT Carrondo, Paula M Alves, Ana P Teixeira. "Towards real-time monitoring of therapeutic protein quality in mammalian cell processes", *Current Opinion in Biotechnology*, 2014, 30:161-167.

Inês A Isidro*, Pedro Vicente*, **Daniel AM Pais**, Mara Domingues, Bernardo Abecasis, Paula M Alves, Margarida Serra. "Dielectric spectroscopy monitoring of a bioreactor process for hiPSC expansion and differentiation" (*in preparation*). * - Denotes co-first authorship

Additional publications on the scope of viral vector production improvement

Pais, D.A.M*, Carinhas, N*, Koshkin, A*, Alves, P. M. and Teixeira, A. P. (2016), "¹³C-metabolic flux analysis of human adenovirus infection: Implications for viral vector production". *Biotechnol. Bioeng.*doi:10.1002/bit.26063 * - Denotes co-first authorship

Pais, D.A.M*, Carinhas, N* et al. "Metabolic flux profiling of MDCK cells during growth and canine adenovirus vector production". *Sci. Rep.* 6, 23529 (2016); * - Denotes co-first authorship

Table of Contents

Chapter I – Introduction.....	1
Chapter II – Enabling PAT in insect cell bioprocesses: in-situ monitoring of recombinant adeno-associated virus production by fluorescence spectroscopy.....	59
Chapter III - Holographic imaging of insect cell cultures: online non-invasive monitoring of adeno associated virus production and cell concentration.....	101
Chapter IV - Dielectric spectroscopy as a PAT tool in the insect cell-baculovirus system: optimization of infection timing and robustness in AAV manufacturing.....	143
Chapter V - Online control strategies.....	177
Chapter VI - Discussion and Future Perspectives	201

List of abbreviations

3CV	3-fold cross-validation
A549	Human lung carcinoma cell line
AAP	Assembly-activating protein
AAV	Adeno-associated virus
AcMNPV	Autographa californica nucleopolyhedrovirus
ADA-SCID	Adenosine deaminase severe combined immunodeficiency
ANN	Artificial neural networks
BHK	Baby Hamster Kidney
BIIC	Baculovirus-infected insect cells
bp	Basepairs
CCD	Charge-coupled device
CCI	Cell concentration at infection
CDE	Cell density effect
CHO	Chinese Hamster Ovary
CMV	Cytomegalovirus promotor
CPP	Critical Process Parameter
CQA	Critical Quality Attribute
CRISPR	Clustered regularly interspaced short palindromic repeats
DDHM	Differential digital holographic imaging
DHM	Digital holographic imaging
DMEM	Dulbecco's modified eagle medium
DNA	Deoxyribonucleic acid
DO	Dissolved oxygen
dsDNA	Double-stranded DNA
<i>E. coli</i>	<i>Escherichia coli</i>
ELISA	Enzyme-linked immunosorbent assay
EMA	European Medicines Agency
FBS	Fetal Bovine serum
fc	Characteristic frequency
FDA	Food and Drug Administration
FTIR	Fourier-transformed Infrared Spectroscopy
GFP	Green Fluorescence Protein
GMP	Good Manufacturing Practices
gp64	Baculovirus major envelope glycoprotein

HCP	Host-cell proteins
HEK293	Human embryonic kidney 293 cell line
HeLa	Human cervical cancer cell line derived from Henrietta Lacks
HighFive	Cell line derived from <i>Trichoplusia ni</i>
hpi	Hours post-infection
HSV	Herpes Simplex Virus
IC-BEVS	Insect cell-baculovirus expression vector system
ILC	Iterative-learning control
IND	Investigational new drug
ITRs	Inverted Terminal Repeats
LOBO	Leave one batch out
MA	Massachusetts
mAb	Monoclonal antibody
MIR	Mid-Infrared spectroscopy
MOI	Multiplicity of infection (number of viruses per cell)
MPC	Model predictive control
MRAC	Model-reference adaptive control
NIR	Near-Infrared spectroscopy
nRMSEcv	Normalized root mean squared error of cross-validation
OUR	Oxygen uptake rate
PAT	Process analytical technology
PCA	Principal component analysis
PI	Proportional-Integrative
PID	Proportional-Integrative-Derivative
PLS	Partial least squares
PTT	Process to target
Q ²	Correlation coefficient for the validation dataset
qPCR	Quantitative Polymerase Chain Reaction
QPI	Quantitative phase imaging
R ²	Correlation coefficient for the calibration dataset
rAAV	Recombinant adeno-associated virus
RMSEC	Root mean squared error for calibration dataset
RMSEV	Root mean squared error for validation dataset
RMSET	Root mean squared error for testing dataset
RNA	Ribonucleic acid
RSD	Relative standard deviation

RTM	Real-time monitoring
SF	Synchronous fluorescence
Sf9	<i>Spodoptera frugiperda</i> clone 9 cell line
ssDNA	Single-stranded DNA
TOH	Time of harvest
TOI	Time of infection
VCC	Viable cell concentration
VLP	Virus-like particle

Chapter I

Introduction

Author contributions

Daniel Pais wrote this chapter based on the published literature

Contents

1. Motivation: The need for real-time monitoring tools for viral vector manufacturing.....	5
2. Gene therapy: the next mAb revolution?.....	6
2.1. Historical perspective.....	6
2.2. Approved products.....	7
2.3. Delivery and therapeutic strategies.....	9
2.3.1. Viral and non-viral delivery.....	9
2.3.2. Therapeutic strategies	9
3. The Adeno-Associated Virus (AAV)	12
3.1. Biology	12
3.2. AAV as a vector for gene therapy	13
3.2.1. Clinical trials using rAAV as delivery vector.....	15
3.3. Comparison of rAAV production systems	17
3.3.1. Transfection of HEK293 cell lines	17
3.3.2. Stable producer mammalian cell lines	18
3.3.3. Infection with Herpes Simplex Virus (HSV).....	18
3.3.4. Insect Cell – Baculovirus expression vector system	19
3.3.5. Novel modalities to produce rAAV	19
3.4. Manufacturing and purification challenges.....	22
3.4.1. AAV vector quality attributes.....	22
3.4.2. Upstream Challenges	23
3.4.3. Downstream process challenges	24
4. The Insect Cell-Baculovirus Expression Vector System.....	25
4.1. Introduction	25
4.2. Baculovirus infection cycle.....	27
4.3. Producing rAAV in the IC-BEVS	28
4.4. IC-BEVS production issues and further improvements	29
5. Real-time monitoring of cell culture processes	32
5.1. Quality by Design and Process Analytical Technology	32
5.2. Real-time monitoring tools	33
5.2.1. The use of real-time monitoring tools for cell culture processes	33

- 5.2.2. Real-time monitoring in the IC-BEVS..... 37
- 5.3. Fluorescence spectroscopy, digital holographic imaging and dielectric spectroscopy 38
 - 5.3.1. Fluorescence spectroscopy 38
 - 5.3.2. In situ microscopy and holographic imaging 40
 - 5.3.3. Dielectric spectroscopy 41
- 6. Thesis scope and outline 44**
- 7. References 46**

Introduction

1. Motivation: The need for real-time monitoring tools for viral vector manufacturing

The interest for the gene therapy field has resurged since the approval of Glybera™, in 2012. The promise of a lifetime treatment for debilitating genetic conditions that dramatically reduce the life expectancy of patients currently attracts the interest of several pharmaceutical companies and shareholders. The World Health Organization (WHO) estimates the existence of 10000 monogenic diseases, with an incidence at birth of 0.4-0.5 % (Venugopal et al., 2018; World Health Organization, 2019). However, gene therapy has potential for treating a whole range of genetic diseases, affecting an estimate of 330 million people worldwide, of which approximately half are children (Goswami et al., 2019). This represents an estimated forecasted global market for gene therapies of USD 11000 million over the next 10 years (Goswami et al., 2019).

The significant investment to study and optimize new viral vectors, new delivery methods and strategies to specifically transduce target cells and improve manufacturing processes translates into a prohibitive cost for the approved gene therapies. As these therapies start entering the commercialization stage, manufacturing the large quantity of vectors necessary in a cost-effective way cannot be achieved only by scaling-up the process but needs to be combined with the development of scalable, compliant and standardized manufacturing processes. Moreover, in the Process Analytical Technology (PAT) initiative (FDA, 2004), the regulatory entities recommend the identification and continuous in-process monitoring of the product quality characteristics, as well as the product itself, in order to

assure product quality at every stage of the manufacturing process. However, the currently developed methods available for bioprocess monitoring were mostly developed for protein-based products, and methods for online monitoring of viral vectors are still lacking (Petiot et al., 2016).

In the scope of the PAT initiative, the work presented in this thesis is focused on the implementation of real-time monitoring tools coupled with advanced pre-treatment and modeling techniques for viral vector manufacturing and increasing AAV vector production process understanding.

2. Gene therapy: the next mAb revolution?

2.1. Historical perspective

Gene therapy is defined as a therapeutic strategy consisting in transferring DNA to patient cells, with the aim of correcting or replacing a defective gene or gene product (Shahryari et al., 2019). The initial concept of gene therapy, the idea to correct defective genes replacing them with their fully functional version, can be traced back to 1972 (Neufeld et al., 1972). The first successful clinical trial occurred 18 years afterwards: in 1990, Ashanti DeSilva, a patient suffering from ADA-SCID, was successfully treated with an adenoviral vector, remaining a success story to this day (Wirth et al., 2013). In the same decade, several trials were followed, culminating with the infamous ornithine transcarbamylase deficiency clinical trial: in 1999, a very high adenovirus vector dose administration induced multiorgan failure in Jesse Gelsinger, resulting in his death (Wirth et al., 2013). This event originated a setback in gene therapy clinical trials, with a consequent focus in improving the safety of viral vectors.

Slowly, the field resurged, with the first approved viral-vector based gene therapy taking place in China in 2003, an adenovirus vector for head and neck

cancer treatment (Wirth et al., 2013). In Europe, the first approved gene therapy viral vector was Glybera™, in 2012, for the treatment of lipoprotein lipase deficiency (Wirth et al., 2013). The approval of Luxturna™ in the USA in 2017, for the treatment of Leber's congenital amaurosis, and Zolgensma® in 2019, for Spinal Muscular Atrophy, marks the definitive establishment of the gene therapy field (Keeler and Flotte, 2019).

2.2. Approved products

Currently, there are 19 gene therapy products approved and currently in the market (Shahryari et al., 2019), 2 of them based on direct AAV vector delivery: Zolgensma® and Luxturna™ (Figure 1.1). Glybera™, an AAV1-based therapy, set the first milestone in AAV-mediated gene therapy, being the first gene therapy product approved in the western world in 2012. Glybera™ was withdrawn from the market in 2017, due to low market demand, despite its effectiveness (Goswami et al., 2019). The current view for the gene therapy field is optimistic, with 70-90 approved products expected by 2025. This projection is based on the current rate of Investigational New Drug (IND) applications to the FDA for gene therapy (800 in 2018 and over 1000 in 2019) (Puri, 2019).

Due to the market risk, the complexity and the cost of the manufacturing process, gene therapies are among the most expensive drugs in the market, which raises concerns on the affordability and profitability of such treatments: when it was launched, Glybera™ had a price tag of over €1 M; Luxturna™ has a cost of USD 770 M for both eyes while Zolgensma®, currently the most expensive gene therapy drug, has a price tag of USD 2.125 M. This has led companies to develop alternative payments schemes, based on pay per-performance annuities and outcome-based rebates (Goswami et al., 2019; Shahryari et al., 2019).

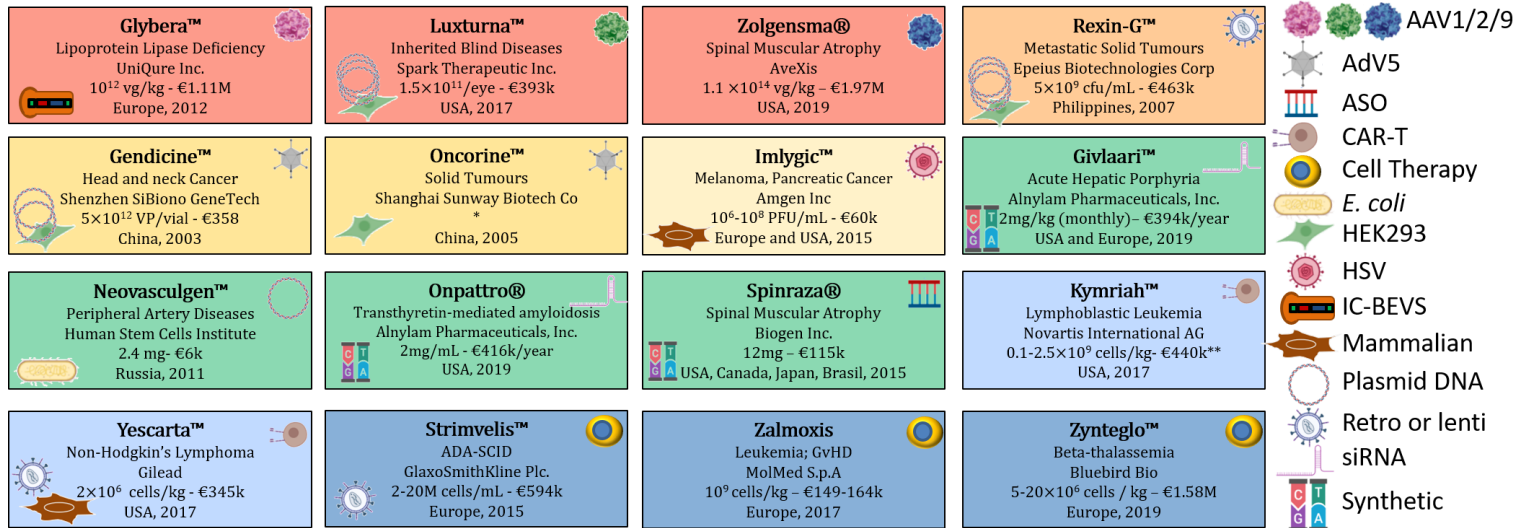


Figure I.1 – Overview of the current gene therapy products approved and currently in the market (Glybera™ was withdrawn from the market in 2017). For each product, we list the therapeutic indication, the manufacturing company, the dosing and pricing and the markets where the drug is approved. The upper right corner indicates the type of product, while the lower left corner depicts the production system. Adapted from (Goswami et al., 2019; Kim et al., 2004; Nemunaitis et al., 2000; Shahryari et al., 2019 and from the corresponding product leaflet in the FDA or EMA websites (accessed on February 2019)). *Oncorine dose and price is indication dependent. **Kymriah™ dose decreases to 0.2-5 × 10⁶ cells/kg for patients less than 50 kg. Missing production systems are proprietary information. AAV – Adeno-Associated Virus; Adenosine deaminase severe combined immunodeficiency; AdV5 – Adenovirus type 5; ASO – Antisense oligonucleotide; CAR-T - Chimeric Antigen Receptor; *E. coli* – Escherichia coli; HSV – Herpes Simplex Virus; IC-BEVS – Insect cell – baculovirus expression vector system; siRNA – small interfering RNA.

2.3. Delivery and therapeutic strategies

2.3.1. Viral and non-viral delivery

“There are only three problems in gene therapy: delivery, delivery and delivery (...)” (I.M. Verma in TIME, 1999; Jan 11). Despite the research and efforts put in viral or cell line development and improvement of manufacturing conditions, to be successful as a therapy the genetic load must be delivered to the target cells. With that aim, both viral and non-viral strategies have been developed (Figure I.2).

Non-viral based strategies have the advantage of being easier to prepare and relatively safer than viral-vector approaches, and include the use of alternatives such as plasmid DNA, liposomes and polymer-based approaches (reviewed in Yin et al., 2014). However, viral vectors have the advantage of their higher transduction potential, since they rely on the natural capacity of viral vectors to infect and express their genetic material in the target cell.

Cucchiari *et al.* published in 2016 a comprehensive review of the current challenges associated with gene therapy delivery, such as physical barriers, immune response, vector capacity, internalization and transgene expression (Cucchiari, 2016).

2.3.2. Therapeutic strategies

According to the European Medicines Agency (EMA), gene therapy comprises several strategies to “regulate, repair, replace, add or delete genetic sequences” in humans (Shorthose, 2017). The chosen strategy is thus dependent on the root cause of the genetic condition (Wang et al., 2019): loss of gene function, gain of toxic mutations or defective protein overexpression or gene modulation (Figure I.3). The challenges associated with each of these strategies and examples of ongoing clinical trials using them are reviewed elsewhere (Wang et al., 2019).






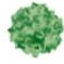
Classes		Advantages	Shortcomings
Nonviral vectors  <ul style="list-style-type: none"> . naked DNA . DNA-protein conjugation . physical methods (microinjection, gene gun, electroporation, sonoporation, photoporation, magnetofection, hydroporation) . chemical methods (inorganic particles: calcium phosphate, silica, gold; synthetic and natural biodegradable compounds: cationic lipids, lipid nano-emulsions and particles, liposome/DNA complexes, peptide-based polyplexes and lipoplexes) 	<ul style="list-style-type: none"> . no toxicity . no immunogenicity . large capacity . ease of preparation 	<ul style="list-style-type: none"> . low efficiency . need for cell division . lysosomal degradation . short-term expression 	
Viral vectors	Retroviral vectors (7-10 kb; 100-150 nm) 	<ul style="list-style-type: none"> . average capacity (8 kb) . stable integration . long-term expression 	<ul style="list-style-type: none"> . low titers (10^6 -10^8 VP/ml) . restricted tropism . low efficiency . need for cell division . insertional mutagenesis . immunogenicity
	Lentiviral vectors (9-10 kb; 100-150 nm) 	<ul style="list-style-type: none"> . average capacity (8 kb) . stable integration . long-term expression . dividing/nondividing cells . high efficiency 	<ul style="list-style-type: none"> . low titers (10^6-10^8 VP/ml) . restricted tropism . insertional mutagenesis . immunogenicity . HIV-derived material
	Adenoviral vectors (~36 kb; ~100 nm) 	<ul style="list-style-type: none"> . high titers (10^{11} VP/ml) . average capacity (7.5 kb) . dividing/nondividing cells . high efficiency 	<ul style="list-style-type: none"> . immunogenicity . no integration . short-term expression
	HSV-derived vectors (150 kb; 120-220 nm) 	<ul style="list-style-type: none"> . high titers (10^{12} VP/ml) . large capacity (>30 kb) . dividing/nondividing cells . high efficiency 	<ul style="list-style-type: none"> . toxicity, immunogenicity . no integration . short-term expression
	rAAV vectors (4.7 kb; ~25 nm) 	<ul style="list-style-type: none"> . high titers (10^{11} VP/ml) . relatively low toxicity . dividing/nondividing cells . high efficiency . episomal maintenance . long-term expression 	<ul style="list-style-type: none"> . small capacity (4.5 kb) . relative immunogenicity . limiting genome conversion . insertional mutagenesis (virus)

Figure I.2 - Comparison of the main advantages and shortcomings in non-viral and viral-based strategies for gene therapy. Adapted from (Cucchiari, 2016). Abbreviations: VP – viral particles; HSV – Herpes simplex virus; rAAV – recombinant adeno-associated virus vectors.

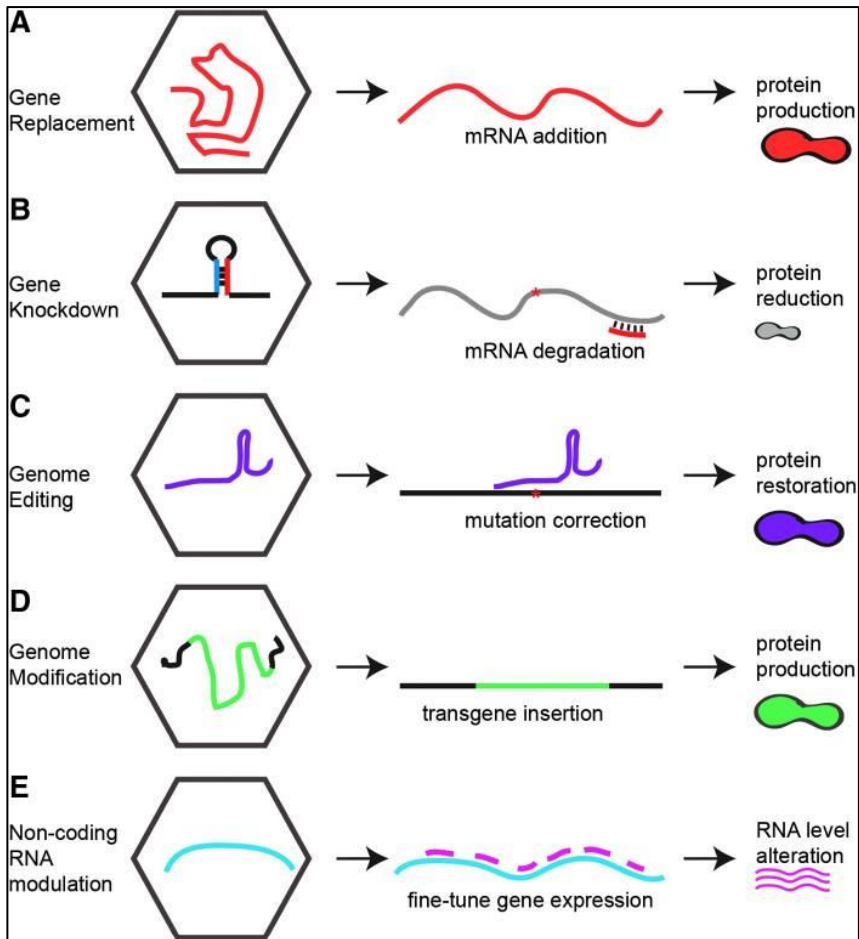


Figure I.3 – Overview of the current gene therapy strategies. **A)** Gene replacement – addition of the correct copy of the defective gene to correct for loss of function mutations. This is the strategy employed for recessive monogenic diseases, such as most eye conditions, hemophilia, Duchenne muscular dystrophy or spinal muscular atrophy. **B)** Gene knockdown - Delivery of interference RNA or use of gene-editing strategies to reduce the expression of the faulty protein. Examples include monogenic diseases (Huntington), tauopathies, such as Alzheimer, or Friedreich Ataxia. **C)** Genome editing – Using strategies such as CRISPR/Cas9 or zinc finger nucleases to edit the mutation causing the disease. **D)** Genome modification or gene addition - introduction of DNA sequences to correct a mutation or provide a therapeutic or suicide gene, such as the Aromatic L-amino acid decarboxylase gene in Parkinson Disease or suicide genes for cancer therapy. **E)** Fine-tuning of the protein expression levels by non-coding RNA modulation, as used for instance for heart failure. Adapted from (Planul and Dalkara, 2017; Valdmanis and Kay, 2017; Wang et al., 2019).

3. The Adeno-Associated Virus (AAV)

3.1. Biology

The adeno-associated virus (AAV) is a small (20-25 nm), icosahedral, non-enveloped, single-stranded DNA (ssDNA) virus belonging to the Parvoviridae family. Its genus name, *Dependoparvovirus*, indicates their dependency on the viral machinery of helper viruses (usually adenovirus or herpes-simplex virus) to replicate in the host cell (Wang et al., 2019). AAV were first detected as a contamination in adenovirus preparations, hence their name (Wang et al., 2019). Currently there are over 108 AAV variants identified, derived from 12 serotypes (Colella et al., 2018). Each serotype has capsid amino acid variations which change their affinity to cellular receptors, and as such their tropism to different cell types, tissues or species (compiled in Keeler and Flotte, 2019 and Saraiva et al., 2016). Despite these inter-serotype differences, recently a new cellular receptor was identified as critical for infection of all AAV serotypes, and accordingly renamed as “universal” AAV receptor (Pillay et al., 2016).

AAV infection starts with attachment of the virus to the cellular receptors, followed by the virus internalization by endocytosis (Nonnenmacher and Weber, 2012). After being released from the endosome into the cytoplasm, the vector is imported into the cell nucleus via the nuclear pore complex, eventually reaching the nucleoplasm, where the viral genome is released by capsid uncoating and the ssDNA is copied into a double stranded DNA. (Brown et al., 2017; Nonnenmacher and Weber, 2012). In the absence of a helper virus, the viral DNA either stays in its episomal form, in the case of viral vectors, or is inserted into the host cell chromosome, in the case of wild type virus (specifically, region AAVS1 in chromosome 19 for human cells) (Keeler and Flotte, 2019).

The AAV DNA consists of a 4.7 kbp linear single stranded genome, which encodes the necessary viral proteins for capsid expression (*cap*) and genome replication (*rep*). These are coded in two open-reading frames, one for *cap* and the other for *rep* genes (Hentzschel et al., 2016). The *cap* gene confers the AAV serotype, and encodes for the three capsid proteins (VP1, VP2 and VP3, with 87, 73 and 62 kDa respectively) (Cecchini et al., 2008). The *rep* gene encodes for the 4 replication proteins, two large proteins (Rep78 and Rep68) and two small ones (Rep52 and Rep40) (Dubielzig et al., 1999). The recently discovered Assembly-Activating Protein (AAP) is encoded out-of-frame in the VP2 gene sequence, and it has important chaperone functions for capsid assembly for most serotypes (Große et al., 2017). AAV genomic material is flanked by Inverted Terminal Repeats (ITRs), palindromic DNA sequences with approximate 140 bp which are essential to provide the encapsidation signal for the cellular machinery (Savy et al., 2017).

3.2. AAV as a vector for gene therapy

AAVs are subject to extensive research in both academia and industrial setting and are one of the most used viral vectors for gene therapy clinical trials (Figure I.4). Reasons for their widespread use are their apparent lack of pathogenicity in humans and the ability to transduce a variety of cell types, while allowing sustained episomal gene expression in replicating and quiescent cells. Finally, recombinant AAVs are resilient, rendering them resistant to industry manufacturing and purification strategies (Naso et al., 2017; Negrete and Kotin, 2009). Some serotypes, such as AAV9, can cross the blood brain barrier, which allows systemic, intravenous administration of vectors targeting the central nervous system, as is the case of Zolgensma®. The main bottlenecks of AAV-based gene therapy (Figure I.2) have been addressed with several interesting strategies:

- Transgene capacity - rAAV possess a very low therapeutic gene capacity (4.7 kbp). While some authors report the slight increase of the rAAV

capacity using molecular biology strategies, such as eliminating VP2 (Grieger and Samulski, 2005), the most used strategies to circumvent the low transgene capacity is dividing large genes into dual rAAV vectors (Chamberlain et al., 2016; McClements and Maclaren, 2017).

- Existence of pre-existing antibodies and immunogenicity – The seroprevalence of neutralizing antibodies for rAAV depends on the serotype. Taking as an example rAAV-2, neutralizing antibodies were detected on average in 45 % of subjects (Louis Jeune et al., 2013); additionally, the similarity between serotypes originates cross reactivity between the corresponding neutralizing antibodies, which was verified in more than 50 % of subjects for any dual serotype combination (Louis Jeune et al., 2013). For multiple dose treatments, the possible generation of rAAV neutralizing antibodies prevents subsequent vector administration. Strategies to prevent rAAV administration-related immune responses (reviewed in Mingozzi and High, 2017) include reduction of the neutralizing antibodies titers pre-vector administration, alternative routes of administration, switching the rAAV serotype or combining AAV vector transduction with non-viral delivery based on exosome vesicles (Meliani et al., 2017; Orefice et al., 2019). This last approach can potentially ameliorate vector uptake by target cells and reduce the associated immune response (reviewed in György and Maguire, 2017).

- Slow onset of transgene expression – In the absence of a helper virus, conversion of rAAV ssDNA into dsDNA has been shown to be a rate-limiting step (Berry and Asokan, 2017). Self-complementary AAV vectors (scAAV) have been developed to shorten the time between vector transduction and transgene expression by eliminating the time for synthesis of the complementary DNA strand. This was achieved by packaging the therapeutic transgene and its complementary DNA strand as the vector payload. However, this approach further reduces the transgene capacity by half (Snyder and Moullier, 2011).

3.2.1. Clinical trials using rAAV as delivery vector

The current landscape of rAAV-based gene therapy is marked by the existence of several companies and a high number of clinical trials under development (219 as of January 2019), targeting a range of eye, blood, muscle, metabolic and central nervous system disorders. The major indications currently being addressed in clinical trials are hemophilia (BioMarin, UniQure, Spark Therapeutics, Pfizer), retinal diseases (Spark Therapeutics, NightStar Therapeutics, Gensight Biologics), metabolic diseases (Adverum), Parkinson and other central nervous system disorders (PTC Therapeutics, Voyager Therapeutics) and muscular diseases (Audentes Therapeutics) (Shahryari et al., 2019). rAAV-based gene therapy is relatively safe, with rare reports of serious adverse events, mostly related with elevation of liver enzymes and immune responses against transduced liver cells, which can be overcome with transient immunosuppression (Kotin and Snyder, 2017).

Currently, rAAV represents 8 % of the gene therapy clinical trials, largely focused in monogenic diseases as target indication (Figure I.4), but with cancer as the next major therapeutic application (Reul et al., 2019; reviewed in Santiago-Ortiz and Schaffer, 2016) followed by neurological disorders (reviewed in Hudry and Vandenberghe, 2019), ocular diseases and cardiovascular diseases (reviewed in Bera and Sen, 2017).

A comprehensive list of the currently active rAAV clinical trials and the corresponding serotype, target tissue and condition is provided elsewhere (Wang et al., 2019).

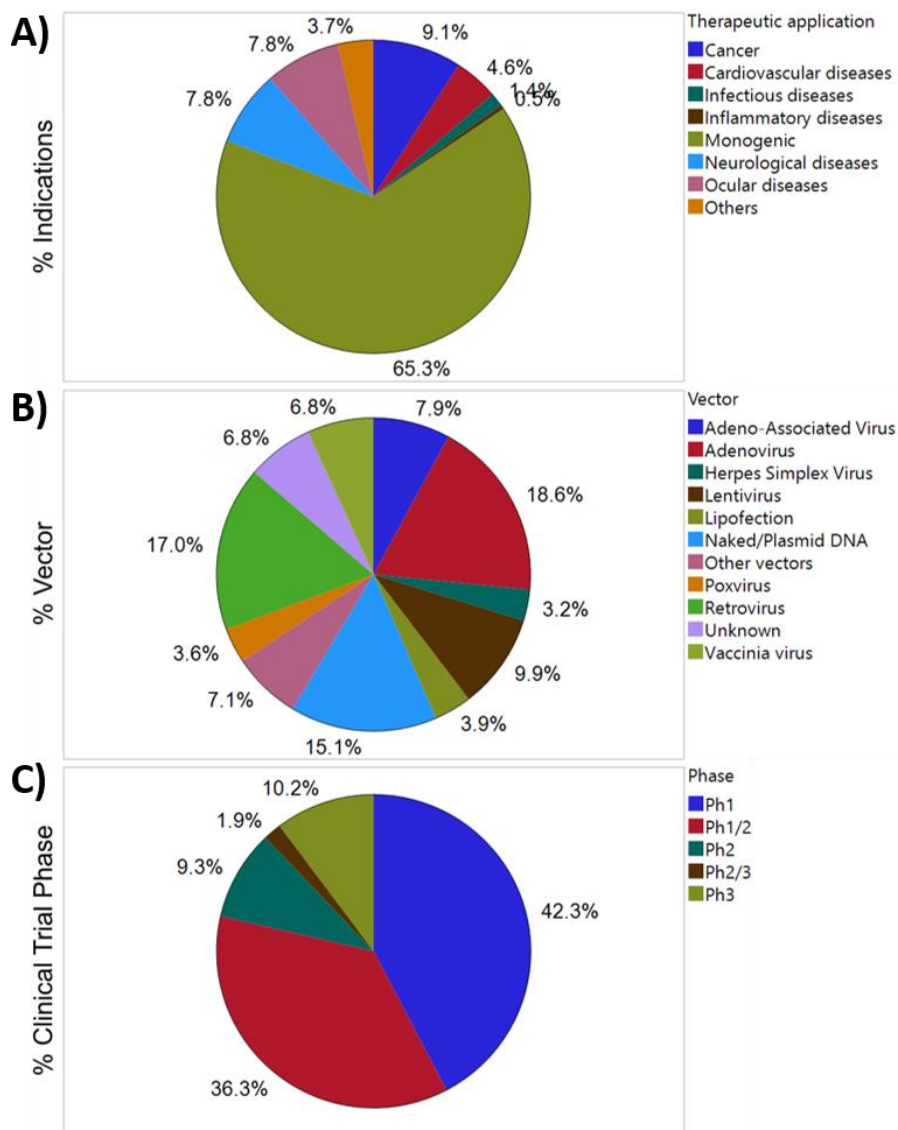


Figure I.4 - Clinical trials using adeno-associated virus (AAV). The data is from <http://www.abedia.com/wiley/>, accessed on January 2019. A) rAAV clinical trials by therapeutic application (n=219). B) Distribution of the clinical trials by vector / non-viral delivery methods (n=3081). C) Distribution by clinical trial phase (total=215).

3.3. Comparison of rAAV production systems

The attractiveness of rAAV for gene therapy led to the development and improvement of several biological production systems. The current state of the art shows the different production systems have comparable cell specific rAAV productivities (Merten, 2016). As such, the choice of the production system is dependent of factors such as the vector quantity needed. For instance, for phase I clinical trials or specific administration sites or routes, where small vector doses are needed, transfection-based systems can be used. For later clinical trial stages and for IV administration, the use of more scalable systems is needed (Merten, 2016; Rininger et al., 2019).

This section will detail each rAAV production system, their strengths and limitations and recent improvements. There are four biological systems considered established for production of AAV vectors, which are detailed in the following sections and compiled in Table I.1. Additionally, Section 3.3.5 briefly addresses the use of new production systems.

3.3.1. Transfection of HEK293 cell lines

This system relies on triple transfection of HEK293 cells, with one plasmid containing the *rep* and *cap* genes, the other one containing the ITR-flanked transgene and the helper plasmid containing the necessary adenoviral genes. A two-plasmid variation has been developed, in which the helper plasmid is combined with the one containing the *rep* and *cap* functions. This system is widely used due to the easiness to design the plasmids and the optimization of the transfection process in these cells throughout the years (Merten, 2016). It is mostly used for screening of new rAAV constructs due to the method simplicity, availability of GMP-grade plasmids and no intellectual property on the manufacturing protocols (Clément, 2019).

These cells are grown in adherent conditions, which poses a constraint for large scale production of the viral vectors. Production in cell stacks or

fixed-bed bioreactors slightly alleviates this issue, although the space requirements are still a concern. The use of suspension and serum free-adapted cells is also reported, in scales of up to 20 L using the WAVE bioreactor system (Chahal et al., 2014; Grieger et al., 2016; Powers et al., 2016) .

3.3.2. Stable producer mammalian cell lines

This system is based on the use of packaging and producer cells which stably express the *rep* and *cap* genes and the ITR-flanked gene of interest (Merten, 2016). In general, either HeLa or A549 cells are preferred due to their easiness to grow in suspension and maintain stably integrated copies of the cytotoxic rep protein (Merten, 2016; Thorne et al., 2009). In order to produce the recombinant AAV vectors, infection with a helper virus is necessary to provide the helper functions required for rAAV replication. Adenovirus is often chosen as helper vector, since it is easy to produce and to demonstrate viral clearance after the purification process (Thorne et al., 2009). This system generates more than 10^5 rAAV viral genomes (vg) *per* cell (Merten, 2016; Sharon and Kamen, 2017), however with the concomitant production of infectious adenovirus, which need to be removed from the final product. This can be partially addressed by using replication deficient or cold-attenuated adenovirus, although with a decrease on the rAAV titers achieved (Merten, 2016; Sharon and Kamen, 2017). The main limitation of this system is the fact that a stable cell clone must be generated for every serotype / therapeutic application (Wang et al., 2019). The use of suspension-adapted producer cell lines has been described in scales up to 2000L (Clément and Grieger, 2016).

3.3.3. Infection with Herpes Simplex Virus (HSV)

The helper functions required for rAAV replication can be provided by the Herpes Simplex Virus. This system relies on co-infection of HEK239 or BHK cells adapted to grow in suspension with two recombinant herpes simplex vectors, one coding for the therapeutic transgene flanked by AAV ITRs and

the other one providing the *rep* and *cap* sequences (Galibert and Merten, 2011). Production scales up to 100 L have been reported (Clément, 2019). Interestingly, when using BHK cells, the decreased virus replication cycle has allowed to harvest rAAV as soon as 24 hpi (Thomas et al., 2009). This system has the potential to generate HSV vectors with immunogenic potential, which need to be removed from the final product. Additionally, a high multiplicity of infection (MOI) of HSV vectors is required for rAAV production, and consequently HSV is produced in suspension culture or fixed bed bioreactors (Knop and Harrell, 2008; Merten, 2016).

3.3.4. Insect Cell – Baculovirus expression vector system

Similarly to the HSV system, the use of the baculovirus system to produce rAAV in insect cells requires two baculovirus: one coding for the AAV *rep* and *cap* functions and the other one providing the transgene flanked by the AAV ITRs (Smith et al., 2009). The main advantage of this system is its scalability, with scales up to 400 L being reported, yielding 2.7×10^{14} vg/L (Cecchini et al., 2011; Kotin and Snyder, 2017).

It is worth referring that Glybera™ was produced using the insect cell baculovirus system. Further details on rAAV production in this system are provided in Section 4.3.

3.3.5. Novel modalities to produce rAAV

The aim to increase cell specific productivity or decrease manufacturing costs led to the development of new rAAV production systems. This section intends to list the current existing alternatives, rather than provide a detailed description of each of the systems:

- Use of CAP® cells, by Cevec Pharmaceuticals – Using a human cell line able to grow in suspension, serum- and animal-free conditions, Cevec reports the production of rAAV using both stable cells and

transient systems. The reported volumetric titers are comparable to existing systems, up to a 10 L scale (Cevec Pharmaceuticals, 2019; Hein et al., 2018).

- Other mammalian-based systems include the use of i) vaccinia virus infection of HEK293 cells, producing superabundant VP1 vectors with increased transduction *in vivo* (Wang et al., 2017); ii) a novel identified AAV helper virus, the bocavirus, which resulted in rAAV titers twice as high as the two-plasmid HEK transfection system (Wang et al., 2018);
- Production in *Saccharomyces cerevisiae*, however the recombinant AAV possessed lower infectivity and full capsid ratio than in the IC-BEVS (Aponte-Ubillus et al., 2018; Barajas et al., 2017);
- Production of AAV2 VP3 protein in *E. coli*, followed by cell-free capsid assembly of Virus-like particles (VLPs) (Le et al., 2019). Further developments are required to encapsidate genomic material into the VLPs and achieve infectious titers similar to the established systems.

Table I.1 - Comparison of several biological systems used for rAAV production. Scale indicated represents the higher reported to date. Adapted from (Aponte-ubillus et al., 2017; Clément, 2019; Clément and Grieger, 2016; Kondratov et al., 2017; Merten, 2016; Wang et al., 2019, 2011).

System	Description	Strengths	Limitations	Companies	Specific productivities (vg and IP)	Selected references
HEK293 transfection	Double or triple transfection of HEK 293	High vector potency; Versatility; Cost; Scales up to 20 L; No need to maintain viral stocks; Track record; Simplicity; Human origin	Scalability; Plasmids contain bacterial backbone; concerns regarding rAAV formation	Spark; AskBio; Neurologix; Abeona; Audentes.	$1.3 \times 10^4 - 9.4 \times 10^5$ vg/cell $10^2 - 10^3$ TU/cell	(Blessing et al., 2019; Chahal et al., 2014; Grieger et al., 2016; Powers et al., 2016)
Herpes Simplex Infection	Co-infection of BHK cells with two HSV1	Scalable up to 100 L; high rAAV vector potency	Large amounts of HSV vector necessary; Viral removal needed	Dimension; SolidBio	$7 \times 10^4 - 1.5 \times 10^5$ vg/cell $6 \times 10^3 - 1 \times 10^4$	(Adamson-Small et al., 2017, 2016; Clément et al., 2009; Knop and Harrell, 2008; Thomas et al., 2009)
Stable Mammalian cells	AdV infection of stable HeLa cells; Human origin	High ratio of full capsids and rAAV vector potency; High specific titer	Flexibility; Viral removal needed; Scalability; need of antibiotic and clone selection.	AGTC	$5 \times 10^4 - 1.3 \times 10^5$ vg/cell $3 \times 10^2 - 2 \times 10^3$ IP/cell	(Chen et al., 2014; Martin et al., 2013; Thorne et al., 2009)
IC-BEVS	Co-infection of insect cells with two baculovirus	Suspension; Scalable up to 400 L; High cell density and vol. productivities achieved; reduced encapsidation of foreign DNA; Absence of mammalian-derived products	Low rAAV potency; Molecular biology strategies for vector improvement; Baculovirus genetic instability; Suboptimal VP ratios; Viral removal needed	Voyager; UniQure; Adverum; Abeona; Virovek; Lacerta	$10^4 - 10^5$ vg/cell; 5×10^5 for stable cells 10^2 IP/cell	(Cecchini et al., 2011; Kotin and Snyder, 2017) Stable cells: (Joshi et al., 2019; Mietzsch et al., 2017, 2014)

rcAAV – replication competent AAV; HEK – human embryonic kidney 293 cell line; BHK – baby hamster kidney cell line; HSV1 – Herpes Simplex Virus 1; AdV – Adenovirus; HeLa - Cancer cell line derived from Henrietta Lacks; vg – vector genomes; TU – transducing units; IP – infectious particles; vol - volumetric

3.4. Manufacturing and purification challenges

3.4.1. AAV vector quality attributes

The main concern regarding recombinant AAV production is the balance between the vector quantities achieved and their quality. The rAAV quality attributes are the ability to infect and transduce the target cell, the ratio of empty to full particles obtained and the encapsidation of undesirable DNA material (Schnödt and Büning, 2017). There is however a common issue in the field, which is the standardization of analytical methods for rAAV quality attributes quantification. As reported in the works by Lock *et al.*, and Ayuso *et al.*, standardization of rAAV2 and 8 characterization assays is indeed a challenge. These authors produced and purified an rAAV2 and 8 vector lot, and characterized it in different labs, using the same protocols and reagents. Despite the standardization efforts, the titration results for the vector total, filled, infectious and transducing capsids were remarkably different between the different labs (Ayuso *et al.*, 2014; Lock *et al.*, 2010). This has profound implications for characterization of the produced vector by any institution or company, but also for comparison studies between different production systems, with discrepancies in the reported values for empty to full ratios and infectivity titers achieved by the different production systems (Kondratov *et al.*, 2017; Merten, 2016; Rumachik *et al.*, 2019). In particular for the vector potency assay, in which biological variability is inherently present, the final infectious titers are dependent on many factors, such as the method used to assess transduction (detection of transduced cell by flow cytometry, protein expression or qPCR) or the cell line used for titration.

The other important quality attribute of rAAV vectors is commonly referred as the ratio of empty to full particles. However, in reality there are three vector “species”: capsids with the correct encapsidated DNA; empty capsids; and capsids with incorrect encapsidated DNA (which includes truncated ssDNA and host cell DNA) (Savy *et al.*, 2017; Schnödt and Büning, 2017). The

majority of incorrectly encapsidated material originates from the vector backbone (Penaud-Budloo et al., 2018, 2017), and although in low percentage, it has immunogenic potential and is considered a major safety concern, being one of the six major product quality concerns identified during Glybera™ licensing assessment (Wright, 2014; Penaud-Budloo et al., 2017). As such, currently the presence of the host cell DNA and partial filled sequences is a concern for rAAV manufacturers (Wright, 2014). Although strongly dependent of the production system (for instance, the IC-BEVS has the lowest percentage of vector with incorrect genomes), some approaches have been developed to reduce foreign DNA encapsidation, such as increasing the length of the packaged transgene, closer to the AAV natural packaging capacity (Penaud-Budloo et al., 2017) and modification of the ITR or rep constructs (Noordman Y, Lubelski J, Bakker, 2016; Savy et al., 2017).

Approaches to increase the percentage of full capsids have mainly been achieved by improvement of the vector molecular design (Kondratov et al., 2017), increasing culture temperature after infection (Aucoin et al., 2007) and altering the ITRs structures (Savy et al., 2017).

3.4.2. Upstream challenges

The main challenges in the upstream process for rAAV production are scalability of the process and stability of the vector during the production process (Merten, 2016).

Scalability of the bioprocess is a concern as therapies advance in the clinical trials phase as large doses are needed. As an example, for AAV therapies the dosage can be as low as 10^{12} vector *per* patient, for eye indications, but three orders of magnitude higher when systemic administration is needed (Rininger et al., 2019). Although for some indications or Phase 1 trials the use of adherent platforms can be used (e.g. cell factories, roller bottles or fixed

bed bioreactors), when larger vector amounts are needed the use of bioreactor systems is necessary (Rininger et al., 2019).

The loss of vector infectivity during the culture is mostly related with rAAV autoproteolytic degradation or external protease activity (Mitchell and Samulski, 2013). The influence of pH and protease activity on rAAV infectivity is reviewed in (Salganik et al., 2012). Strategies to address this issue rely on continuous vector harvest from the culture media (Benskey et al., 2016; Grieger et al., 2016) or addressing the root causes of the vector loss of potency, as demonstrated by Galibert and coworkers. The authors identified the role of baculovirus protease cathepsin on the degradation of rAAV vectors, and report a two to four-fold increase in the vector potency when cathepsin was deleted from the baculovirus construct (Galibert et al., 2018).

Interestingly, this protease-dependent activity has been used for development of myocardial infarction treatments, relying on the elevated protease presence in diseased environments to activate an AAV-based provector (Guenther et al., 2019).

3.4.3. Downstream process challenges

The aim of the downstream process in rAAV manufacturing is to remove process and product-associated impurities while maintaining the vector quality characteristics. Process-related impurities include host cell proteins and DNA and the residual plasmids or helper virus used during the production step, potential causes of geno- or immunotoxicity or even posing infectious risk, as in the case of adenovirus or HSV. Product-associated impurities include capsids with undesirable genetic material (Aponte-ubillus et al., 2017; Wright, 2014).

A typical rAAV downstream process consists in cell lysis, followed by clarification and purification. For the cell lysis step both detergent lysis and

freeze-thaw are reported, although the first is preferred due to its scalability. A nuclease addition step may be added during or after lysis, as well as a concentration step such as tangential flow filtration. For the purification step, chromatography techniques are preferred, usually relying on affinity or ion-exchange (Clément and Grieger, 2016; Florencio et al., 2015).

The choice of the downstream process depends on the upstream conditions, such as cell type and culture volume to process, but it is also dependent on the vector serotype and possibly the vector transgene (Clément and Grieger, 2016; Virag et al., 2009). The different biophysical and chemical properties of the diverse rAAV capsids led to the development of commercially available affinity resins specific for each serotype (Clément and Grieger, 2016). The current challenges for rAAV manufacturing being addressed are the scalable separation of empty and full particles based on ion-exchange chromatography (Lock et al., 2012; Qu et al., 2007) and the development of “universal”, serotype-independent purification strategies for rAAV purification based on chromatography (Nass et al., 2018) or three-phase partitioning (Yu et al., 2020).

4. The Insect Cell-Baculovirus Expression Vector System

4.1. Introduction

The insect cell – baculovirus expression vector system (IC-BEVS) combines the versatility and robustness of insect cells as production host cells and the suitability of the baculovirus as a potent and safe expression vector.

Baculovirus is an enveloped insect cell virus, with a circular double stranded DNA (dsDNA) (80 to 180 kbp) which has been completely sequenced (Ferrelli et al., 2010). Initially studied for their application as insecticide, baculovirus potential as a vector for gene therapy soon emerged, mostly due to their

non-pathogenicity and high recombinant protein production yield (Yee et al., 2018). Nowadays, baculovirus-based systems have proved to be a good production system for difficult-to-express proteins from all organisms (Drugmand et al., 2012). The most studied and widely used baculovirus vector is based in the *Autographa californica* multicapsid nucleopolyhedrovirus (AcMNPV).

Insect cells, the other component of the IC-BEVS, are a robust production system also due to their scale-up and GMP-amenable characteristics: high-cell densities cultivation with modest growth requirements, in serum-free media, at 27 °C, without the need of CO₂ as a buffer for pH control. Insect cells can provide human-like post-translational modifications, have a proven track record for production of virus-like particles (VLPs) and viral vectors and produce lower lactate and ammonia than mammalian-based systems due to their higher TCA cycle utilization (Aponte-ubillus et al., 2017; Monteiro, 2015; Penaud-Budloo et al., 2017; Yee et al., 2018).

This combination resulted in the approval of several products for human use, such as Flublok®, Cervarix®, Provenge® and Glybera™ (reviewed in Monteiro, 2015 and Cox, 2012).

The most used cell lines for biopharmaceutical production are derived from two lepidopteran organisms: Sf9 and Sf21 cell lines, derived from the fall army worm *Spodoptera frugiperda*, and HighFive cells, derived from the cabbage looper *Trichoplusia ni* (van Oers et al., 2015). Both have similar physical characteristics and culture requirements. Despite the higher recombinant protein expression of the HighFive cell line, Sf9 cells are preferred over Sf21 and HighFive due to their higher efficiency in producing infectious baculovirus vectors (Drugmand et al., 2012). For a more detailed comparison of the two cell lines and an overview of the use of insect cells for biopharmaceutical production and their metabolic requirements, the works of Drugmand and

Monteiro are recommended (Drugmand et al., 2012; Monteiro et al., 2016, 2014).

Insect cells can be cultured over long-term passaging, although not without the occurrence of morphological and physiological changes and the decrease in the ability to produce infectious baculovirus (Clement, 2016). Other limitations of the system include the change in chromosome polyploidy during long-term cultivation (Drugmand et al., 2012), inability of insect cells to produce complex N-glycosylation (Steele et al., 2017) and the recent identification of Sf9 cell line contamination with a novel rhabdovirus (Ma et al., 2014). The latter two issues can be addressed by several glycoengineering approaches (compiled in Yee et al., 2018) or the development of rhabdovirus-free insect cell lines (Maghodia and Jarvis, 2017).

Still, the IC-BEVS is now one of the most used production systems for proteins and vaccines for animal and human use, in particular for multi-protein complexes, virus-like particles and rAAV production (Monteiro, 2015; van Oers et al., 2015). Recently, applications as a gene delivery vector for mammalian cells or in cancer therapy have also been reported (Asad et al., 2017; van Oers et al., 2015).

4.2. Baculovirus infection cycle

The baculovirus infection starts with gp64-mediated cell entry, followed by internalization of the virus. A full infection cycle comprises three phases: early, late and very late. The early phase (0-6 hours post-infection, hpi) is characterized by the transcription of the initial baculovirus genes, responsible for the activation of promoters of later genes (Hopkins and Esposito, 2009; van Oers et al., 2015). Detection of these early expressed baculovirus genes is the basis for the development of titration cell lines (Hopkins and Esposito, 2009). In the late infection phase (6 to 20-24 hpi), the baculovirus DNA

replication occurs, with the concomitant production of budded viruses, global shut-off of host cell synthesis and baculovirus-induced cell cycle arrest in the G2/M phase, resulting in the cell growth arrest observed in infected insect cells (Monteiro et al., 2012). The very late phase is characterized by the very strong p10 and polyhedrin promoter expression, which are usually associated with the recombinant protein expression (van Oers et al., 2015).

In the wild-type virus, the baculovirus has a biphasic replication cycle, with two corresponding virions: budded virions, responsible for intra-organism systemic infection, and occlusion derived-virions, responsible for between-organisms infection (Keddie et al., 1989). The very late phase corresponds to the occluded virus production phase, in which very high expression levels of polyhedrin are produced, which will then involve the newly formed baculoviruses and being responsible for their stability outside of the insect larvae. The p10 promoter drives the expression of the P10 protein, also expressed in very large amounts and required for the release of the occluded virus from the infected cell (Monteiro, 2015; van Oers et al., 2015). The finding that both p10 and polyhedrin promoters were very strong promoters but their wild-type genes are not required for recombinant baculovirus replication in infected cells is the main drive of the development of the IC-BEVS (van Oers et al., 2015).

4.3. Producing rAAV in the IC-BEVS

The first report of the IC-BEVS for rAAV production was published by Urabe group (Urabe et al., 2002). This first generation of the system was based in infection with three baculovirus: one baculovirus encoding the *rep* gene, another encoding the *cap* gene and the third baculovirus delivering the ITR-flanked transgene. The helper genes necessary for rAAV expression are provided by the baculovirus itself (Adamson-Small et al., 2017). This approach requires a cell to be simultaneously infected by the three baculovirus, which is only possible at high multiplicities of infection (MOIs).

The second significant improvement using this system was the reduction of the system to two baculovirus, by combining the *rep* and *cap* baculoviruses into one only (Smith et al., 2009). This not only increases the probability of one cell to be infected by all baculovirus, but is also advantageous since there is one less baculovirus stock to generate, amplify, store and titrate (reviewed in Zitzmann et al., 2017).

The necessity of co-infection of the same cell by both baculovirus has led to the development of strategies for system simplification by using one baculovirus only: one of the strategies is based on infection with a transgene-encoding baculovirus of Sf9 cells, which stably express the *rep* and *cap* genes. Because of Rep protein cytotoxicity, the authors developed a switch system and demonstrated the production of rAAV vectors with increased infectivity, although a separate cell line is needed to produce each rAAV serotype (Joshi et al., 2019; Mietzsch et al., 2015, 2014). The other approach relies on using a baculovirus vector which contains all the necessary genes for rAAV production: *rep*, *cap* and ITR-flanked gene of interest. The difficulty with this approach is to find unessential baculovirus genes and a third strong promoter, however the development of a single baculovirus system has been reported (Merten, 2016).

Given that baculovirus is a lytic virus, rAAV production halts due to the baculovirus-induced cell lysis, which also releases the produced rAAVs to the culture medium (Meghrouh et al., 2005). This lytic activity results in release of proteases into the culture supernatant, which can compromise rAAV quality, as introduced in Section 3.4.2.

4.4. IC-BEVS production issues and further improvements

The use of the IC-BEVS for recombinant protein expression always requires optimization of process conditions, such as the optimal cell concentration at infection (CCI), the MOI and the time of harvest (Lecina *et al.*, 2006; Roldão

et al., 2008; Palomares and Ramírez, 2009). All these process variables, together with the cell line and culture medium used can impact product yield (Druzinec *et al.*, 2013; Kwang *et al.*, 2016).

In particular for the CCI, the IC-BEVS shares with other viral-based systems the occurrence of the “cell density effect”, the drop in the cell specific productivity when cells are infected beyond a certain cell concentration (Bernal *et al.*, 2009; Merten, 2016). This effect is likely related with the exhaustion of media components, as demonstrated by Mena *et al*/ who used feeding strategies for infection at high cell densities (Mena *et al.*, 2010).

Regarding MOI, the number of baculovirus per cell added at infection, the main strategies used are infection at low (<0.1) or high (>3) MOI. A high MOI strategy is useful to infect the majority of the cell population (synchronous infection) and maximize the probability that every cell is infected by all baculoviruses for applications where more than one baculovirus is needed (Roldão *et al.*, 2007, 2008). However, this strategy induces cell growth arrest in the first 24 hpi (Palomares and Ramírez, 2009). The low MOI strategy relies on a first infection phase in which a small percentage of cells are infected. The remaining cells are infected in the following rounds of baculovirus replication. This strategy has the advantages of delaying the cell growth arrest phase, needing less amounts of viral stock and decrease the number of defective interfering baculoviruses produced (Palomares and Ramírez, 2009). Still, one more than one baculovirus is used for the production process, the low MOI strategy can result in asynchronous infection of cells by both baculoviruses and more process optimization variables to consider, such as the overall MOI and the MOI for each baculovirus (Aucoin *et al.*, 2006; Roldão *et al.*, 2008).

A rather interesting and scalable approach is the use of Baculovirus-Infected Insect Cells (BII-Cs) as the viral inoculum step. Briefly, insect cells are infected

with baculovirus and cryopreserved, resulting in a drastic reduction in the vector stock volume needed for infection even in the bioreactor scale (Cecchini et al., 2011; Wasilko et al., 2009).

The fact that baculovirus is a lytic virus is also seen as a disadvantage, since the recombinant protein production always reaches an end when the cell enters the apoptotic stage. As such, strategies to prolong the productive lifetime of infected cells have been developed, relying either on stable expression of proteins involved in apoptosis inhibition (Fath-goodin et al., 2009; Steele et al., 2017) optimization of the agitation and aeration rates of the culture (Cruz *et al.*, 1998) or by developing culture strategies to decrease the shear stress sensed by infected cells, such as hollow-fiber bioreactors (Weidner et al., 2017) or the use of the WAVE bioreactor system (Cecchini et al., 2011). Another alternative is to decouple protein production from the baculovirus replication, using baculovirus vectors unable to replicate in infected cells (Marek et al., 2017), efficiently eliminating a contaminating product and in theory redirecting more resources for recombinant protein production.

The most reported issues for rAAV manufacturing in the IC-BEVS are the altered capsid compositions and the low potency of the vectors obtained (Kondratov et al., 2017; Merten, 2016; Wang et al., 2011). However, recent improvements in the baculovirus and AAV vector design have addressed these issues using leaky ribosome scanning and attenuated Kozak sequences (Kondratov et al., 2017); modification of rep and cap sequences (Kohlbrenner et al., 2005); modifying the translation initiation sites for the VP proteins (Bosma et al., 2018) or by deletion of the baculovirus protease cathepsin (Galibert et al., 2018).

With regards to the optimal CCI, published reports of rAAV production in this system use mostly CCI = 1×10^6 cells/mL (Große et al., 2017; Liu et al., 2010;

Penaud-Budloo et al., 2017; Savy et al., 2017) or CCI = 2×10^6 cells/mL (Negrete et al., 2007; Negrete and Kotin, 2007; Potter et al., 2014; Urabe et al., 2002). Depending on the scale and specific application, both low (Große et al., 2017; Liu et al., 2010; Penaud-Budloo et al., 2017; Savy et al., 2017) and high (Meghrouh et al., 2005; Negrete et al., 2007; Negrete and Kotin, 2007; Potter et al., 2014) MOI strategies are reported for rAAV production.

5. Real-time monitoring of cell culture processes

5.1. Quality by design and process analytical technology

Quality by Design (QbD) is an initiative promoted by the pharmaceutical industry regulatory authorities, aiming to yield consistent product quality by switching the traditional product quality testing in the end of each batch into “building quality in the product, by design” (Rathore and Winkle, 2009; Carrondo *et al.*, 2012).

The Process Analytical Technology (PAT) (FDA, 2004) was launched in 2004 by the USA FDA, aiming at facilitating regulatory approval of new drugs. It provides a series of recommendations, which can be summarized into two common goals: to identify the product critical quality attributes (CQAs), and to de-risk the manufacturing process by increasing process understanding, providing quantitative measurements of how changing the process parameters affects the overall process. In particular, PAT highlights the need to identify the process parameters with a significant impact in the product CQAs, termed the critical process parameters (CPP). This knowledge should be used to find the acceptable CPP ranges and define the product Design Space, the proven range of parameter values yielding a product with the desired quality characteristics (FDA, 2004; ICH, 2009; Pais et al., 2014).

As such, the PAT and QbD initiatives are strictly interconnected: only by understanding the manufacturing process and determining the CPP setpoints and acceptable ranges for each of the different phases of the process a product with consistent quality can be obtained. However, deviations from the desired setpoints will occur, and to assure their detection and early correction, the FDA recommendation is to use real-time monitoring tools to monitor the identified CPPs and CQAs, together with the design of control strategies to keep the product from deviating from the acceptable quality profile (FDA, 2004; Pais et al., 2014).

In the following sections, an overview of the real-time monitoring tools commonly used for cell culture processes is provided, with more focus provided to the techniques employed in this thesis.

5.2. Real-time monitoring tools

5.2.1. The use of real-time monitoring tools for cell culture processes

Real-time monitoring tools for cell culture processes should, ideally, be non-invasive, non-destructive, and provide rapid and comprehensive information from the culture in real-time, as well as withstand the sterilization procedure and cellular activity and maintain stability and reliability between batches over long time periods (Carrondo et al., 2012; Glassey, 2013; Guerra et al., 2019; Rowland-Jones et al., 2017). Spectroscopic techniques possess the necessary characteristics mentioned above, and have thus been widely used for cell culture processes, with Raman (Rangan et al., 2018; Santos et al., 2018; Tulsyan et al., 2019; Webster et al., 2018), near infrared (NIR) (Mercier et al., 2016; Rowland-Jones et al., 2017; Wu et al., 2015), dielectric (Kroll et al., 2017; Mercier et al., 2016; Nikolay et al., 2018; Petiot et al., 2016) and fluorescence spectroscopy (Karakach et al., 2018; Schwab and Hesse, 2017) being the most widely used.

Some of these techniques, such as Raman, NIR and fluorescence, are able to track metabolite dynamics in the complex cell culture media of mammalian cells (reviewed in Abu-Absi *et al.*, 2014), providing real-time information simultaneously from different culture components. Dielectric spectroscopy on the other hand, relies on the detection of changes in cell physiology, providing information regarding the cell concentration and overall cell state (Negrete *et al.*, 2007; Petiot *et al.*, 2016; Zeiser *et al.*, 2000). The key features, limitations and selected applications of these techniques for cell culture monitoring are compiled in Table I.2.

A commonality present in real-time monitoring spectroscopic tools for cell culture is the large amount of data obtained due to the cell culture media complexity. Moreover, metabolite spectra in Raman and IR is spread over multiple peaks and bands, which may confound the results (Roberts *et al.*, 2018). As such, adequate pre-processing methods or data analysis techniques are necessary to analyze and model the data available from spectroscopic techniques. Indeed, data preparation is a step that should not be overlooked, with the possibility to “make or break” the success of a model development strategy (Bayer *et al.*, 2019; Glassey, 2013; Pais *et al.*, 2019). Common pre-processing steps are smoothing and baseline correction, particularly for spectroscopic data; and scaling and centering, applied before performing multivariate data analysis to account for only the time-course variation of the variable rather than the absolute value variations (Bayer *et al.*, 2019; Glassey, 2013).

When the variable of interest cannot be measured by the real-time monitoring tool but the probe measurements can be correlated with the variable of interest through chemometrics techniques, we are in the presence of a soft sensor (Kroll *et al.*, 2017; Luttmann *et al.*, 2012; Pais *et al.*, 2019; Zabadaj *et al.*, 2017). Soft sensors in cell culture processes rely on multivariate data analysis techniques for data reduction and elimination of noise in the original

dataset. The multivariate data analysis techniques most used for those purposes are partial least squares (PLS) and principal component analysis (PCA) (Glasse, 2013; Møller et al., 2005; Rathore et al., 2014). Both are projection-based techniques, in which the experimental data is decomposed into a new space using linear combinations of the input variables. These new vectors are the principal components (in the case of PCA) and the latent factors (for PLS).

While PCA is an unsupervised technique, in PLS the decomposition in latent factors maximizes the relationship between input variables and the variables to predict (Rathore et al., 2014; Teixeira et al., 2009). Even when relying in spectroscopic methods such as Raman or IR for metabolite detection, calibration models are needed to correlate the spectral signals to the analytical measurements, and these models are often based in multivariate data analysis (Tulsyan et al., 2019).

Without neglecting the usefulness of PCA and PLS for bioprocess monitoring, one cannot overlook the fact that these are based in linear regression, which limit their applicability for the non-linear nature of biological processes (Glasse, 2013). Recently, the advent of machine learning has also demonstrated its applicability for monitoring cell culture processes, as demonstrated by the use of artificial neural networks (Contreras-Gómez et al., 2017; Liu et al., 2017), support vector machines (Huang et al., 2019; Zavala-Ortiz et al., 2020), genetic algorithms (Pais et al., 2019; Sokolov et al., 2017) or decision-trees (Sawatzki et al., 2018), to name a few. Details on the mode of action of each of the multivariate data analysis and machine learning techniques mentioned is out of the scope of the present thesis, and the reader is referred to the available literature (Glasse, 2013) on the topic. In particular for an extensive review of the different types of artificial neural networks and deep learning and its application to genomics, the work of Eraslan is recommended (Eraslan et al., 2019).

Table I.2 – Overview of the most common spectroscopic techniques used for cell culture monitoring, the measurement principles and selected references of their use for cell culture processes. Adapted from (Lourenço et al., 2012; Moore et al., 2019; Pais et al., 2019; Ribeiro da Cunha et al., 2019; Wu et al., 2015). VCC - Viable cell concentration; mAb - monoclonal antibody.

Technique	Measurement principles	Key features	Current limitations	Measured metabolites and process variables	Selected references
Fluorescence Spectroscopy	Fluorescence	Detection of intracellular fluorophores; Very low detection limit (<0.1 ppm) and high selectivity. Suitable for aqueous media	Applicable only to fluorescent metabolites; Temperature sensitive; Sensitive to sample turbidity	Vitamins, co-factors and fluorescent amino acids	(Bayer et al., 2019; Hakemeyer et al., 2013; Karakach et al., 2018; Ohadi et al., 2015, 2014; Pais et al., 2019; Schwab et al., 2016; Schwab and Hesse, 2017; Teixeira et al., 2011a, 2009; Zabadaj et al., 2017)
Raman Spectroscopy	Vibrational (Raman scattering)	Rapid spectra acquisition. Robust to sample turbidity and aqueous media	Temperature-sensitive; Overlapping of fluorescent signals. Limit of detection (25-150 ppm)	Glucose, glutamine, amino acids, lactate, ammonia, glutamate; mAb titer, VCC.	(Abu-Absi et al., 2011; Berry et al., 2016; Matthews et al., 2016; Rangan et al., 2018; Santos et al., 2018; Whelan et al., 2012)
Infrared Spectroscopy (NIR, MIR, FTIR)	Vibrational (infrared absorption)	High selectivity (FTIR). Rapid measurements (NIR) Optical density probes (NIR)	Poor selectivity using NIR; Strong signal from water absorption (NIR). Temperature sensitive	Glucose, glutamine, amino acids, lactate, ammonia, glutamate; mAb glycosylation	(Clavaud et al., 2013; Hakemeyer et al., 2013; Ribeiro da Cunha et al., 2019; Sandor et al., 2013; Wu et al., 2015; Zavala-Ortiz et al., 2020, 2019)
Dielectric spectroscopy	Dielectric potential of cells in an alternating electrical field	Continuous monitoring; very sensitive for cell culture monitoring	Only able to measure cell-related features	Viable cell concentration; Cell biovolume.	(Ansoerge et al., 2011, 2007; Negrete and Kotin, 2007; Petiot et al., 2016)

All the above-mentioned techniques are the so-called data-driven techniques. However, bioprocess models are increasingly becoming hybrid-models, combining the “black box” approach of multivariate data analysis with first-principles modeling and bioprocess data to increase model predictive power (Bayer et al., 2019; Glassey, 2013; Guerra et al., 2019; Konakovsky et al., 2017; von Stosch et al., 2016).

A label-free alternative to spectroscopic techniques is imaging-based cell culture monitoring, in which the cell itself is measured (Joeris, 2002; Kasprovicz, 2017; reviewed in Höpfner, 2010). Notably examples include the use of Digital Holographic Microscopy (DHM) (Janicke et al., 2017; Kamlund, 2018; Ugele et al., 2018) and Raman microscopy, a combination of Raman spectroscopy, microscopy and multivariate data analysis (applications for cell culture reviewed in Kann et al., 2015).

5.2.2. Real-time monitoring in the IC-BEVS

The already presented characteristics of the IC-BEVS render it inherently amenable to be monitored using real-time monitoring tools. The majority of the literature report on the use of dielectric spectroscopy, which can be used not only for determination of the cell concentration (Zitzmann et al., 2018), but also for monitoring the progress of baculovirus infection (Ansorge et al., 2007; Negrete et al., 2007; Petiot et al., 2016; Zeiser et al., 2000, 1999). NIR has also been used, in particular for measuring glucose, glutamine and lactate concentrations or cell concentration based in the light scattering properties of suspension cells (Qiu et al., 2014; Riley et al., 1997; Zitzmann et al., 2018). Because of the characteristic baculovirus-induced diameter increase, some authors report the use of imaging microscopy for monitoring the progress of baculovirus infection in insect cells (Janakiraman et al., 2006; Laasfeld et al., 2017; Palomares et al., 2001).

5.3. Fluorescence spectroscopy, digital holographic imaging and dielectric spectroscopy

Being the techniques explored in this thesis, in the following sections we provide a more detailed explanation of the working principles of fluorescence spectroscopy, digital holographic imaging and dielectric spectroscopy, as well as selected references of its application for cell culture processes.

5.3.1. Fluorescence spectroscopy

Molecules have various states referred to as energy levels. Fluorescence spectroscopy is primarily concerned with electronic and vibrational states. Generally, the species being examined has a ground electronic state and an excited electronic state of higher energy. Within each of these electronic states there are various vibrational states. Fluorescence spectroscopy is based on the excitation of the species from its ground electronic state to one of the various vibrational states in the excited electronic state. Collisions with other molecules cause the excited molecule to lose vibrational energy until it reaches the lowest vibrational state of the excited electronic state (Figure I.5). When the molecule returns to the ground energy state, it releases energy in the form of light, which is less energetic than the excitation radiation due to the energy loss in the form of vibrational energy during collision with the other molecules. Fluorescence spectroscopy relies on the detection of these changes when both the excitation and emission light belong to the visible spectrum.

Fluorescence spectroscopy has great sensitivity when compared with other vibrational-based spectroscopies. Besides, each excitation emission region in the spectra is associated with very few fluorescent compounds, unlike Raman, NIR or MIR, in which the metabolite spectra is contained over a wide range of frequencies. However, this spectroscopy is only suitable for detection of fluorescence molecules, such as some amino acids, vitamins and

co-factors present inside and outside the cells (Ohadi et al., 2014; Schwab et al., 2016; Teixeira et al., 2011a, 2009; Wolf et al., 2001).

Fluorescence spectroscopy has been extensively used for monitoring water quality (reviewed in Carstea et al., 2016), and demonstrated to be a suitable tool for bioprocessing monitoring in bacteria (Bayer et al., 2019; Schwab et al., 2016), yeast (Karakach et al., 2018; Zabadaj et al., 2017) and mammalian cells (Ohadi et al., 2015; Ohadi, 2014; Teixeira et al., 2011b, 2009), including its use for monitoring critical quality attributes such as monoclonal antibody aggregation (Schwab & Hesse, 2017).

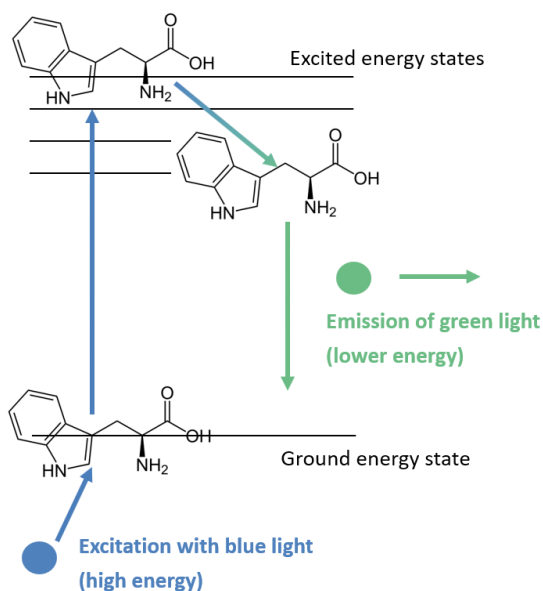


Figure I.5 – Jablonski diagram for tryptophan, exemplifying the fluorescence spectroscopy principle.

Application of fluorescence spectroscopy to cell culture processes relies mostly in two measuring modes: Two-dimensional (2D) fluorescence and synchronous fluorescence.

A 2D fluorescence map is obtained by setting the excitation wavelength and recording the fluorescence emission over the emission range. After obtaining the fluorescence intensity values for all the excitation-emission pairs for the fixed excitation wavelength, the next excitation wavelength is fixed and the whole emission spectra recorded. This process is repeated until the whole range of excitation-emission pairs is tested. This strategy yields very comprehensive datasets, at the cost of a lengthier spectra acquisition process and the need for spectra pre-processing to account of spectral overlap of different fluorescent species (Teixeira et al., 2009).

Synchronous fluorescence is a more rapid acquisition mode, corresponding to a diagonal line in a 2D fluorescence map. In synchronous fluorescence, the difference between the emission and excitation wavelength is kept constant during the whole spectral acquisition, but both the excitation and emission wavelengths are changed simultaneously, resulting in a convolution of the excitation and emission spectra (Kaminski and Purcell, 1982). Besides the more rapid spectral acquisition, the obtained spectra are simpler and with improved peak resolution (Teixeira et al., 2011a). The choice of the offset to apply during spectra acquisition needs to be properly selected to maximize the obtained information using this technique.

5.3.2. *In situ* microscopy and holographic imaging

Microscopy was the first technique developed to observe cells (XVI century). Nowadays, real-time information regarding cell concentration and morphology can be obtained using *in situ* microscopy. This technique combines real-time imaging using a CCD camera immersed in the cell culture medium with image analysis algorithms (Druzinec et al., 2013). The working principle of *in situ* microscopes is either based in detection of backscattering or transmission light. Available commercial systems rely on both methods (Zitzmann et al., 2017) and have been applied for microcarrier-based or

suspension mammalian cell culture (Guez et al., 2004; Höpfner et al., 2010; Rudolph et al., 2008).

A recent image-based technology for cell culture monitoring is quantitative phase imaging (QPI), which has been applied for detecting biological phases based on cell imaging measurements (Kasprowicz et al., 2017; Ugele et al., 2018). QPI is based on quantification of the phase shift of the light after it has passed through the object of focus, such as cells (Kamlund, 2018; Mann et al., 2005). In digital holographic imaging (DHM), this light phase difference is encoded in a hologram which is used to construct high resolution intensity and quantitative phase images of the cell. The way that the light phase changes after interacting with the cells depends on cell factors such as thickness, circularity or intracellular composition (Kasprowicz et al., 2017; Kemper et al., 2010; Mann et al., 2005; Rapoport et al., 2011). As such, DHM can be used to extract important information from the cell state, and has proven useful for several cell-based applications: identification of morphological parameters distinguishing between epithelial and mesenchymal cells (Kamlund, 2018), detecting cell division in endothelial cells (Kemper et al., 2010) and developing cell proliferation (Janicke et al., 2017) or cytotoxic assays (Kühn et al., 2013).

5.3.3. Dielectric spectroscopy

When an electric field is applied to viable cells, those behave like small capacitors and polarize with a frequency-dependent response. This is due to the dielectric properties of the lipid based-cell membrane and the presence of conductive solutes in the extracellular medium and in the cytoplasm (Druzinec et al., 2013). This charge can be detected and quantified, being reported as permittivity (capacitance per membrane area). This property is the working principle behind dielectric spectroscopy, rendering it a very useful technique for measuring viable cell concentration, as demonstrated for bacteria, yeast, plant, insect and mammalian cells (Ansorge et al., 2007;

Grein et al., 2018; Kroll et al., 2017; Liu et al., 2016; Negrete et al., 2007; Nikolay et al., 2018; Opel et al., 2010; Petiot et al., 2016; Zeiser et al., 2000, 1999; reviewed in Justice et al., 2011) and also for monitoring multicellular spheroids (reviewed in Alexander et al., 2013).

The ability of the cell to store charge and polarize is influenced by the frequency of the applied electrical field. In other words, low frequencies will result in the cell being able to fully polarize, while at very high frequencies the applied electric field switches too fast for the cell to be able to polarize. Plotting the permittivity of the culture over a range of applied electrical field frequencies yields the beta-dispersion curve (Figure I.6), which provides information regarding the cell characteristics. For instance, the beta-dispersion curve profile changes depending on the cell concentration, culture biovolume and cell shape and size distribution (Ansorge et al., 2007; Dabros et al., 2009; Petiot et al., 2016).

Consequently, insights on the overall cell physiological state can be obtained by measuring the dielectric properties of the cell. As such, some authors have studied the progress of virus infection using dielectric spectroscopy for several recombinant vectors and host cells: baculovirus infection in insect cells (Ansorge et al., 2007; Petiot et al., 2016), VERO cells infected with rabies virus (Rourou et al., 2010) and lentiviral and influenza vector production in HEK293 cells (Ansorge et al., 2011; Petiot and Kamen, 2012).

For a more in-depth study of the theory behind dielectric spectroscopy and its application to cell culture the works of Zitzmann and Dabros are recommended (Dabros et al., 2009; Zitzmann et al., 2017).

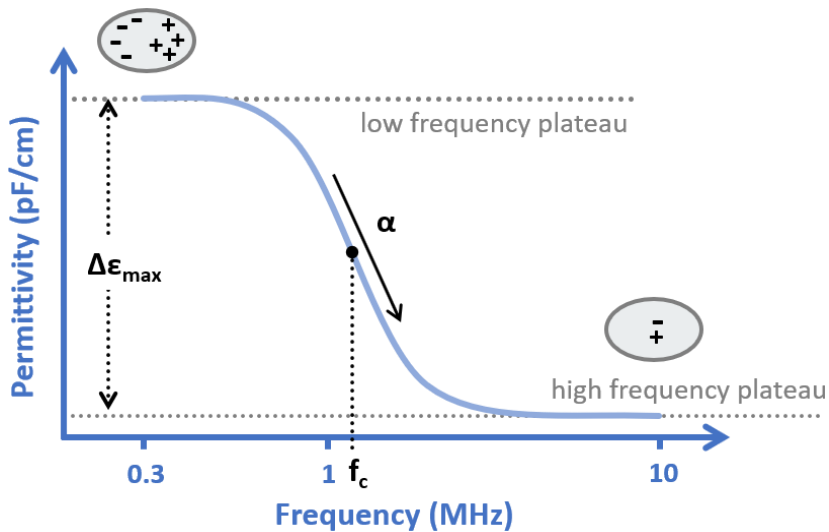


Figure I.6 – Representative diagram of the beta-dispersion curve. The curve can be defined by four parameters: the low and high frequency plateau represent the limit of the capacity of the cell to store electrical charges at low and high frequencies, respectively; the inflexion point of the curve is represented by the characteristic frequency, f_c ; and α quantifies the rate of decrease of the permittivity measurement with increasing frequencies. The difference between the high and low frequency plateaus is often referred to as $\Delta\epsilon_{\max}$.

6. Thesis scope and outline

The overarching purpose of this PhD is the implementation of real-time monitoring tools for rAAV production in IC-BEVS, for real-time determination of critical process variables. Specifically, the focus is to monitor cell concentration, viability and rAAV production. Cell concentration and viability are two of the most significant process variables in this system, important for timing the infection and harvest steps and to follow the overall culture progress. Monitoring in real-time rAAV production kinetics is of special interest for the pharmaceutical manufacturing industry, allowing to identify non-compliant batches during production and increasing process understanding.

The work of this thesis is divided in four parts: **Chapters II to IV** explore the application of three real-time monitoring tools to monitor rAAV production in the insect cell system. **Chapter II** uses fluorescence spectroscopy as a soft sensor to detect rAAV-induced metabolic dynamics in insect cells; the study is complemented with an analysis of the influence of different pre-processing methods for culture predictions. **Chapter III** assesses the suitability of digital holographic imaging for monitoring this system, exploiting the ability of this technology to detect intracellular dynamics in the monitored cells to detect possible rAAV-related variables. In **Chapter IV**, dielectric spectroscopy-based models are developed for monitoring and predicting not only cell concentration and viability profiles, but also intracellular rAAV production kinetics. The tools developed in these chapters generate predictive models for the measured critical process variables, based on the real-time monitoring probe outputs. These models allow to fulfill the final aim of real-time monitoring: to control the process, by acting on the identified critical variables in order to maintain them in the desired setpoint. **Chapter V**, the last part of the thesis, contains an update on the existing control strategies for biological processes.

In light of the previous chapters, **Chapter VI** presents a discussion on how each one of the explored techniques can contribute, by itself or combined with other real-time monitoring tools, to monitor rAAV quality characteristics and address the existing challenges for the field.

Overall, this thesis contributes to increase the knowledge of rAAV production in the insect cell baculovirus system, while simultaneously exploring the application of different real-time monitoring tools to monitor viral production in infected cells. Hopefully, these strategies can be applicable not only to other rAAV serotypes, but for other viral vector manufacturing processes, contributing towards a process analytical technology (PAT) implementation for the gene therapy field.

7. References

- Abu-Absi, N.R., Kenty, B.M., Cuellar, M.E., Borys, M.C., Sakhamuri, S., Strachan, D.J., Hausladen, M.C., Li, Z.J., 2011. Real time monitoring of multiple parameters in mammalian cell culture bioreactors using an in-line Raman spectroscopy probe. *Biotechnol. Bioeng.* 108, 1215–21. <https://doi.org/10.1002/bit.23023>
- Abu-Absi, N.R., Martel, R.P., Lanza, A.M., Clements, S.J., Borys, M.C., Li, Z.J., 2014. Application of spectroscopic methods for monitoring of bioprocesses and the implications for the manufacture of biologics. *Pharm. Bioprocess.* 2, 267–284. <https://doi.org/10.4155/pbp.14.24>
- Adamson-Small, L., Potter, M., Byrne, B.J., Clement, N., 2017. Sodium chloride enhances rAAV production in a serum-free suspension manufacturing platform using the Herpes Simplex Virus System. *Hum. Gene Ther. Methods* hgtb.2016.151. <https://doi.org/10.1089/hgtb.2016.151>
- Adamson-Small, L., Potter, M., Falk, D.J., Cleaver, B., Byrne, B.J., Clément, N., 2016. A scalable method for the production of high-titer and high-quality adeno-associated type 9 vectors using the HSV platform. *Mol. Ther. - Methods Clin. Dev.* 3, 16031. <https://doi.org/10.1038/mtm.2016.31>
- Alexander, F.A., Price, D.T., Bhansali, S., 2013. From cellular cultures to cellular spheroids: Is impedance spectroscopy a viable tool for monitoring multicellular spheroid (MCS) drug models? *IEEE Rev. Biomed. Eng.* 6, 63–76. <https://doi.org/10.1109/RBME.2012.2222023>
- Anson, S., Esteban, G., Schmid, G., 2007. On-line monitoring of infected Sf-9 insect cell cultures by scanning permittivity measurements and comparison with off-line biovolume measurements. *Cytotechnology* 55, 115–24. <https://doi.org/10.1007/s10616-007-9093-0>
- Anson, S., Lanthier, S., Transfiguracion, J., Henry, O., Kamen, A., 2011. Monitoring lentiviral vector production kinetics using online permittivity measurements. *Biochem. Eng. J.* 54, 16–25. <https://doi.org/10.1016/j.bej.2011.01.002>
- Aponte-Ubillus, J.J., Barajas, D., Peltier, J., Bardliving, C., Shamlou, P., Gold, D., 2018. A rAAV2-producing yeast screening model to identify host proteins enhancing rAAV DNA replication and vector yield. *Biotechnol. Prog.* 1–10. <https://doi.org/10.1002/btpr.2725>
- Aponte-ubillus, J.J., Barajas, D., Peltier, J., Bardliving, C., Shamlou, P., Gold, D., Aponte-ubillus, J.J., 2017. Molecular design for recombinant adeno-associated virus (rAAV) vector production. <https://doi.org/10.1007/s00253-017-8670-1>
- Asad, A.S., Moreno Ayala, M.A., Gottardo, M.F., Zuccato, C., Nicola Candia, A.J., Zanetti, F.A., Seilicovich, A., Candolfi, M., 2017. Viral gene therapy for breast cancer: progress and challenges. *Expert Opin. Biol. Ther.* 00, 1–15. <https://doi.org/10.1080/14712598.2017.1338684>
- Aucoin, M.G., Perrier, M., Kamen, A.A., 2007. Improving AAV vector yield in insect cells by modulating the temperature after infection. *Biotechnol. Bioeng.* 97, 1501–1509. <https://doi.org/10.1002/bit.21364>
- Aucoin, M.G., Perrier, M., Kamen, A.A., 2006. Production of Adeno-Associated Viral Vectors in Insect Cells Using Triple Infection: Optimization of Baculovirus Concentration Ratios. *Biotechnol. Bioeng.* 95, 1081–1092. <https://doi.org/10.1002/bit.21069>
- Ayuso, E., Blouin, V., Lock, M., McGorray, S., Leon, X., Alvira, M.R., Auricchio, A., Bucher, S., Chtarto, A., Clark, K.R., Darmon, C., Doria, M., Fountain, W., Gao, G., Gao, K., Giacca, M., Kleinschmidt, J., Leuchs, B., Melas, C., Mizukami, H., Müller, M., Noordman, Y., Bockstael, O., Ozawa, K., Pythoud, C., Sumaroka, M., Surosky, R., Tenenbaum, L., van der Linden, I., Weins, B., Wright, J.F., Zhang, X., Zentilin, L., Bosch, F., Snyder, R.O., Moullier, P., 2014. Manufacturing and characterization of a recombinant adeno-associated virus type 8 reference standard material. *Hum. Gene Ther.* 25, 977–87. <https://doi.org/10.1089/hum.2014.057>
- Barajas, D., Aponte-Ubillus, J.J., Akeefe, H., Cinek, T., Peltier, J., Gold, D., 2017. Generation of infectious recombinant Adeno-associated virus in *Saccharomyces cerevisiae*. *PLoS One* 12, e0173010. <https://doi.org/10.1371/journal.pone.0173010>
- Bayer, B., von Stosch, M., Melcher, M., Duerkop, M., Striedner, G., 2019. Soft sensor based on 2D-fluorescence and process data enabling real-time estimation of biomass in *Escherichia coli* cultivations. *Eng. Life Sci.*

- <https://doi.org/10.1002/elsc.201900076>
- Benskey, M., Sandoval, I., Manfredsson, F.P., 2016. Continuous Collection of AAV from Producer Cell Media Significantly Increases Total Viral Yield. *Hum. Gene Ther. Methods* 1–37.
- Bera, A., Sen, D., 2017. Promise of adeno-associated virus as a gene therapy vector for cardiovascular diseases. *Heart Fail. Rev.* 1–29. <https://doi.org/10.1007/s10741-017-9622-7>
- Bernal, V., Carinhas, N., Yokomizo, A.Y., Carrondo, M.J.T., Alves, P.M., 2009. Cell density effect in the baculovirus-insect cells system: A quantitative analysis of energetic metabolism. *Biotechnol. Bioeng.* 104, 162–180. <https://doi.org/10.1002/bit.22364>
- Berry, B.N., Dobrowsky, T.M., Timson, R.C., Kshirsagar, R., Ryll, T., Wiltberger, K., 2016. Quick generation of Raman spectroscopy based in-process glucose control to influence biopharmaceutical protein product quality during mammalian cell culture. *Biotechnol. Prog.* 32, 224–234. <https://doi.org/10.1002/btpr.2205>
- Berry, G., Asokan, A., 2017. Cellular transduction mechanisms of adeno-associated viral vectors 54–60. <https://doi.org/10.1016/j.coviro.2016.08.001>
- Blessing, D., Vachey, G., Pythoud, C., Rey, M., Padrun, V., Wurm, F.M., Schneider, B.L., Déglon, N., 2019. Scalable Production of AAV Vectors in Orbitally Shaken HEK293 Cells. *Mol. Ther. - Methods Clin. Dev.* 13, 14–26. <https://doi.org/10.1016/j.omtm.2018.11.004>
- Bosma, B., du Plessis, F., Ehlert, E., Nijmeijer, B., de Haan, M., Petry, H., Lubelski, J., 2018. Optimization of viral protein ratios for production of rAAV serotype 5 in the baculovirus system. *Gene Ther.* 25, 415–424. <https://doi.org/10.1038/s41434-018-0034-7>
- Brown, N., Song, L., Kollu, N.R., Hirsch, M., 2017. AAV Vectors and Stem Cells – Friends or Foes? *Hum. Gene Ther.* 27517, hum.2017.038. <https://doi.org/10.1089/hum.2017.038>
- Carrondo, M.J.T., Alves, P.M., Carinhas, N., Glassey, J., Hesse, F., Merten, O.-W., Micheletti, M., Noll, T., Oliveira, R., Reichl, U., Staby, A., Teixeira, A.P., Weichert, H., Mandenius, C.-F., 2012. How can measurement, monitoring, modeling and control advance cell culture in industrial biotechnology? *Biotechnol. J.* 7, 1522–9. <https://doi.org/10.1002/biot.201200226>
- Carstea, E.M., Bridgeman, J., Baker, A., Reynolds, D.M., 2016. Fluorescence spectroscopy for wastewater monitoring: A review. *Water Res.* 95, 205–219. <https://doi.org/10.1016/j.watres.2016.03.021>
- Cecchini, S., Negrete, a, Kotin, R.M., 2008. Toward exascale production of recombinant adeno-associated virus for gene transfer applications. *Gene Ther.* 15, 823–830. <https://doi.org/10.1038/gt.2008.61>
- Cecchini, S., Virag, T., Kotin, R.M., 2011. Reproducible high yields of recombinant adeno-associated virus produced using invertebrate cells in 0.02- to 200-liter cultures. *Hum. Gene Ther.* 22, 1021–1030. <https://doi.org/10.1089/hum.2010.250>
- Cevtec Pharmaceuticals, 2019. Transient AAV production [WWW Document]. URL <https://cevec.com/technology/cap-gt-examples/#stable-aaav> (accessed 20.01.20).
- Chahal, P.S., Schulze, E., Tran, R., Montes, J., Kamen, A.A., 2014. Production of adeno-associated virus (AAV) serotypes by transient transfection of HEK293 cell suspension cultures for gene delivery. *J. Virol. Methods* 196, 163–173. <https://doi.org/10.1016/j.jviromet.2013.10.038>
- Chamberlain, K., Riyad, J.M., Weber, T., 2016. Expressing Transgenes That Exceed the Packaging Capacity of Adeno-Associated Virus Capsids. *Hum. Gene Ther. Methods* 27, 1–12. <https://doi.org/10.1089/hgtb.2015.140>
- Chen, K.G., Mallon, B.S., McKay, R.D.G., Robey, P.G., 2014. Cell Stem Cell Human Pluripotent Stem Cell Culture: Considerations for Maintenance, Expansion, and Therapeutics. *Stem Cell* 14, 13–26. <https://doi.org/10.1016/j.stem.2013.12.005>
- Clavaud, M., Roggo, Y., Von Daeniken, R., Liebler, A., Schwabe, J.-O., 2013. Chemometrics and in-line near infrared spectroscopic monitoring of a biopharmaceutical Chinese hamster ovary cell culture: prediction of multiple cultivation variables. *Talanta* 111, 28–38. <https://doi.org/10.1016/j.talanta.2013.03.044>
- Clement, N., 2016. AAV vector and gene therapy: en route for the American dream? *Cell Gene Ther. Insights* 2, 513–519. <https://doi.org/10.18609/cgti.2016.066>

- Clément, N., 2019. Large-Scale Clinical Manufacturing of AAV Vectors for Systemic Muscle Gene Therapy. *Muscle Gene Ther.* 253–273. https://doi.org/10.1007/978-3-030-03095-7_15
- Clément, N., Grieger, J.C., 2016. Manufacturing of recombinant adeno-associated viral vectors for clinical trials. *Mol. Ther. — Methods Clin. Dev.* 3, 16002. <https://doi.org/10.1038/mtm.2016.2>
- Clément, N., Knop, D.R., Byrne, B.J., 2009. Large-Scale Adeno-Associated Viral Vector Production Using a Herpesvirus-Based System Enables Manufacturing for Clinical Studies. *Hum. Gene Ther.* 20, 796–806. <https://doi.org/10.1089/hum.2009.094>
- Colella, P., Ronzitti, G., Mingozzi, F., 2018. Emerging Issues in AAV-Mediated In Vivo Gene Therapy. *Mol. Ther. - Methods Clin. Dev.* 8, 87–104. <https://doi.org/10.1016/j.omtm.2017.11.007>
- Contreras-Gómez, A., Beas-Catena, A., Sánchez-Mirón, A., García-Camacho, F., Molina Grima, E., 2017. The use of an artificial neural network to model the infection strategy for baculovirus production in suspended insect cell cultures. *Cytotechnology* 70, 555–565. <https://doi.org/10.1007/s10616-017-0128-x>
- Cox, M.M.J., 2012. Recombinant protein vaccines produced in insect cells. *Vaccine* 30, 1759–1766. <https://doi.org/10.1016/j.vaccine.2012.01.016>
- Cruz, P.E., Cunha, A., Peixoto, C.C., Clemente, J., Moreira, J.L., Carrondo, M.J.T., 1998. Optimization of the production of virus-like particles in insect cells. *Biotechnol. Bioeng.* 60, 408–418. [https://doi.org/10.1002/\(SICI\)1097-0290\(19981120\)60:4<408::AID-BIT2>3.0.CO;2-Q](https://doi.org/10.1002/(SICI)1097-0290(19981120)60:4<408::AID-BIT2>3.0.CO;2-Q)
- Cucchiari, M., 2016. Human gene therapy: novel approaches to improve the current gene delivery systems. *Discov Med* 21, 495–506.
- Dabros, M., Dennewald, D., Currie, D.J., Lee, M.H., Todd, R.W., Marison, I.W., Von Stockar, U., 2009. Cole-Cole, linear and multivariate modeling of capacitance data for on-line monitoring of biomass. *Bioprocess Biosyst. Eng.* 32, 161–173. <https://doi.org/10.1007/s00449-008-0234-4>
- Drugmand, J.C., Schneider, Y.J., Agathos, S.N., 2012. Insect cells as factories for biomanufacturing. *Biotechnol. Adv.* 30, 1140–1157. <https://doi.org/10.1016/j.biotechadv.2011.09.014>
- Druzinec, D., Salzig, D., Brix, A., Kraume, M., Vilcinskas, A., Kollwe, C., Czermak, P., 2013. Optimization of Insect Cell Based Protein Production Processes - Online Monitoring, Expression Systems, Scale Up. *Adv. Biochem. Eng. Biotechnol.* 136, 65–100. https://doi.org/10.1007/10_2013_205
- Dubielzig, R., King, J.A., Weger, S., Kern, A., Kleinschmidt, J.A., 1999. Adeno-associated virus type 2 protein interactions: formation of pre-encapsidation complexes. *J Virol* 73, 8989–8998.
- Eraslan, G., Avsec, Ž., Gagneur, J., Theis, F.J., 2019. Deep learning: new computational modelling techniques for genomics. *Nat. Rev. Genet.* 20. <https://doi.org/10.1038/s41576-019-0122-6>
- Fath-goodin, A., Kroemer, J., Webb, B.A., 2009. The Campoletis sonorensis ichnovirus vankyrin protein P-vank-1 inhibits apoptosis in insect Sf9 cells 18, 497–506. <https://doi.org/10.1111/j.1365-2583.2009.00892.x>
- FDA, U.S.D. of H. and H.S., 2004. Guidance for Industry PAT — A Framework for Innovative Pharmaceutical Development, Manufacturing, and Quality Assurance. FDA Off. Doc. 16. <https://doi.org/http://www.fda.gov/CDER/guidance/6419fnl.pdf>
- Ferrelli, M.L., Berretta, M.F., Belaich, M.N., Ghiringhelli, P.D., Sciocco-cap, A., Romanowski, V., 2010. The Baculoviral Genome. *Viral Genomes – Mol. Struct. Divers. Gene Expr. Mech. Host-Virus Interact.* 1–31.
- Florencio, G.D., Precigout, G., Beley, C., Buclez, P.-O., Garcia, L., Benchaouir, R., 2015. Simple downstream process based on detergent treatment improves yield and in vivo transduction efficacy of adeno-associated virus vectors. *Mol. Ther. - Methods Clin. Dev.* 2. <https://doi.org/10.1038/mtm.2015.24>
- Galibert, L., Merten, O.-W., 2011. Latest developments in the large-scale production of adeno-associated virus vectors in insect cells toward the treatment of neuromuscular diseases. *J. Invertebr. Pathol.* 107 Suppl, S80–S93. <https://doi.org/10.1016/j.jip.2011.05.008>
- Galibert, L., Savy, A., Dickx, Y., Bonnin, D., Bertin, B., Mushimiyimana, I., van Oers, M.M., Merten, O.W., 2018. Origins of truncated supplementary capsid proteins in rAAV8 vectors produced with the baculovirus system. *PLoS One*

- 13, 1–20. <https://doi.org/10.1371/journal.pone.0207414>
- Glasse, J., 2013. Multivariate Data Analysis for Advancing the Interpretation of Bioprocess Measurement and Monitoring Data, in: *Adv Biochem Eng Biotechnol* Vol. 132. pp. 167–191. https://doi.org/10.1007/10_2012_171
- Goswami, R., Subramanian, G., Silayeva, L., Newkirk, I., Doctor, D., Chawla, K., Chattopadhyay, S., Chandra, D., Chilukuri, N., Betapudi, V., 2019. Gene Therapy Leaves a Vicious Cycle. *Front. Oncol.* 9, 1–25. <https://doi.org/10.3389/fonc.2019.00297>
- Grein, T.A., Loewe, D., Dieken, H., Salzig, D., Weidner, T., Czermak, P., 2018. High titer oncolytic measles virus production process by integration of dielectric spectroscopy as online monitoring system. *Biotechnol. Bioeng.* 115, 1186–1194. <https://doi.org/10.1002/bit.26538>
- Grieger, J.C., Samulski, R.J., 2005. Packaging Capacity of Adeno-Associated Virus Serotypes: Impact of Larger Genomes on Infectivity and Postentry Steps. *J. Virol.* 79, 9933–9944. <https://doi.org/10.1128/JVI.79.15.9933-9944.2005>
- Grieger, J.C., Soltys, S.M., Samulski, R.J., 2016. Production of Recombinant Adeno-associated Virus Vectors Using Suspension HEK293 Cells and Continuous Harvest of Vector From the Culture Media for GMP FIX and FLT1 Clinical Vector. *Mol. Ther.* 24, 287–97. <https://doi.org/10.1038/mt.2015.187>
- Große, S., Penaud-Budloo, M., Herrmann, A.-K., Börner, K., Fakhiri, J., Laketa, V., Krämer, C., Wiedtke, E., Gunkel, M., Ménard, L., Ayuso, E., Grimm, D., 2017. Relevance of assembly-activating protein for Adeno-associated virus vector production and capsid protein stability in mammalian and insect cells. *J. Virol.* <https://doi.org/10.1128/JVI.01198-17>
- Guenther, C.M., Brun, M.J., Bennett, A.D., Ho, M.L., Chen, W., Zhu, B., Lam, M., Yamagami, M., Kwon, S., Bhattacharya, N., Sousa, D., Evans, A.C., Voss, J., Sevick-Muraca, E.M., Agbandje-McKenna, M., Suh, J., 2019. Protease-Activatable Adeno-Associated Virus Vector for Gene Delivery to Damaged Heart Tissue. *Mol. Ther.* 27, 611–622. <https://doi.org/10.1016/j.ymthe.2019.01.015>
- Guerra, A., von Stosch, M., Glasse, J., 2019. Toward biotherapeutic product real-time quality monitoring. *Crit. Rev. Biotechnol.* 39, 289–305. <https://doi.org/10.1080/07388551.2018.1524362>
- Guez, J.S., Cassar, J.P., Wartelle, F., Dhulster, P., Suhr, H., 2004. Real time in situ microscopy for animal cell-concentration monitoring during high density culture in bioreactor. *J. Biotechnol.* 111, 335–343. <https://doi.org/10.1016/j.jbiotec.2004.04.028>
- György, B., Maguire, C.A., 2017. Extracellular vesicles: nature's nanoparticles for improving gene transfer with adeno-associated virus vectors. *Wiley Interdiscip. Rev. Nanomedicine Nanobiotechnology* e1488. <https://doi.org/10.1002/wnan.1488>
- Hakemeyer, C., Strauss, U., Werz, S., Folque, F., Menezes, J.C., 2013. Near-infrared and two-dimensional fluorescence spectroscopy monitoring of monoclonal antibody fermentation media quality: aged media decreases cell growth. *Biotechnol. J.* 8, 835–46. <https://doi.org/10.1002/biot.201200355>
- Kerstin Hein, Silke Wissing, Nina Riebesehl, Nikola Stempel, Nicole Faust, and Martina Graßl, "Generation of helper virus-free adeno-associated viral vector packaging/producer cell lines based on a human suspension cell line" in "Cell Culture Engineering XVI", A. Robinson, PhD, Tulane University R. Venkat, PhD, MedImmune E. Schaefer, ScD, J&J Janssen Eds, ECI Symposium Series, (2018). <https://dc.engconfintl.org/ccexvi/66>
- Hentzschel, F., Herrmann, A.-K., Mueller, A.-K., Grimm, D., 2016. Plasmodium meets AAV - the (un)likely marriage of parasitology and virology, and how to make the match. *FEBS Lett.* 1–19. <https://doi.org/10.1002/1873-3468.12187>
- Höpfner, T., Bluma, A., Rudolph, G., Lindner, P., Scheper, T., 2010. A review of non-invasive optical-based image analysis systems for continuous bioprocess monitoring. *Bioprocess Biosyst. Eng.* 33, 247–256. <https://doi.org/10.1007/s00449-009-0319-8>
- Hopkins, R.F., Esposito, D., 2009. A rapid method for titrating baculovirus stocks using the Sf-9 Easy Titer cell line. *Biotechniques*. <https://doi.org/10.2144/000113238>
- Huang, Y., Zang, H., Cheng, X., Wu, H., Li, J., 2019. Data-driven soft sensor for animal cell suspension culture process

- based on DRVM. *Appl. Soft Comput.* 77, 34–40. <https://doi.org/10.1016/j.asoc.2018.09.043>
- Hudry, E., Vandenberghe, L.H., 2019. Therapeutic AAV Gene Transfer to the Nervous System: A Clinical Reality. *Neuron* 101, 839–862. <https://doi.org/10.1016/j.neuron.2019.02.017>
- ICH, 2009. ICH Harmonised tripartite guideline Pharmaceutical Development Q8 (R2), International Conference on Harmonisation of Technical Requirements for Registration of Pharmaceuticals for Human Use [WWW Document].
- Janakiraman, V., Forrest, W.F., Chow, B., Seshagiri, S., 2006. A rapid method for estimation of baculovirus titer based on viable cell size. *J. Virol. Methods* 132, 48–58. <https://doi.org/10.1016/j.jviromet.2005.08.021>
- Janicke, B., Kårsnäs, A., Egelberg, P., Alm, K., 2017. Label-free high temporal resolution assessment of cell proliferation using digital holographic microscopy. *Cytom. Part A* 91, 460–469. <https://doi.org/10.1002/cyto.a.23108>
- Joeris, K., Frerichs, J., Konstantinov, K., Scheper, T., 2002. In-situ microscopy: Online process monitoring of mammalian cell cultures. *Cytotechnology* 129–134.
- Joshi, P.R.H., Cervera, L., Ahmed, I., Kondratov, O., Zolotukhin, S., Schrag, J., Chahal, P.S., Kamen, A.A., 2019. Achieving High-Yield Production of Functional AAV5 Gene Delivery Vectors via Fedbatch in an Insect Cell-One Baculovirus System. *Mol. Ther. - Methods Clin. Dev.* 13, 279–289. <https://doi.org/10.1016/j.omtm.2019.02.003>
- Justice, C., Brix, A., Freimark, D., Kraume, M., Pfromm, P., Eichenmueller, B., Czermak, P., 2011. Process control in cell culture technology using dielectric spectroscopy. *Biotechnol. Adv.* 29, 391–401. <https://doi.org/10.1016/j.biotechadv.2011.03.002>
- Kaminski, R., Obenauf, R., Purcell, F. "Focus on Fluorescence," *The Spex Speaker*, Vol. 27, No. 1 (March 1982), pp. 1-9.
- Kamlund, S., 2018. Not all those who wander are lost: A study of cancer cells by digital holographic imaging, fluorescence and a combination thereof, PhD thesis, Lund University, Lund
- Kann, B., Offerhaus, H.L., Windbergs, M., Otto, C., 2015. Raman microscopy for cellular investigations — From single cell imaging to drug carrier uptake visualization. *Adv. Drug Deliv. Rev.* 89, 71–90. <https://doi.org/10.1016/j.addr.2015.02.006>
- Karakach, T.K., Dachon, A., Choi, J., Miguez, C., Masson, L., Tartakovsky, B., 2018. Fluorescence-Based Real Time Monitoring and Diagnostics of Recombinant *Pichia pastoris* Cultivations in a Bioreactor. *Biotechnol. Prog.* 1–9. <https://doi.org/10.1002/btpr.2761>
- Kasprowicz, R., Suman, R., O'Toole, P., 2017. Characterising live cell behaviour: Traditional label-free and quantitative phase imaging approaches. *Int. J. Biochem. Cell Biol.* 84, 89–95. <https://doi.org/10.1016/j.biocel.2017.01.004>
- Keddie, B., Aponte, G., Volkman, L., 1989. The pathway of infection of *Autographa californica* nuclear polyhedrosis virus in an insect host. *Science (80-.)*. 243, 1728–1730. <https://doi.org/10.1126/science.2648574>
- Keeler, A.M., Flotte, T.R., 2019. Recombinant Adeno-Associated Virus Gene Therapy in Light of Luxturna (and Zolgensma and Glybera): Where Are We, and How Did We Get Here? *Annu. Rev. Virol.* 6, 601–621. <https://doi.org/10.1146/annurev-virology-092818-015530>
- Kemper, B., Bauwens, A., Vollmer, A., Ketelhut, S., Langehanenberg, P., Müthing, J., Karch, H., von Bally, G., 2010. Label-free quantitative cell division monitoring of endothelial cells by digital holographic microscopy. *J. Biomed. Opt.* 15, 036009. <https://doi.org/10.1117/1.3431712>
- Kim, H.-J., Jang, S.Y., Park, J.-I., Byun, J., Kim, D.-I., Do, Y.-S., Kim, J.-M., Kim, S., Kim, B.-M., Kim, W.-B., Kim, D.-K., 2004. Vascular endothelial growth factor-induced angiogenic gene therapy in patients with peripheral artery disease. *Exp. Mol. Med.* 36, 336–344. <https://doi.org/10.1038/emm.2004.44>
- Knop, D.R., Harrell, H., 2008. Bioreactor Production of Recombinant Herpes Simplex Virus Vectors. *Biotechnol. Prog.* 23, 715–721. <https://doi.org/10.1021/bp060373p>
- Kohlbrener, E., Aslanidi, G., Nash, K., Shklyayev, S., Campbell-Thompson, M., Byrne, B.J., Snyder, R.O., Muzyczka, N., Warrington, K.H., Zolotukhin, S., 2005. Successful Production of Pseudotyped rAAV Vectors Using a Modified Baculovirus Expression System. *Mol. Ther.* 12, 1217–1225. <https://doi.org/10.1016/j.ymthe.2005.08.018>
- Konakovsky, V., Clemens, C., Müller, M.M., Bechmann, J., Herwig, C., 2017. A robust feeding strategy to maintain set-point glucose in mammalian fed-batch cultures when input parameters have a large error. *Biotechnol. Prog.* 33, 317–336. <https://doi.org/10.1002/btpr.2438>

- Kondratov, O., Marsic, D., Crosson, S.M., Mendez-Gomez, H.R., Moskalenko, O., Mietzsch, M., Heilbronn, R., Allison, J.R., Green, K.B., Agbandje-McKenna, M., Zolotukhin, S., 2017. Direct Head-to-Head Evaluation of Recombinant Adeno-associated Viral Vectors Manufactured in Human versus Insect Cells. *Mol. Ther.* 25, 2661–2675. <https://doi.org/10.1016/j.ymthe.2017.08.003>
- Kotin, R.M., Snyder, R.O., 2017. Manufacturing Clinical Grade Recombinant Adeno-Associated Virus Using Invertebrate Cell Lines. *Hum. Gene Ther.* 28, 350–360. <https://doi.org/10.1089/hum.2017.042>
- Kroll, P., Stelzer, I. V., Herwig, C., 2017. Soft sensor for monitoring biomass subpopulations in mammalian cell culture processes. *Biotechnol. Lett.* 39, 1667–1673. <https://doi.org/10.1007/s10529-017-2408-0>
- Kühn, J., Shaffer, E., Mena, J., Breton, B., Parent, J., Rappaz, B., Chambon, M., Emery, Y., Magistretti, P., Depoursing, C., Marquet, P., Turcatti, G., 2013. Label-free cytotoxicity screening assay by digital holographic microscopy. *Assay Drug Dev. Technol.* 11, 101–107. <https://doi.org/10.1089/adt.2012.476>
- Kwang, T.W., Zeng, X., Wang, S., 2016. Manufacturing of Ac MNPV baculovirus vectors to enable gene therapy trials 1–8. <https://doi.org/10.1038/mtm.2015.50>
- Laasfeld, T., Kopanchuk, S., Rinken, A., 2017. Image-based cell-size estimation for baculovirus quantification. *Biotechniques* 63, 161–168. <https://doi.org/10.2144/000114595>
- Le, D.T., Radukic, M.T., Müller, K.M., 2019. Adeno-associated virus capsid protein expression in *Escherichia coli* and chemically defined capsid assembly. *Sci. Rep.* 9, 18631. <https://doi.org/10.1038/s41598-019-54928-y>
- Lecina, M., Soley, A., Gràcia, J., Espunya, E., Lázaro, B., Cairó, J.J., Gódia, F., Gòdia, F., 2006. Application of on-line OUR measurements to detect actions points to improve baculovirus-insect cell cultures in bioreactors. *J. Biotechnol.* 125, 385–394. <https://doi.org/10.1016/j.jbiotec.2006.03.014>
- Liu, J., Osadchy, M., Ashton, L., Foster, M., Solomon, C.J., Gibson, S.J., 2017. Deep Convolutional Neural Networks for Raman Spectrum Recognition: A Unified Solution. *Analyst* 142, 4067–4074. <https://doi.org/10.1039/C7AN01371J>
- Liu, Y., Wang, Z.J., Li, L., Cui, X., Chu, J., Zhang, S.L., Zhuang, Y.P., 2016. On-line monitoring of the aggregate size distribution of *Carthamus tinctorius* L. cells with multi-frequency capacitance measurements. *RSC Adv.* 6, 89764–89769. <https://doi.org/10.1039/c6ra13527g>
- Liu, Y.K., Yang, C.J., Liu, C.L., Shen, C.R., Shiao, L.D., 2010. Using a fed-batch culture strategy to enhance rAAV production in the baculovirus/insect cell system. *J. Biosci. Bioeng.* 110, 187–193. <https://doi.org/10.1016/j.jbiosc.2010.02.004>
- Lock, M., Alvira, M.R., Wilson, J.M., 2012. Analysis of Particle Content of Recombinant Adeno-Associated Virus Serotype 8 Vectors by Ion-Exchange Chromatography. *Hum Gene Ther Methods* 23, 56–64. <https://doi.org/10.1089/hgtb.2011.217>
- Lock, M., McGorray, S., Auricchio, A., Ayuso, E., Beecham, E.J., Blouin-Tavel, V., Bosch, F., Bose, M., Byrne, B.J., Caton, T., Chiorini, J.A., Chtarto, A., Clark, K.R., Conlon, T., Darmon, C., Doria, M., Douar, A., Flotte, T.R., Francis, J.D., Francois, A., Giacca, M., Korn, M.T., Korytov, I., Leon, X., Leuchs, B., Lux, G., Melas, C., Mizukami, H., Moullier, P., Müller, M., Ozawa, K., Philipsberg, T., Poulard, K., Raupp, C., Rivière, C., Roosendaal, S.D., Samulski, R.J., Soltys, S.M., Surosky, R., Tenenbaum, L., Thomas, D.L., van Montfort, B., Veres, G., Wright, J.F., Xu, Y., Zelenia, O., Zentilin, L., Snyder, R.O., 2010. Characterization of a recombinant adeno-associated virus type 2 Reference Standard Material. *Hum. Gene Ther.* 21, 1273–1285. <https://doi.org/10.1089/hum.2009.223>
- Louis Jeune, V., Joergensen, J.A., Hajjar, R.J., Weber, T., 2013. Pre-existing anti-adeno-associated virus antibodies as a challenge in AAV gene therapy. *Hum. Gene Ther. Methods* 24, 59–67. <https://doi.org/10.1089/hgtb.2012.243>
- Lourenço, N.D., Lopes, J.A., Almeida, C.F., Sarraguça, M.C., Pinheiro, H.M., 2012. Bioreactor monitoring with spectroscopy and chemometrics: A review. *Anal. Bioanal. Chem.* 404, 1211–1237. <https://doi.org/10.1007/s00216-012-6073-9>
- Luttmann, R., Bracewell, D.G., Cornelissen, G., Gernaey, K. V., Glassey, J., Hass, V.C., Kaiser, C., Preusse, C., Striedner, G., Mandenius, C.F., 2012. Soft sensors in bioprocessing: A status report and recommendations. *Biotechnol. J.* 7, 1040–1048. <https://doi.org/10.1002/biot.201100506>
- Ma, H., Galvin, T.A., Glasner, D.R., Shaheduzzaman, S., Khan, A.S., 2014. Identification of a Novel Rhabdovirus in

- Spodoptera frugiperda Cell Lines. *J. Virol.* 88, 6576–6585. <https://doi.org/10.1128/JVI.00780-14>
- Maghodia, A.B., Jarvis, D.L., 2017. Infectivity of Sf-rhabdovirus variants in insect and mammalian cell lines. *Virology* 512, 234–245. <https://doi.org/10.1016/j.virol.2017.09.025>
- Mann, C.J., Yu, L., Lo, C.-M., Kim, M.K., 2005. High-resolution quantitative phase-contrast microscopy by digital holography. *Opt. Express* 13, 8693. <https://doi.org/10.1364/opex.13.008693>
- Marek, M., van Oers, M.M., Merten, O.-W., 2017. Baculovirus-based production of biopharmaceuticals free of contaminating baculoviral virions. US10428315B2.
- Martin, J., Frederick, A., Luo, Y., Jackson, R., Joubert, M., Sol, B., Poulin, F., Pastor, E., Armentano, D., Wadsworth, S., Vincent, K., 2013. Generation and characterization of adeno-associated virus producer cell lines for research and preclinical vector production. *Hum. Gene Ther. Methods* 24, 253–69. <https://doi.org/10.1089/hgtb.2013.046>
- Matthews, T.E., Berry, B.N., Smelko, J., Moretto, J., Moore, B., Wiltberger, K., 2016. Closed loop control of lactate concentration in mammalian cell culture by Raman spectroscopy leads to improved cell density, viability, and biopharmaceutical protein production. *Biotechnol. Bioeng.* 113, 2416–2424. <https://doi.org/10.1002/bit.26018>
- Mcclements, M.E., Maclaren, R.E., 2017. Adeno-associated Virus (AAV) Dual Vector Strategies for Gene Therapy Encoding Large Transgenes 90, 611–623.
- Meghrou, J., Aucoin, M.G., Jacob, D., Chahal, P.S., Arcand, N., Kamen, A.A., 2005. Production of Recombinant Adeno-Associated Viral Vectors Using a Baculovirus / Insect Cell Suspension Culture System : From Shake Flasks to a 20-L Bioreactor. *Biotechnol. Prog.* 154–160. <https://doi.org/10.1021/bp049802e>
- Meliani, A., Boisgerault, F., Fitzpatrick, Z., Marmier, S., Leborgne, C., Collaud, F., Simon Sola, M., Charles, S., Ronzitti, G., Vignaud, A., van Wittenbergh, L., Marolleau, B., Jouen, F., Tan, S., Boyer, O., Christophe, O., Brisson, A.R., Maguire, C.A., Mingozi, F., 2017. Enhanced liver gene transfer and evasion of preexisting humoral immunity with exosome-enveloped AAV vectors. *Blood Adv.* 1, 2019–2031. <https://doi.org/10.1182/bloodadvances.2017010181>
- Mena, J., Aucoin, M., Montes, J., Chahal, P., Kamen, A., 2010. Improving adeno-associated vector yield in high density insect cell cultures. *J. Gene Med.* 157–167. <https://doi.org/10.1002/jgm>
- Mercier, S.M., Rouel, P.M., Lebrun, P., Diepenbroek, B., Wijffels, R.H., Streefland, M., 2016. Process analytical technology tools for perfusion cell culture. *Eng. Life Sci.* 16, 25–35. <https://doi.org/10.1002/elsc.201500035>
- Merten, O., 2016. AAV vector production : state of the art developments and remaining challenges. *Cell Gene Ther.* 521–551. <https://doi.org/10.18609/cgti.2016.067>
- Mietzsch, M., Casteleyn, V., Weger, S., Zolotukhin, S., Heilbronn, R., 2015. OneBac 2.0: Sf9 cell lines for production of AAV5 vectors with enhanced infectivity and minimal encapsidation of foreign DNA. *Hum. Gene Ther.* 1–24.
- Mietzsch, M., Grasse, S., Zurawski, C., Weger, S., Bennett, A., Agbandje-McKenna, M., Muzyczka, N., Zolotukhin, S., Heilbronn, R., 2014. OneBac: platform for scalable and high-titer production of adeno-associated virus serotype 1-12 vectors for gene therapy. *Hum. Gene Ther.* 25, 212–22. <https://doi.org/10.1089/hum.2013.184>
- Mietzsch, M., Hering, H., Hammer, E.-M., Agbandje-McKenna, M., Zolotukhin, S., Heilbronn, R., 2017. OneBac 2.0: Sf9 Cell Lines for Production of AAV1, AAV2 and AAV8 Vectors with Minimal Encapsidation of Foreign DNA. *Hum. Gene Ther. Methods* hgtb.2016.164. <https://doi.org/10.1089/hgtb.2016.164>
- Mingozi, F., High, K.A., 2017. Overcoming the Host Immune Response to Adeno-Associated Virus Gene Delivery Vectors: The Race Between Clearance, Tolerance, Neutralization, and Escape. <https://doi.org/10.1146/annurev-virology>
- Mitchell, A.M., Samulski, R.J., 2013. Mechanistic Insights into the Enhancement of Adeno-Associated Virus Transduction by Proteasome Inhibitors. *J. Virol.* 87, 13035–13041. <https://doi.org/10.1128/JVI.01826-13>
- Møller, S.F., Von Frese, J., Bro, R., 2005. Robust methods for multivariate data analysis. *J. Chemom.* 19, 549–563. <https://doi.org/10.1002/cem.962>
- Monteiro, F., 2015. Rational Design of Insect Cell-based Vaccine Production - Bridging Metabolomics with Mathematical Tools to Study Virus-Host Interactions, PhD thesis, ITQB-UNL, Lisboa
- Monteiro, F., Bernal, V., Chaillet, M., Berger, I., Alves, P.M., 2016. Targeted supplementation design for improved production and quality of enveloped viral particles in insect cell-baculovirus expression system. *J. Biotechnol.* 233,

- 34–41. <https://doi.org/10.1016/j.jbiotec.2016.06.029>
- Monteiro, F., Bernal, V., Saelens, X., Lozano, A.B., Bernal, C., Sevilla, A., Carrondo, M.J.T., Alves, P.M., 2014. Metabolic profiling of insect cell lines: Unveiling cell line determinants behind system's productivity. *Biotechnol. Bioeng.* 111, 816–828. <https://doi.org/10.1002/bit.25142>
- Monteiro, F., Carinhas, N., Carrondo, M.J.T., Bernal, V., Alves, P.M., 2012. Toward system-level understanding of baculovirus-host cell interactions: From molecular fundamental studies to large-scale proteomics approaches. *Front. Microbiol.* 3, 1–16. <https://doi.org/10.3389/fmicb.2012.00391>
- Moore, B., Sanford, R., Zhang, A., 2019. Case study: The characterization and implementation of dielectric spectroscopy (biocapacitance) for process control in a commercial GMP CHO manufacturing process. *Biotechnol. Prog.* 35. <https://doi.org/10.1002/btpr.2782>
- Naso, M.F., Tomkowicz, B., Perry, W.L., Strohl, W.R., 2017. Adeno-Associated Virus (AAV) as a Vector for Gene Therapy. *BioDrugs*. <https://doi.org/10.1007/s40259-017-0234-5>
- Nass, S.A., Mattingly, M.A., Woodcock, D.A., Burnham, B.L., Ardinger, J.A., Osmond, S.E., Frederick, A.M., Scaria, A., Cheng, S.H., O'Riordan, C.R., 2018. Universal Method for the Purification of Recombinant AAV Vectors of Differing Serotypes. *Mol. Ther. - Methods Clin. Dev.* 9, 33–46. <https://doi.org/10.1016/j.omtm.2017.12.004>
- Negrete, A., Esteban, G., Kotin, R.M., 2007. Process optimization of large-scale production of recombinant adeno-associated vectors using dielectric spectroscopy. *Appl. Microbiol. Biotechnol.* 76, 761–72. <https://doi.org/10.1007/s00253-007-1030-9>
- Negrete, A., Kotin, R.M., 2009. Strategies for manufacturing recombinant adeno-associated virus vectors for gene therapy applications exploiting baculovirus technology. *Blood* 7, 303–311. <https://doi.org/10.1093/bfpg/eln034>
- Negrete, A., Kotin, R.M., 2007. Production of recombinant adeno-associated vectors using two bioreactor configurations at different scales. *J. Virol. Methods* 145, 155–61. <https://doi.org/10.1016/j.jviromet.2007.05.020>
- Nemunaitis, J., Ganly, I., Khuri, F., Arseneau, J., Kuhn, J., McCarty, T., Landers, S., Maples, P., Romel, L., Randlev, B., Reid, T., Kaye, S., Kirn, D., 2000. Selective replication and oncolysis in p53 mutant tumors with ONYX-015, an E1B-55kD gene-deleted adenovirus, in patients with advanced head and neck cancer: A phase II trial. *Cancer Res.* 60, 6359–6366.
- Neufeld, E.F., Sweeley, C.C., Rogers, S., Friedmann, T., Roblin, R., 1972. Gene therapy for human genetic disease? *Science (80-)*. 178, 648–649. <https://doi.org/10.1126/science.178.4061.648>
- Nikolay, A., Léon, A., Schwamborn, K., Genzel, Y., Reichl, U., 2018. Process intensification of EB66® cell cultivations leads to high-yield yellow fever and Zika virus production. *Appl. Microbiol. Biotechnol.* 102, 8725–8737. <https://doi.org/10.1007/s00253-018-9275-z>
- Nonnenmacher, M., Weber, T., 2012. Intracellular transport of recombinant adeno-associated virus vectors. *Gene Ther.* 19, 649–658. <https://doi.org/10.1038/gt.2012.6>
- Noordman Y, Lubelski J, Bakker, A., 2016. Mutated rep encoding sequences for use in AAV production. *US* 2013/0023034.
- Ohadi, K., Aghamohseni, H., Legge, R.L., Budman, H.M., 2014. Fluorescence-based soft sensor for at situ monitoring of chinese hamster ovary cell cultures. *Biotechnol. Bioeng.* 111, 1577–1586. <https://doi.org/10.1002/bit.25222>
- Ohadi, K., Legge, R.L., Budman, H.M., 2015. Development of a soft-sensor based on multi-wavelength fluorescence spectroscopy and a dynamic metabolic model for monitoring mammalian cell cultures. *Biotechnol. Bioeng.* 112, 197–208. <https://doi.org/10.1002/bit.25339>
- Ohadi, S.K., 2014. Development of Soft Sensors for Monitoring of Chinese Hamster Ovary Cell Processes.
- Opel, C.F., Li, J., Amanullah, A., 2010. Quantitative modeling of viable cell density, cell size, intracellular conductivity, and membrane capacitance in batch and fed-batch CHO processes using dielectric spectroscopy. *Biotechnol. Prog.* NA-NA. <https://doi.org/10.1002/btpr.425>
- Orefice, N.S., Souchet, B., Braudeau, J., Alves, S., Pigué, F., Collaud, F., Ronzitti, G., Tada, S., Hantraye, P., Mingozzi, F., Ducongé, F., Cartier, N., 2019. Real-Time Monitoring of Exosome Enveloped-AAV Spreading by Endomicroscopy Approach: A New Tool for Gene Delivery in the Brain. *Mol. Ther. - Methods Clin. Dev.* 14, 237–

251. <https://doi.org/10.1016/j.omtm.2019.06.005>
- Pais, D.A.M., Carrondo, M.J.T., Alves, P.M., Teixeira, A.P., 2014. Towards real-time monitoring of therapeutic protein quality in mammalian cell processes. *Curr. Opin. Biotechnol.* 30, 161–167. <https://doi.org/10.1016/j.copbio.2014.06.019>
- Pais, D.A.M., Portela, R.M.C., Carrondo, M.J.T., Isidro, I.A., Alves, P.M., 2019. Enabling Pat in insect cell bioprocesses: *in-situ* monitoring of recombinant adeno-associated virus production by fluorescence spectroscopy. *Biotechnol. Bioeng.* bit.27117. <https://doi.org/10.1002/bit.27117>
- Palomares, L.A., Ramírez, O.T., 2009. Challenges for the production of virus-like particles in insect cells: The case of rotavirus-like particles. *Biochem. Eng. J.* 45, 158–167. <https://doi.org/10.1016/j.bej.2009.02.006>
- Palomares, L. A. and Ramírez, O. T. (2009) 'Challenges for the production of virus-like particles in insect cells: The case of rotavirus-like particles', *Biochemical Engineering Journal*, 45(3), pp. 158–167. doi: 10.1016/j.bej.2009.02.006.
- Penaud-Budloo, M., François, A., Clément, N., Ayuso, E., 2018. Pharmacology of Recombinant Adeno-associated Virus Production. *Mol. Ther. - Methods Clin. Dev.* 8, 166–180. <https://doi.org/10.1016/j.omtm.2018.01.002>
- Penaud-Budloo, M., Lecomte, E., Guy-Duché, A., Saleun, S., Roulet, A., Lopez-Roques, C., Tournaire, B., Cogné, B., Léger, A., Blouin, V., Lindenbaum, P., Moullier, P., Ayuso, E., 2017. Accurate Identification and Quantification of DNA Species by Next-Generation Sequencing in Adeno-Associated Viral Vectors Produced in Insect Cells. *Hum. Gene Ther. Methods* hgtb.2016.185. <https://doi.org/10.1089/hgtb.2016.185>
- Petiot, E., Ansorge, S., Rosa-Calatrava, M., Kamen, A., 2016. Critical phases of viral production processes monitored by capacitance. *J. Biotechnol.* 242, 19–29. <https://doi.org/10.1016/j.jbiotec.2016.11.010>
- Petiot, E., Kamen, A., 2012. Real-time monitoring of influenza virus production kinetics in HEK293 cell cultures. *Biotechnol. Prog.* 29, 275–84. <https://doi.org/10.1002/btpr.1601>
- Pillay, S., Meyer, N.L., Puschnik, A.S., Davulcu, O., Diep, J., Ishikawa, Y., Jae, L.T., Wosen, J.E., Nagamine, C.M., Chapman, M.S., Carette, J.E., 2016. An essential receptor for adeno-associated virus infection. *Nature* 530, 108–112. <https://doi.org/10.1038/nature16465>
- Planul, A., Dalkara, D., 2017. Vectors and Gene Delivery to the Retina. *Annu. Rev. Vis. Sci.* 3, 121–140. <https://doi.org/10.1146/annurev-vision-102016-061413>
- Potter, M., Lins, B., Mietzsch, M., Heilbronn, R., Van Vliet, K., Chipman, P., Agbandje-McKenna, M., Cleaver, B.D., Clément, N., Byrne, B.J., Zolotukhin, S., 2014. A simplified purification protocol for recombinant adeno-associated virus vectors. *Mol. Ther. Methods Clin. Dev.* 1, 14034. <https://doi.org/10.1038/mtm.2014.34>
- Powers, A.D., Piras, B.A., Clark, R.K., Lockey, T.D., Meagher, M.M., 2016. Development and Optimization of AAV hFIX Particles by Transient Transfection in an iCELLis® Fixed-Bed Bioreactor. *Hum. Gene Ther. Methods* 27, 112–121. <https://doi.org/10.1089/hgtb.2016.021>
- Puri, R., 2019. FDA Regulation of Cell and Gene Therapies: Facilitating Advanced Manufacturing. Presented at the American Society for Cell and Gene Therapy (ASGCT) 22nd meeting.
- Qiu, J., Arnold, M.A., Murhammer, D.W., 2014. On-line near infrared bioreactor monitoring of cell density and concentrations of glucose and lactate during insect cell cultivation. *J. Biotechnol.* 173, 106–111. <https://doi.org/10.1016/j.jbiotec.2014.01.009>
- Qu, G., Bahr-Davidson, J., Prado, J., Tai, A., Cataniag, F., McDonnell, J., Zhou, J., Hauck, B., Luna, J., Sommer, J.M., Smith, P., Zhou, S., Colosi, P., High, K.A., Pierce, G.F., Wright, J.F., 2007. Separation of adeno-associated virus type 2 empty particles from genome containing vectors by anion-exchange column chromatography. *J. Virol. Methods* 140, 183–192. <https://doi.org/10.1016/j.jviromet.2006.11.019>
- Rangan, S., Kamal, S., Konorov, S.O., Schulze, H.G., Blades, M.W., Turner, R.F.B., Piret, J.M., 2018. Types of cell death and apoptotic stages in Chinese Hamster Ovary cells distinguished by Raman spectroscopy. *Biotechnol. Bioeng.* 115, 401–412. <https://doi.org/10.1002/bit.26476>
- Rapoport, D.H., Becker, T., Mamlouk, A.M., Schicktanz, S., Kruse, C., 2011. A novel validation algorithm allows for automated cell tracking and the extraction of biologically meaningful parameters. *PLoS One* 6. <https://doi.org/10.1371/journal.pone.0027315>

- Rathore, A., Winkle, H., 2009. Quality by design for biopharmaceuticals. *Nat. Biotechnol.* 27, 26–34.
- Rathore, A.S., Mittal, S., Pathak, M., Arora, A., 2014. Guidance for performing multivariate data analysis of bioprocessing data: Pitfalls and recommendations. *Biotechnol. Prog.* 30, 967–973. <https://doi.org/10.1002/btpr.1922>
- Reul, J., Frisch, J., Engeland, C.E., Thalheimer, F.B., Hartmann, J., Ungerechts, G., Buchholz, C.J., 2019. Tumor-Specific Delivery of Immune Checkpoint Inhibitors by Engineered AAV Vectors. *Front. Oncol.* 9. <https://doi.org/10.3389/fonc.2019.00052>
- Ribeiro da Cunha, B., Fonseca, L.P., Calado, C.R.C., 2019. A phenotypic screening bioassay for *Escherichia coli* stress and antibiotic responses based on Fourier-transform infrared (FTIR) spectroscopy and multivariate analysis. *J. Appl. Microbiol.* 127, 1776–1789. <https://doi.org/10.1111/jam.14429>
- Riley, M.R., Rhiel, M., Zhou, X., Arnold, M.A., Murhammer, D.W., 1997. Simultaneous Measurement of Glucose and Glutamine in Insect Cell Culture Media by Near Infrared Spectroscopy. [https://doi.org/10.1002/\(SICI\)1097-0290\(19970705\)55:1<11::AID-BIT2>3.0.CO;2-#](https://doi.org/10.1002/(SICI)1097-0290(19970705)55:1<11::AID-BIT2>3.0.CO;2-#)
- Rininger, J., Fennell, A., Schoukroun-Barnes, L., Peterson, C., Speidel, J., 2019. Capacity Analysis for Viral Vector Manufacturing: Is There Enough? [WWW Document]. *Bioprocess Int.* URL <https://bioprocessintl.com/manufacturing/emerging-therapeutics-manufacturing/capacity-analysis-for-viral-vector-manufacturing-is-there-enough/>
- Roberts, J., Power, A., Chapman, J., Chandra, S., Cozzolino, D., 2018. The use of UV-Vis spectroscopy in bioprocess and fermentation monitoring. *Fermentation* 4. <https://doi.org/10.3390/fermentation4010018>
- Roldão, A., Carrondo, M.J.T., Alves, P.M., Oliveira, R., 2008. Stochastic simulation of protein expression in the baculovirus/insect cells system. *Comput. Chem. Eng.* 32, 68–77. <https://doi.org/10.1016/j.compchemeng.2007.04.017>
- Roldão, A., Vieira, H.L.A., Charpilienne, A., Poncet, D., Roy, P., Carrondo, M.J.T., Alves, P.M., Oliveira, R., 2007. Modeling rotavirus-like particles production in a baculovirus expression vector system: Infection kinetics, baculovirus DNA replication, mRNA synthesis and protein production. *J. Biotechnol.* 128, 875–894. <https://doi.org/10.1016/j.jbiotec.2007.01.003>
- Rourou, S., Gaumon, S., Kallel, H., 2010. On-Line Monitoring of Vero Cells Cultures During the Growth and Rabies Virus Process Using Biomass Spectrometer, in: *Cells and Culture*. Springer Netherlands, Dordrecht, pp. 829–832. https://doi.org/10.1007/978-90-481-3419-9_145
- Rowland-Jones, R.C., van den Berg, F., Racher, A.J., Martin, E.B., Jaques, C., 2017. Comparison of spectroscopy technologies for improved monitoring of cell culture processes in miniature bioreactors. *Biotechnol. Prog.* 33, 337–346. <https://doi.org/10.1002/btpr.2459>
- Rudolph, G., Lindner, P., Gierse, A., Bluma, A., Martinez, G., Hitzmann, B., Scheper, T., 2008. Online monitoring of microcarrier based fibroblast cultivations with in situ microscopy. *Biotechnol. Bioeng.* 99, 136–145. <https://doi.org/10.1002/bit.21523>
- Rumachik, N.G., Malaker, S.A., Poweleit, N., Maynard, L.H., Adams, C.M., Leib, D., Cirolia, G., Thomas, D., Stamnes, S., Holt, K., Sinn, P., May, A.P., 2019. Methods Matter -- Standard Production Platforms For Recombinant AAV Can Produce Chemically And Functionally Distinct Vectors. *bioRxiv* (2019), p. 640169
- Salganik, M., Venkatakrisnan, B., Bennett, a., Lins, B., Yarbrough, J., Muzyczka, N., Agbandje-McKenna, M., McKenna, R., 2012. Evidence for pH-Dependent Protease Activity in the Adeno-Associated Virus Capsid. *J. Virol.* 86, 11877–11885. <https://doi.org/10.1128/JVI.01717-12>
- Sandor, M., Rüdinger, F., Bienert, R., Grimm, C., Solle, D., Scheper, T., 2013. Comparative study of non-invasive monitoring via infrared spectroscopy for mammalian cell cultivations. *J. Biotechnol.* 168, 636–45. <https://doi.org/10.1016/j.jbiotec.2013.08.002>
- Santiago-Ortiz, J.L., Schaffer, D. V., 2016. Adeno-associated virus (AAV) vectors in cancer gene therapy. *J. Control. Release* 240, 287–301. <https://doi.org/10.1016/j.jconrel.2016.01.001>
- Santos, R.M., Kessler, J.M., Salou, P., Menezes, J.C., Peinado, A., 2018. Monitoring mAb cultivations with in-situ raman spectroscopy: The influence of spectral selectivity on calibration models and industrial use as reliable PAT tool.

- Biotechnol. Prog. 34, 659–670. <https://doi.org/10.1002/btpr.2635>
- Saraiva, J., Nobre, R.J., de Almeida, L.P., 2016. Gene therapy for the CNS using AAVs: The impact of systemic delivery by AAV9. *J. Control. Release* 241, 94–109. <https://doi.org/10.1016/j.jconrel.2016.09.011>
- Savy, A., Dickx, Y., Nauwynck, L., Bonnin, D., Merten, O.-W., Galibert, L., 2017. Impact of ITR integrity on rAAV8 production using baculovirus/Sf9 cells system. *Hum. Gene Ther. Methods* 28, 277–288. <https://doi.org/10.1089/hgtb.2016.133>
- Sawatzki, A., Hans, S., Narayanan, H., Haby, B., Krausch, N., Sokolov, M., Glauche, F., Riedel, S., Neubauer, P., Cruz Bournazou, M., 2018. Accelerated Bioprocess Development of Endopolygalacturonase-Production with *Saccharomyces cerevisiae* Using Multivariate Prediction in a 48 Mini-Bioreactor Automated Platform. *Bioengineering* 5, 101. <https://doi.org/10.3390/bioengineering5040101>
- Schnödt, M., Büning, H., 2017. Improving the Quality of Adeno-Associated Viral Vector Preparations: The Challenge of Product-Related Impurities. *Hum. Gene Ther. Methods* 28, 101–108. <https://doi.org/10.1089/hgtb.2016.188>
- Schwab, K., Hesse, F., 2017. Estimating Extrinsic Dyes for Fluorometric Online Monitoring of Antibody Aggregation in CHO Fed-Batch Cultivations. *Bioengineering* 4, 65. <https://doi.org/10.3390/bioengineering4030065>
- Schwab, K., Lauber, J., Hesse, F., 2016. Fluorometric In Situ Monitoring of an *Escherichia coli* Cell Factory with Cytosolic Expression of Human Glycosyltransferase GalNAcT2: Prospects and Limitations. *Bioengineering* 3, 32. <https://doi.org/10.3390/bioengineering3040032>
- Shahryari, A., Jazi, M.S., Mohammadi, S., Nikoo, H.R., Nazari, Z., Hosseini, E.S., Burtscher, I., Mowla, S.J., Lickert, H., 2019. Development and clinical translation of approved gene therapy products for genetic disorders. *Front. Genet.* 10. <https://doi.org/10.3389/fgene.2019.00868>
- Sharon, D., Kamen, A., 2017. Advancements in the design and scalable production of viral gene transfer vectors. *Biotechnol. Bioeng.* 5, 1–16. <https://doi.org/10.1002/bit.26461>
- Shorthose, S. (Ed.), 2017. *Guide to EU Pharmaceutical Regulatory Law*, Seventh. ed.
- Smith, R.H., Levy, J.R., Kotin, R.M., 2009. A simplified baculovirus-AAV expression vector system coupled with one-step affinity purification yields high-titer rAAV stocks from insect cells. *Mol. Ther.* 17, 1888–1896. <https://doi.org/10.1038/mt.2009.128>
- Snyder, R.O., Moullier, P. (Eds.), 2011. *Adeno-Associated Virus*, *Methods in Molecular Biology*, *Methods in Molecular Biology*. Humana Press, Totowa, NJ. <https://doi.org/10.1007/978-1-61779-370-7>
- Sokolov, M., Ritscher, J., MacKinnon, N., Souquet, J., Broly, H., Morbidelli, M., Butté, A., 2017. Enhanced process understanding and multivariate prediction of the relationship between cell culture process and monoclonal antibody quality. *Biotechnol. Prog.* 33, 1368–1380. <https://doi.org/10.1002/btpr.2502>
- Steele, K.H., Stone, B.J., Franklin, K.M., Fath-goodin, A., Zhang, X., Webb, B.A., Geisler, C., 2017. Improving the Baculovirus Expression Vector System with Vankyrin-enhanced Technology. <https://doi.org/10.1002/btpr.2516>
- Teixeira, A.P., Duarte, T.M., Carrondo, M.J.T., Alves, P.M., 2011a. Synchronous fluorescence spectroscopy as a novel tool to enable PAT applications in bioprocesses. *Biotechnol. Bioeng.* 108, 1852–1861. <https://doi.org/10.1002/bit.23131>
- Teixeira, A.P., Duarte, T.M., Oliveira, R., Carrondo, M.J.T., Alves, P.M., 2011b. High-throughput analysis of animal cell cultures using two-dimensional fluorometry. *J. Biotechnol.* 151, 255–260. <https://doi.org/10.1016/j.jbiotec.2010.11.015>
- Teixeira, A.P., Portugal, C.A.M., Carinhas, N., Dias, J.M.L., Crespo, J.P., Alves, P.M., Carrondo, M.J.T., Oliveira, R., 2009. In situ 2D fluorometry and chemometric monitoring of mammalian cell cultures. *Biotechnol. Bioeng.* 102, 1098–1106. <https://doi.org/10.1002/bit.22125>
- Thomas, D.L., Wang, L., Niamke, J., Liu, J., Kang, W., Scotti, M.M., Ye, G.-J., Veres, G., Knop, D.R., 2009. Scalable Recombinant Adeno-Associated Virus Production Using Recombinant Herpes Simplex Virus Type 1 Coinfection of Suspension-Adapted Mammalian Cells. *Hum. Gene Ther.* 20, 861–870. <https://doi.org/10.1089/hum.2009.004>
- Thorne, B.A., Takeya, R.K., Peluso, R.W., 2009. Manufacturing Recombinant Adeno-Associated Viral Vectors from Producer Cell Clones. *Hum. Gene Ther.* 20, 707–714. <https://doi.org/10.1089/hum.2009.070>

- Tulsyan, A., Schorner, G., Khodabandehlou, H., Wang, T., Coufal, M., Undey, C., 2019. A machine-learning approach to calibrate generic Raman models for real-time monitoring of cell culture processes. *Biotechnol. Bioeng.* 116, 2575–2586. <https://doi.org/10.1002/bit.27100>
- Ugele, M., Weniger, M., Leidenberger, M., Huang, Y., Bassler, M., Friedrich, O., Kappes, B., Hayden, O., Richter, L., 2018. Label-free, high-throughput detection of *P. falciparum* infection in sphered erythrocytes with digital holographic microscopy. *Lab Chip* 18, 1704–1712. <https://doi.org/10.1039/c8lc00350e>
- Urabe, M., Ding, C., Kotin, R.M., 2002. Insect cells as a factory to produce adeno-associated virus type 2 vectors. *Hum. Gene Ther.* 13, 1935–1943. <https://doi.org/10.1089/10430340260355347>
- Valdmanis, P.N., Kay, M.A., 2017. Future of rAAV Gene Therapy : Platform for RNAi , Gene Editing , and Beyond X, 1–12. <https://doi.org/10.1089/hum.2016.171>
- Van Oers, M.M., Pijlman, G.P., Vlak, J.M., 2015. Thirty years of baculovirus-insect cell protein expression: From dark horse to mainstream technology. *J. Gen. Virol.* 96, 6–23. <https://doi.org/10.1099/vir.0.067108-0>
- Venugopal, A., Chandran, M., Eruppakotte, N., Kizhakkilach, S., Breezevilla, S.C., Vellingiri, B., 2018. Monogenic diseases in India. *Mutat. Res. - Rev. Mutat. Res.* 776, 23–31. <https://doi.org/10.1016/j.mrrev.2018.03.003>
- Virag, T., Cecchini, S., Kotin, R.M., 2009. Producing recombinant adeno-associated virus in foster cells: overcoming production limitations using a baculovirus-insect cell expression strategy. *Hum. Gene Ther.* 20, 807–817. <https://doi.org/10.1089/hum.2009.092>
- von Stosch, M., Hamelink, J.-M., Oliveira, R., 2016. Hybrid modeling as a QbD/PAT tool in process development: an industrial *E. coli* case study. *Bioprocess Biosyst. Eng.* 39, 773–84. <https://doi.org/10.1007/s00449-016-1557-1>
- Wang, D., Tai, P.W.L., Gao, G., 2019. Adeno-associated virus vector as a platform for gene therapy delivery. *Nat. Rev. Drug Discov.* 18, 358–378. <https://doi.org/10.1038/s41573-019-0012-9>
- Wang, L., Blouin, V., Brument, N., Bello-roufai, M., Francois, A., 2011. Adeno-Associated Virus. <https://doi.org/10.1007/978-1-61779-370-7>
- Wang, Q., Wu, Z., Zhang, J., Firman, J., Wei, H., Zhuang, Z., Liu, L., Miao, L., Hu, Y., Li, D., Diao, Y., Xiao, W., 2017. A Robust System for Production of Superabundant VP1 Recombinant AAV Vectors. *Mol. Ther. - Methods Clin. Dev.* 7, 146–156. <https://doi.org/10.1016/j.omtm.2017.11.002>
- Wang, Z., Cheng, F., Engelhardt, J.F., Yan, Z., Qiu, J., 2018. Development of a Novel Recombinant Adeno-Associated Virus Production System Using Human Bocavirus 1 Helper Genes. *Mol. Ther. - Methods Clin. Dev.* 11, 40–51. <https://doi.org/10.1016/j.omtm.2018.09.005>
- Wasilko, D.J., Edward Lee, S., Stutzman-Engwall, K.J., Reitz, B.A., Emmons, T.L., Mathis, K.J., Bienkowski, M.J., Tomasselli, A.G., David Fischer, H., 2009. The titerless infected-cells preservation and scale-up (TIPS) method for large-scale production of NO-sensitive human soluble guanylate cyclase (sGC) from insect cells infected with recombinant baculovirus. *Protein Expr. Purif.* 65, 122–132. <https://doi.org/10.1016/j.pep.2009.01.002>
- Webster, T.A., Hadley, B.C., Hilliard, W., Jaques, C., Mason, C., 2018. Development of generic raman models for a GS-KOTM CHO platform process. *Biotechnol. Prog.* 34, 730–737. <https://doi.org/10.1002/btpr.2633>
- Weidner, T., Druzinec, D., Mühlmann, M., Buchholz, R., Czermak, P., 2017. The components of shear stress affecting insect cells used with the baculovirus expression vector system. *Zeitschrift für Naturforsch. C* 72, 429–439. <https://doi.org/10.1515/znc-2017-0066>
- Whelan, J., Craven, S., Glennon, B., 2012. In situ Raman spectroscopy for simultaneous monitoring of multiple process parameters in mammalian cell culture bioreactors. *Biotechnol. Prog.* 28, 1355–1362. <https://doi.org/10.1002/btpr.1590>
- Wirth, T., Parker, N., Ylä-Herttua, S., 2013. History of gene therapy. *Gene* 525, 162–169. <https://doi.org/10.1016/j.gene.2013.03.137>
- Wolf, G., Almeida, J.S., Pinheiro, C., Correia, V., Rodrigues, C., Reis, M. a, Crespo, J.G., 2001. Two-dimensional fluorometry coupled with artificial neural networks: a novel method for on-line monitoring of complex biological processes. *Biotechnol. Bioeng.* 72, 297–306. [https://doi.org/10.1002/1097-0290\(20010205\)72:3<297::AID-BIT6>3.0.CO;2-B](https://doi.org/10.1002/1097-0290(20010205)72:3<297::AID-BIT6>3.0.CO;2-B)

- World Health Organization, 2019. Human Genomics in Global Health - Genes and human diseases [WWW Document]. URL <https://www.who.int/genomics/public/geneticdiseases/en/index2.html> (accessed 2.13.20).
- Wright, J.F., 2014. Product-Related Impurities in Clinical-Grade Recombinant AAV Vectors: Characterization and Risk Assessment. *Biomedicines* 2, 80–97. <https://doi.org/10.3390/biomedicines2010080>
- Wright, J.F., 2014. AAV Empty Capsids: For Better or for Worse? *Mol. Ther.* 22, 2013–2014. <https://doi.org/10.1038/mt.2013.268>
- Wu, H., Read, E., White, M., Chavez, B., Brorson, K., Agarabi, C., Khan, M., 2015. Real time monitoring of bioreactor mAb IgG3 cell culture process dynamics via Fourier transform infrared spectroscopy: Implications for enabling cell culture process analytical technology. *Front. Chem. Sci. Eng.* 9, 386–406. <https://doi.org/10.1007/s11705-015-1533-3>
- Yee, C.M., Zak, A.J., Hill, B.D., Wen, F., 2018. The Coming Age of Insect Cells for Manufacturing and Development of Protein Therapeutics. *Ind. Eng. Chem. Res.* 57, 10061–10070. <https://doi.org/10.1021/acs.iecr.8b00985>
- Yin, H., Kanasty, R.L., Eltoukhy, A.A., Vegas, A.J., Dorkin, J.R., Anderson, D.G., 2014. Non-viral vectors for gene-based therapy. *Nat. Rev. Genet.* 15, 541–555. <https://doi.org/10.1038/nrg3763>
- Yu, Z., Zhou, S., Luo, N., Ho, C.Y., Chen, M., Chen, H., 2020. TPP Combined with DGUC as an Economic and Universal Process for Large-Scale Purification of AAV Vectors. *Mol. Ther. - Methods Clin. Dev.* 17, 34–48. <https://doi.org/10.1016/j.omtm.2019.11.009>
- Zabadaj, M., Chreptowicz, K., Mierzejewska, J., Ciosek, P., 2017. Two-Dimensional Fluorescence as Soft Sensor in the Monitoring of Biotransformation Performed by Yeast. *Biotechnol. Prog.* 33, 299–307. <https://doi.org/10.1002/btpr.2381>
- Zavala-Ortiz, D.A., Ebel, B., Li, M.-Y., Barradas-Dermitz, D.M., Hayward-Jones, P.M., Aguilar-Uscanga, M.G., Marc, A., Guedon, E., 2020. Support Vector and Locally Weighted regressions to monitor monoclonal antibody glycosylation during CHO cell culture processes, an enhanced alternative to Partial Least Squares regression. *Biochem. Eng. J.* 154, 107457. <https://doi.org/10.1016/j.bej.2019.107457>
- Zavala-Ortiz, D.A., Ebel, B., Li, M.-Y., Barradas-Dermitz, D.M., Hayward-Jones, P.M., Aguilar-Uscanga, M.G., Marc, A., Guedon, E., 2019. Interest of locally weighted regression to overcome nonlinear effects during in situ NIR monitoring of CHO cell culture parameters and antibody glycosylation. *Biotechnol. Prog.* 1–10. <https://doi.org/10.1002/btpr.2924>
- Zeiser, A., Bédard, C., Voyer, R., Jardin, B., Tom, R., Kamen, a, 1999. On-line monitoring of the progress of infection in Sf-9 insect cell cultures using relative permittivity measurements. *Biotechnol. Bioeng.* 63, 122–6. [https://doi.org/10.1002/\(SICI\)1097-0290\(19990405\)63:1<122::AID-BIT13>3.0.CO;2-I](https://doi.org/10.1002/(SICI)1097-0290(19990405)63:1<122::AID-BIT13>3.0.CO;2-I)
- Zeiser, A., Elias, C.B., Voyer, R., Jardin, B., Kamen, A.A., 2000. On-line monitoring of physiological parameters of insect cell cultures during the growth and infection process. *Biotechnol. Prog.* 16, 803–808. <https://doi.org/10.1021/bp000092w>
- Zitzmann, J., Sprick, G., Weidner, T., Schreiber, C., Czermak, P., 2017. Process Optimization for Recombinant Protein Expression in Insect Cells. *New Insights into Cell Cult. Technol.* <https://doi.org/10.5772/67849>
- Zitzmann, J., Weidner, T., Eichner, G., Salzig, D., Czermak, P., 2018. Dielectric Spectroscopy and Optical Density Measurement for the Online Monitoring and Control of Recombinant Protein Production in Stably Transformed *Drosophila melanogaster* S2 Cells. *Sensors* 18, 900. <https://doi.org/10.3390/s18030900>

Chapter II

Enabling PAT in insect cell bioprocesses: *in-situ* monitoring of recombinant adeno-associated virus production by fluorescence spectroscopy

This chapter is adapted from the manuscript:

Pais, DAM, Portela, RMC, Carrondo, MJT, Isidro, IA, Alves, PM. 2019. "Enabling PAT in insect cell bioprocesses: In situ monitoring of recombinant adeno-associated virus production by fluorescence spectroscopy", *Biotechnology and Bioengineering*, Nov;116(11):2803-2814

Author Contribution

Daniel Pais participated in the experimental setup and design, executed the experiments, analyzed the data and wrote this chapter.

Abstract

The process analytical technology (PAT) initiative shifted the bioprocess development mindset towards real-time monitoring and control tools to measure relevant process variables online and acting accordingly when undesirable deviations occur. Online monitoring is especially important in lytic production systems in which released proteases and changes in cell physiology are likely to affect product quality attributes, as is the case of the insect cell-baculovirus expression vector system (IC-BEVS), a well-established system for production of viral vectors and vaccines.

Here, we applied fluorescence spectroscopy as a real-time monitoring tool for recombinant adeno-associated virus (rAAV) production in the IC-BEVS. Fluorescence spectroscopy is simple, yet sensitive and informative. To overcome the strong fluorescence background of the culture medium and improve predictive ability, we combined artificial neural network models with a genetic algorithm-based approach to optimize spectra pre-processing.

We obtained predictive models for cell viability, cell concentration and rAAV intra and extracellular titer with normalized root mean squared errors of 4 %, 7 %, 16 % and 7 %, respectively, for leave-one-batch-out cross-validation.

Our approach shows fluorescence spectroscopy allows real-time determination of the best time of harvest in order to maintain rAAV infectivity, an important quality attribute, and detection of deviations from the golden batch profile. Spectra acquisition takes 22 minutes for 2D-fluorescence maps, but less than 2 minutes for the synchronous fluorescence mode. This methodology can be applied to other biopharmaceuticals produced in the IC-BEVS, supporting the use of fluorescence spectroscopy as a versatile PAT tool.

Contents

1.	Introduction	63
2.	Materials and Methods	66
2.1.	Cell line and culture medium.....	66
2.2.	Viruses, infection and titration.....	66
2.3.	Bioreactor cultures and sample processing	67
2.4.	Fluorescence spectra acquisition.....	68
2.5.	Spectra pre-processing.....	70
2.6.	Artificial neural network (ANN) and partial least squares (PLS) predictors.....	71
2.7.	Sensitivity analysis.....	72
3.	Results	73
3.1.	Culture conditions and rAAV production	73
3.2.	Fluorescence spectra dynamics	75
3.3.	Fluorescence-based ANN models can predict important process variables.....	75
3.4.	Assessment of model robustness and fluorescence regions important for prediction.....	78
4.	Discussion	80
5.	Conclusions	87
6.	Acknowledgements	87
7.	Supplementary Data	89
8.	References	97

1. Introduction

Following the introduction of the process analytical technology (PAT) initiative (FDA, 2004), new process development efforts have focused on: i) a thorough characterization of product quality; ii) increasing process understanding; and iii) the use of real-time monitoring and control tools to implement robust bioprocesses. The use of PAT tools allows minimizing the impact of process variations in product quality, ensuring its consistency, cost savings and real-time release, ultimately easing regulatory approval of new drugs. Nevertheless, the potential benefits brought on by PAT are hindered by resistance in implementing new tools to existent bioprocesses and the concern that the investment in these technologies will exceed the benefits of their implementation (reviewed in Henriques et al., 2018; Pais et al., 2014).

For a wide implementation of PAT, real-time monitoring solutions are needed. Spectroscopic methods are ideal for use as analyzers to support process control, enabling its use to assure product quality during production and to act in conformity when undesirable changes are observed (FDA, 2004; Teixeira et al., 2011; reviewed in Pais et al., 2014).

Several spectroscopic techniques have been used for cell culture processes and virus production monitoring, with Raman (Rangan et al., 2018; Santos et al., 2018; Webster et al., 2018), near-infrared (Mercier et al., 2015; Rowland-Jones et al., 2017), dielectric (Kroll et al., 2017; Mercier et al., 2015; Nikolay et al., 2018; Petiot et al., 2016) and fluorescence spectroscopy (Karakach et al., 2018; Schwab & Hesse, 2017) being the most widely used. All possess characteristics desirable for PAT: spectroscopic techniques are non-invasive, non-destructive, and able to provide rapid information from several components simultaneously (Ohadi et al., 2014, 2015; Rowland-Jones et al., 2017; Teixeira et al., 2011, 2009), including product quality attributes (Chopda et al., 2017; Li et al., 2019). Both Raman and fluorescence have proven worthy for monitoring recombinant protein production and cell density in cell culture processes, due to their ability to

track metabolite dynamics in the complex cell culture media of mammalian cells (reviewed in Abu-Absi et al., 2014). Fluorescence spectroscopy has the advantages of a more straightforward spectra acquisition, pre-processing and interpretation, coupled with high sensitivity and low cost. It also can detect fluorophores inside and outside the cells (Ohadi et al., 2014; Schwab et al., 2016; Teixeira et al., 2011, 2009; Wolf et al., 2001). When compared with dielectric spectroscopy for monitoring virus and protein production, fluorescence has the advantage of incorporating information from metabolite dynamics, rather than using changes in cell physiology (Negrete et al., 2007; Petiot et al., 2016; Zeiser et al., 2000).

Fluorescence spectroscopy has proven useful to monitor cell and product formation, as well as metabolite consumption and production in different biological systems. Examples include prediction of biomass and recombinant protein production in *E. coli* (Schwab et al., 2016) and prediction of product titer, glucose consumption, optical density and overall culture progression in yeast cultures (Karakach et al., 2018; Zabadaj et al., 2017), to name a few. Our group and others have also shown the applicability of fluorescence spectroscopy to monitor viable cell concentration and recombinant protein titers in mammalian cell culture systems (Ohadi et al., 2014, 2015, Teixeira et al., 2011, 2009), or critical quality attributes such as monoclonal antibody aggregation (Schwab & Hesse, 2017).

In this work, we investigate the use of fluorescence spectroscopy as a soft sensor to monitor recombinant adeno-associated virus (rAAV) production in the insect cell-baculovirus expression vector system (IC-BEVS). Soft sensors infer information for process variables that cannot be measured directly based on other measured variables. For fluorescence spectroscopy, the spectra reflect changes in the concentrations of fluorophores such as amino acids, co-factors and vitamins present in the cell culture medium, which can then be correlated with culture progression and viral production. As with other

spectroscopic techniques, fluorescence-based soft sensors require adequate spectra pre-processing combined with multivariate models to predict relevant process variables accurately (reviewed in Glassey, 2013). Chemometrics employs mostly linear methods, but to model the non-linear nature of biological systems, non-linear learning models can be used. These include artificial neural networks (ANN), which have a broad track record of applications to bioprocess monitoring (Contreras-Gómez et al., 2017; Wolf et al., 2001).

Recombinant adeno-associated viruses (rAAV) are increasingly gaining interest as viral vectors for gene therapy. Reasons include their safety profile, long term transgene expression and the existence of several serotypes, which allow transduction of cells from different tissues (Gray et al., 2012). Large-scale manufacturing of rAAV is still a challenge, with several biological systems competing for establishment as the preferred platform for rAAV production. One of those systems is the IC-BEVS, which is well established for manufacturing of recombinant products, with several approved biopharmaceuticals on the market. Advantages of this system include high productivity, scalability and GMP-compatible characteristics (Cox, 2012; Merten, 2016).

Here, we combine *in-situ* fluorescence spectroscopy with ANN models to predict relevant process variables, such as viability and product titer, in the IC-BEVS platform during rAAV production. As mentioned previously, in fluorescence spectroscopy the useful information obtained is highly dependent on adequate spectra pre-processing (Wolf et al., 2001). In the insect cell medium, this is even more relevant due to the existence of a strong background fluorescence signal. As such, a genetic algorithm-based approach was applied to maximize predictive power through optimization of spectra pre-processing, using different combinations of common spectra pre-treatments.

2. Materials and Methods

2.1. Cell line and culture medium

Spodoptera frugiperda Sf9 cells were obtained from Thermo Fisher Scientific (No 11496015) and routinely cultivated in 500 mL glass Erlenmeyer flasks with 50 mL working volume of SF900-II medium (Gibco™), at 27 °C with an agitation rate of 100 rpm in an Innova 44R incubator (orbital motion diameter = 2.54 cm, Eppendorf). Cell concentration and viability were determined using a Cedex HiRes Analyzer (Roche).

HT1080 cells (Agilent), used for titrating infectious rAAV, were maintained in a 37 °C humidified atmosphere incubator with 5 % CO₂ in air, cultured in high glucose DMEM medium (Gibco™) supplemented with 10 % Fetal Bovine Serum (Gibco™).

2.2. Viruses, infection and titration

The recombinant *Autographa californica* nucleopolyhedrovirus encoding the GFP transgene under the control of the cytomegalovirus promoter (CMV-GFP) and flanked by AAV2 inverted terminal repeats (ITR) regions was kindly provided by Généthon and was titrated and amplified *in house* as described for the *rep/cap* baculovirus (below).

The plasmid containing rAAV2 *rep* and *cap* genes was a gift from Robert Kotin (Addgene plasmid #65214) (Smith et al., 2009). Recombinant baculovirus was produced using the Bac-to-Bac® Baculovirus Expression System (Invitrogen), according with manufacturer instructions. Baculovirus amplification was performed infecting exponential growing suspension Sf9 cells at 1×10⁶ cells/mL at a multiplicity of infection (MOI) of 0.01 plaque forming units (pfu) per cell. When cell viability was between 80-85%, culture was harvested and centrifuged at 200 g for 10 min at 4 °C. After discarding the pellet, the supernatant was centrifuged at 2000 g for 20 min at 4 °C, and the resulting supernatant titrated and stored at 4 °C in clarified culture

medium, protected from light and periodically titrated in Sf9 cells using the MTT assay as described elsewhere (Roldão et al., 2009).

Recombinant adeno-associated virus (rAAV) intra and extracellular titer was estimated separately using a commercially available sandwich ELISA kit (Progen Biotechnik GmbH), according to the manufacturer instructions. This kit detects a conformational epitope present in assembled rAAV capsids. Infectious rAAV titer was determined by titrating intra and extracellular samples using the HT1080 cell line. Briefly, 3×10^4 cells were infected with serial dilutions of rAAV virus in 200 μ L DMEM+2% FBS, in 24-well plates. The plate was gently shaken every 30 minutes until 4 hours after infection, at the time a fresh DMEM+12 % FBS was added to reach a final concentration of DMEM+10 % FBS. Cells were harvested 42 hours post-infection, and infectious titer was calculated by determining the percentage of GFP-expressing cells in a flow cytometer (CyFlow Space, Partec).

2.3. Bioreactor cultures and sample processing

Four independent bioreactor runs (BR1-4) were performed using 1 L BIOSTAT® DCU-3 (Sartorius), equipped with two Rushton turbines. Temperature control (27 °C) was achieved using a water recirculation jacket and gas supply was provided by a ring sparger in the bottom of the vessel. Two additional bioreactor cultures (BR5 and 6) were performed using the QPlus system (Sartorius), with a working volume of 0.5 L and equivalent hydrodynamic characteristics to the 1 L bioreactors. Figure II.1 summarizes the experimental methodology: Sf9 cells were inoculated at 0.5×10^6 cells/mL and infected with rAAV2 and GFP-expressing baculoviruses the day after, when cell concentration reached 1×10^6 cells/mL. The progress of infection was monitored *in situ* for the 4 BIOSTAT® cultures using fluorescence spectroscopy. Sf9 infection was performed at varying MOIs (total of 0.02, 0.1 or 10 pfu/cell, with the two baculoviruses in equal proportions). Dissolved

oxygen (DO) concentration was kept at 30 % by controlling the stirring rate (70-270 rpm) and the N₂/air ratios in a mixture of air and N₂ (0.01 vvm).

At each sampling point, cell concentration and viability were measured, and a clarification step was performed (200 g, 10 min, 4 °C). Supernatant was subjected to a further clarification step (2000 g, 20 min, 4 °C) and stored at -80 °C for offline analysis. Cell pellets were used for intracellular rAAV quantification, by extraction with TNT buffer, consisting of 20 mM Tris-HCl (pH 7.5), 150 mM NaCl, 1% Triton X-100, 10 mM MgCl₂ (Smith et al., 2009), to which a 0.5 % solution of sodium deoxycholate was added to further increase the release of intracellular rAAV from pelleted cells (Gray et al., 2012). After 10 minutes of incubation at 22 °C, the suspension was centrifuged (2000 g, 20 min, 4 °C) and the supernatant stored at -80 °C for offline analysis.

2.4. Fluorescence spectra acquisition

Online fluorescence data was acquired *in situ* using a spectrofluorometer (Horiba Jobin Yvon Fluoromax-4) equipped with a bifurcated optical fiber cable. To accommodate the optical fiber, we designed and built *in house* a cylindrical stainless-steel probe which fits into a bioreactor 19 mm top port and accommodates a quartz lens (CVI laser optics) in the bottom, in contact with culture media. The bioreactors were covered with a blackout material to prevent interference of outside light with the fluorescence acquisition. For the 2 Qplus bioreactors, fluorescence acquisition was performed offline in a Tecan Spark® 10 M microplate reader (Tecan Group Ltd), with 250-520 nm excitation range and 280-640 nm emission range.

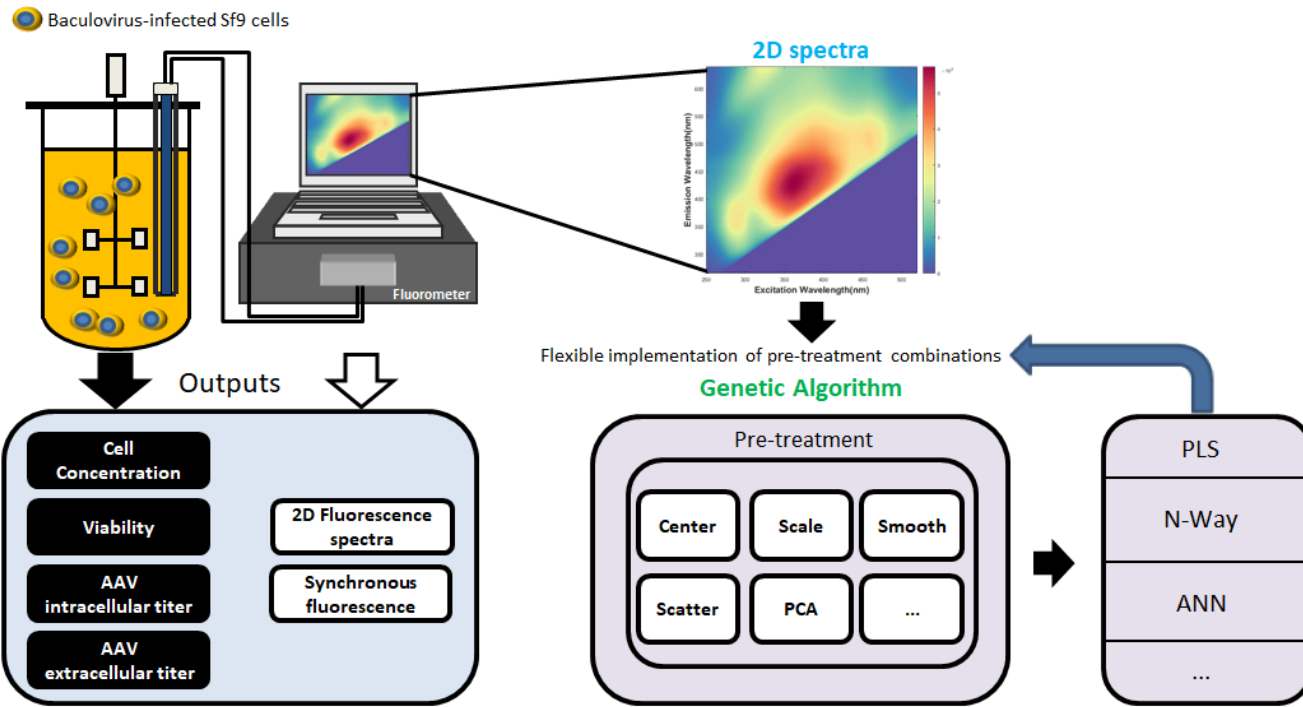


Figure II.1 - Experimental and computational setup. Exponential growing Sf9 cells were cultured in stirred tank bioreactors and co-infected by two baculoviruses (encoding a CMV-GFP gene and AAV rep-cap2 genes). Fluorescence spectra were acquired online using an in-situ probe, connected to the fluorometer through optical fibers. Samples were collected at several culture time points to determine relevant process variables and fluorescence spectra were acquired in two modes (2D maps and synchronous fluorescence). These spectra were pre-processed to maximize predictive power, based on genetic algorithm-guided computational approach. To correlate fluorescence signals with experimental process variables, different prediction models were tested: PLS – partial least squares regression; N-way – multi-way PLS; ANN – artificial neural network regression.

For the 4 BIOSTAT bioreactors, 2D fluorescence maps and synchronous spectra were acquired online (no cell centrifugation) simultaneously to sampling. 2D fluorescence maps were acquired with 5 nm steps in the 250-520 nm excitation range and 265-640 nm emission range. Synchronous fluorescence is a fluorescence acquisition mode in which the difference between excitation and emission ($\Delta\lambda$) is kept constant throughout the scan. In this work we evaluated $\Delta\lambda$ values of 20, 80 and 140 nm, in the 250-520 nm excitation range, with 2 nm steps. Synchronous fluorescence data was concatenated and utilized as one dataset only. Slit widths were set to 2.5 nm for excitation and emission in the two fluorescence acquisition modes.

In addition to acquisitions done simultaneously with sampling, fluorescence spectra were also acquired between two samples to increase the data available for model training. The reference data values for these spectra were estimated using MATLAB (Mathworks Inc, USA) cubic smoothing spline function.

2.5. Spectra pre-processing

Several pre-processing methods for 2D maps and synchronous fluorescence spectroscopy were implemented using *in house* MATLAB code. The choice of the spectra pre-processing combinations that could increase predictive power and increase accuracy of reference data prediction was guided by a genetic algorithm. The pre-treatments available to the genetic algorithm for 2D maps and synchronous fluorescence spectra are listed in Supplementary Table II.1. 2D maps were converted from two- to one-dimensional arrays for pre-processing and algorithm training.

Optimization of the extent of Rayleigh and Raman scattering removal was performed visually, by gradually increasing the excised excitation-emission pairs below and above the excitation wavelength of the known scatter area using the drEEM toolbox (Murphy et al., 2013). The chosen values (60 and

25 nm for 1st and 2nd order Rayleigh and 5 nm for 1st and 2nd order Raman) represent a compromise between extent of scatter removed without loss of important information. For the Qplus the obtained spectra were normalized to the 1 L bioreactors culture medium fluorescence spectrum.

Each data point consists of a 2D map, 3 synchronous fluorescence scans and the corresponding set of reference data (cell concentration, viability, rAAV total concentration, rAAV intracellular percentage and rAAV titer). The sampling time was added to the fluorescence data.

2.6. Artificial neural network (ANN) and partial least squares (PLS) predictors

For the artificial neural networks, partial least squares and principal component analysis (PCA) calculations, MATLAB built-in functions and standard toolboxes were used. ANN models were trained using the Levenberg-Marquardt backpropagation algorithm. To avoid overfitting, only ANN structures with up to two hidden layers were considered, with a maximum of 4 nodes in each layer, in a total of 9 different architectures. Leave-one-batch-out (LOBO) cross-validation was employed by using all batches but one for model training and predicting the remaining batch feeding its fluorescence spectra to the trained model. The optimal number of latent variables for PLS and ANN architecture was obtained by cross-validation. Specifically, for PLS the number of latent variables was increased until the obtained models started overfitting the predicted batches (measured by the normalized root mean squared error of cross-validation (nRMSE_{cv}), normalized to the range of the variable, Equation 1). For ANN, the nRMSE_{cv} was calculated for all predicted batches for each of the 9 architectures, and the one presenting the lowest nRMSE_{cv} was chosen as the optimal model.

$$nRMSEcv = \frac{\sqrt{\frac{\sum_{i=1}^{nsamples} (\hat{y} - y)^2}{nsamples}}}{\max(y) - \min(y)} \quad (1)$$

In equation 1, \hat{y} represents a vector of model-predicted values and y represents the corresponding reference data for the validation set; $nsamples$ is the total number of data points and $\max(y)$ and $\min(y)$ refer to the maximum and minimum values for the standardized reference data, respectively.

The correlation coefficients of calibration and validation (R^2 and Q^2) were calculated according to equations 2 and 3, respectively using calibration ($ncal$) or validation ($nval$) samples. σ^2 represents sample variance and RMSEC and RMSEV stand for root mean-squared error of the calibration and validation set, respectively.

$$RMSEC = \sqrt{\frac{\sum_{i=1}^{ncal} (\hat{y} - y)^2}{ncal}} \quad RMSEV = \sqrt{\frac{\sum_{i=1}^{nval} (\hat{y} - y)^2}{nval}} \quad (2)$$

$$R^2 = 1 - \frac{RMSEC^2}{\sigma^2} \quad Q^2 = 1 - \frac{RMSEV^2}{\sigma^2} \quad (3)$$

2.7. Sensitivity analysis

A Monte Carlo sensitivity analysis was performed to find the fluorescence regions contributing more for the prediction of each process variable. Briefly, for each principal component (PC) of the 2D map obtained after pre-processing, 10000 new data points were generated, with random noise added to that PC with a normal distribution with average and standard deviation calculated from all PC values. The remaining values were kept constant and equal to the average of each PC. ANN outputs for the new data points were computed, and a relative standard deviation, RSD, was

calculated. The Monte Carlo results were converted back to the form of a 2D map by reversing the PCA transformation.

3. Results

3.1. Culture conditions and rAAV production

The main purpose in this study was to correlate fluorescence spectra dynamics with rAAV production in Sf9 cells using the baculovirus expression vector system. In order to build a robust fluorescence-based monitoring platform, a range of culture conditions was covered (Table II.1), including low and high multiplicities of infection (MOI) and the use of different fluorometers for online and offline spectra acquisition. Overall MOIs tested ranged from 0.02 to 10 pfu/cell, yielding between 1.4 and 13.3×10^{10} total rAAV capsids/mL. Infectious rAAV concentration was strongly correlated with total titer ($R^2=0.935$), ranging from 0.8 to 7.4×10^7 infectious rAAV/mL. To improve process understanding, the intra- and extracellular rAAV capsid titer and infectious titer were quantified (Supplementary Figure II.1 C, D and E respectively), as well as cell concentration and viability (Supplementary Figure II.1 A and B, respectively). In order to provide the model with a wider training space, the experiments included common harvest times described in other works (day 3 and 4 post-infection) as well as an extra day of production.

The different experimental conditions translated into a high and desirable experimental variability, where similar trends between cultures can be observed, although with significant differences in rAAV titer and quality profiles.

Table II.1 - Summary of the culture conditions, spectra acquisition mode, maximum total rAAV achieved and number of samples for each batch. The MOI indicated is overall MOI for the culture. The same MOI was used for each baculovirus (rep-cap2 and CMV-GFP), and as such individual MOI for each baculovirus is half of the presented value. Cell samples represent number of samples used to build models for prediction of viability and cell concentration. Product samples represent the number of samples used to build models for prediction of rAAV titer and total rAAV.

Bioreactor number	Fluorescence acquisition mode	Overall MOI (pfu/cell)	Day of harvest	Maximum rAAV (10^{10} total capsids/mL)	Maximum infectious rAAV (10^7 infectious rAAV/mL)	2D spectra		SF spectra	
						Cell samples	Product samples	Cell samples	Product samples
1	Online	0.02	4	1.4	0.8	27	15	27	16
2	Online	0.1	5	13.3	6.4	33	28	33	28
3	Online	0.1	5	12.4	7.4	34	26	52	42
4	Online	0.1	5	4.9	2.9	35	21	33	20
5	Offline	0.02	5	1.7	1.7	13	5	NA	NA
6	Offline	10	5	1.7	2.5	13	5	NA	NA

rAAV – recombinant adeno-associated virus; MOI – multiplicity of infection (pfu/cell); CMV-GFP - GFP transgene under the control of the cytomegalovirus promoter; pfu=plaque forming units; NA – not applicable.

3.2. Fluorescence spectra dynamics

Despite the differences in the experimental determination of process variables, common trends in the temporal fluorescence profiles for all cultures were identified (Figure II.2). Although some fluorescence regions have a clear trend over culture time, either with decreasing intensity (e.g. excitation/emission pair 290/350 nm, corresponding to tryptophan) or increasing intensity (e.g. 440/530 nm, corresponding to riboflavin), overall most fluorescence regions associated with important co-factors and vitamins are difficult to correlate with process variables using univariate analysis methods. Nevertheless, fluorescence regions correlated with cell viability profiles could be identified in the spectra with the two fluorescence acquisition methods evaluated: 2D maps (Figure II.2 A, riboflavin region) and synchronous fluorescence (Figure II.2 B), highlighting the potential of this spectroscopy for real-time monitoring in this system.

3.3. Fluorescence-based ANN models can predict important process variables

The first approach into developing 2D fluorescence-based models for rAAV production was based on the four online bioreactors. When coupled with PCA and adequate spectra pre-processing, ANN models yielded good predictions that captured the correct trend of the experimental data for all relevant process variables (Figure II.3).

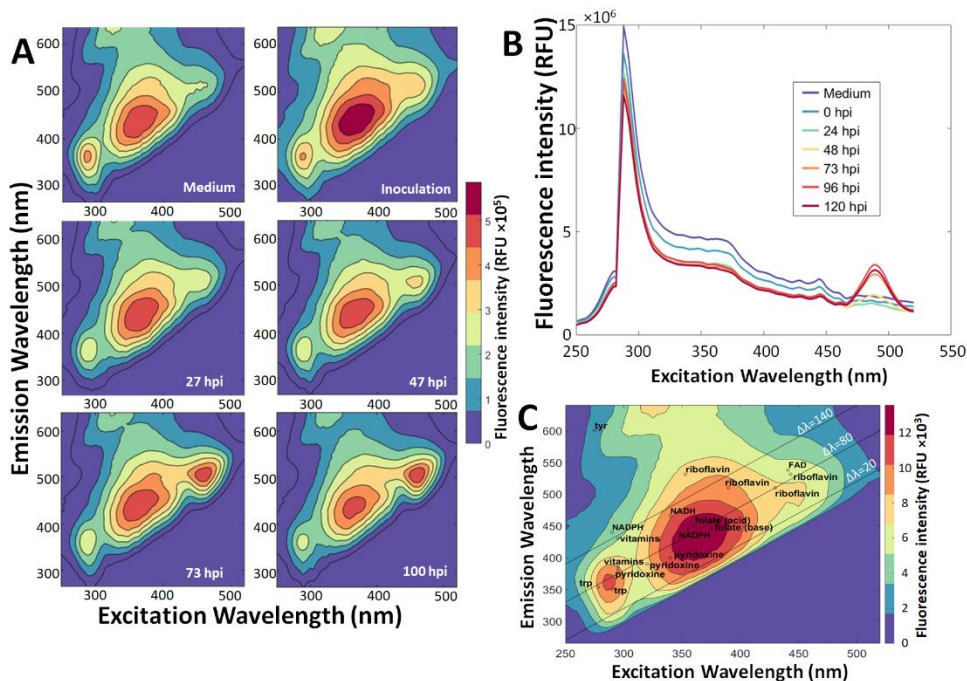


Figure II.2 - Representative fluorescence spectra collected at different time points. (A) 2D fluorescence maps; (B) Synchronous fluorescence spectra, with $\Delta\lambda$ of 20 nm; (C) 2D map for the culture media with indication of synchronous fluorescence regions used (black lines) and expected location for known fluorophores.

The best prediction model was obtained for cell viability, with a nRMSEcv of 4% (Figure II.3 A). The nRMSEcv was 7% for both extracellular rAAV titer and viable cell concentration models (Figure II.3 B and C) and 16% for total rAAV concentration (Figure II.3 D), which are good predictions considering the demanding leave-one-batch-out validation strategy used and the variability of the dataset. For each variable, the number and size of hidden layers in the ANN model was optimized (limited to 2 hidden layers and 4 nodes per layer) and different pre-processing combinations were used, as indicated in Supplementary Table II.2.

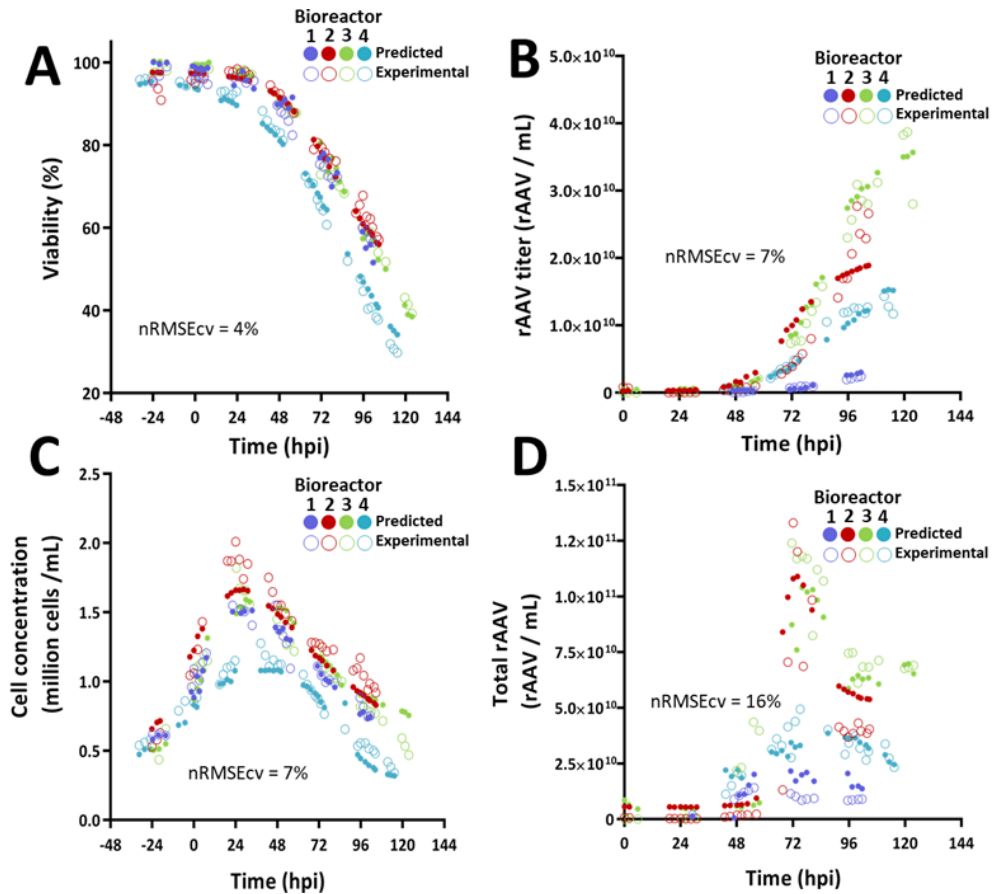


Figure II.3 - Experimental and predicted values for four bioreactor runs using online 2D fluorescence maps and artificial neural network (ANN) models. **(A)** Cell viability; **(B)** Extracellular rAAV titer; **(C)** Viable cell concentration; **(D)** Total rAAV concentration (intra and extracellular rAAV). Model-predicted values for a bioreactor are based on ANN models trained using data from the other three bioreactors (leave-one-batch-out cross-validation). Colors represent different batches, open circles represent experimental data and filled circles show model predictions. The different ANN architectures and the spectra pre-processing used are described in Supplementary Table II.2.

The culture time was used as an input variable, in addition to the 2D maps, which improved accuracy of model predictions (Supplementary Table II.3).

Similarly to 2D maps, synchronous fluorescence spectra can be used with ANN models to predict process variables (Supplementary Figure II.2). Nevertheless, when all culture predictions are considered, predictors based on 2D maps are more accurate than those based on synchronous fluorescence, despite the similar nRMSE_{cv} (Table II.2), indicating the former contain important spectral information missing in the synchronous spectra.

The final ANN models were benchmarked against linear partial least squares (PLS) regression models. The non-linearity of the system is confirmed in the inability of using PLS for modeling, translating into much higher nRMSE_{cv} values (Table II.2).

Table II.2 - Comparison of ANN and PLS regression models for different process variables, using 2D and synchronous fluorescence data for the four online cultures (bioreactors 1-4). Values represent the cross-validation error calculated using leave-one-batch-out after optimization of pre-processing. For ANN models, values in parentheses represent the ANN architecture, e.g., an ANN with two hidden layers, with 3 nodes on the first one and 2 nodes on the second layer would be represented as (3 2). For PLS models, values in parentheses represent the number of latent factors.

Predicted Variable	2D		SF
	ANN	PLS	ANN
Cell concentration	11% (4 1)	19% (2)	9% (2)
Viability	4% (2)	14% (3)	4% (1)
Total rAAV concentration	16% (2 3)	28% (1)	14% (4)
% Intracellular rAAV	16% (4)	26% (2)	14% (3 2)
rAAV extracellular titer	7% (3 2)	22% (1)	7% (4)

ANN – artificial neural network; PLS – partial least squares; 2D –two-dimensional fluorescence data; SF – synchronous fluorescence data; rAAV – recombinant adeno-associated virus.

3.4. Assessment of model robustness and fluorescence regions important for prediction

Model robustness was assessed by performing bioreactor cultures with variable profiles and acquiring fluorescence data in two different fluorometers (Table II.1). As before, ANN models with a leave-one-batch-out validation strategy were used and pre-processing was optimized guided by a genetic

algorithm. The resulting predictive models for the complete dataset (Figure II.4) showed similar predictive capabilities (as shown by the nRMSEcv) to the models using online fluorescence data only. This demonstrates that fluorescence data from different fluorometers can be combined for model training, independently of the fluorometer or culture condition, when combined with adequate pre-processing, tailored for each process variable (see also Supplementary Figure II.3).

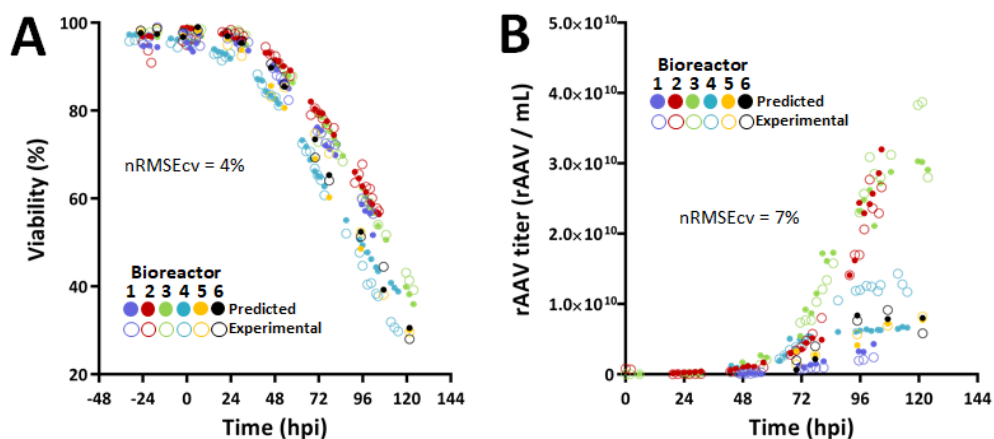


Figure II.4 - Assessment of fluorescence models robustness by combination of fluorescence data acquired in different fluorometers. Fluorescence spectra for bioreactors 1-4 was acquired online, whereas for bioreactors 5 and 6 this data was acquired offline in another fluorometer. (A) Cell viability; (B) rAAV extracellular titer. Colors represent different batches, open circles represent experimental data and filled circles show model predictions. The different artificial neural network (ANN) architectures used are the same as in Figure 3 A-B, respectively, and the spectra pre-processing combinations used are described in Supplementary Table II.2.

Sensitivity analysis using Monte Carlo simulations highlights that the most important excitation-emission pairs are different for each predicted process variable (Figure II.5). The metabolites associated with each region provide information which can be used for process improvement. Noteworthy, the

sensitivity analysis results are highly associated with the PCA coefficients for each variable (Supplementary Figure II.4).

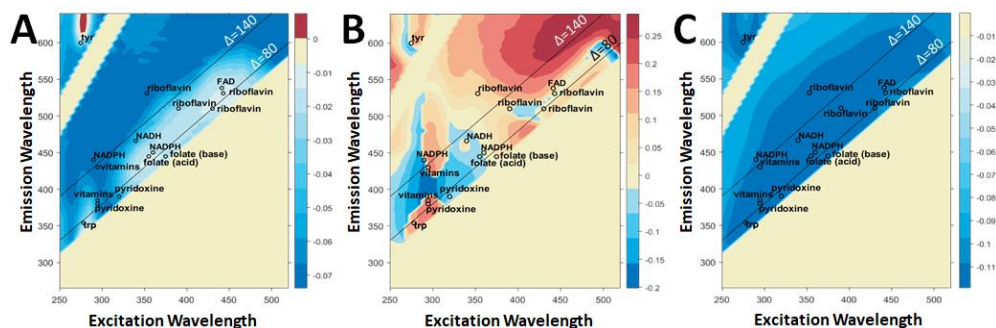


Figure II.5 - Regions of the fluorescence spectra more meaningful for prediction based on Monte Carlo simulations using the artificial neural network (ANN) models from Figure 3. **(A)** Cell viability; **(B)** Total rAAV concentration; **(C)** Extracellular rAAV titer. Expected location for known fluorophores is indicated in black. Black lines represent synchronous fluorescence regions using a $\Delta\lambda$ of 80 and 140. Monte Carlo sensitivity scores are colored according to their positive (red) or negative (blue) values, which arise from the principal component scores and the relative standard deviation (RSD) obtained for each principal component after Monte Carlo.

4. Discussion

The aim of this study was the development of a fluorescence spectroscopy-based approach to monitor rAAV production in IC-BEVS to enable PAT implementation in this system. Fluorescence spectra predictive power was maximized through a combination of pre-processing techniques, efficiently circumventing the strong fluorescence background of insect cell culture medium to predict rAAV production profiles and supporting the time of harvest decision, an important process parameter for virus-based processes (Grein et al., 2018; Nikolay et al., 2018).

The best time of harvest is dependent on many different factors. These include not only bioprocess parameters like cell concentration at infection (CCI), MOI and culture medium, but also the baculovirus construct, making it

difficult to draw general conclusions. In previous reports (Aucoin et al., 2006, 2007; Meghrous et al., 2005), the maximum rAAV total and infectious titer was obtained at 72 hpi, using a high MOI. Here, using a low MOI strategy, the maximum rAAV total and infectious titer were achieved at the same culture time. Additionally, the aforementioned reports found a plateau in infectious rAAV concentration after 72 hpi, whilst in this work infectious titer peaks at 72 hpi, and then decreases (Supplementary Figure II.1 E). The concentration of infectious rAAV particles is a critical determinant of the product quality, and as such the knowledge of the process variables that affect it is critical to obtain higher rAAV quality. This decrease in infectious rAAV titer can be explained with the decrease in cell viability upon baculovirus-induced cell lysis and the consequent release of proteases to the culture medium, to which rAAV is sensitive (Florencio et al., 2015). Therefore, to have a process able to monitor in real-time the decrease of viability of infected cells is critical to ensure rAAV infectious titers remain at their peak.

The high complexity of the cell culture medium, together with its strong fluorescence signal, justifies a two-fold approach for developing fluorescence spectroscopy-based tools for real-time monitoring in this system: first, increasing the predictive power of the fluorescence spectra, by optimizing spectra pre-processing; second, to make use of PCA and chemometric tools for dimensionality reduction and correlation of relevant fluorescence regions with process variables.

The first approach was guided by a genetic algorithm. Although a widely used computational technique for numerous applications, the use of genetic algorithms for optimization of fluorescence spectra pre-processing has not been reported before. Based on pre-processing combinations optimized for each model (Supplementary Table II.2), we concluded that for 2D matrices, dividing each excitation-emission pair by its integral and standard deviation for all samples was one of the most important pre-processing steps.

Subtracting the average of emission wavelengths and scaling by standard deviation of excitation wavelengths, or vice-versa, was also a pre-processing combination useful for model prediction, since in the same step information from excitation and emission wavelengths for all samples is considered. These are scaling approaches which minimize the effects of variability among different spectra acquisitions and batches. Performing a PCA reduction to manage the highly redundant 2D maps before training the ANN model (Teixeira et al., 2009; Zabadaj et al., 2017) greatly improved not only the prediction but also the time needed for model training.

As a viral-dependent production process, the system under study is characterized by non-linear dynamics (Roldão et al., 2007), which can be perceived in the viable cell concentration and total rAAV titer profiles (Figure II.3 C and D respectively). In particular, cell concentration increases significantly in the beginning of the culture when the fluorescence spectra show less variation. Additionally, fluorescence spectra can present fluorophore overlapping and inner-filter effects, further increasing non-linear behavior (Teixeira et al., 2009). As such, the second approach was based on the use of non-linear modeling tools combined with chemometrics for process monitoring. Specifically, artificial neural networks (ANN) were tested and benchmarked against partial least squares (PLS) regression, a standard linear model for chemometrics (Teixeira et al., 2009). In PLS, the aim is to maximize the relationship between inputs (fluorescence spectra) and outputs (variables to predict). This is achieved by extracting the most relevant information from the input data in the form of latent variables, hence simultaneously offering dimensionality reduction, by transforming the N input variables into M orthogonal latent factors or principal components ($M \leq N$). The ideal number of latent factors is determined to prevent overfitting. Unlike PLS, ANN can describe non-linear relationships between inputs and outputs. To do so, an ANN has a number of hidden layers, each with a number of nodes

with variable connectivity. The nodes on the input layer receive the inputs and apply a non-linear transformation to the data. According to the results of the transformation, these nodes will activate specific nodes on the subsequent layer until the output layer is reached. The number of hidden layers and the number of nodes in each layer is adjusted by testing several configurations in training and validation data.

Linear models based on PLS regression did not predict well process variables using leave-one-batch-out (LOBO) cross-validation, a consequence of the system non-linearity (Table II.2). To use the 2D fluorescence maps in their 2D format, rather than converting them in one-dimensional arrays (Teixeira et al., 2009), N-way PLS was also tested (Murphy et al., 2013). However, the results obtained were similar to PLS, and consequently PLS was preferred. ANN have been used previously to model non-linear interactions in bioprocesses, including also in the IC-BEVS (Contreras-Gómez et al., 2017; Wolf et al., 2001), and therefore were chosen for chemometric modeling.

The best predictors were obtained for viability and extracellular rAAV concentration, variables which have an expected higher impact on extracellular medium composition and thus on the supernatant fluorescence. Viability profiles in the beginning of the culture have less accurate predictions (Figure II.3 A) because there is no significant release of the fluorescent compounds into the culture medium before cells start lysing. Model-based prediction of variables such as cell concentration or intracellular rAAV accumulation based on secretion and uptake of fluorescent metabolites is less direct, and highly dependent on the quality of the obtained spectra and the number of batches. Still, both biomass and assembled rAAV particles have fluorescent compounds in their composition. In fact, according to published data regarding AAV2 capsid composition (UniProt, 2002), 12 % of the assembled AAV capsid is composed of the fluorescent amino acids tryptophan, phenylalanine and tyrosine. One possible strategy to improve

prediction of cell concentration and total rAAV concentration would be to use two *in-situ* probes, combining fluorescence and dielectric spectroscopy. In this way, medium components information from the fluorescence probe could be combined with the cell concentration and cell physiology information from the capacitance probe, which has proven useful for insect cell culture (Negrete et al., 2007; Petiot et al., 2016; Zeiser et al., 2000).

The robustness of the fluorescence-based models is confirmed by prediction of the rAAV titer for a bioreactor with a low production profile (Figure II.3 B and D, bioreactor 1), using fluorescence data from the other batches. The similar prediction ability when using fluorescence spectra from different fluorimeters and from cultures with dissimilar rAAV production profiles at high and low MOIs (Figure II.4 and Table II.1) also sustain the claim that adequate pre-processing is critical for accurate predictions (Supplementary Figure II.3), allowing combination of data from different fluorimeters. As expected, when adding the fluorescence spectra acquired from the different fluorimeters, a better model was obtained when normalization to culture medium was performed. Taken together, this work demonstrates that fluorescence-based models, coupled with adequate spectra pre-processing, are robust and can be used to detect deviations to a standard rAAV production profile in the IC-BEVS.

One disadvantage of using 2D maps is the lengthier spectra acquisition time (22 minutes per sample). As such, the suitability to apply synchronous fluorescence for this system was assessed. Synchronous fluorescence allows faster spectra acquisition (1.5 minutes per sample) by focusing on excitation-emission pairs with a fixed offset between them ($\Delta\lambda$) (Teixeira et al., 2011). The acceptable predictions obtained (Supplementary Figure II.2), coupled with the knowledge of the spectral regions more important for prediction, can make this a valid strategy to support PAT implementation in this system (Pais et al., 2014; Teixeira et al., 2011). However, 2D maps-based

models yielded better predictions, since the ones based on synchronous fluorescence were not able to capture rAAV titer production trends for some batches nor provide predictions for complex variables such as rAAV total titer (Supplementary Figure II.2 B). Identifying the $\Delta\lambda$ which captures a higher amount of relevant process information together with incorporation of more bioreactor data in training models will prove useful to address this issue.

The most important fluorescence spectra regions for each process variable were evaluated using Monte Carlo simulations, highlighting differences for each of the variables under study (Figure II.5). The corresponding fluorophores associated to each region may provide valuable insights for process understanding. However, the fluorescence of a compound is highly dependent on culture medium composition, pH and temperature. While other fluorophores which also contribute to the overall spectra may exist in the identified regions, for simplicity the most commonly identified in culture media were considered.

The predictors for cell viability are correlating the release of intracellular compounds (e.g. NAD(P)H, riboflavin or tyrosine) with the decrease in cell viability, which is also confirmed by the negative sensitivity scores (Figure II.5 A); indeed, NADH-dependent fluorescence has been reported to be used for monitoring the progress of baculovirus infection (Zeiser et al., 1999). Fluorescence regions for these metabolites are identified in the sensitivity analysis as having a lower importance for the prediction than whole regions of the spectra which do not correspond to known fluorophores. This may be because the PCA reduction captured the background signal (mainly unchanged regions), which the model uses to establish the baseline value for prediction. Then, the information contained in the fluorophore regions is used to adjust the prediction over time for each bioreactor.

Because changes in cell viability are associated with release of rAAV to the supernatant, many of the most important excitation-emission pairs for extracellular rAAV prediction are common to those important for viability (Figure II.5 C).

For total rAAV concentration (Figure II.5 B), interpretation of the results is not straightforward due to the rAAV production profile, which increases until 72 hpi followed by a decrease and plateau throughout the remaining culture time (Figure II.3 D). Still, fluorescence regions corresponding to NAD(P)H, riboflavin, tryptophan and tyrosine also have large absolute sensitivity scores, which are likely related to the increased metabolic needs required for rAAV production and amino acid incorporation into viral particles. The fact that NAD(P)H regions appear as important for rAAV production can be a consequence of the modulation of energetic metabolism by baculovirus infection, independently of the transgene carried by the baculovirus (Zeiser et al., 1999). Another region that is also important for the model is approximately at 300 nm excitation and 360 nm emission wavelengths. This region likely corresponds to rAAV fluorescence, based on the 2D fluorescence map of a purified rAAV2 solution in PBS. In this solution, the fluorescence signal in the regions between 270-300 nm excitation and 310-370 nm emission wavelength was higher than in the PBS control, likely due to fluorescence signal of the amino acids incorporated into the assembled rAAV capsid, whose fluorescence signal changes when integrated in a protein (Teixeira et al., 2009). This finding was confirmed in the work of (Fu et al., 2019), in which AAV empty and full capsid separation was monitored using a fluorescence detector with excitation wavelength of 280 nm and emission wavelength of 350 nm.

5. Conclusions

The present study reports for the first time the use of fluorescence spectroscopy as a soft sensor to monitor recombinant adeno-associated virus (rAAV) production in the insect cell-baculovirus expression system (IC-BEVS). Using a combination of spectra pre-processing methods and artificial neural network models, prediction of important process variables such as cell viability, rAAV titer and intra and extra rAAV concentration was achieved. Monitoring the rAAV production process online allows determination of the best time for harvest to maintain rAAV infectivity, as well as detection of deviations from the expected batch profile.

The straightforward implementation of fluorescence spectroscopy coupled with a suitable data analysis framework and the substantial information it provides from rapid culture medium measurements renders this spectroscopic technique a powerful tool for bioprocessing monitoring. As such, this demonstration of fluorescence spectroscopy for real-time monitoring can be applicable to other rAAV serotypes and biopharmaceuticals produced in the IC-BEVS.

Overall, this demonstration of fluorescence spectroscopy as a tool for real-time monitoring and for improving process understanding represents one step further towards a process analytical technology (PAT) implementation for rAAV production in the IC-BEVS.

6. Acknowledgements

Financial support for this work was provided by the Portuguese “*Fundação para a Ciência e Tecnologia*” through individual PhD grant PD/BD/105873/2014 and project grant EXPL/BBBBIO/1129/2013. iNOVA4Health Research Unit (LISBOA-01-0145-FEDER-007344), which is

cofounded by *Fundação para a Ciência e Tecnologia / Ministério da Ciência e do Ensino Superior*, through national funds, and by FEDER under the PT2020 Partnership Agreement, is acknowledged.

The authors would like to acknowledge Généthon for kindly providing the CMV-GFP baculovirus, as well as Dr. Otto Merten, Prof. José Cardoso Menezes and Dr. Matthias Hebben for comments and useful discussions on this work.

The authors wish to thank Marcos Sousa and Paulo Galvão for their support in the bioreactor process, and Tiago Escobar for the help building the fluorescence stainless steel probe.

7. Supplementary Data

Supplementary Table II.1 – Complete list of pre-processing steps available for the genetic algorithm, for 2D maps and synchronous spectra.

2D spectra	Synchronous fluorescence
Divide by the integral of map	Divide by the integral of sample
Subtract sample average	Subtract sample average
Divide by sample standard deviation	Divide by sample standard deviation
Normalize each sample by its maximum	Divide by integral per wavelength
Divide by integral per excitation wavelength	Subtract average by wavelength
Divide by integral per emission wavelength	Divide by standard deviation of wavelength
Subtract average by excitation wavelength	Subtract or divide by culture medium spectra
Subtract average by emission wavelength	Normalize each sample by its maximum
Divide by standard deviation of emission wavelength	Moving average smoothing
Divide by standard deviation of excitation wavelength	PCA reduction
Subtract or divide by culture medium spectra	
Subtract average and divide by standard deviation for excitation-emission wavelength pairs	
Smooth using moving average	
Remove Rayleigh scatter (1 st and 2 nd order)	
Remove Raman scatter (1 st and 2 nd order)	
Interpolate the removed scatter values using the remaining spectra	
PCA reduction	

Supplementary Table II.2 – Optimal pre-processing combinations, number of PCA components and ANN architectures used for each model. For ANN, values in parentheses represent the ANN architecture, e.g., an ANN with two hidden layers, with three nodes on the first one and two nodes on the second layer would be represented as (3 2). R^2 and Q^2 were calculated according to equations 2 and 3 from main text, and indicate the correlation coefficients of calibration and validation, respectively.

Model	Figure	Pre-processing combinations	Number of PCA components (ANN architecture)	R^2	Q^2	Total data points
Viability (2D data, 4 BR) nRMSE _{cv} =4 %	Figure II.3 A / Supplementary Figure II.3 C	Removed Rayleigh 1 st and 2 nd order scatter; subtracted average and divided by standard deviation of excitation-emission wavelength pairs; subtracted average of excitation wavelengths and divided by standard deviation of emission wavelengths; samples normalized by their maximum; reduced by PCA.	2 (2)	0.99	0.98	129
rAAV titer (2D data, 4 BR) nRMSE _{cv} =7 %	Figure II.3 B	Removed Rayleigh and Raman 1 st and 2 nd order scatter; subtracted average and divided by standard deviation of excitation-emission wavelength pairs; subtracted average of excitation wavelengths and divided by standard deviation of emission wavelengths; smoothed using moving average and reduced by PCA.	3 (3 2)	0.99	0.93	89
Viable cell concentration (2D data, 4 BR) nRMSE _{cv} =7 %	Figure II.3 C	Removed Rayleigh 1 st and 2 nd order scatter and Raman 1 st order scatter, and interpolated removed values using remaining spectra; subtracted average and divided by standard deviation of excitation-emission wavelength pairs; divided each sample by the culture medium spectrum; subtracted average of emission wavelengths and divided by standard deviation of excitation wavelengths; reduced by PCA.	2 (4)	0.97	0.90	129
Total rAAV concentration (2D data, 4 BR) nRMSE _{cv} =16 %	Figure II.3 D	Removed Rayleigh and Raman 1 st and 2 nd order scatter and interpolated removed values using remaining spectra; subtracted for each sample the culture medium spectrum; subtracted average and divided by standard deviation of excitation-emission wavelength pairs; divided emission wavelengths by their standard deviation; smoothed using moving average and reduced by PCA.	4 (2 3)	0.97	0.82	90

Supplementary Table II.2 (cont.)

Model	Figure	Pre-processing combinations	Number of PCA components (ANN architecture)	R ²	Q ²	Total data points
Viability (2D data, 6 BR) nRMSEcv=4 %	Figure II.4 A	Removed Rayleigh and Raman 2 nd order scatter and Rayleigh 1 st order, and interpolated removed values using remaining spectra; divided each sample by the culture medium spectrum; subtracted average and divided by standard deviation of excitation-emission wavelength pairs; smoothed using moving average and reduced by PCA.	9 (2)	0.99	0.98	155
rAAV titer (2D data, 6 BR) nRMSEcv=7 %	Figure II.4 B	Removed Rayleigh and Raman 1 st and 2 nd order scatter, and interpolated removed values using remaining spectra; Subtracted the culture medium spectrum for each sample; subtracted the average and divided for standard deviation for the emission wavelengths; calculated the integral of the sample spectrum along the emission wavelength; reduced by PCA.	6 (3 2)	0.99	0.91	98
Viability (SF data, 4 BR) nRMSEcv=4 %	Supplementary Figure II.2 A	Subtracted average per sample; divided each sample by the culture medium spectrum and by integral per wavelength; samples normalized by their maximum PCA reduction.	4 (1)	0.99	0.98	145
rAAV titer (SF data, 4 BR) nRMSEcv=7 %	Supplementary Figure II.2 B	Subtracted average per sample; subtracted culture medium spectrum from each sample; samples normalized by their maximum and reduced by PCA.	5 (4)	0.99	0.95	104
Viable cell concentration (SF data, 4 BR) nRMSEcv=9 %	Supplementary Figure II.2 C	Divided each sample by the culture medium spectrum, by the integral per wavelength and by sample standard deviation; samples normalized by their maximum and reduced by PCA.	1 (2)	0.70	0.84	147

Supplementary Table II.2 (cont.)

Model	Figure	Pre-processing combinations	Number of PCA components (ANN architecture)	R ²	Q ²	Total data points
Total rAAV concentration (SF data, 4 BR)	Supplementary Figure II.2 D	Divided each sample by its integral and by culture medium spectrum, and reduced by PCA	4 (4)	0.97	0.75	106

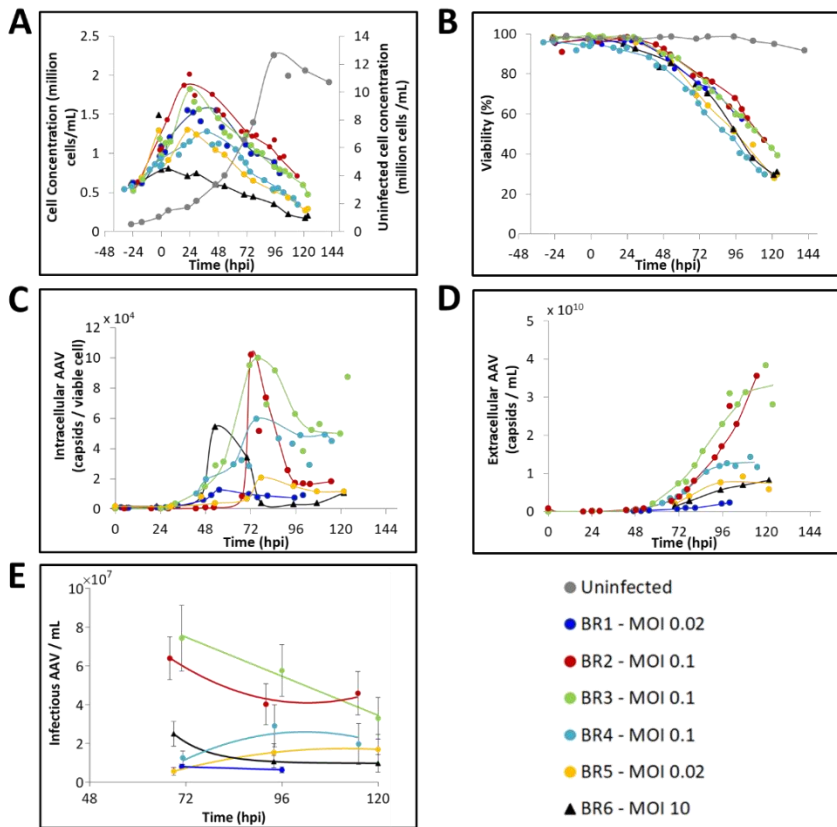
nRMSEcv=14 %

PCA – principal component analysis; ANN – artificial neural network; 2D – two-dimensional fluorescence data; BR - bioreactor; rAAV -recombinant adeno-associated virus; SF – synchronous fluorescence data.

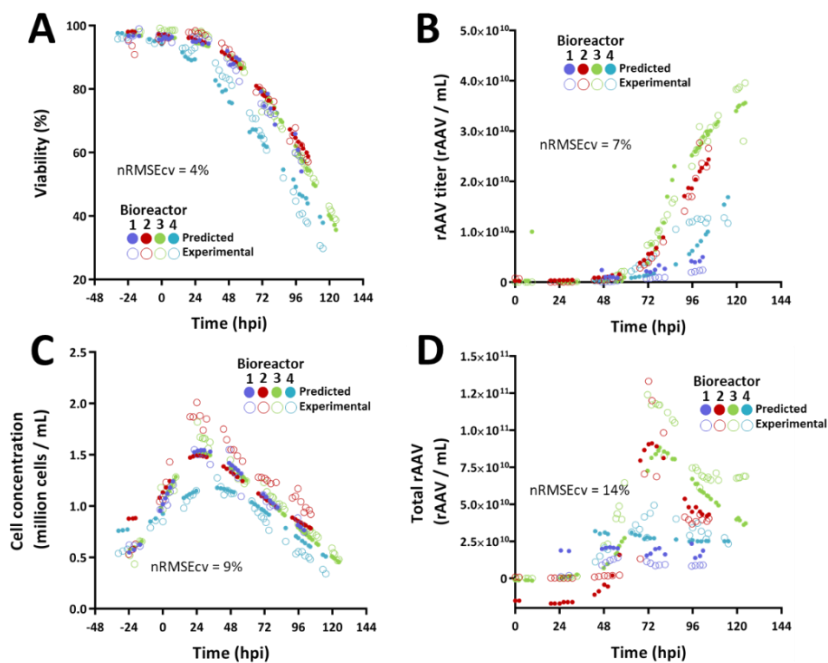
Supplementary Table II.3 - Comparison of ANN models for different process variables with and without adding culture time as a predictor variable, using the 2D fluorescence data for the four online bioreactors. Values represent the cross-validation error calculated using leave-one-batch-out after optimization of pre-processing and ANN structure for each model. For ANN, values in parentheses represent the ANN architecture, e.g., an ANN with two hidden layers, with three nodes on the first one and two nodes on the second layer would be represented as (3 2).

Predicted variable	nRMSEcv using time (ANN architecture)	nRMSEcv without using time (ANN architecture)
Viable cell concentration	7 % (4)	18 % (4)
Cell viability	4 % (2)	16 % (2 2)
rAAV extracellular titer	7 % (3 2)	9 % (1)
Total rAAV titer	16 % (2 3)	15 % (4)
Intracellular rAAV fraction	16 % (4)	21 % (2 3)

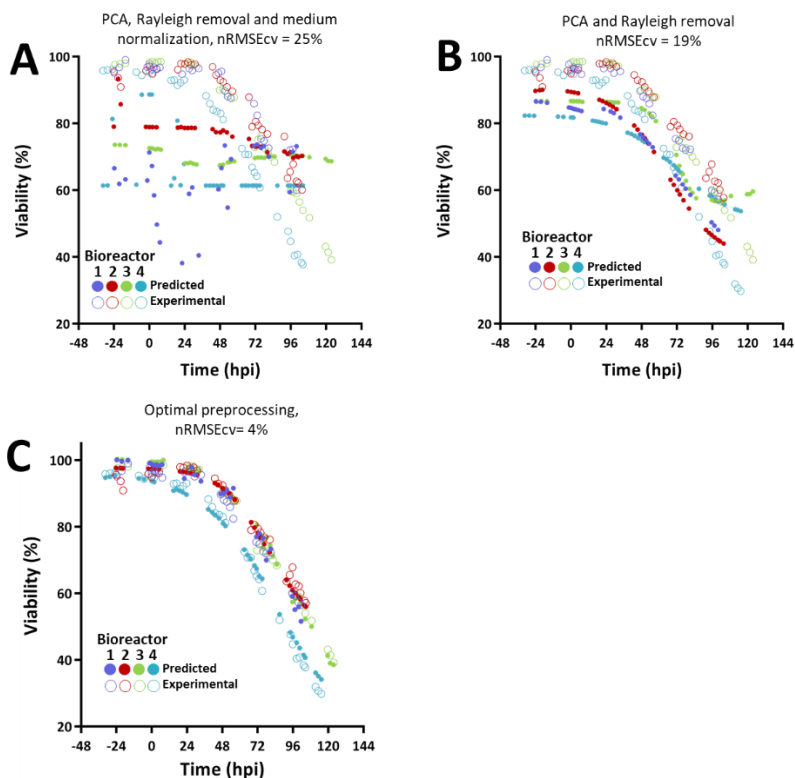
ANN – artificial neural network; 2D – two-dimensional fluorescence data; rAAV – recombinant adeno-associated virus; nRMSEcv - normalized root mean squared error of cross-validation.



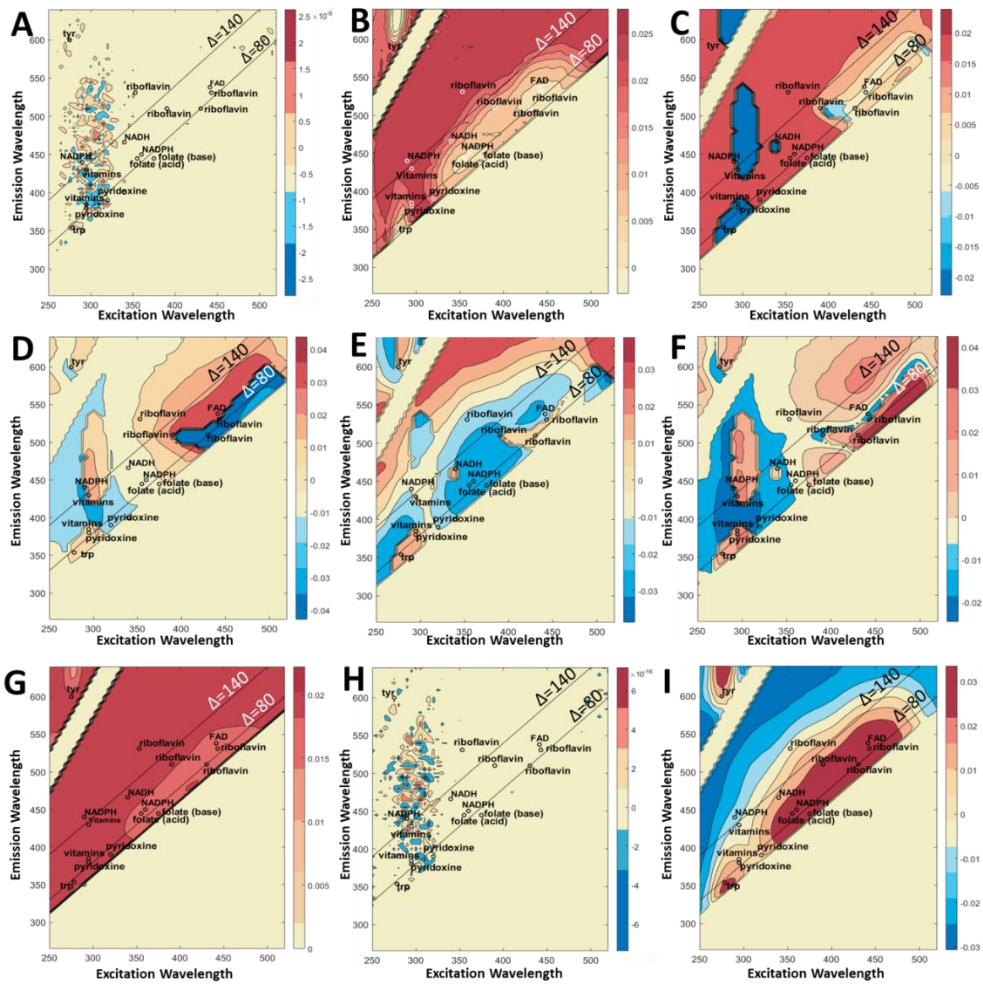
Supplementary Figure II.1 - Time course profiles for the experimentally determined process variables for all cultures. (A) Viable cell concentration; (B) Cell viability; (C) Intracellular rAAV titer; (D) Extracellular rAAV titer; (E) Infectious rAAV titer (intra- and extracellular); error bars represent standard error propagated from measurement replicates). hpi - hours post-infection.



Supplementary Figure II.2 - Experimental and predicted values for four bioreactor runs using online synchronous fluorescence spectra and artificial neural network (ANN) models. **(A)** Cell viability; **(B)** rAAV extracellular titer; **(C)** Viable cell concentration; **(D)** Total rAAV concentration (intra and extracellular rAAV). Model-predicted values for a bioreactor are based on ANN models trained using the other three bioreactors data (leave-one-batch-out cross-validation). Colors represent different batches, open circles represent experimental data and filled circles show model predictions. The different ANN architectures and spectra pre-processing used are described in Supplementary Table II.2.



Supplementary Figure II.3 - Example of the importance of pre-processing for 2D fluorescence maps and ANN models. Choosing one of the optimized models (Figure II.3 A, viability prediction), we kept the optimal ANN architecture for that model but tested standard fluorescence spectra pre-processing before batch prediction. Pre-processing used are as follows: (A) PCA, 1st and 2nd order Rayleigh removal and medium normalization, $R^2=0.97$, $Q^2=-0.62$; (B) Same as before, without medium normalization, $R^2=0.88$, $Q^2=0.61$; (C) Optimal pre-processing (Supplementary Table II.2), $R^2=0.99$, $Q^2=0.98$.



Supplementary Figure II.4 - Principal components (PC) loadings for each of the 2D maps excitation-emission pairs: (A) and (B) - First and second PC loadings for viability; (C), (D), (E), (F) – second, third and fourth PC loadings for total rAAV concentration; (G), (H), (I) – First, second and third component coefficients for rAAV titer. Maps are colored according to their positive (red) or negative (blue) values, which arise from the principal component scores.

8. References

- Abu-Absi, N. R., Martel, R. P., Lanza, A. M., Clements, S. J., Borys, M. C., & Li, Z. J. (2014). Application of spectroscopic methods for monitoring of bioprocesses and the implications for the manufacture of biologics. *Pharmaceutical Bioprocessing*, 2(3), 267–284. <https://doi.org/10.4155/pbp.14.24>
- Aucoin, M. G., Perrier, M., & Kamen, A. A. (2006). Production of Adeno-Associated Viral Vectors in Insect Cells Using Triple Infection: Optimization of Baculovirus Concentration Ratios. *Biotechnol. Bioeng*, 95(6), 1081–1092. <https://doi.org/10.1002/bit.21069>
- Aucoin, M. G., Perrier, M., & Kamen, A. A. (2007). Improving AAV vector yield in insect cells by modulating the temperature after infection. *Biotechnology and Bioengineering*, 97(6), 1501–1509. <https://doi.org/10.1002/bit.21364>
- Chopda, V. R., Pathak, M., Batra, J., Gomes, J., & Rathore, A. S. (2017). Enabler for process analytical technology implementation in *Pichia pastoris* fermentation: Fluorescence-based soft sensors for rapid quantitation of product titer. *Engineering in Life Sciences*, 17(4), 448–457. <https://doi.org/10.1002/elsc.201600155>
- Contreras-Gómez, A., Beas-Catena, A., Sánchez-Mirón, A., García-Camacho, F., & Molina Grima, E. (2017). The use of an artificial neural network to model the infection strategy for baculovirus production in suspended insect cell cultures. *Cytotechnology*, 70, 555–565. <https://doi.org/10.1007/s10616-017-0128-x>
- Cox, M. M. J. (2012). Recombinant protein vaccines produced in insect cells. *Vaccine*, 30(10), 1759–1766. <https://doi.org/10.1016/j.vaccine.2012.01.016>
- FDA. (2004). Guidance for industry: PAT — a framework for innovative pharmaceutical development, manufacturing, and quality assurance. Retrieved from <https://www.fda.gov/downloads/Drugs/GuidanceComplianceRegulatoryInformation/Guidances/UCM070305.pdf>
- Florencio, G. D., Precigout, G., Beley, C., Buclez, P.-O., Garcia, L., & Benchaouir, R. (2015). Simple downstream process based on detergent treatment improves yield and in vivo transduction efficacy of adeno-associated virus vectors. *Molecular Therapy - Methods & Clinical Development*, 2(15024). <https://doi.org/10.1038/mtm.2015.24>
- Glasse, J. (2013). Multivariate Data Analysis for Advancing the Interpretation of Bioprocess Measurement and Monitoring Data. In *Adv Biochem Eng Biotechnol Vol. 132* (pp. 167–191). https://doi.org/10.1007/10_2012_171
- Gray, S. J., Choi, V. W., Asokan, A., Haberman, R. A., Thomas, J., & Samulski, R. J. (2012). Production of Recombinant Adeno-Associated Viral Vectors and Use in In Vitro and In Vivo Administration. *Current Protocols in Neuroscience*, Oct(Chapter: Unit4.17), 1–36. <https://doi.org/10.1002/0471142301.ns0417s7>
- Grein, T. A., Loewe, D., Dieken, H., Salzig, D., Weidner, T., & Czermak, P. (2018). High titer oncolytic measles virus production process by integration of dielectric spectroscopy as online monitoring system. *Biotechnology and Bioengineering*, 115(5), 1186–1194. <https://doi.org/10.1002/bit.26538>
- Henriques, J., Sousa, J., Veiga, F., Cardoso, C., & Vitorino, C. (2018). Process analytical technologies and injectable drug products: is there a future? *International Journal of Pharmaceutics*, 554(August 2018), 21–35. <https://doi.org/10.1016/j.ijpharm.2018.10.070>
- Karakach, T. K., Dachon, A., Choi, J., Miguez, C., Masson, L., & Tartakovsky, B. (2018). Fluorescence-Based Real Time Monitoring and Diagnostics of Recombinant *Pichia pastoris* Cultivations in a Bioreactor. *Biotechnology Progress*, 1–9. <https://doi.org/10.1002/btpr.2761>
- Kroll, P., Stelzer, I. V., & Herwig, C. (2017). Soft sensor for monitoring biomass subpopulations in mammalian cell culture processes. *Biotechnology Letters*, 39(11), 1667–1673. <https://doi.org/10.1007/s10529-017-2408-0>
- Li, M. Y., Ebel, B., Blanchard, F., Paris, C., Guedon, E., & Marc, A. (2019). Control of IgG glycosylation by in situ and real-time estimation of specific growth rate of CHO cells cultured in bioreactor. *Biotechnology and Bioengineering*, (June 2018). <https://doi.org/10.1002/bit.26914>

- Meghrou, J., Aucoin, M. G., Jacob, D., Chahal, P. S., Arcand, N., & Kamen, A. A. (2005). Production of Recombinant Adeno-Associated Viral Vectors Using a Baculovirus / Insect Cell Suspension Culture System : From Shake Flasks to a 20-L Bioreactor. *Biotechnology Progress*, (2), 154–160. <https://doi.org/10.1021/bp049802e>
- Mercier, S. M., Rouel, P. M., Lebrun, P., Diepenbroek, B., Wijffels, R. H., & Streefland, M. (2015). Process analytical technology tools for perfusion cell culture. *Engineering in Life Sciences*, n/a-n/a. <https://doi.org/10.1002/elsc.201500035>
- Merten, O. (2016). AAV vector production : state of the art developments and remaining challenges. *Cell & Gene Therapy*, (February), 521–551. <https://doi.org/10.18609/cgti.2016.067>
- Murphy, K. R., Stedmon, C. A., Graeber, D., & Bro, R. (2013). Fluorescence spectroscopy and multi-way techniques. *PARAFAC. Analytical Methods*, 5(23), 6557–6566. <https://doi.org/10.1039/c3ay41160e>
- Negrete, A., Esteban, G., & Kotin, R. (2007). Process optimization of large-scale production of recombinant adeno-associated vectors using dielectric spectroscopy. *Applied Microbiology and Biotechnology*, 76(4), 761–772. <https://doi.org/10.1007/s00253-007-1030-9>
- Nikolay, A., Léon, A., Schwamborn, K., Genzel, Y., & Reichl, U. (2018). Process intensification of EB66® cell cultivations leads to high-yield yellow fever and Zika virus production. *Applied Microbiology and Biotechnology*, 102(20), 8725–8737. <https://doi.org/10.1007/s00253-018-9275-z>
- Ohadi, K., Aghamohseni, H., Legge, R. L., & Budman, H. M. (2014). Fluorescence-based soft sensor for at situ monitoring of chinese hamster ovary cell cultures. *Biotechnology and Bioengineering*, 111(8), 1577–1586. <https://doi.org/10.1002/bit.25222>
- Ohadi, K., Legge, R. L., & Budman, H. M. (2015). Development of a soft-sensor based on multi-wavelength fluorescence spectroscopy and a dynamic metabolic model for monitoring mammalian cell cultures. *Biotechnology and Bioengineering*, 112(1), 197–208. <https://doi.org/10.1002/bit.25339>
- Pais, D. A. M., Carrondo, M. J. T., Alves, P. M., & Teixeira, A. P. (2014). Towards real-time monitoring of therapeutic protein quality in mammalian cell processes. *Current Opinion in Biotechnology*, 30, 161–167. <https://doi.org/10.1016/j.copbio.2014.06.019>
- Petiot, E., Ansoorge, S., Rosa-Calatrava, M., & Kamen, A. (2016). Critical phases of viral production processes monitored by capacitance. *Journal of Biotechnology*, 242, 19–29. <https://doi.org/10.1016/j.jbiotec.2016.11.010>
- Rangan, S., Kamal, S., Konorov, S. O., Schulze, H. G., Blades, M. W., Turner, R. F. B., & Piret, J. M. (2018). Types of cell death and apoptotic stages in Chinese Hamster Ovary cells distinguished by Raman spectroscopy. *Biotechnology and Bioengineering*, 115(2), 401–412. <https://doi.org/10.1002/bit.26476>
- Roldão, A., Oliveira, R., Carrondo, M. J. T., & Alves, P. M. (2009). Error assessment in recombinant baculovirus titration: Evaluation of different methods. *Journal of Virological Methods*, 159(1), 69–80. <https://doi.org/10.1016/j.jviromet.2009.03.007>
- Roldão, A., Vieira, H. L. A., Charpillienne, A., Poncet, D., Roy, P., Carrondo, M. J. T., Alves, P. M., & Oliveira, R. (2007). Modeling rotavirus-like particles production in a baculovirus expression vector system: Infection kinetics, baculovirus DNA replication, mRNA synthesis and protein production. *Journal of Biotechnology*, 128(4), 875–894. <https://doi.org/10.1016/j.jbiotec.2007.01.003>
- Rowland-Jones, R.C.; van den Berg, F.; Racher, A.J.; Martin, E.B.; Jaques, C. (2017). Comparison of spectroscopy technologies for improved monitoring of cell culture processes in miniature bioreactors. *Biotechnol. Prog.* 33, 337–346. <https://doi.org/10.1002/btpr.2459>
- Santos, R. M., Kessler, J. M., Salou, P., Menezes, J. C., & Peinado, A. (2018). Monitoring mAb cultivations with in-situ raman spectroscopy: The influence of spectral selectivity on calibration models and industrial use as reliable PAT tool. *Biotechnology Progress*, 34(3), 659–670. <https://doi.org/10.1002/btpr.2635>
- Schwab, K., & Hesse, F. (2017). Estimating Extrinsic Dyes for Fluorometric Online Monitoring of Antibody Aggregation in CHO Fed-Batch Cultivations. *Bioengineering*, 4(3), 65. <https://doi.org/10.3390/bioengineering4030065>

- Schwab, K., Lauber, J., & Hesse, F. (2016). Fluorometric In Situ Monitoring of an Escherichia coli Cell Factory with Cytosolic Expression of Human Glycosyltransferase GalNAcT2: Prospects and Limitations. *Bioengineering*, 3(4), 32. <https://doi.org/10.3390/bioengineering3040032>
- Smith, R. H., Levy, J. R., & Kotin, R. M. (2009). A simplified baculovirus-AAV expression vector system coupled with one-step affinity purification yields high-titer rAAV stocks from insect cells. *Molecular Therapy: The Journal of the American Society of Gene Therapy*, 17(11), 1888–1896. <https://doi.org/10.1038/mt.2009.128>
- Teixeira, A. P., Duarte, T. M., Carrondo, M. J. T., & Alves, P. M. (2011). Synchronous fluorescence spectroscopy as a novel tool to enable PAT applications in bioprocesses. *Biotechnology and Bioengineering*, 108(8), 1852–1861. <https://doi.org/10.1002/bit.23131>
- Teixeira, A. P., Portugal, C. A. M., Carinhas, N., Dias, J. M. L., Crespo, J. P., Alves, P. M., Carrondo, M. J. T., & Oliveira, R. (2009). In situ 2D fluorometry and chemometric monitoring of mammalian cell cultures. *Biotechnology and Bioengineering*, 102(4), 1098–1106. <https://doi.org/10.1002/bit.22125>
- UniProt. (2002). AAV2 capsid protein VP1 composition. UniProt. Retrieved November 20, 2016, from <https://www.uniprot.org/uniprot/P03135>
- Webster, T. A., Hadley, B. C., Hilliard, W., Jaques, C., & Mason, C. (2018). Development of generic raman models for a GS-KOTM CHO platform process. *Biotechnology Progress*, 34(3), 730–737. <https://doi.org/10.1002/btpr.2633>
- Wolf, G., Almeida, J. S., Pinheiro, C., Correia, V., Rodrigues, C., Reis, M. a, & Crespo, J. G. (2001). Two-dimensional fluorometry coupled with artificial neural networks: a novel method for on-line monitoring of complex biological processes. *Biotechnology and Bioengineering*, 72, 297–306. [https://doi.org/10.1002/1097-0290\(20010205\)72:3<297::AID-BIT6>3.0.CO;2-B](https://doi.org/10.1002/1097-0290(20010205)72:3<297::AID-BIT6>3.0.CO;2-B)
- Zabadaj, M., Chreptowicz, K., Mierzejewska, J., & Ciosek, P. (2017). Two-dimensional fluorescence as soft sensor in the monitoring of biotransformation performed by yeast. *Biotechnology Progress*, 33(2), 299–307. <https://doi.org/10.1002/btpr.2381>
- Zeiser, A., Bédard, C., Voyer, R., Jardin, B., Tom, R., & Kamen, a a. (1999). On-line monitoring of the progress of infection in Sf-9 insect cell cultures using relative permittivity measurements. *Biotechnology and Bioengineering*, 63(1), 122–126. [https://doi.org/10.1002/\(SICI\)1097-0290\(19990405\)63:1<122::AID-BIT13>3.0.CO;2-I](https://doi.org/10.1002/(SICI)1097-0290(19990405)63:1<122::AID-BIT13>3.0.CO;2-I)
- Zeiser, A., Elias, C. B., Voyer, R., Jardin, B., & Kamen, A. A. (2000). On-line monitoring of physiological parameters of insect cell cultures during the growth and infection process. *Biotechnology Progress*, 16, 803–808. <https://doi.org/10.1021/bp000092w>

Chapter III

Holographic imaging of insect cell cultures: online non-invasive monitoring of adeno associated virus production and cell concentration

This chapter is adapted from the manuscript:

Pais, DAM, Galvão, PRS, Kryzhanska, A, MJT, Barbau, J, Isidro, IA, Alves, PM. 2020. "Holographic imaging of insect cell cultures: online non-invasive monitoring of adeno associated virus production and cell concentration", *Processes*, 8 (4), 487.

Author Contribution

Daniel Pais participated in the experimental setup and design, run the majority of the experiments, analyzed the data and wrote this chapter.

Abstract

The insect cell-baculovirus vector system has become one of the favorite platforms for expression of viral vectors for vaccination and gene therapy purposes. Being a lytic system, it is essential to balance maximum recombinant product expression with harvest time, minimizing product exposure to detrimental proteases. With that purpose, new bioprocess monitoring solutions are needed to accurately estimate culture progression.

Herein, we used online digital holographic microscopy (DHM) to monitor bioreactor cultures of Sf9 insect cells. Batches of baculovirus infected Sf9 cells producing recombinant adeno-associated virus (rAAV) and non-infected cells were used to evaluate DHM prediction capabilities for viable cell concentration, culture viability and rAAV titer. Over 30 cell-related optical attributes were quantified using DHM, followed by a forward stepwise regression to select the most significant ($p < 0.05$) parameters for each variable. We then applied multiple linear regression to obtain models which were able to predict culture variables with root mean squared errors (RMSE) of 7×10^5 cells/mL, 3% for cell viability and 2×10^3 rAAV/cell for 3-fold cross-validation.

Overall this work shows that DHM is a valuable tool for online monitoring of Sf9 concentration and viability, permitting also to monitor product titer, namely rAAV, or culture progression in lytic systems, making it a valuable tool to support the time of harvest decision and for the establishment of controlled feeding strategies.

Contents

1.	Introduction	105
2.	Materials and Methods	108
2.1.	Cell line and culture medium.....	108
2.2.	AAV and baculovirus infection and titration.....	108
2.3.	Bioreactor cultures and sample processing	109
2.4.	Modeling strategy and software	111
2.4.1.	Dataset	111
2.4.2.	Attribute selection and stepwise regression	111
2.4.3.	Model training and validation	112
3.	Results	114
3.1.	Digital holographic microscopy can be used for monitoring viable cell concentration and viability	114
3.2.	Prediction of rAAV titers using digital holographic microscopy	117
3.3.	Time-course profiles of morphological and optical parameters measured with DDHM	119
3.4.	Model parameters have biological significance.....	121
4.	Discussion	122
5.	Conclusions	128
6.	Acknowledgements	129
7.	Conflicts of interest	129
8.	Supplementary Data	130
9.	References	139

1. Introduction

After the FDA launched the Process Analytical Technology (PAT) initiative in 2004 (FDA, 2004), an increased effort has been put in place by the manufacturers of biological products to comply with PAT requirements. The PAT initiative is a guidance for the pharmaceutical industry for the development of new products and production processes, with the main focus on: **i)** increasing product and process knowledge through identification of the product critical quality attributes and the process parameters affecting it; and **ii)** monitoring in real-time the identified critical process parameters and the product quality characteristics, ensuring manufacturing robustness and an increased quality assurance to achieve the required levels of compliance (FDA, 2004; Pais et al., 2014; Petiot et al., 2016).

Label-free methodologies are preferred, especially in biopharmaceutical processes, since they allow the monitoring of cell culture without adding any compounds which would influence cellular behavior. Most cell culture monitoring methods employing label-free methodologies are based on spectroscopic techniques, which have been widely used for cell culture process monitoring. Examples include the use of dielectric spectroscopy and turbidimetry/light scattering probes for determination of cell concentration (Loutfi et al., 2020; Moore et al., 2019), as well as the use of Raman (Santos et al., 2018; Tulsyan et al., 2020), infrared (Zavala-Ortiz et al., 2019) and fluorescence (Pais et al., 2019) spectroscopy, which allow quantification of metabolites based on direct spectra quantification, but also indirect determination of cell concentration and product formation based on chemometric analysis.

A label-free alternative to spectroscopic techniques is imaging-based cell culture monitoring. Since cells are mostly transparent, these systems rely on several strategies to generate the needed image contrast (Kasproicz et al.,

2017; Mann et al., 2005). One example of a imaging technique with proven demonstrations for live cell imaging is Digital Holographic Microscopy (DHM) (Janicke et al., 2017). Briefly, DHM provides quantitative phase imaging (QPI), quantifying the phase shift of the light after it has passed through the object of focus, such as cells. This light phase difference is encoded in a hologram which is used to construct high resolution intensity and quantitative phase images of the cell, while also providing quantitative parameters related with light phase and intensity (Kamlund, 2018; Mann et al., 2005). The way light is scattered after interacting with cells depends on factors such as cell thickness, circularity or intracellular composition (Kasprowicz et al., 2017; Kemper et al., 2010; Mann et al., 2005; Rapoport et al., 2011). As such, DHM can be used to extract important information from the cell state, and has proven useful for several cell-based applications: identification of morphological parameters distinguishing between epithelial and mesenchymal cells (Kamlund, 2018), detecting cell division in endothelial cells (Kemper et al., 2010) and developing cell proliferation (Janicke et al., 2017) or cytotoxic assays (Kühn et al., 2013). In particular, infected cells will have different intracellular structure than uninfected cells (Altschuler and Wu, 2010; Petiot et al., 2016; Ugele et al., 2018). Furthermore, as demonstrated by Ugele and colleagues, DHM-based detection of the intracellular composition of infected erythrocytes even allowed to distinguish between different infection phases in the malaria *P. falciparum* life cycle (Ugele et al., 2018). The ability to detect infected cells as well as cell concentration and viability makes DHM inherently attractive to monitor the progress of infection-based biopharmaceutical production systems, such as the insect cell-baculovirus system (Hidalgo et al., 2017).

Insect cells are one of the preferred hosts for viral vector manufacturing for vaccines and gene therapy purposes, since they can be grown in suspension to high cell densities in serum free media (Cox, 2012; Negrete et al., 2007).

However, to maximize product yields it is determinant to infect cells at low cell concentration, to prevent the so called “cell density effect”, a drop on the specific productivity of the cell when infection takes place at high cell concentration. The optimal cell concentration for infection and the definition of “low” and “high” cell concentration are dependent on the cell type, culture medium used and recombinant product being expressed (Bernal et al., 2009; Sequeira et al., 2018). Moreover, baculovirus is a lytic virus, which can lead to the release of intracellular proteases into the culture medium, possibly degrading the recombinant product after it has been released into the medium. As such, both culture viability and cell concentration are critical process parameters for this system.

Other authors have addressed ways to monitor this system using dielectric (Negrete et al., 2007; Petiot et al., 2016; Zeiser et al., 2000, 1999) or fluorescence spectroscopies (Pais et al., 2019), as well as using image-based technologies, in particular for measuring the progress of baculovirus infection (Janakiraman et al., 2006; Laasfeld et al., 2017; Palomares et al., 2001). DHM can go one step further, by monitoring not only the cell diameter increase after baculovirus infection, but also the evolution profile of several cell characteristics, allowing to explore the possibility to observe baculovirus or rAAV-induced changes in suspension insect cells in real-time.

In this chapter, we used iLine F differential DHM microscope (DDHM) (Ovizio Imaging Systems SA/NV) for real-time monitoring of a Sf9 culture infected with baculovirus, expressing recombinant adeno-associated virus (rAAV) type 2. rAAV is widely used as a gene therapy viral vector, due to its lack of known pathogenicity, broad tissue tropism coupled with long term transgene expression and ability to withstand harsh manufacturing conditions (Naso et al., 2017). Estimation of rAAV titer in real-time is desirable in order to harvest when its concentration is higher. Moreover, monitoring this system in real-time can support the time of harvest decision, an important process

variable to consider giving the lytic nature of the baculovirus and consequential release of proteases to the medium when cells start lysing.

Since DDHM can be used to detect infected cells, we further explored this capability for monitoring the AAV titer in our cultures along with the development of predictive models for viable cell concentration and viability. Using the culture-related morphologic and optical attributes quantified with iLine F, we used forward stepwise regression to find the attributes associated with viable cell concentration, viability and intra and extracellular rAAV titer. We validated this approach using leave one batch out (LOBO) and 3-fold cross-validation strategies. As such, we demonstrate DDHM can be used not only for monitoring Sf9 cell concentration and viability but also for assessing rAAV production kinetics in this biological system.

2. Materials and Methods

2.1. Cell line and culture medium

Spodoptera frugiperda Sf9 cells were obtained from Thermo Fisher Scientific (No 11496015) and routinely cultivated in 500 mL glass Erlenmeyer flasks with 50 mL working volume of SF900-II medium (Gibco™), at 27 °C with an agitation rate of 100 rpm in an Innova 44R incubator (orbital motion diameter = 2.54 cm, Eppendorf). Cell concentration and viability were determined using a Cedex HiRes Analyzer (Roche).

2.2. AAV and baculovirus infection and titration

The recombinant *Autographa californica* nucleopolyhedrovirus encoding the GFP transgene under the control of the cytomegalovirus promoter (CMV-GFP) and flanked by AAV2 inverted terminal repeats (ITR) regions was kindly provided by Généthon and was titrated and amplified *in house* as described for the *rep/cap* baculovirus (below).

The plasmid containing AAV2 *rep* and *cap* genes was a gift from Robert Kotin (Addgene plasmid #65214) (Smith et al., 2009). Recombinant baculovirus was produced using the Bac-to-Bac® Baculovirus Expression System (Invitrogen), according with manufacturer instructions. Baculovirus amplification was performed as described elsewhere (Pais et al., 2019).

Recombinant adeno-associated virus (rAAV) intra and extracellular titer was estimated separately using a commercially available sandwich ELISA kit (Progen Biotechnik GmbH), according to the manufacturer instructions. This kit detects a conformational epitope present in assembled rAAV capsids.

2.3. Bioreactor cultures and sample processing

Benchtop 1 L bioreactor runs were performed in BIOSTAT® DCU-3 (Sartorius), equipped with two Rushton turbines. Temperature control (27 °C) was achieved using a water recirculation jacket and gas supply was provided by a ring sparger in the bottom of the vessel. Dissolved oxygen (DO) concentration was kept at 30 % by cascade controlling the stirring rate (70-270 rpm) and the N₂/air ratios in a mixture of air and N₂ (0.01 vvm).

Several runs were performed to establish the standard culture progression profile. However, due to equipment constraints, only two bioreactors were monitored using the iLine F system (Ovizio Imaging Systems). These included a growth batch, consisting of a Sf9 batch culture monitored until cell death due to nutrient starvation, which occurred after ten days of culture; and an infected batch, in which a Sf9 culture was infected with two baculovirus vectors to express recombinant adeno-associated virus type 2, harvested on day six. Both bioreactors follow similar process trends to their biological replicates (*vide* Supplementary Figure II.1 in the previous chapter, page 93).

Sf9 cells were inoculated at 0.5×10^6 cells/mL for both bioreactors. The “infected batch” was infected 31 hours after inoculation, when viable cell

concentration reached 1×10^6 cells/mL, with a multiplicity of infection (MOI) of 0.05 plaque forming units per cell, for each baculovirus. The two baculovirus strategy was used, in which one baculovirus codes for the AAV2 *rep* and *cap* genes and the other provides the GFP transgene flanked by the AAV ITRs.

In the iLine F system, a single-use, autoclavable closed-loop tube is inserted in a standard 19 mm bioreactor top port. This sampling tube contains in the other end a cartridge with the imaging chamber. After sterilization, the sampling tube is connected to a pump motor. Cell culture is continuously aspirated through the sampling tube to the imaging chamber and then returned to the cell culture vessel. The setup is controlled using the *OsOne* software (Ovizio Imaging Systems SA/NV), which controls the sampling rate and image analysis by the holographic microscope. Images are acquired every minute, but image processing occurs in batches of 25, thus yielding a new timepoint every 30 minutes (the 5 remaining minutes are used for background elimination and attribute calculations). Image processing consists in (1) image focus, (2) holographic fingerprint acquisition for every cell present in the image, (3) computation of 66 image-related attributes for every cell. Supplementary Figure III.1 exemplifies the cell culture and hologram evolution profiles.

Sampling for determination of reference variables was performed daily for the growth batch and three times per day for infected batch. At each sampling point, cell concentration and viability were measured using Cedex HiRes Analyzer (Roche). Additionally, for the infected batch a clarification step was performed (200 g, 10 min, 4 °C) to recover intra and extracellular rAAV. Supernatant was subjected to a further clarification step (2000 g, 20 min, 4 °C) and stored at -80 °C for offline analysis. Intracellular rAAV was extracted from cell pellets with TNT buffer, consisting of 20 mM Tris-HCl (pH 7.5), 150 mM NaCl, 1% Triton X-100, 10 mM MgCl₂ (Smith et al., 2009), to which a 0.5% solution of sodium deoxycholate was added to further increase

the release of intracellular rAAV from pelleted cells (Gray et al., 2012). After 10 minutes of incubation at 22 °C, the suspension was centrifuged (2000 g, 20 min, 4 °C) and the supernatant stored at -80 °C for offline analysis.

2.4. Modeling strategy and software

2.4.1. Dataset

After run completion, for each timepoint the average for each attribute was calculated, considering all cells present in the 25 images acquired per timepoint. This resulted in 499 timepoints for growth batch and 275 timepoints for infected batch (online data). This data was smoothed using a moving average of two hours, corresponding to four datapoints. The reference data consisted of 14 samples for growth batch and 23 samples for infection batch, with determination of the four reference variables (viable cell concentration, viability, extracellular volumetric rAAV titer and intracellular specific rAAV titer) for each sample. The data for modeling consisted of each one of the reference datapoints time-aligned with the corresponding online datapoints, yielding a matrix of [37 rows × 4 reference variables columns × 66 columns with averaged attributes].

All analysis and modeling were performed in JMP v14 (Statistical Analysis System institute).

Potential outliers in the reference data were identified by visual inspection of the data time-course profile and confirmed by calculating the jackknife distances for each datapoint. JMP jackknife outlier identification method relies on estimates of the mean, standard deviation, and correlation matrix that do not include the observation itself.

2.4.2. Attribute selection and stepwise regression

OsOne calculates 66 attributes per each cell. However, due to high collinearity of some attributes and to prevent model over-fitting (Feng et al.,

2009), the Pearson correlation coefficient was calculated for every attribute pair. For pairs with a high correlation (Pearson correlation coefficient absolute value >0.95), one of the attributes was excluded from further analysis. This process was iterated until no attributes had a correlation coefficient higher than 0.95 or lower than -0.95, reducing the initial 66 attributes to 30.

For model training, JMP “Fit model” platform was used. Briefly, the selected 30 attributes were subjected to a forward stepwise regression to find the most significant for the prediction of each of the reference variables. In a forward stepwise regression method, the most significant attribute is identified and added to the model, followed by identification and inclusion in the model of the second most significant attribute and so on. This process was stopped when the next term added was considered not significant ($p\text{-value}>0.05$).

Since this biological system has non-linear variables, which can be observed on the viable cell concentration and rAAV titer profiles, after identification of the most significant attributes for every variable, a second model was created, by performing the same forward stepwise regression technique using the significant terms (“main effects”) and their interactions and quadratics. The final forward stepwise regression model (main effects only or with interactions) was chosen by comparison of prediction profiles and root mean squared error (RMSE).

2.4.3. Model training and validation

Multiple linear regression models were built based on the stepwise forward regression strategy. Two validation strategies were used to assess model prediction capabilities and overfitting: leave one batch out (LOBO) and 3-fold cross-validation (3CV). For LOBO models, the stepwise attribute selection strategy mentioned in the previous section was applied to one batch only. After finding the most significant parameters and determining the model coefficients for each parameter by multiple linear regression, the model was

applied to the remaining batch for validation. This strategy was successfully applied to viability models but resulted in significant overfitting for viable cell concentration due to the significant differences in the variable ranges between the two batches. As such, an alternative LOBO strategy was used, in which parameter selection was performed using the reference data from both batches, followed by training of each batch separately. The obtained model was then used for predicting the remaining batch for validation purposes.

For 3CV, the significant parameters were identified applying forward stepwise regression to the reference data from both batches, followed by multiple linear regression for model fitting using both batches. Model validation was performed by dividing the dataset (37 timepoints) into three random partitions, using two for model training with the selected parameters and predicting the third partition. The process was repeated for the two remaining partitions.

The contribution of each parameter to the final model was calculated dividing the logworth value for each parameter by the sum of the logworth for all parameters (logworth is defined as $-\log_{10}(\text{p-value})$).

RMSEs for calibration (RMSEC) and validation (RMSEV) were calculated for all models (equation 1). In equation 1, \hat{y} represents a vector of model-predicted values and y represents the corresponding reference data; n_{cal} and n_{val} represent the number of samples in the calibration or validation set, respectively; $\max(y)$ and $\min(y)$ refer to the maximum and minimum values for the reference data, respectively. Normalized RMSE (nRMSE) was obtained by dividing the RMSE by the variable range.

The correlation coefficients of calibration and validation were calculated according to equation 2 using calibration (R^2) or validation (Q^2) data. R^2 is a measure of how well the chosen model fits the calibration data while Q^2

measures how the obtained model fits the validation dataset, which is not used to fit the model, being indicative of the model predictive power for new data. σ^2 represents sample variance.

$$RMSEC = \sqrt{\frac{\sum_{i=1}^{ncal}(\hat{y} - y)^2}{ncal}} \quad RMSEV = \sqrt{\frac{\sum_{i=1}^{nval}(\hat{y} - y)^2}{nval}} \quad nRMSE = \frac{RMSE}{\max(y) - \min(y)} \quad (1)$$

$$R^2 = 1 - \frac{RMSEC^2}{\sigma^2}. \quad Q^2 = 1 - \frac{RMSEV^2}{\sigma^2}. \quad (2)$$

3. Results

3.1. Digital holographic microscopy can be used for monitoring viable cell concentration and viability

In this chapter, we study applicability of iLine F system for online monitoring of critical process variables in the insect cell-baculovirus system, for production of recombinant adeno associated viral vectors (rAAV). The critical process variables under analysis were viable cell concentration, cell viability and intra and extracellular rAAV titers.

Models were trained using two batches, one infected (rAAV production) and one uninfected (cell growth). These have similar viability profiles (Figure III.1 A), differing only in the time to onset of viability decrease, but are distinct in the viable cell concentration ranges achieved (Figure III.1 B), as well as the rAAV production profiles (Figure III.2).

The preferential validation strategy consisted in using one batch for model calibration and the other one as validation set (leave one batch out, LOBO). The high Q^2 obtained for viability (0.72 and 0.92 for validation with growth and infected batches, Figure III.1 B) support the feasibility of using iLine F for monitoring viability in this process, even using only one batch for model

calibration. The lower Q^2 score obtained for growth batch is mainly due to an underestimation of viability in the growth phase, but the prediction profiles for the death phase (more relevant for this system) are accurate for both runs. For viable cell concentration, the large range difference between runs causes the model to overfit the calibration batch, therefore severely underestimating viable cell concentration when predicting the growth batch, although with the correct profile ($Q^2=0.66$) and failing to capture the correct viable cell concentration trend for the infected batch ($Q^2=0.34$) (Figure III.1 B).

The second validation strategy tested for viability and viable cell concentration was the 3-fold cross-validation (3CV) (Figure III.1 C and D). Models were built using data from both batches, and a 3CV strategy was applied to measure the model predictive power and confirm these are not overfitting, while simultaneously allowing identification of the DDHM attributes more important for variable prediction. Applying the 3CV model to iLine F real-time data, as expected, yields greatly improved predictions when compared with LOBO models (Figure III.1, $Q^2=0.98$ for viability and $Q^2=0.93$ for viable cell concentration). Although less robust, this strategy was necessary so that model coefficients could account for the differences in the variable range between the two batches. The final model parameters and coefficients are presented in Supplementary Table III.1. For comparison purposes, the predictions for viable cell concentration and viability using Ovizio proprietary models are shown in Supplementary Figure III.2. Except for the viable cell concentration LOBO model calibrated in the infected batch, no models consider parameter interactions, since the models containing only the main effects possess an equal or better predictive score than the ones considering interactions and quadratics.

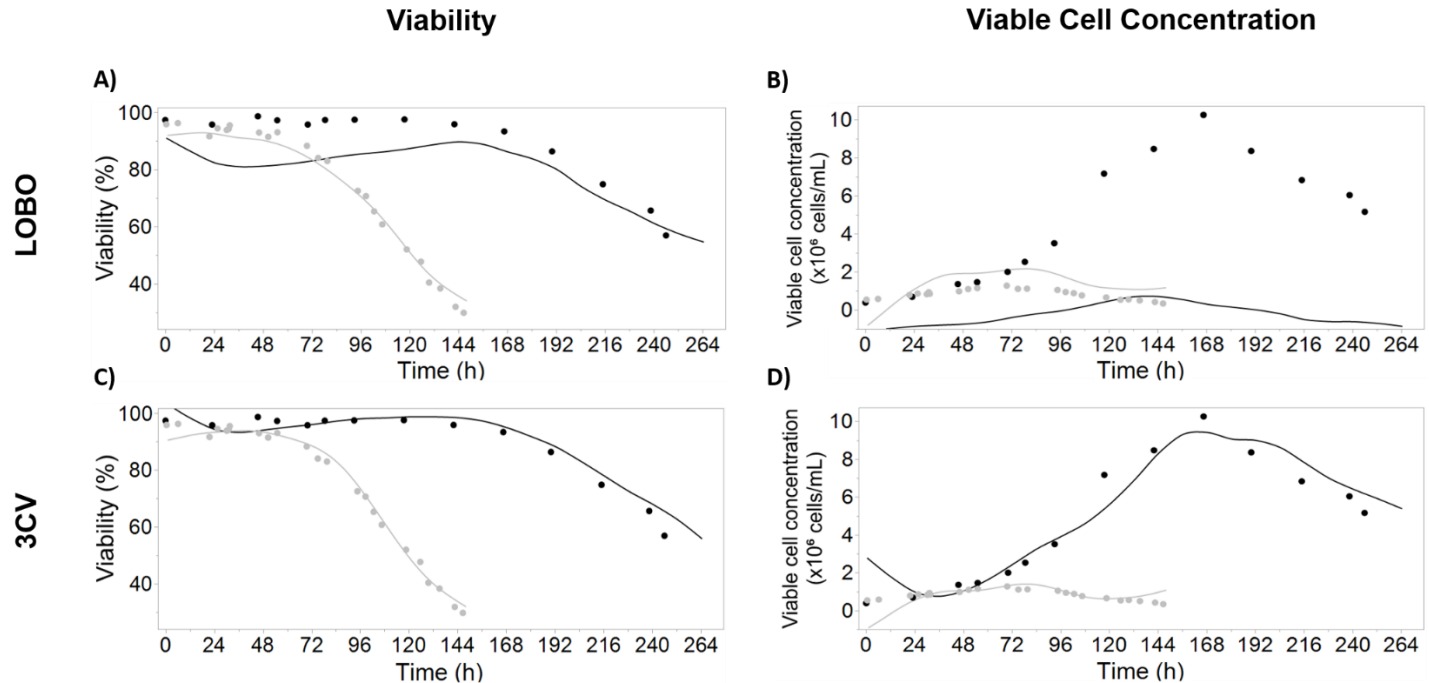


Figure III.1 - Viability (left) and viable cell concentration (VCC, right) predictions using leave one batch out (LOBO, top) and 3-fold cross-validation (3CV, bottom) models. Growth batch is represented in black and infected batch is colored in grey. Lines represent model-predicted values; filled circles represent reference data; empty circles were considered outliers and excluded from modeling. For LOBO models, only the model prediction is shown (i.e. when the growth batch was used for model calibration, the calibration model is not shown, only the prediction for the infected batch). For 3CV models, the model shown was built using data from both batches. **(A)** Observed and predicted values for viability using LOBO for model validation. **(B)** Observed and predicted values for VCC using LOBO for model validation. **(C)** Observed and predicted values for viability using 3CV for model validation. **(D)** Observed and predicted values for VCC using 3CV for model validation. Model parameters and coefficients are presented in Supplementary Table III.1.

3.2. Prediction of rAAV titers using digital holographic microscopy

Given that the used dataset consists of two batches, from which only one is expressing rAAV, the LOBO strategy cannot be used for modeling rAAV-related variables. As such, the 3-fold cross-validation (3CV) strategy described in the previous section was used to calibrate prediction models for extracellular volumetric rAAV titer ($Q^2 = 0.97$) and intracellular specific rAAV titer ($Q^2 = 0.99$) (Figure III.2). rAAV production trend is captured with our modeling strategy, highlighting the potential of using multiple linear regression for identification of the most important optical attributes measured with DDHM and monitoring rAAV production profiles in this biological system.

To confirm the obtained models are not overfitting the data, the coefficients of correlation for the calibration and validation set for every partition were calculated, for the four variables under study (Supplementary Table III.2). For each variable, the nRMSE for each partition are comparable in magnitude. Moreover, for each partition the nRMSE values obtained for validation are on average 1.8 % higher than the ones obtained for calibration, confirming the 3CV models are not overfitting the data.

The high adjusted coefficients of correlation for calibration and validation for the models shown in Figure III.1 and Figure III.2 indicate that good prediction models were obtained, with the exception of the LOBO viable cell concentration model (Figure III.3, Supplementary Table III.3). The feasibility of using DDHM for bioprocessing monitoring is demonstrated by the acceptable Q^2 (0.74) using LOBO for viability prediction, and by the high cross-validation Q^2 for all variables (0.93 to 0.98). For LOBO viable cell concentration models, the negative value is obtained when considering the Q^2 for both batches simultaneously, due to the high discrepancy in the variable range and the overfitting in each calibration model. Individual Q^2 are 0.66 for prediction of growth batch and 0.34 for prediction of infected batch. The Q^2 values for 3CV models are very close to the corresponding R^2 ,

demonstrating that the chosen model is appropriate to describe both the calibration data and new datapoints. Altogether, this demonstrates that using only two batches with different rAAV production profiles is enough to find the DDHM attributes likely relevant for rAAV production.

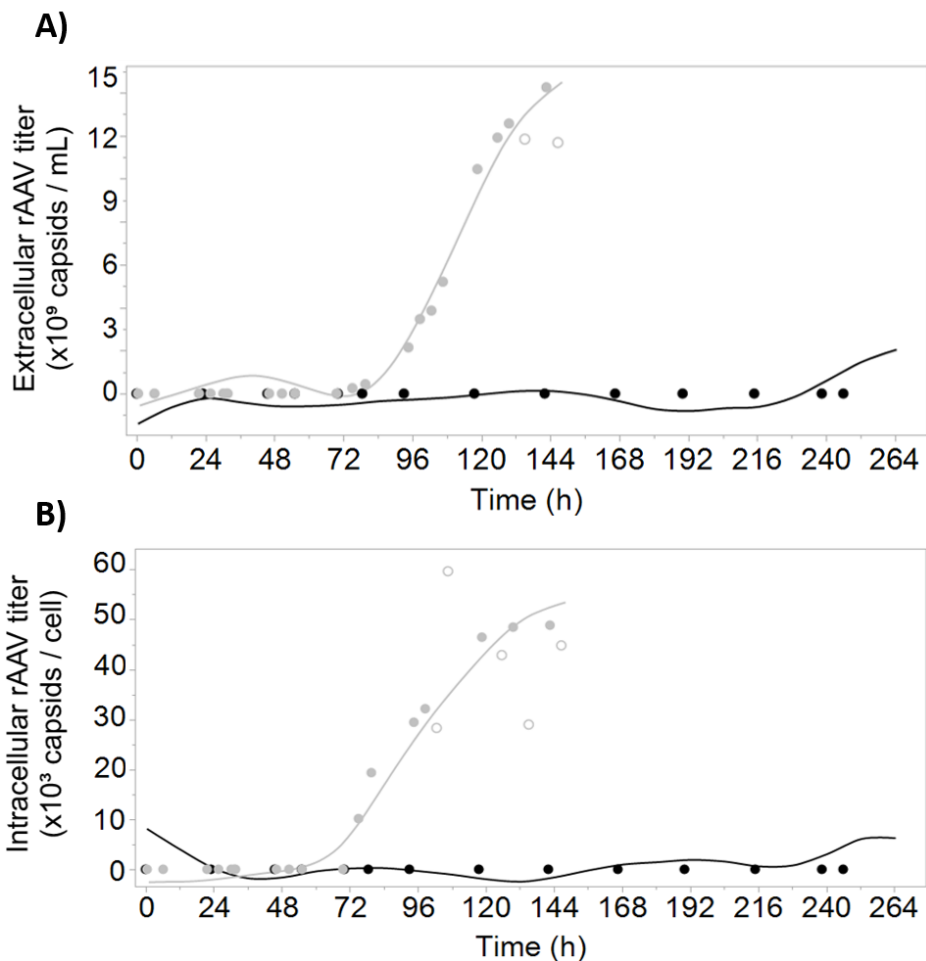


Figure III.2 – rAAV titer predictions for both batches. Growth batch is represented in black and infected batch is colored in grey. Lines represent model-predicted values; filled circles represent reference data; empty circles represent datapoints considered outliers and excluded from modeling. Models were calibrated using the reference data for both batches (filled circles). The prediction data represented by the smooth lines was obtained by applying the model to the real-time differential digital holographic microscopy data. (A) Observed and predicted values for extracellular rAAV titer; (B) Observed and predicted values for intracellular specific rAAV titer. Model parameters and coefficients are presented in Supplementary Table III.1.

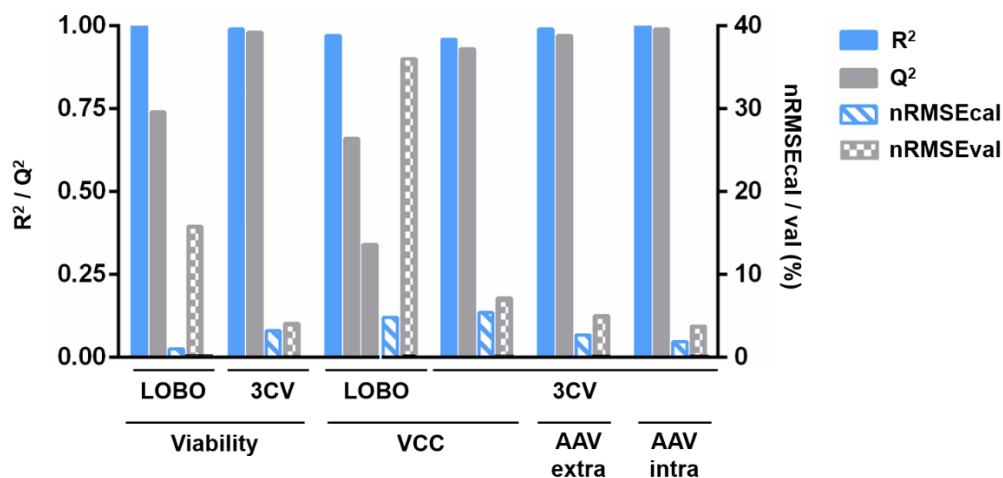


Figure III.3 – Quality characteristics overview for the models presented in Figure III.1 and 2. R^2 and Q^2 are the correlation coefficients of calibration and validation, respectively. Also depicted are the normalized root mean squared errors (nRMSE) for calibration and validation which are scaled by the variable range. For the LOBO VCC models, the difference in the cell concentration ranges and the fact that the prediction models overfit the calibration batch result in a negative Q^2 (-0.69) when data from both batches is considered. As such, we chose to depict the Q^2 for each batch separately (0.66 for prediction of growth batch and 0.34 for prediction of infected batch). 3CV – 3-fold cross-validation; LOBO – leave one batch out; R^2 -correlation coefficient of calibration; nRMSE - normalized root mean squared error; Q^2 -correlation coefficient of validation; VCC – viable cell concentration. Raw data is provided in Supplementary Table III.3.

3.3. Time-course profiles of morphological and optical parameters measured with DDHM

One of the advantages of using DDHM for monitoring biological systems in real-time is the number of cell and image attributes that are calculated and the possibility to analyze the attribute evolution profile over culture time. These attributes are related with the cell morphology and with image optical characteristics, such as intensity of the light and light phase differences. While some of these attributes have an obvious biological meaning (for instance “Cell Radius”), most of them do not have a direct biological meaning *per se*. Still, some of the attributes clearly show an evolution over culture progression, and some are clearly correlated with the critical process variables studied in

this work, such as culture viability (Figure III.4 C, E and F), viable cell concentration (Figure III.4 C and G) and extracellular rAAV titer profiles (Figure III.4 A, B and D). These attributes were included in the final multiple linear regression prediction models with varying contributions for the overall model (Figure III.5 and Supplementary Table III.1). Our final models have between 5 and 12 parameters, excluding the intercept term (Figure III.5 and Supplementary Table III.2).

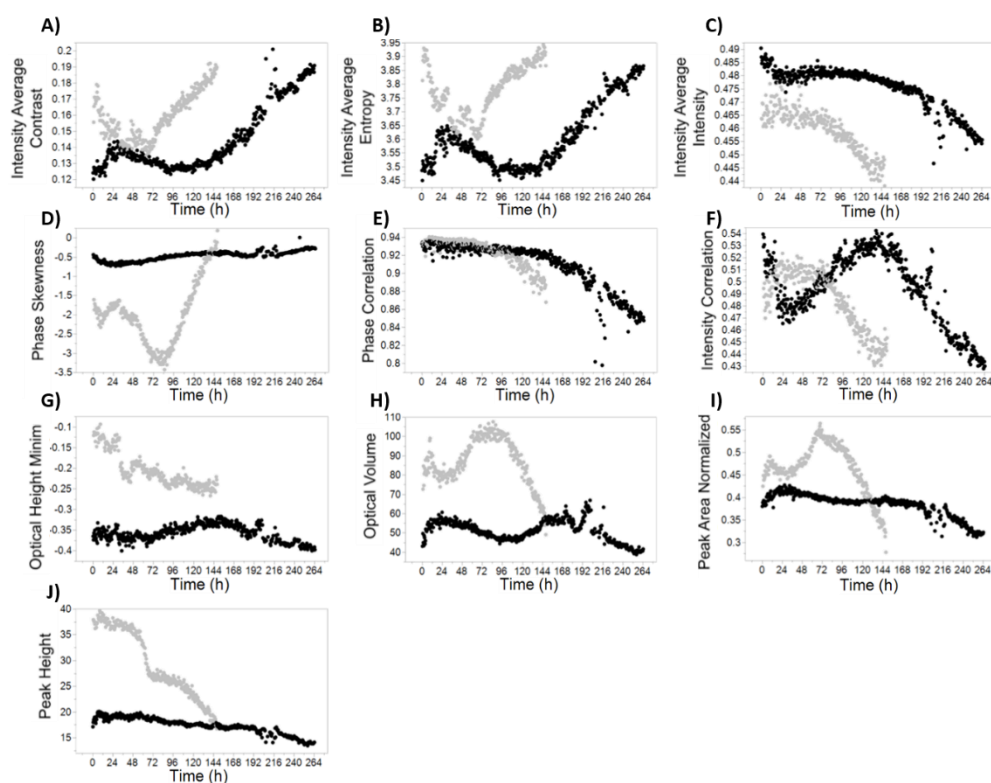


Figure III.4 – Time-course profiles for selected DDHM attributes. Growth batch is represented in black, while infection batch is colored in grey. Measurements are obtained every 30 minutes. (A) Intensity Average Contrast; (B) Intensity Average Entropy; (C) Intensity Average Intensity; (D) Phase Skewness; (E) Phase Correlation; (F) Intensity Correlation; (G) Optical Height Minimum; (H) Optical Volume; (I) Peak Area Normalized; (J) Peak Height.

3.4. Model parameters have biological significance

With iLine F, more than 60 attributes are calculated per cell. These are related with the cell morphology (e.g. “circularity”), the light optical characteristics (e.g. “maximum intensity”), the light phase texture (e.g. “phase skewness”) or the light intensity texture (e.g. “intensity correlation”). Overall, the parameters with a larger contribution for the obtained models are related with light intensity and phase characteristics (Figure III.5).

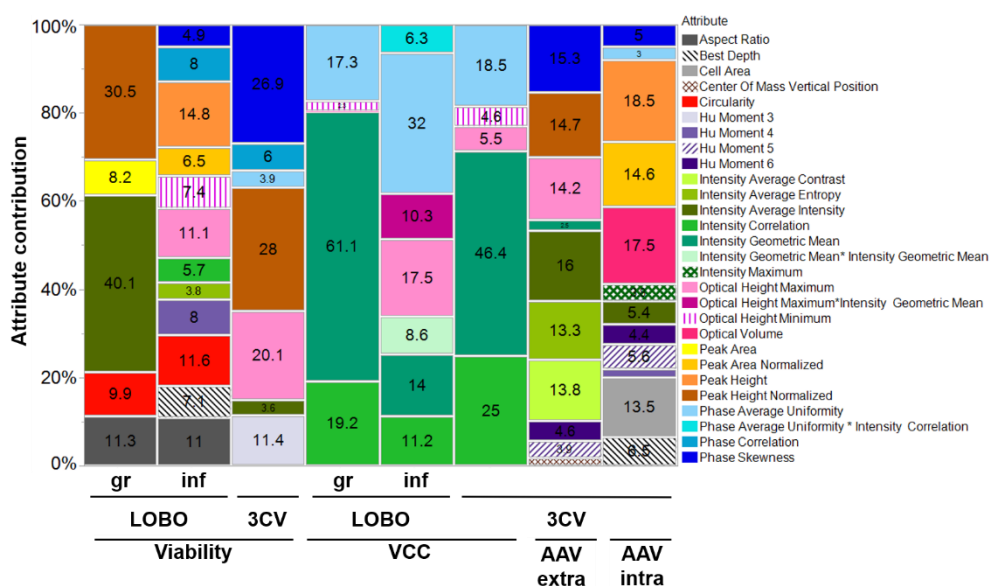


Figure III.5 - Relative contribution of each parameter to the final models. For leave one batch out (LOBO) models, the batch used for model calibration is indicated (gr – growth; inf - infected). For 3CV models, the coefficients presented are related to the model using both batches. Relative importance was calculated using the logworth for each parameter (Supplementary Table III.1).

Regardless of their relative contribution, some parameters are present in most of the models. Examples include “optical height maximum”, “phase average uniformity”, “intensity correlation”, “intensity average intensity” and “phase skewness”. Parameters present in the predictive models for viability, VCC and rAAV extracellular titer are specially interesting because the

respective variables are also correlated: viability is the quantitative measurement of the decrease in viable cell concentration, and rAAV extracellular titer increase is mostly due to cell lysis (Meghrou et al., 2005).

Another important consideration is the presence of highly correlated attributes, which may confound biological interpretation of the model contributions. For instance, “phase average uniformity”, a measure of the uniformity of the light phase in each cell, is strongly correlated ($R^2=0.91$) with “radius variance”, the variance of the cell radius, which is inversely correlated with circularity ($R^2=-0.97$). In conclusion, a cell with an increased “phase average uniformity” has a less spherical shape ($R^2=-0.88$). The pairwise Pearson correlations for every pair of attributes are shown in Supplementary Figure III.3.

4. Discussion

The aim of this study was to demonstrate the applicability of differential digital holographic microscopy (DDHM) to monitor important process parameters in the insect cell-baculovirus system, including the rAAV production kinetics. Specifically, Ovizio iLine F system was used. A forward stepwise regression technique combined with multiple linear regression was applied to the morphological and physiological attributes quantified by DDHM, successfully identifying attributes relevant for viable cell concentration, viability and intra and extracellular rAAV titer.

Currently there is a lack of methods available for online monitoring of viral particles production during cell culture (Petiot et al., 2016). Existing methods explore chemometrics approaches, by measuring process variables related with the viral production kinetics (Pais et al., 2019), or changes in the morphological and physiological alterations of the cells (Grein et al., 2018; Petiot et al., 2016). In particular for the baculovirus system, these methods

are mostly based on the known increase of cell diameter upon baculovirus infection (Janakiraman et al., 2006; Laasfeld et al., 2017; Palomares et al., 2001), although they were used as an assay rather than for in-culture determination.

Viability is one of the most important process variables to consider in many viral-based systems, being related with product quality and influencing harvest decision (Grein et al., 2018; Nikolay et al., 2018; Pais et al., 2019). In both batches cell viability decreases in the end of the culture. However, the onset of viability decrease occurs at different process times (150 h for growth and 60 h for infected batch) and with different biological triggers: while in the infected batch cell viability decreases due to baculovirus-induced cell lysis, in the growth batch cells died by nutrient starvation. This validates the applicability of DDHM, but also provides a possible explanation to why the parameters present in each LOBO viability model are different (Figure III.5), since the biological reason for the cell death was different. While some of the identified model parameters have a clear similarity with viability profiles (e.g. Figure III.4 C, E and F), in general these are not the most important for the viability prediction models. Given the small dataset used, the parameters more important for the models may be in fact distinguishing between infected and growth batch (e.g. Figure III.4 J, “peak height”) followed by fine-tuning using the attributes with the similar viability profile. While addition of more calibration batches would be essential for determination of the parameters associated with viability, the prediction profiles using LOBO (Figure III.1 A) show DDHM possess enough predictive power for prediction of viability using only one batch for calibration, and additional batches are expected to further improve the prediction accuracy.

Although the lack of an independent testing set for VCC and rAAV predictions prevents assessment of model validation for new batches, our aim was to explore iLine F applicability to study this system. Furthermore, the

identification and analysis of the parameters correlated with the modeled variables provides valuable biological insights for rAAV production in this system.

Most of the attributes calculated with DDHM have no biological meaning *per se*, but can be used to characterize a dynamic phenotype, indicative of the cell adaptation to different biological situations (Feng et al., 2009; Kasprowicz et al., 2017). However, some of these parameters may have a possible biological explanation. For instance, “phase correlation”, a measure of how neighboring pixels are correlated, has a time-profile very similar to the culture viability profiles (Figure III.4 E). A possible explanation may be related with the increase in intracellular complexity during baculovirus infection. The cellular phenotype alterations occurring throughout baculovirus infection and the release of intracellular compounds to the culture supernatant during lysis will increase the entropy inside the cell, consequently resulting in less correlation of each pixel with its neighbors and a decrease in the phase correlation profiles. For viable cell concentration, it is expected that the attributes more predictive for viable cell concentration are related to light intensity, due to light dispersion caused by suspension cells, analogous to turbidimetry-based measurements. In fact, one of the parameters common to all three viable cell concentration models is “intensity correlation” (Figure III.4 F), a measure of how correlated the intensity of one pixel is to the intensity of its neighbours over the cell surface.

One of the aims of this work was to find image attributes associated with rAAV production. Some parameters are common for extracellular rAAV and viability models (Figure III.5), which is expected since rAAV release into the culture supernatant is mostly due to cell lysis (Galibert and Merten, 2011; Meghroun et al., 2005). Common parameters include “intensity average intensity”, “peak height normalized”, “phase skewness” and “optical height maximum”. Interestingly, “phase skewness” has a time-course profile very similar with

extracellular rAAV production (Figure III.4 D) for both batches. We believe this increase in “phase skewness” concomitant with AAV production is due to a combination of several factors: The cell nucleus and nucleolus possess a higher molecular density than surrounding regions, and are likely the cell organelles better detected using QPI due to their higher phase contrast (Kemper et al., 2010). Additionally, rAAV capsid assembly takes place in the nucleolus (Bennett et al., 2017). We hypothesize that AAV production in the nucleolus of infected cells increases the phase contrast of that nuclear region but not in the surrounding regions, creating an asymmetry. The attribute “phase skewness” measures the lack of symmetry for the phase histogram of the cell and would therefore increase. A similar explanation can be derived for baculovirus, which also assembles in the nucleus (Ohkawa et al., 2010). Moreover, infection at low baculovirus multiplicity of infection (MOI) yields a first round of baculovirus release from infected cells, approximately 24 hours after infection. The released baculovirus will then infect more insect cells, originating a second round of infection. In the phase skewness profiles shown in Figure III.4 D all these phases can be observed, likely validating our hypothesis: first baculovirus infection cycle from 24 h (infection time) to 48 h; and second infection from 48 to 72 hours. The fact that baculovirus and rAAV induce a different phase skewness profile (decrease for baculovirus and increase for rAAV) may be due to their different shape (rod vs icosahedral, respectively), and the fact that baculovirus nucleocapsid is assembled in another nucleus region, the virogenic stroma (Zhao et al., 2019), among other factors.

“Phase skewness” was considered significant for both rAAV models, with a total contribution for the overall model of 15 % for extracellular rAAV and 5 % for specific rAAV (Figure III.5). Although a much higher contribution for the intracellular specific rAAV model was expected, the fact that “phase skewness” is also present in some viability models may explain its high

contribution for extracellular rAAV. As expected, this parameter has negative coefficients for viability models and positive for the extracellular rAAV prediction model (Supplementary Table III.1).

Finally, it is important to consider the influence of biological factors such as cell passage or similar. Since we have a small dataset, we cannot be sure whether some of the model parameters are accounting with biological variability between the two runs.

Comparison of the number of parameters in the 3CV models allows to have a sense of the difficulty in measuring the rAAV signals when compared to VCC and viability, which have a more “macroscopic” change. More simple models (with 5 and 7 terms) were enough to describe VCC and viability, respectively, while for rAAV, models with 10 and 12 parameters were needed (for extracellular rAAV and intracellular specific rAAV, respectively). This is also expected due to the complexity of measuring viral-induced cell changes, in which a combination of methods (measuring nucleus, diameter, cell intracellular complexity) is needed. Another possibility relies in the very different ranges and time profiles for VCC in the two batches, while for rAAV only one range is available. Higher range variations allow to better discriminate between significant and non-significant attributes. We expect these models to be refined with more batches, excluding parameters which are less relevant and clearly highlighting the attributes relevant for each variable.

Other authors have monitored the IC-BEVS using real-time monitoring tools, mainly using dielectric spectroscopy (Mena et al., 2010; Negrete et al., 2007; Pais et al., 2019; Petiot et al., 2016; Zeiser et al., 2000, 1999). Compared with other published reports using RTM in this system, DHM provides a simpler workflow: First, iLine F assembly in the bioreactor is straightforward and no preliminary calibrations are needed; data analysis is in real-time (every

30 minutes) and immediate (no pre-processing needed) and, in *OsOne*, there is a beta-version algorithm to estimate the percentage of baculovirus-infected cells, which we tried for the infected batch (Supplementary Figure III.2). Further optimization of this algorithm could be helpful to monitor the baculovirus replication kinetics and optimize the production conditions, such as the overall MOI to use, and contribute to understanding how this parameter correlates with infection progression. Moreover, the attribute stepwise selection coupled with MLR methodology presented in this work has the advantage of generating more interpretable models, when compared with partial least squares (PLS) or other projection-based methods: MLR models are easier to interpret regarding the biological meaning of each parameter, enabling process understanding under the PAT initiative. This is because in MLR the coefficients of the parameters itself are analyzed, differing from PLS in which the focus is on the principal components, which are linear combinations of several parameters.

In future experiments using this modeling approach, more “perturbation” batches will be useful to determine an rAAV-related “label-free dynamic phenotype” (Kasprowicz et al., 2017), identifying the attributes related with rAAV production and gaining insights on their biological meaning. Batches that would strengthen the VCC model calculations include more “growth only” runs, at different cell seeding densities. For rAAV models, examples include runs allowing to decouple rAAV production signals from other signals which may be correlated with VCC or baculovirus production. For instance, infection with empty baculovirus (a baculovirus vector which is devoid of any transgene, but still can infect and replicate in insect cells, and thus generate the normal cytopathic effects expected in this system) or only with the rep-encoding baculovirus. Infection with only the cap-encoding baculovirus would possibly be useful for finding attributes associated with empty or full rAAV capsid formation, which together with the infectivity profile, is one of the

most important quality attributes for AAV vectors (Merten, 2016). Regarding the empty to full ratio, runs using other rAAV production systems can also be performed, particularly using systems known by their high full particle ratio, as is the case of the herpes simplex production system (Merten and Gaillet, 2016). Exploring the application of DHM to other AAV-producing systems, such as the HEK293 transfection system, could elucidate the differences for AAV production in transfection and infection processes and between different producer cells. Moreover, DHM could provide further insights on the reason why suspension-based transfection is less efficient than adherent-transfection. An alternative DHM device with equivalent image processing capabilities, the QMod (also by Ovizio Imaging Systems), could be used to enable a similar approach in adherent cell culture. Finally, combining the DDHM attributes with process data (e.g., DO profiles, total oxygen flow) may further increase prediction capabilities due to the increase of complementary information available (Bayer et al., 2019).

Finally, one of the most promising functionalities of *OsOne* is the ability to analyze individual cells and the values of their attributes. Once the attributes correlated with rAAV production are found, clone screening can be performed to identify high and low producing cells, or at least allow a deeper understanding of why some cells produce more rAAV than others. This would be feasible combining one of the other available Ovizio systems, the qMod, a camera equipped with DDHM technology, with omics technologies for determination of rAAV-associated transcriptomics and proteomics profiles (Kasprowicz et al., 2017).

5. Conclusions

Overall, we demonstrate the suitability of this methodology and DDHM technology for monitoring two of the most important variables for this

biological system, cell concentration and viability, with potential for the development of feeding strategies schemes for rAAV production. The approach described in this chapter enables model interpretability, increasing process understanding and allowing to draw conclusions regarding the biological state of the cell at each infection stage.

Moreover, models for determination of rAAV production were developed, and correlations between DHM attributes and rAAV measurements were determined, identifying for the first-time attributes related with rAAV production detectable using phase microscopy.

For future work, it would be relevant to employ the same strategy for identification of the DDHM attributes relevant for prediction of AAV infectivity and full to empty ratio, in order to fully explore the potential of this method to optimize AAV titer and quality, in line with the PAT initiative.

6. Acknowledgements

Financial support for this work was provided by the Portuguese “Fundação para a Ciência e Tecnologia” through individual PhD grant PD/BD/105873/2014. iNOVA4Health Research Unit (LISBOA-01-0145-FEDER-007344), which is cofounded by Fundação para a Ciência e Tecnologia / Ministério da Ciência e do Ensino Superior, through national funds, and by FEDER under the PT2020 Partnership Agreement, is acknowledged.

The authors would like to acknowledge Généthon for kindly providing the CMV-GFP baculovirus.

7. Conflicts of interest

Jérémie Barbau is an employee of Ovizio Imaging Systems SA/NV.

8. Supplementary Data

Supplementary Table III.1 - Estimates, corresponding standard error, t-ratio and logworth / p-value for all the models shown in Figure III.1 and III.2. For leave one batch out (LOBO) models, the batch used for model calibration is indicated between brackets. Logworth is defined as $-\log_{10}(\text{p-value})$.

Model	Parameter	Estimate	Std Error	t-Ratio	Logworth	p-value
Extracellular rAAV titer - 3CV	Intensity Average Intensity	-2.5E+11	1.7E+10	-14.4	12.6	2.5E-13
	Phase Skewness	3.9E+09	2.9E+08	13.6	12.0	9.7E-13
	Peak Height Normalized	-3.3E+10	2.5E+09	-12.9	11.6	2.8E-12
	Optical Height Maximum	4.5E+09	3.7E+08	12.3	11.2	7.0E-12
	Intensity Average Contrast	2.8E+11	2.4E+10	12.0	10.9	1.3E-11
	Intensity Average Entropy	-4.1E+10	3.6E+09	-11.4	10.4	3.7E-11
	Hu Moment 6	-1.7E+15	4.0E+14	-4.3	3.6	2.4E-04
	Hu Moment 5	3.9E+16	1.0E+16	3.8	3.1	8.7E-04
	Intensity Geometric Mean	1.2E+10	4.3E+09	2.7	1.9	1.1E-02
	Center of Mass Vertical Position	3.4E+07	1.5E+07	2.2	1.5	3.5E-02
	Intercept	2.0E+11	1.4E+10	14.2		
Specific rAAV titer - 3CV	Peak Height	-3.2E+03	1.5E+02	-21.4	14.0	9.2E-15
	Optical Volume	3.2E+03	1.7E+02	19.4	13.3	5.3E-14
	Peak Area Normalized	-5.0E+05	3.4E+04	-14.7	11.1	8.1E-12
	Cell Area	-6.2E+02	4.8E+01	-13.1	10.2	5.8E-11
	Best Depth	2.8E+03	4.8E+02	5.9	4.9	1.1E-05
	Hu Moment 5	1.7E+11	3.3E+10	5.2	4.2	5.6E-05
	Intensity Average Intensity	4.3E+05	8.6E+04	5.0	4.1	8.4E-05
	Phase Skewness	9.4E+03	2.0E+03	4.7	3.8	1.6E-04

Supplementary Table III.1 (cont.)

Model	Term	Estimate	Std Error	t-Ratio	Logworth	p-value
Specific rAAV titer - 3CV	Hu Moment 6	-6.4E+09	1.5E+09	-4.2	3.3	4.7E-04
	Intensity Maximum	-3.5E+04	9.1E+03	-3.8	2.9	1.3E-03
	Phase Average Uniformity	-5.0E+05	1.6E+05	-3.2	2.3	5.0E-03
	Hu Moment 4	-2.5E+08	1.1E+08	-2.3	1.5	3.1E-02
	Intercept	9.1E+04	3.5E+04	2.6		
Viable cell concentration - 3CV	Intensity Geometric Mean	-6.4E+07	4.0E+06	-16.2	15.7	2.2E-16
	Intensity Correlation	5.2E+07	6.3E+06	8.2	8.4	3.7E-09
	Phase Average Uniformity	-1.6E+08	2.5E+07	-6.3	6.2	5.8E-07
	Optical Height Maximum	-8.9E+05	3.4E+05	-2.6	1.9	1.4E-02
	Optical Height Minimum	-9.2E+06	4.0E+06	-2.3	1.6	2.8E-02
	Intercept	9.0E+06	6.2E+06	1.5		
Viability - 3CV	Peak Height Normalized	1.7E+02	1.3E+01	13.4	13.2	5.7E-14
	Phase Skewness	-1.4E+01	1.1E+00	-12.8	12.7	1.8E-13
	Optical Height Maximum	-2.5E+01	2.7E+00	-9.3	9.5	3.0E-10
	Hu Moment 3	8.9E+04	1.6E+04	5.7	5.4	3.8E-06
	Phase Correlation	4.8E+02	1.3E+02	3.5	2.8	1.4E-03
	Phase Average Uniformity	-1.0E+03	3.9E+02	-2.6	1.8	1.5E-02
	Intercept	-4.2E+02	1.4E+02	-3.0		
	Intensity Average Intensity	3.3E+02	1.3E+02	2.5	1.7	1.9E-02
Viable cell concentration -LOBO (growth)	Intensity Geometric Mean	-6.3E+07	7.7E+06	-8.2	4.4	3.7E-05
	Intensity Correlation	6.2E+07	2.6E+07	2.4	1.4	4.1E-02
	Phase Average Uniformity	-1.3E+08	5.9E+07	-2.2	1.3	5.6E-02

Supplementary Table III.1 (cont.)

Model	Term	Estimate	Std Error	t-Ratio	Logworth	p-value
Viable cell concentration -LOBO (growth)	Optical Height Minimum	-1.6E+07	3.7E+07	-0.4	0.2	6.8E-01
	Optical Height Maximum	-6.7E+04	2.0E+06	0.0	0.0	9.7E-01
	Intercept	-2.9E+06	3.0E+07	-0.1		
VCC LOBO (infected)	Phase Average Uniformity	1.0E+08	4.6E+07	2.2	1.4	4.4E-02
	Optical Height Maximum	7.1E+05	5.0E+05	1.4	0.7	1.8E-01
	Intensity Geometric Mean	1.1E+07	9.2E+06	1.2	0.6	2.6E-01
	Intensity Correlation	6.1E+06	6.1E+06	1.0	0.5	3.4E-01
	Optical Height Maximum*Intensity Geometric Mean	9.7E+06	1.0E+07	0.9	0.4	3.7E-01
	Intensity Geometric Mean*	-2.1E+08	2.5E+08	-0.8	0.4	4.3E-01
	Intensity Geometric Mean					
	Phase Average Uniformity * Intensity Correlation	7.1E+08	1.1E+09	0.6	0.3	5.4E-01
	Intercept	-1.3E+07	6.3E+06	-2.0		
		Intensity Average Intensity	1.6E+03	1.1E+02	15.0	6.4
Viability LOBO (growth)	Peak Height Normalized	8.3E+01	8.8E+00	9.4	4.9	1.4E-05
	Aspect Ratio	7.3E+01	2.4E+01	3.1	1.8	1.6E-02
	Circularity	4.6E+02	1.7E+02	2.7	1.6	2.6E-02
	Peak Area	4.9E-01	2.1E-01	2.3	1.3	4.8E-02
	Intercept	-1.3E+03	1.6E+02	-7.7		
Viability LOBO (infected)	Peak Height	2.1E+00	2.3E-01	9.2	5.5	3.3E-06
	Circularity	-7.7E+02	1.1E+02	-6.7	4.3	5.3E-05

Supplementary Table III.1 (cont.)

Model	Term	Estimate	Std Error	t-Ratio	Logworth	p-value
Viability LOBO (infected)	Optical Height Maximum	-2.8E+01	4.3E+00	-6.4	4.1	7.6E-05
	Aspect Ratio	-6.8E+01	1.1E+01	-6.3	4.1	8.8E-05
	Hu Moment 4	2.9E+05	6.3E+04	4.6	3.0	1.1E-03
	Phase Correlation	5.3E+02	1.2E+02	4.5	2.9	1.1E-03
	Optical Height Minimum	7.7E+01	1.8E+01	4.2	2.7	1.8E-03
	Best Depth	3.7E+00	9.0E-01	4.1	2.6	2.3E-03
	Peak Area Normalized	1.4E+02	3.6E+01	3.7	2.4	3.9E-03
	Intensity Correlation	1.6E+02	4.7E+01	3.3	2.1	7.6E-03
	Phase Skewness	-5.8E+00	2.0E+00	-2.9	1.8	1.5E-02
	Intensity Average Entropy	2.5E+01	1.0E+01	2.4	1.4	3.9E-02
	Intercept	3.0E+02	8.2E+01	3.6		

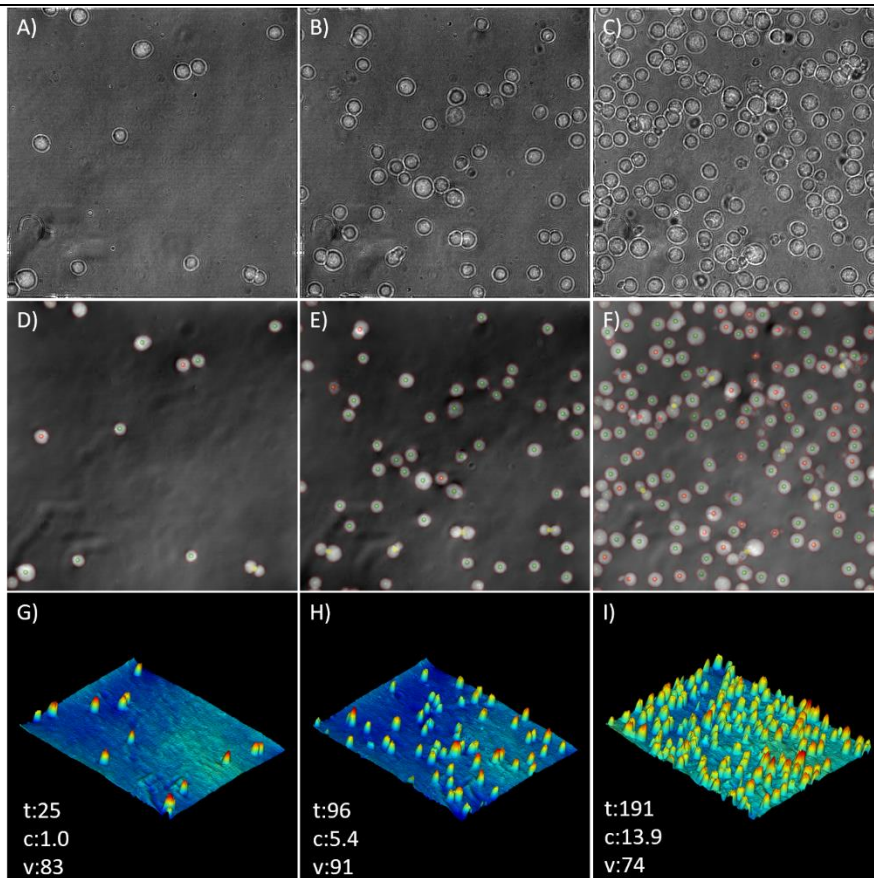
Supplementary Table III.2 - RMSE for calibration and validation models, scaled for the variable range, using the 3-fold cross-validation strategy. The dataset was divided in three partitions. Two partitions were used for model calibration, which was used for prediction of the reference data for the third partition. This process was repeated for the three partitions.

Model	Partition for testing	R ²	RMSE calibration	Normalized RMSE calibration	Q ²	RMSE validation	Normalized RMSE validation	Number of model datapoints	Number of model parameters
Extracellular rAAV titer	1	0.98	4.5E+08	3.2	0.95	8.8E+08	6.2	23	10
	2	0.99	3.9E+08	2.7	0.98	7.4E+08	5.2	24	
	3	0.99	2.8E+08	2.0	0.98	4.9E+08	3.4	23	
Specific rAAV titer	1	1.00	7.5E+02	1.5	1.00	1.0E+03	2.1	22	12
	2	0.99	1.3E+03	2.6	0.98	2.1E+03	4.4	23	
	3	1.00	7.2E+02	1.5	0.98	2.2E+03	4.5	20	
Viable cell concentration	1	0.97	4.5E+05	4.5	0.92	7.6E+05	7.7	23	5
	2	0.94	7.2E+05	7.3	0.93	7.7E+05	7.8	26	
	3	0.98	4.4E+05	4.5	0.94	7.0E+05	7.1	23	
Viability	1	0.99	2.6E+00	3.7	0.98	3.6E+00	5.2	24	7
	2	0.99	1.9E+00	2.8	0.99	2.1E+00	3.1	26	
	3	0.98	2.1E+00	3.1	0.98	2.6E+00	3.7	24	

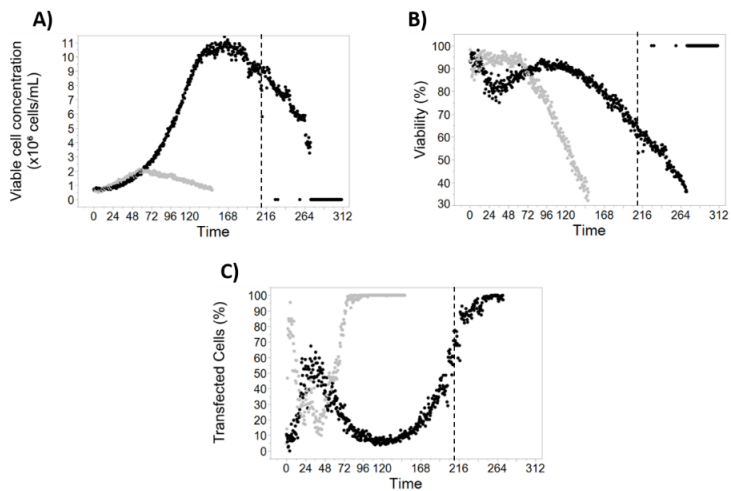
Supplementary Table III.3 - Quality characteristics overview for the models presented in Figure III.1 and 2. R^2 and Q^2 are the correlation coefficients of calibration and validation, respectively. Also shown are the root mean squared errors (RMSE) for calibration and validation and the RMSE scaled by the variable range.

Variable	Validation Method	R^2	RMSE calibration	Normalized	Q^2	RMSE validation	Normalized
				RMSE calibration (%)			RMSE validation (%)
Viability	LOBO	1.00	6.8×10^{-1}	1.0	0.74	1.1×10^1	15.8
Viable cell concentration	LOBO	0.97	4.7×10^5	4.8	-0.69	3.6×10^6	36
Viability	3CV	0.99	2.2	3.2	0.98	2.9	4.1
Viable cell concentration	3CV	0.96	5.4×10^5	5.4	0.93	7.1×10^5	7.2
Intracellular specific rAAV titer	3CV	1.00	9.1×10^2	1.9	0.99	1.9×10^3	3.8
Extracellular rAAV titer	3CV	0.99	3.8×10^8	2.7	0.97	7.2×10^8	5.0

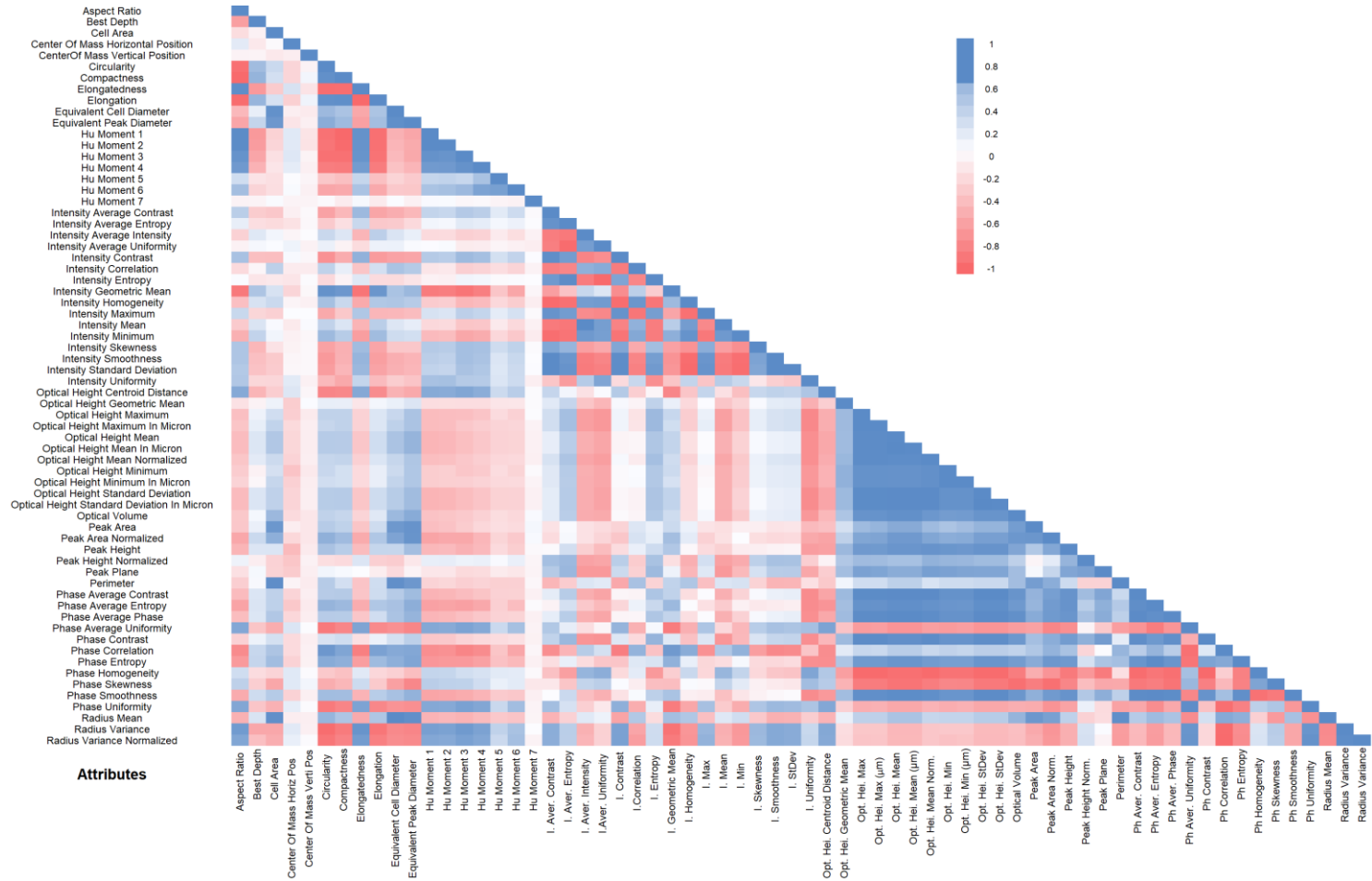
LOBO – leave one batch out; 3CV – 3-fold cross-validation; R^2 – correlation coefficient of calibration; RMSE - Root Mean Squared Error; Q^2 – correlation coefficient of validation.



Supplementary Figure III.1 - Overview of the cell culture evolution profile over time, as captured by OsOne software. Phase images are presented in top row; middle row shows OsOne identification of each cell, with indication of the cell viability by a coloured circle in the middle of each cell: green - viable cells, red - non-viable, yellow - cell cluster; the corresponding calculated holograms are shown in bottom row. Each column represents different image types from the same culture timepoint, indicated in the bottom of the column. Abbreviations: t – culture time (h); c - viable cell concentration (10^6 cells/mL); v: viability (%).



Supplementary Figure III.2 - Evolution of the predicted process variables using Ovizio proprietary models. Growth batch is represented in black, while infection batch is colored in grey. **A)** Viable cell concentration. **B)** Viability. **C)** Percentage of transfected cells. Dashed line indicates the time when controller setpoints were changed, with noticeable alterations in the iLine F profiles.



Supplementary Figure III.3 – Pearson correlation coefficients for all attributes. A heatmap representation is shown, with blue colors indicating positive correlation and red colors indicating negative correlations.

9. References

- Altschuler, S.J., Wu, L.F., 2010. Cellular Heterogeneity: Do Differences Make a Difference? *Cell* 141, 559–563. <https://doi.org/10.1016/j.cell.2010.04.033>
- Bayer, B., von Stosch, M., Melcher, M., Duerkop, M., Striedner, G., 2019. Soft sensor based on 2D-fluorescence and process data enabling real-time estimation of biomass in *Escherichia coli* cultivations. *Eng. Life Sci.* <https://doi.org/10.1002/elsc.201900076>
- Bennett, A., Mietzsch, M., Agbandje-mckenna, M., 2017. Understanding capsid assembly and genome packaging for adeno-associated viruses. <https://doi.org/10.2217/fvl-2017-0011>
- Bernal, V., Carinhas, N., Yokomizo, A.Y., Carrondo, M.J.T., Alves, P.M., 2009. Cell density effect in the baculovirus-insect cells system: A quantitative analysis of energetic metabolism. *Biotechnol. Bioeng.* 104, 162–180. <https://doi.org/10.1002/bit.22364>
- Cox, M.M.J., 2012. Recombinant protein vaccines produced in insect cells. *Vaccine* 30, 1759–1766. <https://doi.org/10.1016/j.vaccine.2012.01.016>
- FDA, U.S.D. of H. and H.S., 2004. Guidance for Industry PAT — A Framework for Innovative Pharmaceutical Development, Manufacturing, and Quality Assurance. FDA Off. Doc. 16. <https://doi.org/http://www.fda.gov/CDER/guidance/6419fnl.pdf>
- Feng, Y., Mitchison, T.J., Bender, A., Young, D.W., Tallarico, J.A., 2009. Multi-parameter phenotypic profiling: Using cellular effects to characterize small-molecule compounds. *Nat. Rev. Drug Discov.* 8, 567–578. <https://doi.org/10.1038/nrd2876>
- Galibert, L., Merten, O.-W., 2011. Latest developments in the large-scale production of adeno-associated virus vectors in insect cells toward the treatment of neuromuscular diseases. *J. Invertebr. Pathol.* 107 Suppl, S80–S93. <https://doi.org/10.1016/j.jip.2011.05.008>
- Gray, S.J., Choi, V.W., Asokan, A., Haberman, R.A., Thomas, J., Samulski, R.J., 2012. Production of Recombinant Adeno-Associated Viral Vectors and Use in In Vitro and In Vivo Administration. *Curr. Protoc. Neurosci.* Oct, 1–36. <https://doi.org/10.1002/0471142301.ns0417s57>
- Grein, T.A., Loewe, D., Dieken, H., Salzig, D., Weidner, T., Czermak, P., 2018. High titer oncolytic measles virus production process by integration of dielectric spectroscopy as online monitoring system. *Biotechnol. Bioeng.* 115, 1186–1194. <https://doi.org/10.1002/bit.26538>
- Hidalgo, D., Paz, E., Palomares, L.A., Ramírez, O.T., 2017. Real-time imaging reveals unique heterogeneous population features in insect cell cultures. *J. Biotechnol.* 259, 56–62. <https://doi.org/10.1016/j.jbiotec.2017.08.019>
- Janakiraman, V., Forrest, W.F., Chow, B., Seshagiri, S., 2006. A rapid method for estimation of baculovirus titer based on viable cell size. *J. Virol. Methods* 132, 48–58. <https://doi.org/10.1016/j.jviromet.2005.08.021>
- Janicke, B., Kårsnäs, A., Egelberg, P., Alm, K., 2017. Label-free high temporal resolution assessment of cell proliferation using digital holographic microscopy. *Cytom. Part A* 91, 460–469. <https://doi.org/10.1002/cyto.a.23108>
- Kamlund, S., 2018. Not all those who wander are lost: A study of cancer cells by digital holographic imaging, fluorescence and a combination thereof, PhD thesis, Lund University, Lund
- Kasprowicz, R., Suman, R., O'Toole, P., 2017. Characterising live cell behaviour: Traditional label-free and quantitative phase imaging approaches. *Int. J. Biochem. Cell Biol.* 84, 89–95. <https://doi.org/10.1016/j.biocel.2017.01.004>
- Kemper, B., Bauwens, A., Vollmer, A., Ketelhut, S., Langehanenberg, P., Müthing, J., Karch, H., von Bally, G., 2010. Label-free quantitative cell division monitoring of endothelial cells by digital holographic microscopy. *J. Biomed. Opt.* 15, 036009. <https://doi.org/10.1117/1.3431712>
- Kühn, J., Shaffer, E., Mena, J., Breton, B., Parent, J., Rappaz, B., Chambon, M., Emery, Y., Magistretti, P., Depeursinge, C., Marquet, P., Turcatti, G., 2013. Label-free cytotoxicity screening assay by digital holographic microscopy. *Assay Drug Dev. Technol.* 11, 101–107. <https://doi.org/10.1089/adt.2012.476>
- Laasfeld, T., Kopanchuk, S., Rinken, A., 2017. Image-based cell-size estimation for baculovirus quantification. *Biotechniques* 63, 161–168. <https://doi.org/10.2144/000114595>

- Loutfi, H., Pellen, F., Le Jeune, B., Lteif, R., Kallassy, M., Le Brun, G., Abboud, M., 2020. Real-time monitoring of bacterial growth kinetics in suspensions using laser speckle imaging. *Sci. Rep.* 10, 1–11. <https://doi.org/10.1038/s41598-019-57281-2>
- Mann, C.J., Yu, L., Lo, C.-M., Kim, M.K., 2005. High-resolution quantitative phase-contrast microscopy by digital holography. *Opt. Express* 13, 8693. <https://doi.org/10.1364/opex.13.008693>
- Meghrouh, J., Aucoin, M.G., Jacob, D., Chahal, P.S., Arcand, N., Kamen, A.A., 2005. Production of Recombinant Adeno-Associated Viral Vectors Using a Baculovirus / Insect Cell Suspension Culture System: From Shake Flasks to a 20-L Bioreactor. *Biotechnol. Prog.* 154–160. <https://doi.org/10.1021/bp049802e>
- Mena, J., Aucoin, M., Montes, J., Chahal, P., Kamen, A., 2010. Improving adeno-associated vector yield in high density insect cell cultures. *J. Gene Med.* 157–167. <https://doi.org/10.1002/jgm>
- Merten, O., 2016. AAV vector production: state of the art developments and remaining challenges. *Cell Gene Ther.* 521–551. <https://doi.org/10.18609/cgti.2016.067>
- Merten, O., Gaillet, B., 2016. Viral vectors for gene therapy and gene modification approaches. *Biochem. Eng. J.* 108, 98–115. <https://doi.org/10.1016/j.bej.2015.09.005>
- Moore, B., Sanford, R., Zhang, A., 2019. Case study: The characterization and implementation of dielectric spectroscopy (biocapacitance) for process control in a commercial GMP CHO manufacturing process. *Biotechnol. Prog.* 35. <https://doi.org/10.1002/btpr.2782>
- Naso, M.F., Tomkowicz, B., Perry, W.L., Strohl, W.R., 2017. Adeno-Associated Virus (AAV) as a Vector for Gene Therapy. *BioDrugs.* <https://doi.org/10.1007/s40259-017-0234-5>
- Negrete, A., Esteban, G., Kotin, R.M., 2007. Process optimization of large-scale production of recombinant adeno-associated vectors using dielectric spectroscopy. *Appl. Microbiol. Biotechnol.* 76, 761–72. <https://doi.org/10.1007/s00253-007-1030-9>
- Nikolay, A., Léon, A., Schwamborn, K., Genzel, Y., Reichl, U., 2018. Process intensification of EB66® cell cultivations leads to high-yield yellow fever and Zika virus production. *Appl. Microbiol. Biotechnol.* 102, 8725–8737. <https://doi.org/10.1007/s00253-018-9275-z>
- Ohkawa, T., Volkman, L.E., Welch, M.D., 2010. Actin-based motility drives baculovirus transit to the nucleus and cell surface. *J. Cell Biol.* 190, 187–195. <https://doi.org/10.1083/jcb.201001162>
- Pais, D.A.M., Carrondo, M.J.T., Alves, P.M., Teixeira, A.P., 2014. Towards real-time monitoring of therapeutic protein quality in mammalian cell processes. *Curr. Opin. Biotechnol.* 30, 161–167. <https://doi.org/10.1016/j.copbio.2014.06.019>
- Pais, D.A.M., Portela, R.M.C., Carrondo, M.J.T., Isidro, I.A., Alves, P.M., 2019. Enabling PAT in insect cell bioprocesses: In situ monitoring of recombinant adeno-associated virus production by fluorescence spectroscopy. *Biotechnol. Bioeng.* bit.27117. <https://doi.org/10.1002/bit.27117>
- Palomares, L.A., Pedroza, J.C., Ramírez, O.T., 2001. Cell size as a tool to predict the production of recombinant protein by the insect-cell baculovirus expression system. *Biotechnol. Lett.* 23, 359–364. <https://doi.org/10.1023/A:1005688417525>
- Petiot, E., Ansoorge, S., Rosa-Calatrava, M., Kamen, A., 2016. Critical phases of viral production processes monitored by capacitance. *J. Biotechnol.* 242, 19–29. <https://doi.org/10.1016/j.jbiotec.2016.11.010>
- Rapoport, D.H., Becker, T., Mamlouk, A.M., Schick Tanz, S., Kruse, C., 2011. A novel validation algorithm allows for automated cell tracking and the extraction of biologically meaningful parameters. *PLoS One* 6. <https://doi.org/10.1371/journal.pone.0027315>
- Santos, R.M., Kessler, J.M., Salou, P., Menezes, J.C., Peinado, A., 2018. Monitoring mAb cultivations with in-situ raman spectroscopy: The influence of spectral selectivity on calibration models and industrial use as reliable PAT tool. *Biotechnol. Prog.* 34, 659–670. <https://doi.org/10.1002/btpr.2635>
- Sequeira, D.P., Correia, R., Carrondo, M.J.T., Roldão, A., Teixeira, A.P., Alves, P.M., 2018. Combining stable insect cell lines with baculovirus-mediated expression for multi-HA influenza VLP production. *Vaccine* 36, 3112–3123. <https://doi.org/10.1016/j.vaccine.2017.02.043>

- Smith, R.H., Levy, J.R., Kotin, R.M., 2009. A simplified baculovirus-AAV expression vector system coupled with one-step affinity purification yields high-titer rAAV stocks from insect cells. *Mol. Ther.* 17, 1888–1896. <https://doi.org/10.1038/mt.2009.128>
- Tulsyan, A., Wang, T., Schomer, G., Khodabandehlou, H., Coufal, M., Undey, C., 2020. Automatic real-time calibration, assessment, and maintenance of generic Raman models for online monitoring of cell culture processes. *Biotechnol. Bioeng.* 117, 406–416. <https://doi.org/10.1002/bit.27205>
- Ugele, M., Weniger, M., Leidenberger, M., Huang, Y., Bassler, M., Friedrich, O., Kappes, B., Hayden, O., Richter, L., 2018. Label-free, high-throughput detection of *P. falciparum* infection in sphered erythrocytes with digital holographic microscopy. *Lab Chip* 18, 1704–1712. <https://doi.org/10.1039/c8lc00350e>
- Zavala-Ortiz, D.A., Ebel, B., Li, M.Y., Barradas-Dermitz, D.M., Hayward-Jones, P.M., Aguilar-Uscanga, M.G., Marc, A., Guedon, E., 2019. Interest of locally weighted regression to overcome nonlinear effects during in situ NIR monitoring of CHO cell culture parameters and antibody glycosylation. *Biotechnol. Prog.* 1–10. <https://doi.org/10.1002/btpr.2924>
- Zeiser, A., Bédard, C., Voyer, R., Jardin, B., Tom, R., Kamen, a a, 1999. On-line monitoring of the progress of infection in Sf-9 insect cell cultures using relative permittivity measurements. *Biotechnol. Bioeng.* 63, 122–6. [https://doi.org/10.1002/\(SICI\)1097-0290\(19990405\)63:1<122::AID-BIT13>3.0.CO;2-I](https://doi.org/10.1002/(SICI)1097-0290(19990405)63:1<122::AID-BIT13>3.0.CO;2-I)
- Zeiser, A., Elias, C.B., Voyer, R., Jardin, B., Kamen, A.A., 2000. On-line monitoring of physiological parameters of insect cell cultures during the growth and infection process. *Biotechnol. Prog.* 16, 803–808. <https://doi.org/10.1021/bp000092w>
- Zhao, S., He, G., Yang, Y., Liang, C., 2019. Nucleocapsid assembly of baculoviruses. *Viruses* 11. <https://doi.org/10.3390/v11070595>

Chapter IV

Dielectric spectroscopy as a PAT tool in the insect cell-baculovirus system: optimization of infection timing and robustness in rAAV manufacturing

This chapter is adapted from the manuscript:

Pais, DAM, Brown, C, Grewal, H, Isidro, IA, Alves, PM, Slade, PG. 2020. "Dielectric spectroscopy as a PAT tool in the insect cell-baculovirus system: optimization of infection timing and robustness in rAAV manufacturing" (*in preparation*).

Author Contribution

The data presented in this chapter results from the work Daniel Pais performed at Voyager Therapeutics, Inc., Cambridge, MA, while doing a PhD Co-Op in the Upstream Process Development group. Daniel Pais participated in the experimental setup and design, executed the experiments, analyzed the data and wrote this chapter.

Abstract

The insect cell – baculovirus expression vector system is established as one of the preferred methods for large scale recombinant adeno-associated virus (rAAV) production, largely due to its scalability potential and the high volumetric productivities achieved. However, rAAV production and infectious titers can be affected by several process parameters, of which Sf9 cell concentration at infection and cell viability at harvest are the most critical. Furthermore, these parameters are dependent on the rAAV serotype, and as such are pipeline dependent.

Herein we demonstrate the use of dielectric spectroscopy as a process analytical technology (PAT) tool to continuously monitor Sf9 cell growth in 2 L stirred tank bioreactors and accurately predict the infection time up to 24 hours in advance. Furthermore, we developed prediction models for important process variables based on the dielectric measurements of the culture. These multiple linear regression-based models resulted in correlation coefficients (Q^2) of 0.89 for viable cell concentration, 0.97 for viability, 0.92 for diameter and 0.77 for intracellular rAAV titer in an independent testing set. These models provide the capability to distinguish between high and low production batches and reliably estimate the time of harvest, avoiding unnecessary prolonged exposure of viral vector to protease activity due to baculovirus-induced cell lysis.

We show dielectric spectroscopy can be used for narrowing the range for the infection window, consequently ensuring process robustness and reasonable rAAV prediction ability, while decreasing the probability of contamination due to reduced sampling needs. Dielectric spectroscopy proves useful for real-time monitoring of rAAV-production, and its FDA compliance renders it readily available for use in existing processes.

Contents

1.	Introduction	147
2.	Materials and Methods	149
2.1.	Cell line and culture medium.....	149
2.2.	Viruses, infection and titration.....	150
2.3.	Bioreactor cultures and sample processing	150
2.4.	Process-to-target script.....	152
2.5.	Modeling strategy and software	153
2.5.1.	Dataset	153
2.5.2.	Model calibration and testing	153
3.	Results	155
3.1.	Accurate prediction of infection timing using continuous permittivity monitoring.....	155
3.2.	Dielectric spectroscopy can be used for monitoring the progress of baculovirus infection.....	158
3.3.	rAAV production kinetics in the insect cell – baculovirus system.....	162
3.4.	Detection of rAAV-induced signals using multiple linear regression	162
4.	Discussion	164
5.	Conclusions	169
6.	Conflicts of interest	169
7.	Supplementary Data	170
8.	References	172

1. Introduction

Recombinant adeno-associated viruses (rAAV) are an ideal candidate gene therapy vector for many rare diseases, due to their ability to transduce non-dividing cells from several tissues maintaining a long-term gene expression. Besides, rAAV possess low immunogenicity compared to other viral vectors, and are physical resistant to harsh conditions, making it resilient to industry manufacturing methodologies, long-time storage, and *in vivo* administration (Galibert and Merten, 2011; Xu et al., 2014).

While several biological systems have been adapted for rAAV production, the insect cell - baculovirus expression vector system (IC-BEVS) is the system more amenable for large scale rAAV production. Insect cells possess scalable and GMP-compatible characteristics, since they can grow in suspension to high cell densities in serum-free conditions (Penaud-Budloo et al., 2017); as for the baculovirus, its use as a vector relies on the high recombinant protein production yields achieved and the absence of mammalian-derived products (Yee et al., 2018). This combination resulted in several approved products, targeting Influenza (Flublok®), cancer (Cervarix® and Provenge®) and at least one rAAV-based gene therapy (Glybera™) (Monteiro, 2015; Shahryari et al., 2019).

Since 2004, with the introduction of the PAT initiative (FDA, 2004), regulatory entities have become increasingly more stringent regarding the end product quality attributes of biopharmaceutical products (Pais et al., 2014). By encouraging the pharmaceutical industry to develop tools to characterize the pharmaceutical product and manufacturing process, in the end yielding biological products with consistent quality, the PAT initiative facilitates regulatory approval of new drugs. With that aim, the use of real-time monitoring tools for process characterization and product monitoring is strongly encouraged (Guerra et al., 2019; Pais et al., 2014).

The ability to monitor in real-time the insect cell-baculovirus system can support the time of harvest decision, an important process variable to consider given the lytic nature of the baculovirus and consequential release of proteases, which can compromise the quality of the end-product (Grein et al., 2018; M Lecina et al., 2006; Nikolay et al., 2018; Pais et al., 2019). Moreover, the ability to estimate the rAAV titer in real-time is also desirable to harvest rAAV when its concentration is higher.

Several types of sensors have been applied for monitoring of cell culture processes. Substantial work has been developed using spectroscopy tools, mainly infrared (mid and near), Raman and fluorescence (Marison et al., 2013; Mercier et al., 2016; Pais et al., 2019; Qiu et al., 2014; Riley et al., 1997).

Another spectroscopy tool with proven applications for monitoring cell size and biovolume is dielectric spectroscopy (Justice et al., 2011; Mercier et al., 2016; Moore et al., 2019; Opel et al., 2010), with several authors reporting its application for monitoring insect cells in suspension (Ansorge et al., 2007; Elias et al., 2000; Negrete et al., 2007; Petiot et al., 2016; Zeiser et al., 2000, 1999). This technique is based on the detection of the cell dielectric potential, which is dependent on the intracellular composition. As such, dielectric spectroscopy is ideal for monitoring infection-based processes, because of the effect that virus formation and release have in the cell membrane (Petiot et al., 2016; Petiot and Kamen, 2012).

The application of dielectric spectroscopy to monitor the production of viral vector production processes is reported in several other works: Zeiser and coworkers correlated permittivity measurements with cell swelling due to intracellular baculovirus production (Zeiser et al., 1999); Ansorge *et al.* followed lentivirus budding process by monitoring physiological changes in infected producer cells (Ansorge et al., 2011); Petiot *et al.* identified critical

infection phases in enveloped and non-enveloped viruses, produced using transfection and infection methods (Petiot et al., 2016); Grein and coworkers used the culture permittivity measurements to detect the optimal harvest time in an oncolytic virus (Grein et al., 2018); and Negrete *et al.* correlated Sf9 cell diameter with rAAV production yield, decreasing the optimal harvest time by 24 hours (Negrete et al., 2007). However, so far there is a lack of real-time monitoring solutions to monitor the accumulation of viral vectors in real-time (Petiot et al., 2016), which was not addressed in the cited works.

Herein, we explored the capabilities of dielectric spectroscopy to monitor the cell physiological state to build prediction models for viable cell concentration, viability, diameter and intracellular rAAV for the insect cell-baculovirus system. We used a commercially available permittivity and conductivity probe to monitor in situ the dielectric properties of the culture. By combining the permittivity readings at 18 different frequencies with the beta-dispersion parameters determined for the system, we built a permittivity-based soft sensor for accurate prediction of the infection timing and for estimation of intracellular rAAV titers in real-time.

2. Materials and Methods

2.1. Cell line and culture medium

Spodoptera frugiperda Sf9 cells were routinely cultivated in 5 L Corning shake flasks with 3 L working volume of ESF-AF medium (Expression Systems™), at 27 °C with an agitation rate of 80 rpm in an Innova 44R incubator (orbital motion diameter = 2.54 cm, Eppendorf). Cell concentration and viability were determined using a Vi-Cell XR Cell Counter (Beckman Coulter).

2.2. Viruses, infection and titration

Three recombinant *Autographa californica* nucleopolyhedrovirus were used as expression vector, which due to confidentiality reasons will not be fully described. For the standard rAAV production process, cells were infected with a “transgene” and “repcap” baculovirus as described in the following section. These batches are referred as “standard” throughout this chapter. The “transgene” baculovirus encodes an interference RNA gene to selectively knock down, or reduce, the mRNA levels of a specific neurodegenerative disease. This gene is flanked by the AAV inverted terminal repeats (ITRs). The “repcap” baculovirus encodes for the expression of an AAV1 serotype.

The third recombinant baculovirus vector used in some experiments did not encode for any recombinant transgene (hence named “empty Bac”), but it is still able to infect and replicate in Sf9 cells.

After generation of the bacmids for the above mentioned baculoviruses, those were used to transfect Sf9 suspension cells. As described elsewhere (Wasilko et al., 2009), infected cells were grown until the diameter increased, indicating successful baculovirus infection and replication, but before the viability started to decrease. At that culture time, cells were frozen and cryopreserved as baculovirus-infected insect cells (BIICs), which were subsequently used as the viral inoculum for bioreactor experiments.

Recombinant adeno-associated virus (rAAV) intracellular titer was estimated by an *in-house* qPCR assay.

2.3. Bioreactor cultures and sample processing

Bioreactor cultures were performed in benchtop Finesse 3 L bioreactors with 1.6 L culture volume, equipped with one turbine with three blades tilted at 45 ° angle (“elephant ear” turbine). Temperature control (27 °C) was achieved using a heating jacket. Dissolved oxygen (DO) concentration was kept at

40 % by continuous flow of air over the headspace and on-demand supply of air and O₂ mixtures using a L-shaped sparger in the bottom of the vessel. The stirring rate was kept at 200 rpm. All controller action was ensured by Finesse Controllers and DeltaV software.

Bioreactors were seeded at 1.1×10^6 Sf9 cells/mL. Infection was performed at different cell densities: 3×10^6 cells/mL for “standard”, “empty” and “blend” batches and 5×10^6 cells/mL for “cell density effect” batches (see Figure IV.1 for details on each type of batch). All batch types except “empty” were infected using both “repcap” and “transgene” BIIcs at specific volume of culture to BIIc volume ratios. For “empty” runs, “empty” BIIcs (“empty” baculovirus cryopreserved in infected Sf9 cells) were added to the Sf9 cultures at a total volume to volume ratio as both the “repcap” and “transgene” BIIcs. For “blend” batches, both “standard” and “empty” infections were performed in separate bioreactors. On day 2 post-infection, cells from both reactors were transferred to another bioreactor, with the following ratios of “standard” to “empty” (100:0; 65:35; 40:60; 10:90), in a total of 1.3 L working volume. The multiplicity of infection (MOI) was kept constant for every batch.

The *Incyte* sensor (Hamilton) was inserted in a standard 19 mm bioreactor top port, to perform *in situ* permittivity and conductivity measurements. After sterilization, sensor readings were zeroed with culture medium, after allowing enough time for the permittivity and conductivity signals to stabilize at 27 °C. Permittivity and conductivity measurements were performed every six minutes, with permittivity measurements obtained in a range of 18 frequencies between 300 to 10000 kHz. Measurements were recorded using the ArcView instrument (Hamilton). In the “blend” experiments, only the “blend” bioreactors were monitored with *Incyte*, this being the reason why there are no permittivity measurements before day 2 post-infection.

Sampling for determination of reference variables was done three times per day before infection and four times per day after infection. At each sampling point, cell concentration and viability were measured using Vi-cell Counter. For rAAV determination, 10 mL of culture supernatant were subjected to a clarification step (1000 g, 10 min) to separate intra and extracellular rAAV. Supernatant was discarded, and the pellet resuspended in an equal volume of fresh medium, to which a 1.3 mL of lysis solution was added. Samples were left agitating at 27 °C, 200 rpm, for approximately 24 hours, centrifuged (4000 g, 5 minutes), filtrated through a 0.2 µm syringe filter and stored at 4 °C until analysis.

2.4. Process-to-target script

The process-to-target (PTT) is an *in-house* script which runs in the JMP (SAS Institute) programming language. The PTT script predicts the infection timing based on all the measured permittivity values for the 1000 kHz frequency, considering timepoints from cell seeding to the moment the script is run. It is based in a time-weighted linear model of permittivity. Briefly, the script plots the permittivity values from the *Incyte* probe and the corresponding time in hours since the beginning of the run. Each data point is given a weight (Time^7), with later timepoints having a significantly higher weight when compared to earlier time points, avoiding the inherent non-linearity of the initial portion of the permittivity curve (corresponding to the lag phase). A weighted linear model is then fit to the data and the model values are saved. Using the target permittivity, the model values are used to calculate the time in hours at which the culture will reach infection density. The time remaining to infection is also calculated using the current time. The script outputs the graphical results as demonstrated in the results section.

2.5. Modeling strategy and software

2.5.1. Dataset

A total of 14 bioreactors were run in different conditions: 6 “standard” runs, 2 “cell density effect” runs, 2 “empty” runs and 4 “blend” runs (Figure IV.1).

All analysis and modeling were performed in JMP v14 (SAS institute).

The *Incyte* data consists of 22 variables: permittivity measured at 18 different frequencies, medium conductivity and 3 beta-dispersion curve parameters (alpha, characteristic frequency and $\Delta\epsilon$). All these variables are automatically calculated by the *Incyte* sensor. After run completion, the *Incyte* data was smoothed using a 30-minute (5 datapoints) moving average filter. This data was time-aligned with the corresponding sampling points (reference data).

Biovolume was calculated based on the viable cell concentration and the cell diameter measurements, considering cells as perfect spheres.

2.5.2. Model calibration and testing

For calibrating the models, the offline reference data and corresponding online averages were used. The dataset was divided in calibration and testing set, with two “standard” batches (numbered 5 and 7) as testing set and the remaining belonging to calibration set. For the “empty” runs, random rAAV titers were generated, with a normal distribution of rAAV titers below the qPCR limit of detection. These random datapoints were divided by the real cell concentration to calculate the specific rAAV titers for “empty” batches. For modeling rAAV data, only the data after 2.5 days post-infection was used, when rAAV titer was above the limit of detection of the assay.

JMP “Fit model” platform was used. Briefly the 22 parameters were subjected to forward and backwards stepwise regression to find the most significant parameters to each of the reference variables.

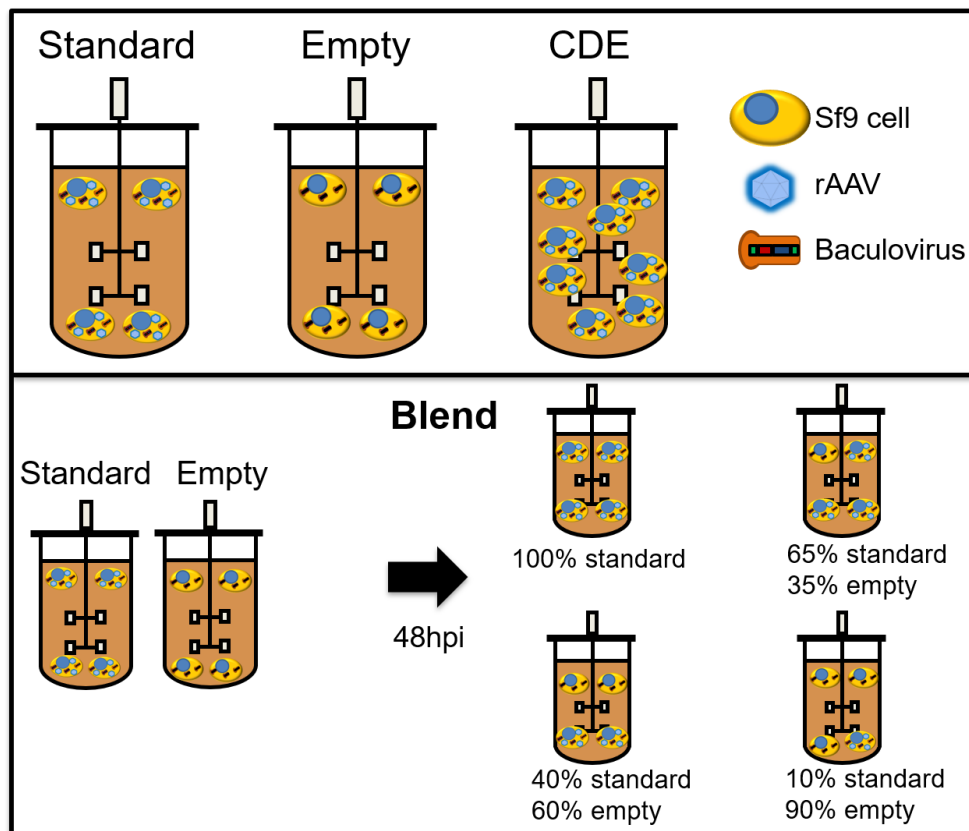


Figure IV.1 - Overview of the different batches used for model calibration. “Standard” runs represent a normal infection process, with co-infection with repcap- and transgene-Baculovirus Infected Insect Cells (BIICs). “Empty” runs were infected with an empty-BIIC, a BIIC which was infected with a baculovirus vector devoid of any transgene, but still able to replicate and induce cytopathic effects in infected cells. Cell density effect (CDE) runs are like “standard” runs, except that infection was performed at 5×10^6 cells/mL instead of 3×10^6 . “Blend” runs consisted of separate “standard” and “empty” batches. 2 days after infection, cells from both reactors were transferred to new bioreactors, with the indicated proportions of each batch. Hpi – Hours post-infection.

In a forward stepwise regression method, the most significant attribute is identified and added to the model, followed by identification and inclusion in the model of the second most significant attribute and so on. In a backwards stepwise regression method, all parameters are added to the model in the beginning and are stepwise removed according to their lack of significance to the model. The significance level considered was $p\text{-value} = 0.05$. For the most

significant attributes, their two-level interactions and quadratics were also considered, using the same combination of forward and backwards stepwise regression.

RMSEs for calibration (RMSEC) and testing (RMSET) were calculated for all models (equation 1). The correlation coefficients of calibration and testing were calculated according to equation 2 using calibration (R^2) or testing (Q^2) data.

In equation 1, \hat{y} represents a vector of model-predicted values and y represents the corresponding reference data; $ncal$ and n_{test} represent the number of samples in the calibration or testing set, respectively. σ^2 represents sample variance.

$$RMSEC = \sqrt{\frac{\sum_{i=1}^{ncal} (\hat{y} - y)^2}{ncal}} \quad RMSET = \sqrt{\frac{\sum_{i=1}^{n_{test}} (\hat{y} - y)^2}{n_{test}}} \quad (1)$$

$$R^2 = 1 - \frac{RMSEC^2}{\sigma^2} \quad Q^2 = 1 - \frac{RMSET^2}{\sigma^2} \quad (2)$$

3. Results

3.1. Accurate prediction of infection timing using continuous permittivity monitoring

Our target cell concentration at infection (CCI) is pipeline dependent. For this specific vector, the infection target is 3×10^6 cells/mL. However, inter-batch differences of up to 24 hours can occur for the cells to reach the target concentration (Figure IV.2 A). In order to accurately predict infection timing, an operator-independent strategy was developed. This strategy, entitled “process-to-target”, is based on the real-time continuous availability of permittivity measurements provided by the *Incyte* sensor. The first step was

then to determine the correlation between permittivity and viable cell concentration, which is linear during the exponential growth stage. As such, the permittivity corresponding to the target cell concentration was determined to be 2.2 pF/cm (2.18-2.34 pF/cm, 95 % confidence interval, Figure IV.2 B).

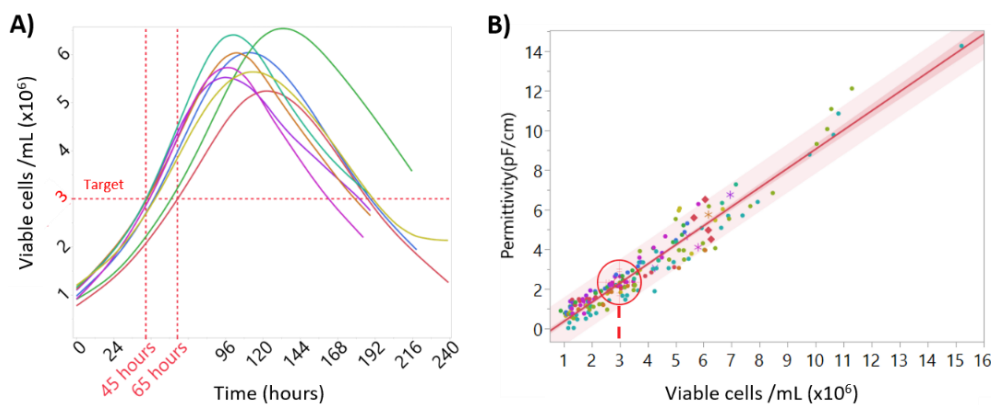


Figure IV.2 - Process variability and correlation between permittivity and viable cell concentration. **A)** Viable cell concentration time-course profiles for the “standard” batches, with co-infection with repcap and transgene BIICs. The time when the cells reached the target cell concentration at infection can vary up to 24 hours. **B)** Correlation between viable cell concentration measured by Vi-cell and permittivity values measured by the Incyte sensor. The target value of VCC=3x10⁶ cells is represented by a target, corresponding to a permittivity value of 2.2 (95% CI = 2.18-2.34). $R^2_{\text{adj}}=0.94$.

The obtained permittivity target was used as input for the “process-to- target” script. The other inputs are the permittivity time-profile data until the present time. The PTT script will then return the estimated predicted time when cells will be at the desired permittivity value (Figure IV.3).

Prediction accuracy improves significantly with the availability of more datapoints, but accurate predictions are obtained as early as 24 hours after seeding (Table IV.1).

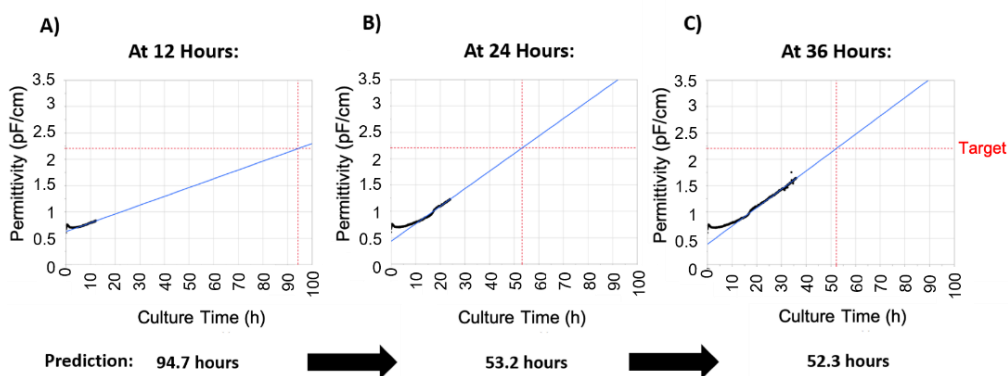


Figure IV.3 – Outputs of the process-to-target (PTT). The script was run at different times after inoculation, and the infection timing predictions are indicated below each image. For this figure, batch 5 was used, in which the target was reached at 50.8 h. Permittivity data is represented in black, the blue line represents model predictions and the red lines are the target (y axis) and the predicted time the target will be reached (x axis). A) PTT script run 12 hours after seeding. B) PTT script run 24 hours after seeding C) PTT script run 36 hours after seeding.

Table IV.1 – Application of the PTT script to each of ten batches monitored using the Incyte probe at several process timepoints after seeding. The numbers in the prediction columns represent the predicted infection time (in hours post seeding). Actual time indicates the time in hours that the permittivity equaled the nominal target of 2.2 pF/cm. “N/A” indicates a timepoint that was past the point where the target was reached. CDE = Cell density effect. The data presented in this table was calculated after batch completion.

Batch number	Batch type	Prediction					Actual time
		6 h	12 h	24 h	36 h	48 h	
1	Standard	-648	129	53	78	54	55
2	Standard	-299	73	59	67	59	59
3	Empty	458	95	64	56	53	52
4	Standard	196	114	59	57	56	55
5	Standard	213	95	53	52	50	51
6	Standard	136	56	37	N/A	N/A	36
7	Standard	-92	108	53	55	57	52
8	CDE	-120	156	65	73	65	61
9	Empty	-746	112	50	52	N/A	48
10	CDE	553	107	56	60	55	54

3.2. Dielectric spectroscopy can be used for monitoring the progress of baculovirus infection

Analysis of the variables measured by the *Incyte* probe allows to find similarities between those variables and the critical process variables of this system, such as cell concentration, viability and virus production (Figure IV.4). The first observation is that the culture conductivity increases simultaneously with the onset of baculovirus-induced cell lysis, suggesting that conductivity can be used for prediction of viability decrease (Figure IV.4 A). *Incyte* measurements of permittivity over a wide range of frequencies allows to plot the beta-dispersion curve, and the subsequent calculation of the curve parameters: $\Delta\epsilon$, α and characteristic frequency, which indicate changes in the cell state during the production process (Petiot et al., 2016) (Figure IV.4 B).

Specifically for the IC-BEVS system, permittivity measurements allow to follow the progress of the culture and baculovirus infection in real-time, due to the correlation between permittivity and the cell biovolume (Ansorge et al., 2007; Petiot et al., 2016). This way, this technology is suited to follow a complete IC-BEVS infection process: cell seeding and growth until the infection density, baculovirus-induced cell diameter increase and cell growth arrest and finally cell death phase (Figure IV.4 C). Baculovirus budding from infected cells has been postulated before to be detectable in the characteristic frequency signal (Petiot et al., 2016). In this work, the previous-reported “v-shaped” profile can also be observed (Figure IV.4 D) (Petiot et al., 2016).

Figure IV.4 has a two-fold purpose: to provide an overview of the parameters measured with *Incyte*, and prove those parameters have a close interconnection with critical process variables in this system and are thus suitable for building prediction models for those variables.

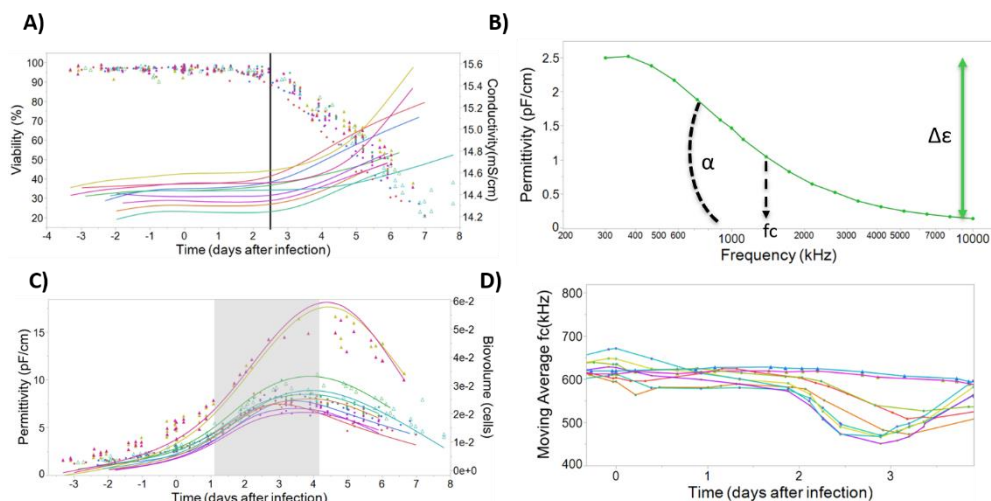


Figure IV.4 - *Incyte* measurements can be correlated with the progress of baculovirus infection in insect cells. **A)** The onset of baculovirus-induced cell lysis (viability, represented with circles) can be detected by the simultaneous onset of conductivity increase (smooth lines, measured by *Incyte*). **B)** Beta-dispersion curve 24 hours after seeding, for batch number 1. The beta-dispersion allows calculation of variables such as $\Delta\epsilon$, α and characteristic frequency, which are indicative of the cell state during the infection process. **C)** Visual inspection of the permittivity profile allows to follow the three phases of the production process (separated by the shaded area): cell growth, cell diameter increase due to baculovirus infection and baculovirus-induced cell lysis. Circles represent biovolume calculations based on the measured diameter and considering cells as perfect spheres, and smooth lines the *Incyte* permittivity measurements at 1000 kHz. **D)** The characteristic frequency (frequency corresponding to the beta-dispersion curve inflection point) time profile is shown. The “v shaped” profile after 2 days post infection has been postulated to be correlated with baculovirus release from cells elsewhere (Petiot et al., 2016).

As such, prediction models for viable cell concentration (Figure IV.5), viability (Figure IV.6) and diameter (Figure IV.7) were built based on the *Incyte* data. Regarding viable cell concentration, the observed vs predicted values for the calibration set (Figure IV.5 A) are shown. To complement the information, the viable cell concentration time-course profiles for the two batches used as testing set are compared with the corresponding time-course predictions (Figure IV.5 B). The obtained models are very accurate ($Q^2=0.89$), with only a slight underestimation of the viable cell concentration.

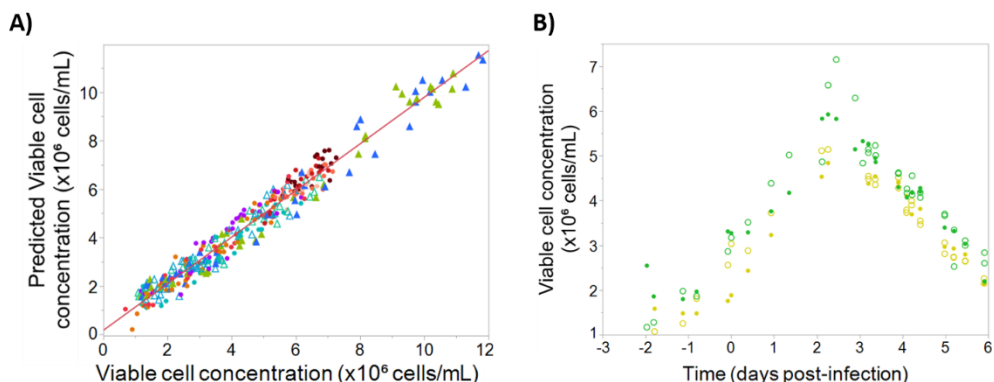


Figure IV.5 - Calibration and testing data for viable cell concentration. **A)** Observed and predicted values for the dataset used for model calibration, $R^2=0.96$. Batches are represented by different colors, with filled triangles representing “cell density effect” batches, empty triangles representing “empty” batches and filled circles representing “standard” and “blend” batches. **B)** Viable cell concentration time-course profiles for the testing set, $Q^2=0.89$. Reference data is represented by open circles and corresponding model-predicted values are shown as filled circles.

For the viability models (Figure IV.6), the prediction profiles are remarkably accurate ($Q^2=0.98$), for both culture phases, demonstrating the same prediction model can be deployed for the whole cultivation.

The increase in cell diameter induced by baculovirus infection can be used as indicator of the progress of baculovirus infection. Similar to the viability models, the models created for prediction of cell diameter are accurate during all phases of the infection process (Figure IV.7).

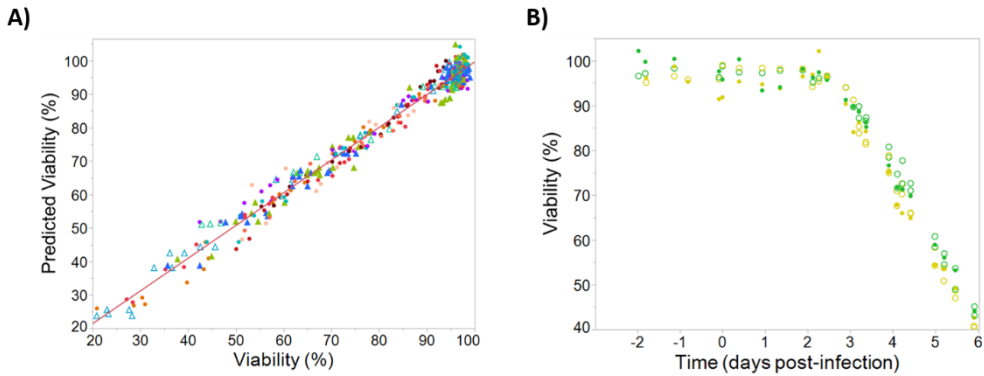


Figure IV.6 - Calibration and testing data for viability. Batches are represented by different colors. **A)** Observed and predicted values for the dataset used for model calibration, $R^2=0.98$. Batches are represented by different colors, with filled triangles representing “cell density effect” batches, empty triangles representing “empty” batches and filled circles representing “standard” and “blend” batches. **B)** Viability time-course profiles for the testing set, $Q^2=0.97$. Reference data is represented by open circles and corresponding model-predicted values are shown as filled circles.

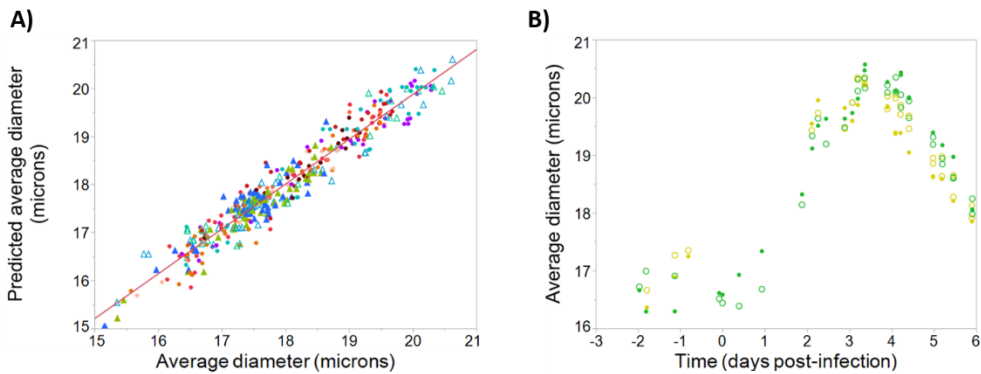


Figure IV.7 - Calibration and testing data for diameter. Batches are represented by different colors. **A)** Observed and predicted values for the dataset used for model calibration, $R^2=0.94$. Batches are represented by different colors, with filled triangles representing “cell density effect” batches, empty triangles representing “empty” batches and filled circles representing “standard” and “blend” batches. **B)** Diameter time-course profiles for the testing set, $Q^2=0.92$. Reference data is represented by open circles and corresponding model-predicted values are shown as filled circles.

3.3. rAAV production kinetics in the insect cell – baculovirus system

The same modeling strategy used for the process variables was employed for developing prediction models for intracellular rAAV production. Supernatant rAAV concentrations were not considered on the assumption that dielectric spectroscopy measures variations in the intracellular composition of the cell. The chosen bioreactor dataset translated into desirable and intended variability (Figure IV.8). Both the intracellular rAAV titer (rAAV quantified in the supernatant of the lysed pellet solution, Figure IV.8 A) and the specific rAAV titer are presented (Figure IV.8 B, intracellular titer normalized by viable cell concentration).

In particular, the effect of infecting cells at high cell density in the specific rAAV production titer can be observed (Figure IV.8 B, blue and green triangles). The “blend batch” strategy (depicted in Figure IV.1) also has the desired effect of providing rAAV concentration profiles at different ranges (Figure IV.8, open circles).

3.4. Detection of rAAV-induced signals using multiple linear regression

The same modeling strategy used for the critical process variables was applied to the specific rAAV data from Figure IV.8 B. The model predictions obtained (Figure IV.9) demonstrate this strategy yields acceptable predictions for the testing set ($Q^2=0.77$).

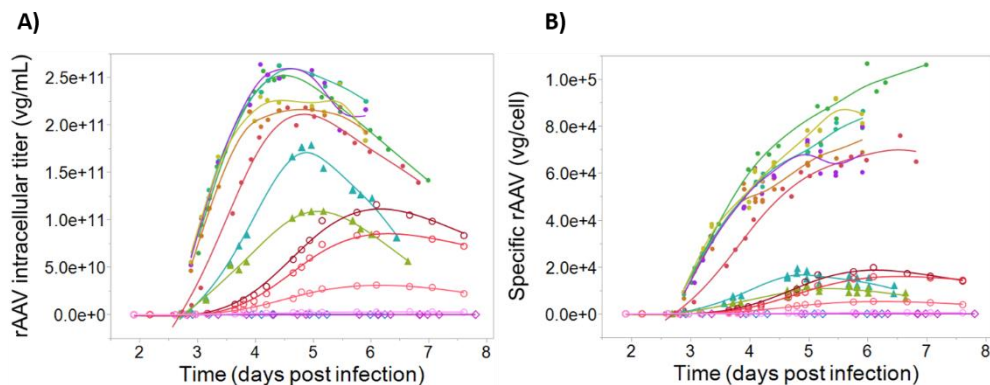


Figure IV.8 - rAAV intracellular production profiles. The datapoints represent vector genomes quantification. Filled circles represent “standard” batches, triangles represent “cell density effect” batches, empty diamonds represent “empty batches” and the empty circles represent “blend batches”. For the details on batch nomenclature, the reader is referred to Figure IV.1. Lines represent a smooth of the reference data, unrelated with model predictions. **A)** rAAV intracellular titer, the rAAV concentration after lysing pellet from 10 mL of culture. **B)** Specific rAAV titer. Same data as **A** normalized by the number of viable cells at the corresponding sampling time.

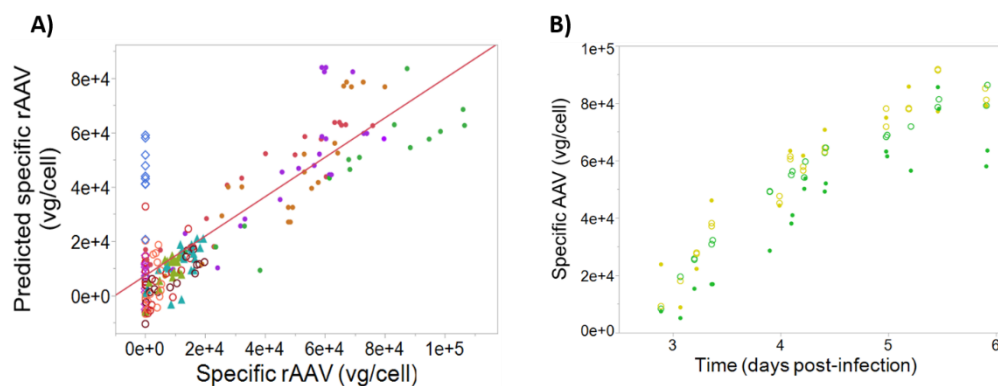


Figure IV.9 - Calibration and testing data for intracellular specific rAAV. Batches are represented by different colors. **A)** Observed and predicted values for the dataset used for model calibration, $R^2=0.71$. Batches are represented by different colors, with filled triangles representing “cell density effect” batches, empty triangles representing “empty” batches, filled circles representing “standard” batches and empty circles representing “blend” batches. **B)** Intracellular specific rAAV time-course profiles for the testing set, $Q^2=0.77$. Reference data is represented by open circles and corresponding model-predicted values are shown as filled circles.

4. Discussion

In this work we employed dielectric spectroscopy for accurate prediction of infection timing in the insect cell-baculovirus system. Moreover, we developed predictive models for cell concentration, viability, diameter and rAAV production, which can be used to follow the progress of baculovirus infection and recombinant AAV production in real-time.

The time of infection is one of the most important process parameters that need optimization in the insect cell system, with direct implication on the overall process results (Druzinec et al., 2013; M. Lecina et al., 2006). Current methods for infection timing require frequent, offline cell-counting, subjected to equipment variability and operator dependency, frequently resulting in more than 10 % variability. Additionally, frequent sampling increases the changes for contamination. Real-time, continuous monitoring of viable cell concentration can alleviate this issue. One of the real-time monitoring tools extensively applied to monitor cell concentration in cell culture processes is dielectric spectroscopy (Kroll et al., 2017; Mercier et al., 2016; Nikolay et al., 2018). In particular for the insect-cell system, dielectric spectroscopy has been extensively used (Ansorge et al., 2007; Elias et al., 2000; Negrete et al., 2007; Petiot et al., 2016; Zeiser et al., 2000, 1999) owing to the scalable properties of the system and the increase in cell diameter induced by baculovirus infection. Taking advantage of the frequent *Incyte* permittivity measurements and the high correlation between permittivity and cell concentration (before the cells increase diameter due to baculovirus infection, Figure IV.2), we applied dielectric spectroscopy to predict infection timing (Figure IV.3). An *in-house* JMP script (PTT – “process-to-target”) was developed, which uses the current batch historical permittivity data to accurately predict infection timing. As expected, the more historical data is available for the current batch, the better the predictions (Table IV.1). This tool was able to predict infection timing within 10 % of the actual infection time

as early as 24 hours post-inoculation. This amount of prior notice would allow for more accurate infection timing and could help alleviating resources in manufacturing facilities. Additionally, the PTT script is operator independent, allowing for easy transfer to Contract Manufacturing Organizations. Currently the script relies on a weighted linear regression, and the occasional permittivity spikes or the initial cell lag phase can impact prediction accuracy (Table IV.1, predictions at 36 h and 6 h, respectively). Although for our current process the weighted linear regression model used in the PTT allow accurate enough predictions, the script can be adjusted for using other prediction models.

Our script relies on the target permittivity value as an input. This target is obtained by a simple linear regression between viable cell concentration and permittivity for all the dataset. Since permittivity values are correlated with the culture biovolume, rather than cell concentration, this linear relationship is maintained until the cell diameter starts increasing. However, cell permittivity can be indicative not only of the cell biovolume, but more importantly of the overall cell state (Ansorge et al., 2007; Petiot et al., 2016). As such, we envision to move from a cell concentration-based infection process, to a permittivity-based infection. Further experiments with cells infected at different permittivity values is ongoing.

Moreover, and taking into account the inverse linear correlation between the onset of viability decrease and the onset of conductivity increase (Figure IV.4 A and Supplementary Figure IV.1), we are conducting experiments to switch from a “by day”-based harvest into a viability-based harvest, adapting the PTT to the conductivity measurements to accurately predict harvest time. The choice of the best viability to harvest is dependent not only on the final rAAV titer but also the vector potency and the overall downstream yield (Grein et al., 2018; M Lecina et al., 2006; Nikolay et al., 2018).

The PTT relies only in current data historical profiles, since for any current batch and during exponential growth phase, a linear correlation can be obtained between permittivity and cell concentration and viability and conductivity (Supplementary Figure IV.2). However, the correlation obtained for one batch cannot be used directly in another batch. We even detected a significant difference in the obtained linear regression slope for permittivity and cell concentration in different cell banks (results not shown). Moreover, even though the same medium was used in parallel bioreactors and the *Incyte* probe is zeroed in the medium, the conductivity measurements have a baseline reading which is different between batches (Figure IV.4 A). For manufacturing purposes, it is useful to have robust prediction models which are less sensitive of the small variations in probe measurements and the cell biological variations. As such, conductivity or permittivity-only based models cannot be used for the development of robust process prediction models, and consequently the beta-dispersion curve was considered for modeling the critical process variables in this process. This curve changes during the culture progression, being indicative of the cell physiological alterations during the overall growth and infection progress (Supplementary Figure IV.3). These changes can be quantified by calculating the beta-dispersion curve parameters along time: the difference between the low and high frequency plateaus ($\Delta\epsilon$), the Cole-Cole α (α) and the curve inflexion point (characteristic frequency, f_c). These parameters have been shown to be useful for characterizing the culture. For instance, α is related with the distribution of the dielectric properties in the population and the cell shape and size (Ansorge et al., 2007; Dabros et al., 2009); $\Delta\epsilon$ is proportional to cell concentration and biovolume (Petiot et al., 2016) and f_c has been demonstrated to be correlated with the cell death phase and virus budding (Ansorge et al., 2011; Petiot et al., 2016). For a more in-depth review of the biological meaning of each parameter, the reader is referred to the work of Dabros (Dabros et al., 2009).

The models shown in Figure IV.5 to Figure IV.9 were built using the calibration dataset introduced before and the above mentioned beta-dispersion parameters and frequency measurements. Besides multiple linear regression, we also tested partial least squares (PLS) regression and artificial neural networks. Multiple linear regression models combined simplicity with accurate predictions, and thus it was the strategy followed for developing predictive models. The high Q^2 obtained (0.78-0.97) show that dielectric spectroscopy signals can be used to predict critical process variables for this system and highlight the importance of a variable dataset.

Although not explored in this work, dielectric spectroscopy can be used to monitor baculovirus release kinetics from infected cells. Petiot and coworkers found a characteristic “V-shape” profile in the characteristic frequency time-course profile, and associated that signal with viral budding from the infected cells (Petiot et al., 2016). In Figure IV.4 D, we also observed a significant drop in the permittivity around day 2 post-infection. Given that our infection process takes place at a very low MOI, it takes two days to infect a significant proportion of the Sf9 population and the baculovirus release from the cells be detectable. As a control group, the two cell density effect batches do not show the decrease in the f_c value on day 2, but instead on day 4, since the higher cell concentration at infection is able to delay detection of the cell growth arrest induced by baculovirus. Moreover, we developed good prediction models for the cell diameter, a good indicator of the progress of baculovirus infection (Janakiraman et al., 2006; Laasfeld et al., 2017). Altogether, this knowledge may be useful for characterizing the baculovirus release kinetics for each baculovirus, developing dielectric spectroscopy-based models for prediction of baculovirus release from infected cells and possibly for baculovirus and BIIC titration.

The permittivity-based models were expanded to prediction of intracellular specific rAAV titer (Figure IV.9). rAAV extracellular titer was excluded from

the models because our hypothesis was that most rAAV-induced alterations in the cell state would be detected through variations in the intracellular composition of the cell. However, as mentioned in previous chapters, increase of rAAV concentration in the medium is mostly due to cell lysis. As good viability prediction models were developed using dielectric spectroscopy, we believe building extracellular rAAV prediction models would also be feasible, as demonstrated in **Chapter III** with digital holographic microscopy.

Still, measuring intracellular rAAV data contributed to an increase in understanding of our production process (Figure IV.8). For instance, rAAV production per cell seems to halt around day 5 post-infection. As such, we may be able to harvest our process one day earlier, although this decision is also dependent on the rAAV quality profiles. As culture progresses and cell lysis starts to occur, the number of viable cells producing rAAV decreases. However, since the rAAV profiles plateau around day 5 and the viability decrease starts around day 2.5, there are probably other factors related other than cell viability.

We clearly show the impact of baculovirus infection at high cell density for specific rAAV production (Figure IV.8). The addition of cultures infected at higher cell density was intended to introduce variability in the model, based on the well-known cell density effect, a drop in cell specific productivities when infecting high cell density cultures (Bernal et al., 2009; Ferreira et al., 2009; Merten, 2016). Similarly, the “blend” batch strategy intended to decouple rAAV permittivity signals from cell and baculovirus-induced permittivity changes. This strategy was successful in generating batches with decreasing rAAV concentration, keeping the cell concentration and baculovirus production at similar levels (Figure IV.8). However, even though infection was performed at 3×10^6 cells/mL, these runs have a similar rAAV production profile with the “cell density effect” batches (Supplementary Figure IV.4). The

existence of a “blend” batch with 0 % “empty” (theoretically, a “standard” production run) but still with low rAAV production titers seem to indicate there was an unknown problem in the “blend” batch runs. Regardless, the positive impact of the “blend” strategy in the overall model is incontestable.

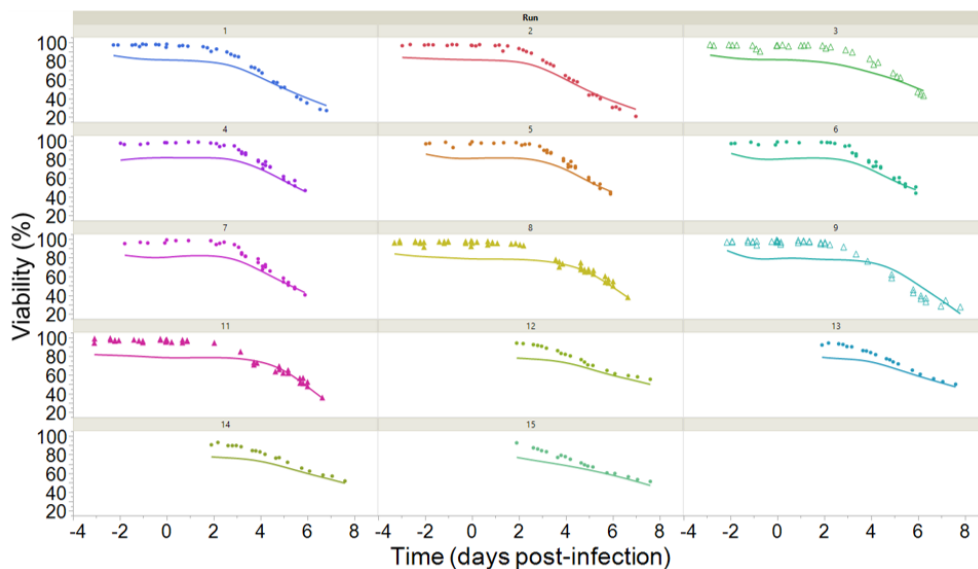
5. Conclusions

The work developed clearly shows dielectric spectroscopy can be used as PAT tool for this system, not only by allowing accurate infection time determination, but also for rAAV production monitoring. The ability to estimate the time of infection more than 24 hours before is invaluable for GMP settings, proving the usefulness of the PTT approach. The predictive models developed for critical process variables demonstrate accurate predictions for all variables in an independent testing set, validating the chosen strategy, and can be used for developing viability-based harvest methods. The determined intracellular rAAV production profiles, together with the developed rAAV prediction models, allow to increase process knowledge regarding this process, and to possibly unveil new factors influencing rAAV production by conducting process alterations and supplements administration and assess their impact on rAAV production in real-time. Future studies will address the possibility of applying this tool for determination of rAAV quality characteristics, such as potency or ratio of empty to full particles.

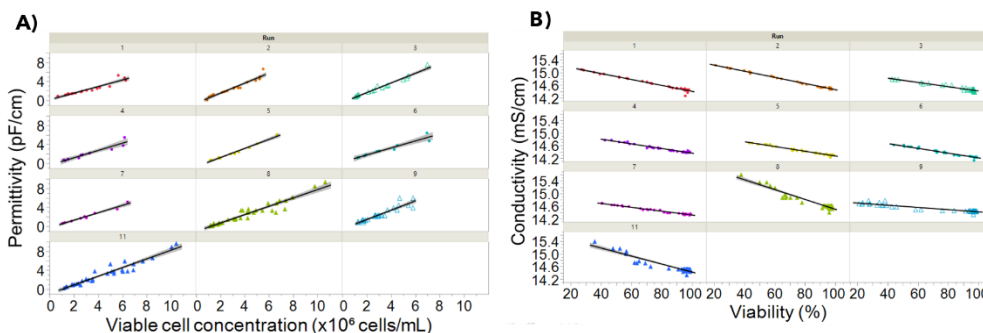
6. Conflicts of interest

Peter Slade and Harvir Grewal are currently employees at Voyager Therapeutics, Cambridge, MA. Chris Brown is currently an employee at Vedere Bio, Cambridge, MA.

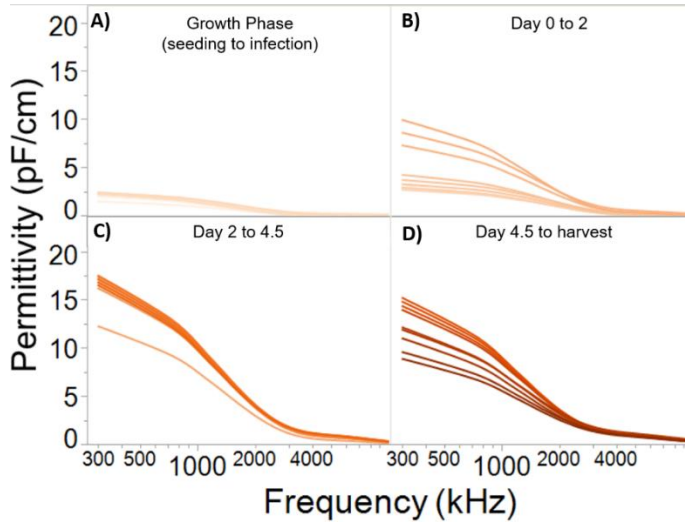
7. Supplementary Data



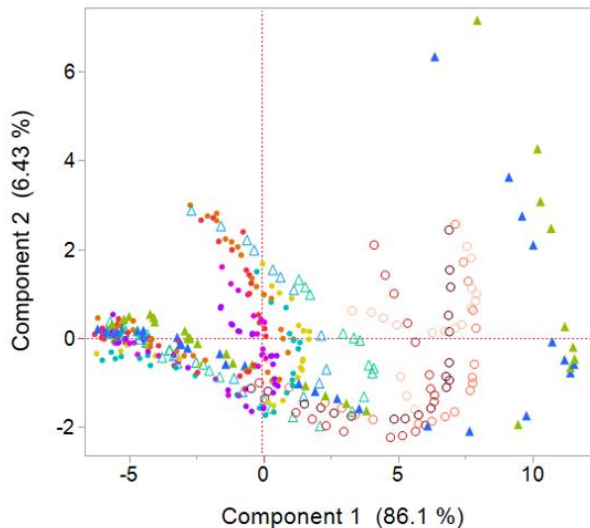
Supplementary Figure IV.1 - Viability reference data and corresponding predictions using only the conductivity data. For each run, a linear fit was obtained between conductivity and viability, considering only the data after viability started to decrease. This simple fit can be applied in the PTT.



Supplementary Figure IV.2 – Linear correlation between permittivity and viable cell concentration (A) and conductivity and viability (B). For viable cell concentration, only data until day two post infection is shown, since after day 2 cell diameter increases. For viability, only data after day two post-infection is shown, corresponding to the timepoints of viability decrease.



Supplementary Figure IV.3 – Representative beta-dispersion curve evolution profiles for different culture phases, here shown for batch number 1. Each curve is colored according to the culture time (the darker the color, the closer the timepoint is to the harvest time).



Supplementary Figure IV.4 – Scores for the two first principal components for all runs. The 22 permittivity-related variables were utilized to calculate the principal components. Filled circles represent “standard” batches, filled triangles represent “cell density effect” batches, empty triangles represent “empty batches” and the empty circles represent “blend batches”. As it can be observed, even though “blend” batches were infected at the same cell concentration as the “standard” batches, their permittivity data is more similar to the “cell density effect” ones, similar to what was observed in the specific rAAV titers (Figure IV.8)

8. References

- Ansonge, S., Esteban, G., Schmid, G., 2007. On-line monitoring of infected Sf-9 insect cell cultures by scanning permittivity measurements and comparison with off-line biovolume measurements. *Cytotechnology* 55, 115–24. <https://doi.org/10.1007/s10616-007-9093-0>
- Ansonge, S., Lanthier, S., Transfiguracion, J., Henry, O., Kamen, A., 2011. Monitoring lentiviral vector production kinetics using online permittivity measurements. *Biochem. Eng. J.* 54, 16–25. <https://doi.org/10.1016/j.bej.2011.01.002>
- Bernal, V., Carinhas, N., Yokomizo, A.Y., Carrondo, M.J.T., Alves, P.M., 2009. Cell density effect in the baculovirus-insect cells system: A quantitative analysis of energetic metabolism. *Biotechnol. Bioeng.* 104, 162–180. <https://doi.org/10.1002/bit.22364>
- Dabros, M., Dennewald, D., Currie, D.J., Lee, M.H., Todd, R.W., Marison, I.W., Von Stockar, U., 2009. Cole-Cole, linear and multivariate modeling of capacitance data for on-line monitoring of biomass. *Bioprocess Biosyst. Eng.* 32, 161–173. <https://doi.org/10.1007/s00449-008-0234-4>
- Druzinec, D., Salzig, D., Brix, A., Kraume, M., Vilcinskas, A., Kollwe, C., Czermak, P., 2013. Optimization of Insect Cell Based Protein Production Processes - Online Monitoring, Expression Systems, Scale Up. *Adv. Biochem. Eng. Biotechnol.* 136, 65–100. https://doi.org/10.1007/10_2013_205
- Elias, C.B., Zeiser, A., Bedard, C., Kamen, A.A., 2000. Enhanced growth of Sf-9 cells to a maximum density of 5.2×10^7 cells per mL and production of β -galactosidase at high cell density by fed batch culture. *Biotechnol. Bioeng.* 68, 381–388. [https://doi.org/10.1002/\(SICI\)1097-0290\(20000520\)68:4<381::AID-BIT3>3.0.CO;2-D](https://doi.org/10.1002/(SICI)1097-0290(20000520)68:4<381::AID-BIT3>3.0.CO;2-D)
- FDA, U.S.D. of H. and H.S., 2004. Guidance for Industry PAT — A Framework for Innovative Pharmaceutical Development, Manufacturing, and Quality Assurance. FDA Off. Doc. 16. <https://doi.org/http://www.fda.gov/CDER/guidance/6419fnl.pdf>
- Ferreira, T.B., Perdigão, R., Silva, A.C., Zhang, C., Aunins, J.G., Carrondo, M.J.T., Alves, P.M., 2009. 293 Cell cycle synchronisation in adenovirus vector production. *Biotechnol. Prog.* 25, 235–243. <https://doi.org/10.1002/btpr.64>
- Galibert, L., Merten, O.-W., 2011. Latest developments in the large-scale production of adeno-associated virus vectors in insect cells toward the treatment of neuromuscular diseases. *J. Invertebr. Pathol.* 107 Suppl, S80–S93. <https://doi.org/10.1016/j.jip.2011.05.008>
- Grein, T.A., Loewe, D., Dieken, H., Salzig, D., Weidner, T., Czermak, P., 2018. High titer oncolytic measles virus production process by integration of dielectric spectroscopy as online monitoring system. *Biotechnol. Bioeng.* 115, 1186–1194. <https://doi.org/10.1002/bit.26538>
- Guerra, A., von Stosch, M., Glassey, J., 2019. Toward biotherapeutic product real-time quality monitoring. *Crit. Rev. Biotechnol.* 39, 289–305. <https://doi.org/10.1080/07388551.2018.1524362>
- Janakiraman, V., Forrest, W.F., Chow, B., Seshagiri, S., 2006. A rapid method for estimation of baculovirus titer based on viable cell size. *J. Virol. Methods* 132, 48–58. <https://doi.org/10.1016/j.jviromet.2005.08.021>
- Justice, C., Brix, A., Freimark, D., Kraume, M., Pfromm, P., Eichenmueller, B., Czermak, P., 2011. Process control in cell culture technology using dielectric spectroscopy. *Biotechnol. Adv.* 29, 391–401. <https://doi.org/10.1016/j.biotechadv.2011.03.002>
- Kroll, P., Stelzer, I. V., Herwig, C., 2017. Soft sensor for monitoring biomass subpopulations in mammalian cell culture processes. *Biotechnol. Lett.* 39, 1667–1673. <https://doi.org/10.1007/s10529-017-2408-0>
- Laasfeld, T., Kopanchuk, S., Rinken, A., 2017. Image-based cell-size estimation for baculovirus quantification. *Biotechniques* 63, 161–168. <https://doi.org/10.2144/000114595>
- Lecina, M., Soley, A., Gràcia, J., Espunya, E., Lázaro, B., Cairó, J.J., Gódià, F., Gódià, F., 2006. Application of on-line OUR measurements to detect actions points to improve baculovirus-insect cell cultures in bioreactors. *J. Biotechnol.* 125, 385–394. <https://doi.org/10.1016/j.jbiotec.2006.03.014>
- Marison, I., Hennessy, S., Foley, R., Schuler, M., Sivaprakasam, S., Freeland, B., 2013. The Choice of Suitable Online Analytical Techniques and Data Processing for Monitoring of Bioprocesses. *Adv. Biochem. Eng. Biotechnol.* 132, 249–280. https://doi.org/10.1007/10_2012_175

- Mercier, S.M., Rouel, P.M., Lebrun, P., Diepenbroek, B., Wijffels, R.H., Streefland, M., 2016. Process analytical technology tools for perfusion cell culture. *Eng. Life Sci.* 16, 25–35. <https://doi.org/10.1002/elsc.201500035>
- Merten, O., 2016. AAV vector production : state of the art developments and remaining challenges. *Cell Gene Ther.* 521–551. <https://doi.org/10.18609/cgti.2016.067>
- Monteiro, F., 2015. Rational Design of Insect Cell-based Vaccine Production - Bridging Metabolomics with Mathematical Tools to Study Virus-Host Interactions.
- Moore, B., Sanford, R., Zhang, A., 2019. Case study: The characterization and implementation of dielectric spectroscopy (biocapacitance) for process control in a commercial GMP CHO manufacturing process. *Biotechnol. Prog.* 35. <https://doi.org/10.1002/btpr.2782>
- Negrete, A., Esteban, G., Kotin, R.M., 2007. Process optimization of large-scale production of recombinant adeno-associated vectors using dielectric spectroscopy. *Appl. Microbiol. Biotechnol.* 76, 761–72. <https://doi.org/10.1007/s00253-007-1030-9>
- Nikolay, A., Léon, A., Schwamborn, K., Genzel, Y., Reichl, U., 2018. Process intensification of EB66® cell cultivations leads to high-yield yellow fever and Zika virus production. *Appl. Microbiol. Biotechnol.* 102, 8725–8737. <https://doi.org/10.1007/s00253-018-9275-z>
- Opel, C.F., Li, J., Amanullah, A., 2010. Quantitative modeling of viable cell density, cell size, intracellular conductivity, and membrane capacitance in batch and fed-batch CHO processes using dielectric spectroscopy. *Biotechnol. Prog.* NA-NA. <https://doi.org/10.1002/btpr.425>
- Pais, D.A.M., Carrondo, M.J.T., Alves, P.M., Teixeira, A.P., 2014. Towards real-time monitoring of therapeutic protein quality in mammalian cell processes. *Curr. Opin. Biotechnol.* 30, 161–167. <https://doi.org/10.1016/j.copbio.2014.06.019>
- Pais, D.A.M., Portela, R.M.C., Carrondo, M.J.T., Isidro, I.A., Alves, P.M., 2019. Enabling Pat in insect cell bioprocesses: *in-situ* monitoring of recombinant adeno-associated virus production by fluorescence spectroscopy. *Biotechnol. Bioeng.* bit.27117. <https://doi.org/10.1002/bit.27117>
- Penaud-Budloo, M., Lecomte, E., Guy-Duché, A., Saleun, S., Roulet, A., Lopez-Roques, C., Tournaire, B., Cogné, B., Léger, A., Blouin, V., Lindenbaum, P., Moullier, P., Ayuso, E., 2017. Accurate Identification and Quantification of DNA Species by Next-Generation Sequencing in Adeno-Associated Viral Vectors Produced in Insect Cells. *Hum. Gene Ther. Methods* hgtb.2016.185. <https://doi.org/10.1089/hgtb.2016.185>
- Petiot, E., Ansoorge, S., Rosa-Calatrava, M., Kamen, A., 2016. Critical phases of viral production processes monitored by capacitance. *J. Biotechnol.* 242, 19–29. <https://doi.org/10.1016/j.jbiotec.2016.11.010>
- Petiot, E., Kamen, A., 2012. Real-time monitoring of influenza virus production kinetics in HEK293 cell cultures. *Biotechnol. Prog.* 29, 275–84. <https://doi.org/10.1002/btpr.1601>
- Qiu, J., Arnold, M.A., Murhammer, D.W., 2014. On-line near infrared bioreactor monitoring of cell density and concentrations of glucose and lactate during insect cell cultivation. *J. Biotechnol.* 173, 106–11. <https://doi.org/10.1016/j.jbiotec.2014.01.009>
- Riley, M.R., Rhiel, M., Zhou, X., Arnold, M.A., Murhammer, D.W., 1997. Simultaneous Measurement of Glucose and Glutamine in Insect Cell Culture Media by Near Infrared Spectroscopy. [https://doi.org/10.1002/\(SICI\)1097-0290\(19970705\)55:1<11::AID-BIT2>3.0.CO;2-#](https://doi.org/10.1002/(SICI)1097-0290(19970705)55:1<11::AID-BIT2>3.0.CO;2-#)
- Shahyari, A., Jazi, M.S., Mohammadi, S., Nikoo, H.R., Nazari, Z., Hosseini, E.S., Burtscher, I., Mowla, S.J., Lickert, H., 2019. Development and clinical translation of approved gene therapy products for genetic disorders. *Front. Genet.* 10. <https://doi.org/10.3389/fgene.2019.00868>
- Wasilko, D.J., Edward Lee, S., Stutzman-Engwall, K.J., Reitz, B.A., Emmons, T.L., Mathis, K.J., Bienkowski, M.J., Tomasselli, A.G., David Fischer, H., 2009. The titerless infected-cells preservation and scale-up (TIPS) method for large-scale production of NO-sensitive human soluble guanylate cyclase (sGC) from insect cells infected with recombinant baculovirus. *Protein Expr. Purif.* 65, 122–132. <https://doi.org/10.1016/j.pep.2009.01.002>
- Xu, Z., Shi, C., Qian, Q., 2014. Scalable manufacturing methodologies for improving adeno-associated virus-based pharmaprojects. *Chinese Sci. Bull.* 59, 1845–1855. <https://doi.org/10.1007/s11434-014-0197-6>

- Yee, C.M., Zak, A.J., Hill, B.D., Wen, F., 2018. The Coming Age of Insect Cells for Manufacturing and Development of Protein Therapeutics. *Ind. Eng. Chem. Res.* 57, 10061–10070. <https://doi.org/10.1021/acs.iecr.8b00985>
- Zeiser, A., Bédard, C., Voyer, R., Jardin, B., Tom, R., Kamen, a a, 1999. On-line monitoring of the progress of infection in Sf-9 insect cell cultures using relative permittivity measurements. *Biotechnol. Bioeng.* 63, 122–6. [https://doi.org/10.1002/\(SICI\)1097-0290\(19990405\)63:1<122::AID-BIT13>3.0.CO;2-I](https://doi.org/10.1002/(SICI)1097-0290(19990405)63:1<122::AID-BIT13>3.0.CO;2-I)
- Zeiser, A., Elias, C.B., Voyer, R., Jardin, B., Kamen, A.A., 2000. On-line monitoring of physiological parameters of insect cell cultures during the growth and infection process. *Biotechnol. Prog.* 16, 803–808. <https://doi.org/10.1021/bp000092w>

Chapter V

Online control strategies

This chapter is adapted from the book chapter:

Isidro, IA, **Pais, DAM**, Alves, PM, Carrondo, MJT, 2019. "Online control strategies", *Comprehensive Biotechnology*, 3rd edition, Volume 2, 2019: 943-951

Author Contribution

This publication is an update of the book chapter “A.P. Teixeira, R. Oliveira, P.M. Alves, M.J.T. Carrondo, 2.63 - Online Control Strategies, Editor: Murray Moo-Young, Comprehensive Biotechnology (Second Edition), Academic Press, 2011, Pages 875-882”, published in 2019. Daniel Pais co-wrote the chapter update, conducting literature review and introducing recent application examples, as well as updating introduction and conclusion sections to reflect recent developments in the state of the art.

Contents

1.	Introduction.....	178
2.	Current Practice of Bioprocess Control	181
2.1.	Manual Control Based on Infrequent Measurements.....	182
2.2.	Closed-loop Control Based on At- or Online Measurements	182
2.3.	Inferential Control Methods.....	183
3.	Advanced Process Control Strategies.....	185
3.1.	Adaptive Control	185
3.1.1.	Gain scheduling	186
3.1.2.	Self-tuning controller.....	188
3.1.3.	Model reference adaptive control	189
3.2.	Linearization-based Control	190
3.3.	Iterative Learning Control.....	191
3.4.	Model Predictive Control.....	192
4.	Concluding remarks	195
5.	Acknowledgements	196
6.	Glossary.....	197
7.	References	198

1. Introduction

The biotechnology industry is largely contributing to the global economy. Its growth is mainly attributed to an in-depth understanding of biological systems, fostered by developments in 'omics' technologies (Lee et al., 2005) and to an ever-increasing demand for biotech-derived products, such as biopharmaceuticals, food and feed products or biofuels (Matasci et al., 2009; Rude and Schirmer, 2009). Despite the large amount of research conducted in the last few years, process control has played a minor role in the industrial practice, with the majority of established industrial processes still manually following empirical state trajectories obtained after a significant experimental effort (Henson, 2006). Nevertheless, the economic interest in process control is increasing as a mean to effectively compete in the marketplace, especially against cheaper generic alternatives due to expiration of blockbuster drugs patents (Kresse, 2009) and also due to the process analytical technology (PAT) guidance introduced by the Food and Drug Administration (FDA) in 2004 (Munson et al., 2008), encouraging pharmaceutical and biopharmaceutical companies to implement advanced control strategies to achieve operational excellence.

Well established control technologies apply classical proportional-integral-derivative (PID) feedback loops to easily measurable physicochemical variables, such as dissolved oxygen (DO), temperature, and pH. The control of these variables, although important, is not enough to guarantee optimal operation. The success of PID control schemes is primarily founded on the reliability of the measurement technologies.

Currently, key bioprocess variables like biomass concentration, nutrient uptake rates and product titer cannot be measured directly and online. In fact, this is one of the main limitations preventing wider adoption of classical online control in bioprocesses. Process control approaches based on online sensors

that are able to estimate key variables indirectly are becoming more common in biomanufacturing, based on recent developments in bioprocess monitoring technologies (Zhao et al., 2015).

State-of-the-art bioprocess control schemes rely on more sophisticated approaches, which find still limited acceptance in the industry due to their complexity in implementation, maintenance and use and the need for accurate bioprocess models to achieve reliable performance.

For any bioreactor operation mode (batch, fed-batch, or continuous), the goal in process control is most often to maximize total production of the desired product, while assuring consistent quality. The choice of specific control objective may vary from maximization of cell concentration, maximization of product titer or specific productivity, by-product minimization, improvement of a quality attribute or reproducing an established process trajectory.

Continuous operation involves control of the nutritional environment at an operating point that maximizes the steady-state productivity. Zhao and Skogestad (Zhao and Skogestad, 1997) compare various control configurations for continuous bioreactors. The most common control structures employ the dilution rate or the feed concentration of the rate-limiting substrate as manipulated variables. When a sufficiently accurate mathematical model is available, the optimal operating state can be determined offline through computer simulation and optimization (the optimal control problem), and then implemented in the process in the form of either an open-loop operating protocol or a closed-loop control system that forces the measured process state to track the optimal state.

Process control of batch and fed-batch operations is more challenging, as the optimization is a dynamic programming problem. The fed-batch operation mode is the most employed, as it often avoids substrate inhibition and

overflow metabolism while still allowing some operational flexibility. A comprehensive review of fed-batch control strategies was published by Lee and coworkers (Lee et al., 1999). The most frequently addressed process control problem in fed-batch reactors is designing substrate-feeding strategies to maximize product quantity at the end of the culture. If a reliable dynamic model of the process is available, dynamic programming is adopted to solve the control problem (Li and Biegler, 1988). In general, the biotech industry prefers the open-loop implementation as it does not rely on complex instrumentation; still this method is often suboptimal due to the unavoidable process-model mismatch.

Apart from the theory-practice gap, the choice of adequate control theory for biotechnological applications is still surprisingly challenging due to the nonlinear and time-varying nature of bioprocesses and their poorly understood kinetics (van Impe and Bastin, 1995). Nonetheless, by using the available bioprocess information together with tools from control theory, it is possible to develop control strategies that overrule some of the empiricism associated with the operation of bioreactors.

Process control is a rich field in the literature with many different strategies, methods and algorithms that can be combined in multiple ways to address a control problem. Consequently, specific implementations can be classified according to different criteria. Here we attempt to highlight common and defining attributes of different approaches to bioprocess control, but these approaches inherently have conceptual and method overlaps. The examples presented focus on upstream processing. A recent review by Hong and coworkers (Hong et al., 2018) highlights how process control can be used in different steps of biopharmaceutical manufacturing.

The objective of this article is to review some of the strategies that have been developed to design bioprocess control systems. The first part summarizes

several works employing classical control strategies, while the second part is focused on applications of advanced control strategies. Here, we focus on the techniques that we think are closer to practice and thus with higher industrial potential.

2. Current Practice of Bioprocess Control

Simple semiautomatic control strategies developed based on extensive experimental testing are the current industrial practice to control bioprocesses, employing either open- or closed-loop protocols (Gnoth et al., 2008). Process control based on open-loop operation is well accepted in the biotechnology industry because of its simple technological implementation and quasi-guaranteed reproducibility of manipulated variables; these factors are concomitant with a safe operation strategy, which is highly valued by industry. In open-loop control, the optimization of the process is performed offline, and then the resulting policy is implemented online. This type of control is applied when a good prediction model exists but information about the process state is not enough to be used for online feedback actions when deviations from the desired behavior occur. The weaknesses of an open-loop protocol when model-process mismatches exist are illustrated in the work by Vanichsriratana and coworkers (Vanichsriratana et al., 1996) through simulations. They introduced a 10 % error in the parameters of the mathematical model for the process and then used this model to calculate the optimal substrate concentration that maximized biomass production. The performance of the open-loop control was much poorer than that of a closed-loop control using model predictive control (MPC), since the modeling error could be compensated by a feedback control action in the latter case.

The variables usually monitored in industrial bioreactors are temperature, pH, DO concentration, bioreactor head pressure, and, often, the oxygen and

carbon dioxide composition in the off gas. Relying on these basic measurements and, sometimes, on more sophisticated determinations of rate-limiting substrates, toxic metabolites, and cell biomass, simple closed-loop algorithms have been developed for bioreactor control. Normally, an optimal policy is derived based on empirical biochemical knowledge or simplistic models representing the cellular biochemical reactions. This solution is then implemented online with likely deviations corrected whenever new measurements are available.

2.1. Manual Control Based on Infrequent Measurements

A predictive control configuration based on infrequent measurements of glucose was applied by Dowd *et al.* (Dowd *et al.*, 2001), to keep the concentration of this substrate at a defined set point in a perfusion culture of Chinese hamster ovary (CHO) cells. Glucose concentration in the culture bulk was analyzed off-line every 24 h, from which a consumption rate was predicted and used to adjust the feeding rate for the next 24 h. Despite the infrequent sampling, glucose deviation from the set point was less than 0.4 mM. A similar strategy was followed by Cruz and coworkers (Cruz *et al.*, 2000) to control both glucose and glutamine concentrations at extremely low levels to reduce byproduct formation during fed-batch cultures of recombinant baby hamster kidney (BHK) cells. Feeding rates were adjusted daily after offline analysis of both the nutrients. This empirical way of controlling key state variables is still very common in industrial practice.

2.2. Closed-loop Control Based on At- or Online Measurements

There are many examples in literature of standard closed-loop controllers based on variables that are measured in real-time employing sophisticated measurement technologies. An example of this type of control is given in the work by Turner *et al.* (Turner *et al.*, 1994), in which a fully automated system for the online monitoring of acetate and closed-loop control of a fed-batch fermentation of recombinant *Escherichia coli* is developed to prevent acetate

formation. Samples from the bioreactor are collected through an aseptic sampling device, then the supernatant is separated from biomass in a microcentrifuge and injected into a high-performance liquid chromatography for acetate analysis. The results were used by a control algorithm that determined the feeding strategy to limit acetate concentration to a low level throughout the fermentation.

Ozturk and coworkers (Ozturk et al., 1997) employed a similar strategy, in which a simple algorithm was derived to maintain glucose and lactate levels at their set points during hybridoma perfusion cultures. In their study, every 60 min, a cell-free sample was drawn from the bioreactor to quantify glucose and lactate concentrations using a biochemical analyzer YSI2700 upgraded with an aseptic sampling module. Then, the perfusion rate was adjusted according to a simple model, which accounted with the specific consumption/secretion rates previously observed.

2.3. Inferential Control Methods

In this type of control, unmeasured control variables are estimated from other more easily measured variables and then feedback control is applied to maintain the estimated control variable at the desired set point. This enables real-time control of variables for which direct measurements are only available offline. The combination of hardware sensors with a software-based estimator is known as a soft sensor, and their current applications in bioprocessing have been reviewed in Luttmann *et al.* (Luttmann et al., 2012).

For example, Zhou and coworkers (Zhou et al., 1995) established a closed-loop scheme to control glucose concentration at a desired set point in high cell density cultures of mammalian cells by measuring oxygen uptake rates (OUR) and assuming a constant stoichiometric ratio between glucose and oxygen uptake. Using the same principle, Konstantinov *et al.* (Konstantinov et al., 1990) estimated the glucose consumption rate from

real-time measurements of the exit gas composition in an *E. coli* fed-batch culture. The control objective was to keep the specific glucose feed rate below a critical limit to prevent acetate formation. This controller allowed negligible acetic acid accumulation and improved phenylalanine synthesis. Hiller *et al.* (Hiller et al., 2017) demonstrated a simple but interesting strategy to control perfusion rate in CHO cell cultures based on pH measurements. CHO cells will produce lactate if glucose concentration is high and will consume lactate when glucose drops to limiting levels, leading to variations in pH. By keeping the pH to a specific set point by turning perfusion on and off, the authors were able to ensure adequate glucose supply.

Spectroscopic probes are commonly used in inferential control methods, often in combination with soft sensors. Raman spectroscopy, for example, allows simultaneous estimation of multiple metabolite concentrations and has been increasingly used in bioprocess monitoring practice (Esmonde-White et al., 2016). In Matthews *et al.* (Matthews et al., 2016), the authors used Raman spectroscopy and partial least squares (PLS) regression to control glucose feeding and minimize lactate accumulation in mammalian fed-batch cultures.

Dielectric spectroscopy sensors, or biocapacitance probes, are a promising solution to monitor viable cells. Zhang and coworkers (Zhang et al., 2015) showed that dielectric spectroscopy can be used with an online feedback loop to adjust nutrient feeding in a CHO fed-batch, as long as the viability is high. In this study, the control loop kept the feeding proportional to the cumulative integral of cell growth.

3. Advanced Process Control Strategies

Model-based control strategies based on well-established control theory have been effectively employed in the chemical industry for decades. Their application to biotechnological processes has also received considerable attention in academia over the last few years. Examples include adaptive control, linearization-based control, iterative learning control (ILC), and MPC. These are described below, and their block diagrams represented in Figure V.1. In many of the published studies, the additional benefits of these strategies in relation to classical control are demonstrated, laying primarily on the possibility of correcting not only the manipulated variables, but also the underlying model parameters as fresh process data become available. Nevertheless, only a small number of published works provide the proof of concept in real process conditions; the majority presents simulation results, assuming that the required state variables are accurately measured or estimated, which many times is technically unfeasible. In practice, the estimation of unmeasured state variables is not trivial, particularly if unknown parameters also have to be estimated (Bequette, 1991). The lack of online sensors providing high-quality data for key bioprocess variables is one of the main factors hindering the industrial implementation of advanced control algorithms. A recent review (Portner et al., 2017) covers monitoring and modelling considerations for the implementation of advanced bioprocess control strategies.

3.1. Adaptive Control

In adaptive control, controller parameters are updated to reflect variability in the process or uncertainty in initial parameter estimation. Adaptive control has been widely used as a way to cope with process-model mismatch (Bastin and Dochain, 1990); the controller structure can be designed on the basis of a simple model, and then one or more feedback actions compensate for both model uncertainties and major disturbances. Three main classes of adaptive

control, differing on the way parameter adaptation is implemented, are gain scheduling, model reference adaptive control, and self-tuning control.

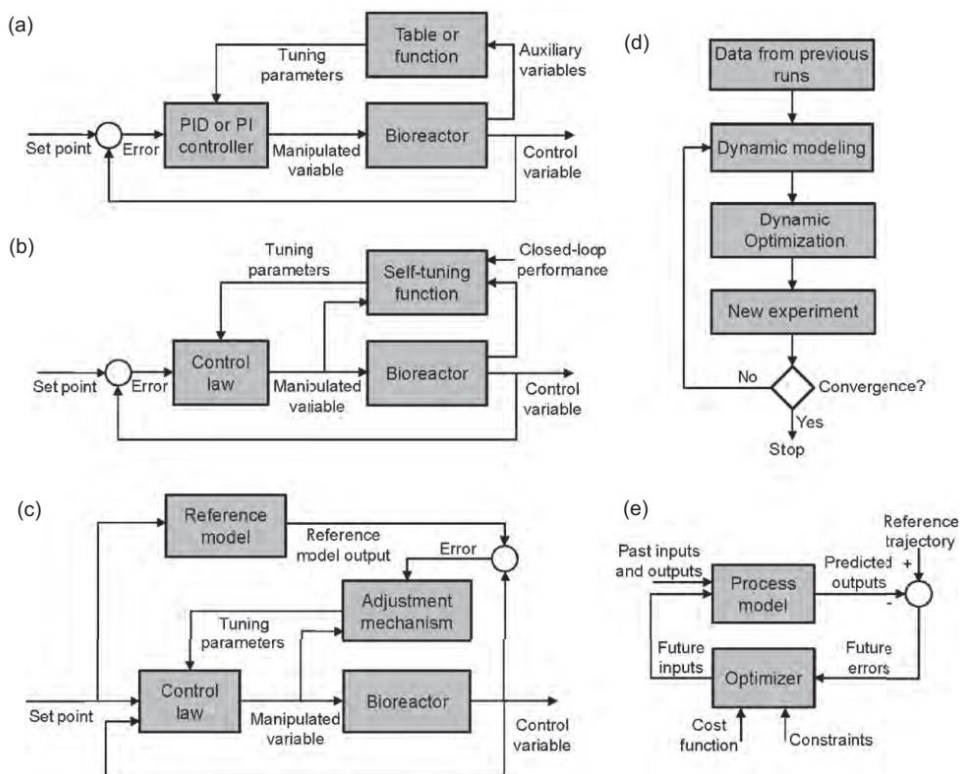


Figure V.1 - Block diagram of advanced control strategies: **A)** gain-scheduling controller; **B)** self-tuning controller; **C)** model reference adaptive controller; **D)** iterative learning control; and **E)** model predictive controller.

3.1.1. Gain scheduling

Gain scheduling, the simplest version of an adaptive control system, adjusts the controller gain, or the strength of the response, of proportional-integral (PI) or PID controllers to obtain a good performance at different operating regions. It is convenient especially if the process dynamics have good

correlation with easily measurable variables that can be used as scheduling variables.

This type of control has been mainly used to improve performance of DO concentration control in batch and fed-batch processes. Several authors have reported tuning problems when PID controllers with fixed parameters are used to control DO concentration during the whole process; a controller tuned at one operating condition may not maintain a satisfactory response at different operating conditions. One of the main disturbances in DO control is the change in OUR over culture time. Cardello and San (Cardello and San, 1988) applied the OUR as the auxiliary variable to fine-tune the parameters of the PID controller for DO in a batch reactor. Also Kuprijanov *and* coworkers (Kuprijanov et al., 2009) based the update of the parameters of a PI controller on changes in OUR. These authors developed a linear relationship between the controller parameters and OUR, which was then used to adapt online those parameters and guarantee a good performance of the DO controller. The performance of the controller was further improved by using the information from the substrate feeding rate (the variable that mostly influences the DO) in a feed-forward fashion. This part of the controller is important for a quick response when the substrate feed rate or the mass transfer coefficient changes rapidly.

In the Åkesson and Hagander (Åkesson and Hagander, 1999) study, a gain-scheduling PID controller for DO concentration was developed using the stirrer speed as manipulated variable. The working range for the stirrer speed was divided into different operating regions and then for each region the controller parameters were obtained using auto-tuning experiments. The controller was applied to a recombinant *E. coli* cultivation and good disturbance rejection was achieved.

Despite the simplicity of implementation and the quick response provided, the design of gain scheduling controllers presents two main drawbacks: it is time-consuming since the parameters have to be determined for many operating conditions, and, because the schedule is defined *a priori*, it provides no feedback to compensate for incorrect schedules.

3.1.2. Self-tuning controller

In a self-tuning controller, the algorithm learns from experience and self-adjusts the parameters to improve closed-loop control performance after process variations. Often, this learning process builds up a mathematical model based on experimental input/output data. It has been used to tune classical PID controllers and more complex control laws. Machine learning methods, such as fuzzy logic and artificial neural networks (ANN), have been used for the adaptation mechanism of controller parameters.

Ramkumar and Chidambaram (Ramkumar and Chidambaram, 1995) employed an online fuzzy logic mechanism to self-tune a PI controller designed to maintain cellular concentration at the optimal steady-state in a continuous bioreactor. The controller parameters were determined based on the Ziegler-Nichols tuning formula. This fuzzy self-tuning method takes the process output error as input and the tuning parameters as outputs. Simulation studies showed that the controller is robust to the uncertainty and disturbances in the model parameters, giving improved responses in relation to a PI controller with fixed parameters. On the other hand, in the Mohseni *et al.* study (Mohseni *et al.*, 2008), an ANN was designed to tune online the parameters of a PI controller, the weights of the ANN being updated at each sampling time by means of the error between the desired output and the actual output of the system. This self-tuning controller was employed to follow a desired reference trajectory for the cellular growth rate by manipulating the substrate feed rate in a fed-batch culture of recombinant *E. coli*. It demonstrated improved performance in relation to the classical PI controller

tracking the growth rate and could reject large disturbances and parameter variations.

Radhakrishnan *et al.* (Radhakrishnan et al., 1999) adopted a nonlinear self-tuning controller based on the NARMAX approach (nonlinear autoregressive moving average with exogenous inputs) to regulate a continuous bioreactor near its optimum productivity. The dilution was the manipulated input and cell concentration was the controlled variable. Simulation studies showed a smooth response of the controller when changes in both load and set point occurred, and a better control performance when compared to a classical PI controller.

3.1.3. Model reference adaptive control

Model reference adaptive control (MRAC) systems aim at updating the parameters of the control law such that the behavior of the resulting closed-loop system becomes as close as possible to that of a given reference model. The controller parameters are adapted in a way such that the plant response matches the response of the reference model.

In Oliveira *et al.* (Oliveira et al., 2005), a high cell density *Pichia pastoris* culture was operated near maximum oxygen transfer capacity by manipulating glycerol feeding (limiting substrate). Two adaptive control algorithms, a MRAC controller, based on the known stoichiometry between glycerol and oxygen consumption, and a PI feedback controller with adaptive gain, were designed and tested in a pilot plant bioreactor with online measurements of DO and off-gas composition. Both controllers proved to be robust and accurate, but the MRAC was more sensitive to errors in the measurements of oxygen transfer rate since it relies on the exact mass balance of oxygen. Nevertheless, the MRAC has the advantage of being easily tuned by choosing a first-order time constant for the convergence to the set point (the reference model).

Maher *et al.* (Maher et al., 1995) developed a different MRAC to follow a predetermined trajectory for the substrate concentration by manipulating the dilution rate in a continuous culture of *S. cerevisiae*. They compared the proposed controller to a classical PI controller in terms of regulation, tracking, and overshooting after set point changes, demonstrating improved performance of the MRAC controller with less overshoot and the absence of oscillatory phenomena.

As adaptive controllers cannot guarantee optimality of the results obtained, Smets *et al.* (Smets et al., 2004) proposed optimal adaptive control, which consists of first deriving and carefully analyzing a nearly optimal solution based on biochemical knowledge, which is then implemented in an adaptive way.

3.2. Linearization-based Control

Given the inherently nonlinear nature of bioprocesses, an increasing interest is directed to the application of nonlinear control theory (Mailleret et al., 2004). However, when nonlinear models are used in a model-based control structure, the control law cannot be analytically obtained. The computational effort increases considerably, and numerical stability is not guaranteed. To circumvent these problems, exact linearization control theory became a concept of paramount importance (Wang et al., 1993). This strategy consists of finding a feedback control law and a state variable transformation such that the closed-loop system model becomes linear in the new coordinate variables; the input-output nonlinearities are canceled under the assumption of a perfect knowledge of the kinetics.

Exact linearization has been mainly used to control continuous bioreactors. With the objective of keeping the bioreactor near the optimal productivity, Henson and Seborg (Henson and Seborg, 1992) showed that exact input-output linearizing control provides good control behavior when the

manipulated variable is the dilution rate, but not when it is the feed substrate concentration. Wang *et al.* (Wang et al., 1993) also emphasized the importance of the control structure selection in the application of exact linearization control to continuous bioreactors.

In general, however, the nonlinear terms are not fully known, making impossible their cancelation and leading to a poor performance of the linearized controller. In the case of uncertainty in kinetic rates, parameter adaptation appears as an attractive way to improve feedback-linearizing control. This is called adaptive feedback-linearization control; the nonlinear problem is solved by linearizing the process model as the process moves into different operating regions (Guardabassi and Savaresi, 2001). The majority of reported studies on adaptive linearizing control employs the MRAC methodology to define the update law for estimation of parameters for the input-output linearization (McLain and Henson, 2000).

In the Ignatova *et al.* (Ignatova et al., 2008) study, an indirect adaptive linearizing control was evaluated by simulations of the gluconic acid production process in a continuous culture of *Aspergillus niger*. The kinetics were considered as fully unknown and treated as time-varying parameters to be estimated online. The results of the stability and convergence analysis of the closed-loop system confirmed a good global performance.

3.3. Iterative Learning Control

ILC has been used to improve process performance from batch-to-batch. The basic idea of ILC is to update the control trajectory of the next run using the information from previous runs so that the output trajectory converges asymptotically to the desired reference trajectory (Lee and Lee, 2007). The parameter values used in the process model are updated at the end of the batch based on the progression of the previous runs and then an optimization is carried out to determine the new optimal policy for the next batch. This

strategy exhibits the limitations of open-loop control with respect to the current run, without feedback correction for disturbances, but generates useful data variability for optimizing subsequent runs (Srinivasan and Bonvin, 2007).

Xiong et al. (Xiong et al., 2008) presented an ILC scheme based on a feed-forward ANN to gradually improve the endpoint product quality of fed-batch processes. The performance of the controller was illustrated on a simulated fed-batch ethanol fermentation process, where convergence to the desired product quality was achieved after six runs. In the Teixeira *et al.* (Teixeira et al., 2006) study, a methodology for fast bioprocess optimization employing iterative batch-to-batch dynamic programming was developed and applied to three simulation case studies widely reported in the literature. The relationship between process performance and control inputs was established by means of hybrid models combining parametric and nonparametric structures. The main features of this iterative procedure include the supervision of model reliability during the optimization step, crucial to increase the speed of convergence, and sampling schedule optimization to explore new input domains, minimizing overlapping measurements, thereby reducing experimental effort.

3.4. Model Predictive Control

In the control strategies described before, the desired output trajectory is given *a priori*. The control objective is to track the predetermined output trajectory by either one or repetitive cultures. Since the mathematical models used to support the optimization studies approximate the process behavior, the obtained output trajectories are suboptimal. Online optimizing control or MPC strategies represent a way to overcome this problem.

In MPC, the control policy is obtained by solving online (at each sampling point) a finite horizon open-loop optimal control problem, using the current state of the process as the initial state (Henson, 1998). Upon the current

computation of the optimal trajectories, the values of the manipulated variables are updated. This procedure is repeated at each sampling point when direct or indirect measurements of the controlled variables are available. The objective of applying MPC is to keep pursuing the optimal state.

MPC has been widely used in industrial applications as it can guarantee closed-loop stability. Its implementation is particularly well suited for slow response processes such as mammalian cultivations since the calculations are complex and time-consuming. If a nonlinear model is used, a nonlinear optimization problem needs to be solved at every time step. Nonlinear model predictive control (NLMPC) is computationally demanding and the solution of the optimization problem may not converge to global minima or it may take a long time to converge. This makes the online implementation of NLMPC a nontrivial task. The numerical solution of NLMPC optimal control problems is typically based on direct methods using Newton-type optimization schemes. Sommeregger and coworkers (Sommeregger et al., 2017) provide an overview of enabling technologies and current issues for the implementation of MPC in biopharmaceutical manufacturing.

In the Frahm *et al.* (Frahm et al., 2003) study, a model-based controller was developed and applied to a fed-batch of NS0 cells expressing an antibody. Using this strategy, the performance of the process model could be improved by optimizing the model parameters when new data became available. The same control strategy was followed by our group (Teixeira et al., 2007) to control glucose and glutamine feeding rates over fed-batch cultures of BHK cells expressing a fusion antibody. In this case, a hybrid structure including knowledge from active metabolic pathways was employed to establish the relationship between state variables and process performance.

Soni and Parker (Soni and Parker, 2004) applied an MPC algorithm to fed-batch cultures of *S. cerevisiae* with the goal of re-optimizing the glucose feeding at each sampling time to maximize ethanol concentration at the end of the fermentation. Closed-loop MPC showed an equivalent performance to that of the open-loop strategy optimized offline, but simulation tests pointed to a better performance in the presence of disturbances. Saha *et al.* (Saha *et al.*, 1999) developed an MPC strategy to control a continuous bioreactor at its optimum operating state employing a nonlinear model to describe the process. The efficiency of the proposed algorithm was demonstrated by simulating shifts in the optimum state as a response to changes in the maximum specific growth rate. The algorithm was able to track the optimum in the presence of measurement noise and allowed a considerable improvement in productivity. Zhu and coworkers (Zhu *et al.*, 2000) employed a segregated unstructured model to describe oscillations that adversely affected the stability and productivity of a continuous culture of budding yeast. Then, a linear model obtained by linearizing and temporally discretizing the NL ordinary differential equation was used to develop MPC formulations, which were further evaluated via simulation. The best results were obtained when a subset of the cell number distribution is employed as the control variable.

Using Raman spectroscopy to monitor glucose levels online, Craven *et al.* (Craven *et al.*, 2014) implemented NLMPC for closed-loop control of the feed rate in a CHO fed-batch process. The bioprocess model used classical ordinary differential equations to describe cell growth, death and consumption/production of main metabolites, and provided the controller with an estimation of future changes in glucose consumption at each point. The strategy was implemented in a 15 L bioreactor with glucose concentration successfully maintained at a fixed set point. Aehle *et al.* (Aehle *et al.*, 2012) used a similar kinetic model to control the growth rate of EPO-producing CHO

cultures to an optimum level known to lead to higher productivity and product quality. The growth rate was controlled indirectly by changing oxygen supply based on model predictions and OUR was calculated online from in- and off-gas composition. This approach demonstrated high batch-to-batch consistency in cell profiles, as well as product titer and quality.

4. Concluding remarks

The importance of process control to maintain an extracellular environment promoting cell growth and product synthesis is well recognized, in view of the extensive literature on the application of simple and advanced control strategies to biotechnological processes. However, few experimental applications have been reported using these strategies, most works reporting results on simulation studies. The lack of compelling published evidence of such algorithms significantly increasing bioprocess performance, together with higher implementation costs has hampered their widespread adoption by industry.

Because advanced control strategies are usually based on a dynamic model of the process, the accuracy of the model is another key concern; it should properly describe the relationship between intracellular metabolic pathways and extracellular parameters, including all process aspects relevant to achieve the control objectives. First-principle models are preferred, although for many bioprocesses these not readily available. Purely data-driven models are a useful alternative when there is little process knowledge available and time/cost constraints, but they do not contribute much to process understanding and have limited generalizability. Consequently, there has been a considerable interest in developing hybrid models for process identification, combining first-principle knowledge with nonparametric functions, to describe the unknown parts of the process. Due to their inherent

capacity to mimic any nonlinear function after proper training, artificial neural networks (ANNs) have been used for a variety of applications in bioprocess control, including developing dynamic models, self-tuning controllers, and assisting batch-to-batch optimization.

Choosing a control strategy for a specific process is a non-trivial task that must consider the process objective, sources of variation, availability of a process model and/or previous data, availability of reliable sensors for critical variables, as well as cost and development time considerations.

The availability of monitoring techniques to reliably estimate key process variables is a hard constraint when developing a control strategy. Further advances in this area will also contribute to the increased industrial application of advanced process control in biotechnology. In this regard, the development of noninvasive methods based on *in situ* spectroscopic techniques has been an active area of research in recent years (Teixeira et al., 2009). These tools provide series of spectra from which online information on multiple key bioprocess and/or metabolic variables can be extracted using data-mining techniques. Once the potential of applying such techniques for process control is clearly demonstrated, they will progressively become routine at the industrial environment.

5. Acknowledgements

Financial support for this work was provided by the Portuguese *Fundação para a Ciência e Tecnologia* through the project PTDC/EBB-EBI/102750/2008 and scholarship PD/BD/105873/2014.

6. Glossary

Open-loop control - The optimal trajectory is computed off-line and then implemented online. No feedback loop is employed, thus eventual deviations of the controlled variable from the desired value are not corrected.

Closed-loop or feedback control - The controlled variable is measured, and its value is sent to the controller where it is compared with a desired value or set point. Then, the controller adjusts the manipulated variable as necessary to minimize the error.

Feed-forward control - Detects disturbances in an input variable and applies corrective action to prevent or minimize impact on the process. Because process outputs are not measured, this cannot correct for disturbances in the process itself.

Inferential or indirect control - Uses easy to measure process variables to infer variables that are more difficult to measure.

Adaptive control - A class of control algorithms that deal with system uncertainties by continuously adapting the control law to compensate for those uncertainties.

Model predictive control - A class of control algorithms that apply an explicit model of the process to predict the future response of the process. At each sampling instant, the future process behavior is optimized by computing a sequence of adjustments to the manipulated variable.

7. References

- Aehle, M., Bork, K., Schaepe, S., Kuprijanov, A., Horstkorte, R., Simutis, R., Lübbert, A., 2012. Increasing batch-to-batch reproducibility of CHO-cell cultures using a model predictive control approach. *Cytotechnology* 64, 623–634. <https://doi.org/10.1007/s10616-012-9438-1>
- Akesson, M., Hagander, P., 1999. A gain-scheduling approach for control of dissolved oxygen in stirred bioreactors 7608–7613.
- Bastin, D., Dochain, D., 1990. *On-line estimation and adaptive control of Bioreactors*. Elsevier.
- Bequette, B.W., 1991. Nonlinear Control of Chemical Processes: A Review 1391–1413. <https://doi.org/10.1021/ie00055a001>
- Cardello, R.J., San, K., 1988. The Design of Controllers for Batch Bioreactors 32, 519–526.
- Craven, S., Whelan, J., Glennon, B., 2014. Glucose concentration control of a fed-batch mammalian cell bioprocess using a nonlinear model predictive controller. *J. Process Control* 24, 344–357. <https://doi.org/10.1016/j.jprocont.2014.02.007>
- Cruz, H.J., Moreira, J.L., Carrondo, M.J.T., 2000. Metabolically optimised BHK cell fed-batch cultures. *J. Biotechnol.* 80, 109–118. [https://doi.org/10.1016/S0168-1656\(00\)00254-6](https://doi.org/10.1016/S0168-1656(00)00254-6)
- Dowd, J.E., Kwok, K.E., Piret, J.M., 2001. Predictive modeling and loose-loop control for perfusion bioreactors. *Biochem. Eng. J.* 9, 1–9. [https://doi.org/10.1016/S1369-703X\(01\)00119-X](https://doi.org/10.1016/S1369-703X(01)00119-X)
- Esmonde-White, K.A., Cuellar, M., Uerpmann, C., Lenain, B., Lewis, I.R., 2016. Raman spectroscopy as a process analytical technology for pharmaceutical manufacturing and bioprocessing. *Anal. Bioanal. Chem.* 1–13. <https://doi.org/10.1007/s00216-016-9824-1>
- Frahm, B., Lane, P., Märkl, H., Pörtner, R., 2003. Improvement of a mammalian cell culture process by adaptive, model-based dialysis fed-batch cultivation and suppression of apoptosis. *Bioprocess Biosyst. Eng.* 26, 1–10. <https://doi.org/10.1007/s00449-003-0335-z>
- Gnoth, S., Jenzsch, M., Simutis, R., Lübbert, A., 2008. Control of cultivation processes for recombinant protein production: A review. *Bioprocess Biosyst. Eng.* 31, 21–39. <https://doi.org/10.1007/s00449-007-0163-7>
- Guardabassi, G.O., Savaresi, S.M., 2001. Approximate linearization via feedback—an overview. *Automatica* 37, 1–15. [https://doi.org/10.1016/S0005-1098\(00\)00117-5](https://doi.org/10.1016/S0005-1098(00)00117-5)
- Henson, M.A., 2006. Biochemical reactor modeling and control. *IEEE Control Syst.* 26, 54–62. <https://doi.org/10.1109/MCS.2006.1657876>
- Henson, M.A., 1998. Nonlinear model predictive control: current status and future directions. *Comput. Chem. Eng.* 23, 187–202. [https://doi.org/10.1016/S0098-1354\(98\)00260-9](https://doi.org/10.1016/S0098-1354(98)00260-9)
- Henson, M.A., Seborg, D.E., 1992. Nonlinear Control Strategies for Continuous Culture. *Chem. Eng. Sci.* 47, 821–835.
- Hiller, G.W., Ovalle, A.M., Gagnon, M.P., Curran, M.L., Wang, W., 2017. Cell-controlled hybrid perfusion fed-batch CHO cell process provides significant productivity improvement over conventional fed-batch cultures. *Biotechnol. Bioeng.* 114, 1438–1447. <https://doi.org/10.1002/bit.26259>
- Hong, M.S., Severson, K.A., Jiang, M., Lu, A.E., Love, J.C., Braatz, R.D., 2018. Challenges and opportunities in biopharmaceutical manufacturing control. *Comput. Chem. Eng.* 110, 106–114. <https://doi.org/10.1016/j.compchemeng.2017.12.007>
- Ignatova, M.N., Lyubenova, V.N., García, M.R., Vilas, C., Alonso, A.A., 2008. Indirect adaptive linearizing control of a class of bioprocesses - Estimator tuning procedure. *J. Process Control* 18, 27–35. <https://doi.org/10.1016/j.jprocont.2007.06.001>
- Konstantinov, K.B., Nishio, N., Yoshida, T., 1990. Glucose feeding strategy accounting for the decreasing oxidative capacity of recombinant *Escherichia coli* in fed-batch cultivation for phenylalanine production. *J. Ferment. Bioeng.* 70, 253–260. [https://doi.org/10.1016/0922-338X\(90\)90058-5](https://doi.org/10.1016/0922-338X(90)90058-5)
- Kresse, G.B., 2009. Biosimilars - Science, status, and strategic perspective. *Eur. J. Pharm. Biopharm.* 72, 479–486. <https://doi.org/10.1016/j.ejpb.2009.02.014>

- Kuprijanov, A., Gnath, S., Simutis, R., Lübbert, A., 2009. Advanced control of dissolved oxygen concentration in fed batch cultures during recombinant protein production. *Appl. Microbiol. Biotechnol.* 82, 221–229. <https://doi.org/10.1007/s00253-008-1765-y>
- Lee, J., Lee, S.Y., Park, S., Middelberg, A.P.J., 1999. Control of fed-batch fermentations. *Biotechnol. Adv.* 17, 29–48. [https://doi.org/10.1016/S0734-9750\(98\)00015-9](https://doi.org/10.1016/S0734-9750(98)00015-9)
- Lee, J.H., Lee, K.S., 2007. Iterative learning control applied to batch processes: An overview. *Control Eng. Pract.* 15, 1306–1318. <https://doi.org/10.1016/j.conengprac.2006.11.013>
- Lee, S.Y., Lee, D.-Y., Kim, T.Y., 2005. Systems biotechnology for strain improvement. *Trends Biotechnol.* 23, 349–358. <https://doi.org/10.1016/j.tibtech.2005.05.003>
- Li, W.C., Biegler, L.T., 1988. Process control strategies for constrained nonlinear systems. *Ind. Eng. Chem. Res.* 27, 1421–1433. <https://doi.org/10.1021/ie00080a014>
- Luttmann, R., Bracewell, D.G., Cornelissen, G., Gernaey, K. V., Glassey, J., Hass, V.C., Kaiser, C., Preusse, C., Striedner, G., Mandenius, C.F., 2012. Soft sensors in bioprocessing: A status report and recommendations. *Biotechnol. J.* 7, 1040–1048. <https://doi.org/10.1002/biot.201100506>
- Maher, M., Dahhou, B., Zeng, F.Y., 1995. Experimental results in model reference adaptive estimation and control of a fermentation process. *Control Eng. Pract.* 3, 313–320. [https://doi.org/10.1016/0967-0661\(95\)00002-C](https://doi.org/10.1016/0967-0661(95)00002-C)
- Mailleret, L., Bernard, O., Steyer, J.P., 2004. Nonlinear adaptive control for bioreactors with unknown kinetics. *Automatica* 40, 1379–1385. <https://doi.org/10.1016/j.automatica.2004.01.030>
- Matasci, M., Hacker, D.L., Baldi, L., Wurm, F.M., 2009. Recombinant therapeutic protein production in cultivated mammalian cells: current status and future prospects. *Drug Discov. Today Technol.* 5, 37–42. <https://doi.org/10.1016/j.dtecc.2008.12.003>
- Matthews, T.E., Berry, B.N., Smelko, J., Moretto, J., Moore, B., Wiltberger, K., 2016. Closed loop control of lactate concentration in mammalian cell culture by Raman spectroscopy leads to improved cell density, viability, and biopharmaceutical protein production. *Biotechnol. Bioeng.* 113, 2416–2424. <https://doi.org/10.1002/bit.26018>
- McLain, R.B., Henson, M.A., 2000. Nonlinear model reference adaptive Control with Embedded Linear Models. *Ind. Eng. Chem. Res.* 39, 3007–3017. <https://doi.org/10.1021/ie990088t>
- Mohseni, S., Vali, A.R., Babaeipour, V., 2008. Designing appropriate schemes for the control of fed-batch cultivation of recombinant E.coli. *Int. J. Comput. Commun. Control* 3, 396–401. <https://doi.org/10.1109/CHICC.2008.4604899>
- Munson, J., Stanfield, C.F., Gujral, B., 2008. A Review of Process Analytical Technology (PAT) in the U . S . Pharmaceutical Industry 405–414.
- Oliveira, R., Clemente, J.J., Cunha, A.E., Carrondo, M.J.T., 2005. Adaptive dissolved oxygen control through the glycerol feeding in a recombinant *Pichia pastoris* cultivation in conditions of oxygen transfer limitation. *J. Biotechnol.* 116, 35–50. <https://doi.org/10.1016/j.jbiotec.2004.09.016>
- Ozturk, S.S., Thrift, J.C., Blackie, J.D., Naveh, D., 1997. Real-time monitoring and control of glucose and lactate concentrations in a mammalian cell perfusion reactor. *Biotechnol. Bioeng.* 53, 372–378. [https://doi.org/10.1002/\(SICI\)1097-0290\(19970220\)53:4<372::AID-BIT3>3.0.CO;2-K](https://doi.org/10.1002/(SICI)1097-0290(19970220)53:4<372::AID-BIT3>3.0.CO;2-K)
- Portner, R., Platas Barradas, O., Frahm, B., Hass, V.C., 2017. Advanced Process and Control Strategies for Bioreactors, in: *Current Developments in Biotechnology and Bioengineering*. Elsevier, pp. 463–493. <https://doi.org/https://doi.org/10.1016/B978-0-444-63663-8.00016-1>
- Radhakrishnan, T.K., Sundaram, S., Chidambaram, M., 1999. Non-linear control of continuous bioreactors. *Bioprocess Eng.* 20, 173–178. <https://doi.org/10.1007/s004490050577>
- Ramkumar, K.B., Chidambaram, M., 1995. Fuzzy self-tuning PI controller for bioreactors. *Bioprocess Eng.* 12, 263–267. <https://doi.org/10.1007/BF00369500>
- Rude, M.A., Schirmer, A., 2009. New microbial fuels: a biotech perspective. *Curr. Opin. Microbiol.* 12, 274–281. <https://doi.org/10.1016/j.mib.2009.04.004>
- Saha, P., Patwardhan, S.C., Ramachandra Rao, V.S., 1999. Maximizing productivity of a continuous fermenter using

- nonlinear adaptive optimizing control. *Bioprocess Eng.* 20, 15–21. <https://doi.org/10.1007/s004490050553>
- Smets, I.Y., Claes, J.E., November, E.J., Bastin, G.P., van Impe, J.F., 2004. Optimal adaptive control of (bio)chemical reactors: Past, present and future. *J. Process Control* 14, 795–805. <https://doi.org/10.1016/j.jprocont.2003.12.005>
- Sommeregger, W., Sissolak, B., Kandra, K., von Stosch, M., Mayer, M., Striedner, G., 2017. Quality by control: Towards model predictive control of mammalian cell culture bioprocesses. *Biotechnol. J.* 1600546, 1–7. <https://doi.org/10.1002/biot.201600546>
- Soni, A.S., Parker, R.S., 2004. Closed-Loop Control of Fed-Batch Bioreactors: A Shrinking-Horizon Approach. *Ind. Eng. Chem. Res.* 43, 3381–3393. <https://doi.org/10.1021/ie030535b>
- Srinivasan, B., Bonvin, D., 2007. Controllability and stability of repetitive batch processes. *J. Process Control* 17, 285–295. <https://doi.org/10.1016/j.jprocont.2006.10.009>
- Teixeira, A.P., Alves, C., Alves, P.M., Carrondo, M.J.T., Oliveira, R., 2007. Hybrid elementary flux analysis/nonparametric modeling: Application for bioprocess control. *BMC Bioinformatics* 8, 1–15. <https://doi.org/10.1186/1471-2105-8-30>
- Teixeira, A.P., Clemente, J., Cunha, E., Carrondo, M.J.T., 2006. Bioprocess Iterative Batch-to-Batch Optimization Based on Hybrid Parametric / Nonparametric Models. *Optimization*.
- Teixeira, A.P., Oliveira, R., Alves, P.M., Carrondo, M.J.T., 2009. Advances in on-line monitoring and control of mammalian cell cultures: Supporting the PAT initiative. *Biotechnol. Adv.* 27, 726–732. <https://doi.org/10.1016/j.biotechadv.2009.05.003>
- Turner, C., Gregory, M.E., Thornhill, N.F., 1994. Closed-loop control of fed-batch cultures of recombinant *Escherichia coli* using on-line HPLC. *Biotechnol. Bioeng.* 44, 819–29. <https://doi.org/10.1002/bit.260440707>
- Van Impe, J., Bastin, G., 1995. Optimal adaptive control of fed-batch fermentation processes. *Control Eng. Pract.* 3, 939–954. [https://doi.org/10.1016/0967-0661\(95\)00077-8](https://doi.org/10.1016/0967-0661(95)00077-8)
- Vanichsriratana, W., McFarlane, D., Keshavarz, T., Leigh, J.R., 1996. Comparison of Open Loop Optimal Control and Closed Loop Optimal Control of a fermentation process, in: *UKACC International Conference on CONTROL '96*. pp. 258–263.
- Wang, Z.-Q., Skogestad, S., Zhao, Y., 1993. Exact Linearization Control of continuous bioreactors: A comparison of various control structures. *Second IEEE Conf. Control Appl.* 107–112.
- Xiong, Z., Xu, Y., Zhang, J., Dong, J., 2008. Batch-to-batch control of fed-batch processes using control-affine feedforward neural network. *Neural Comput. Appl.* 17, 425–432. <https://doi.org/10.1007/s00521-007-0142-6>
- Zhang, A., Tsang, V.L., Moore, B., Shen, V., Huang, Y.M., Kshirsagar, R., Ryll, T., 2015. Advanced process monitoring and feedback control to enhance cell culture process production and robustness. *Biotechnol. Bioeng.* 112, 2495–2504. <https://doi.org/10.1002/bit.25684>
- Zhao, L., Fu, H.-Y., Zhou, W., Hu, W.-S., 2015. Advances in process monitoring tools for cell culture bioprocesses. *Eng. Life Sci.* n/a-n/a. <https://doi.org/10.1002/elsc.201500006>
- Zhao, Y., Skogestad, S., 1997. Comparison of Various Control Configurations for Continuous Bioreactors 5885, 697–705.
- Zhou, W., Rehm, J., Hu, W. -S., 1995. High viable cell concentration fed-batch cultures of hybridoma cells through on-line nutrient feeding. *Biotechnol. Bioeng.* 46, 579–587. <https://doi.org/10.1002/bit.260460611>
- Zhu, G.-Y., Zamamiri, A., Henson, M.A., Hjortsø, M.A., 2000. Model predictive control of continuous yeast bioreactors using cell population balance models. *Chem. Eng. Sci.* 55, 6155–6167. [https://doi.org/10.1016/S0009-2509\(00\)00208-6](https://doi.org/10.1016/S0009-2509(00)00208-6)

Chapter VI

Discussion and Future Perspectives

Contents

1. General discussion.....203

1.1. Comparison of real-time monitoring strategies205

1.2. Manufacturing challenges for rAAV in the insect cell system208

2. Contributions to the field and future directions.....212

3. References214

1. General discussion

Gene therapies are now finding their path into the clinic and the market, as confirmed by the 454 clinical trials currently active (clinicaltrials.gov, accessed on February 2019) and the recent increase in product approvals. Although substantially improving the life of patients suffering from devastating diseases, gene therapy product manufacturing is complex and costly, translating into a high selling cost, and starting the debate on the reimbursement strategies. Zolgensma, an rAAV-based gene therapy, is currently the most expensive drug in the world, with an one-time administration price tag of €1.92 M (Shahryari et al., 2019). At the current rate of Investigational New Drug (IND) applications submitted to the FDA (1000 in 2019), it is projected that 70-90 gene therapy products will be approved by 2025 (Puri, 2019) and that the demand for viral vector manufacturing will exceed the contract manufacturing organization capacity by March 2020 (Rininger et al., 2019). As such, it is paramount to increase the production titers and decrease the manufacturing costs of the current manufacturing systems.

AAV-derived vectors are one of the most commonly used gene therapy vectors, mainly targeting monogenic diseases. In the specific case of rAAV production, strategies for increasing the vector yield include the development of high productive cell lines (Martin et al., 2013), production process improvements (Aucoin et al., 2007; Joshi et al., 2019; Mena et al., 2010) and increasing rAAV recovery yields in the downstream process (Qu et al., 2015).

This PhD aimed at contributing for the decrease of gene therapy manufacturing costs. First, by assessing applicability of different real-time monitoring techniques for prediction of important process variables for the insect cell-baculovirus system, including the prediction of rAAV titers; second, by increasing process understanding in this system, by elucidating possible

rAAV production pathways (**Chapter II**, fluorescence spectroscopy) and rAAV-associated cell attributes (**Chapter III**, digital holographic microscopy and **Chapter IV**, dielectric spectroscopy) and supporting the decision on the optimal harvest time according to the intra and extracellular rAAV profiles. The major achievements obtained for each chapter are depicted in Figure VI.1.

The first step for this PhD was the implementation of the rAAV production process, with the assessment of the optimal infection and harvest conditions and the establishment of the analytical methodologies for rAAV quantification. Only with this process knowledge the implementation of real-time monitoring tools of **Chapters II-IV** could be studied.

Implementation of real-time monitoring tools in the biopharmaceutical manufacturing processes is one of the main drives of the Process Analytical Technology (PAT) initiative, but its application is still lagging behind the chemical industry (Guerra et al., 2019). In particular, for recombinant viral vector production processes, application of real-time monitoring tools is still limited to few works (Grein et al., 2018; Negrete et al., 2007; Petiot et al., 2016). However, these publications do not explore the predictive model generation, being mainly based in correlations between the monitored signals and the viral production phases. The ability to clearly identify the onset of rAAV production and the rAAV titer during the culture is critical to identify the best harvest time and predict the batch productivity even before its end.

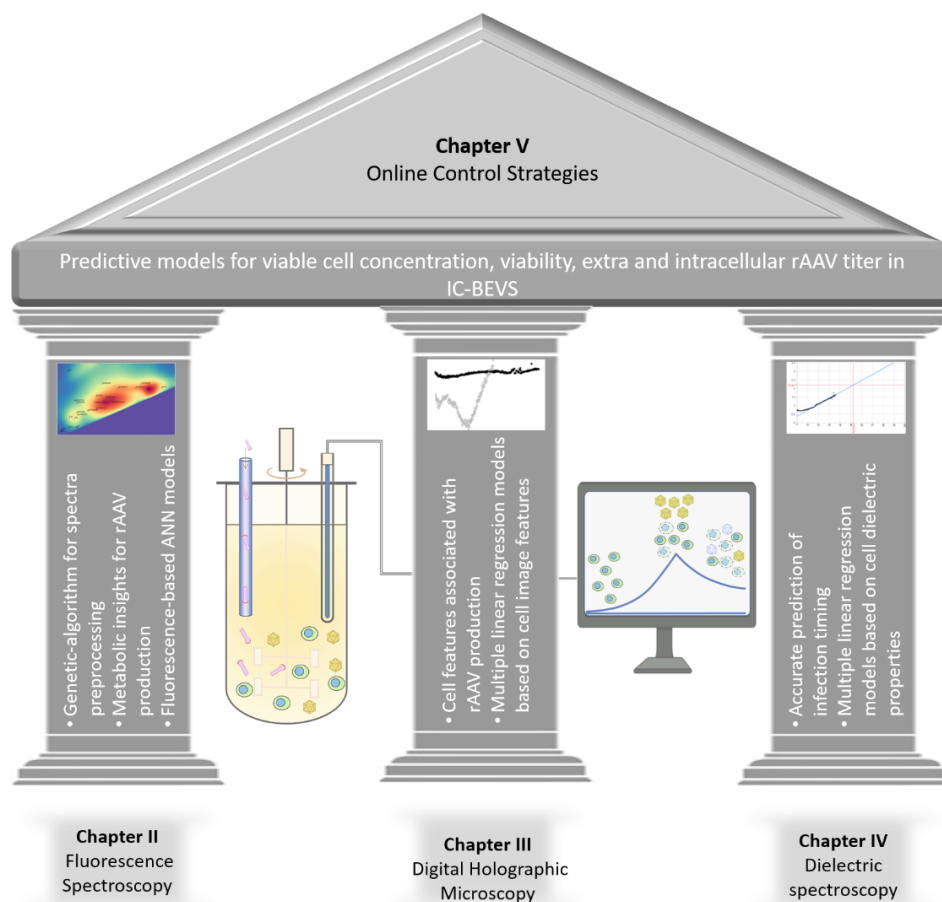


Figure VI.1 - Schematic representation of the work developed in this thesis. Each pillar represents the main achievements for each real-time monitoring chapter, culminating in the generation of predictive models for rAAV titer, viable cell concentration and viability. Online control strategies are the next step towards implementation of PAT systems for viral vector monitoring and control. rAAV – recombinant adeno-associated virus; IC-BEVS - Insect cell - baculovirus expression vector system; ANN – Artificial neural networks.

1.1. Comparison of real-time monitoring strategies

The suitability of three real-time monitoring tools for the IC-BEVS was assessed: fluorescence spectroscopy (**Chapter II**), digital differential holographic microscopy (**Chapter III**) and dielectric spectroscopy (**Chapter IV**). For each technique, predictive models for cell concentration, viability,

extracellular rAAV titer and intracellular specific rAAV titer were developed, either based on direct or indirect (soft sensor) measurements.

Fluorescence spectroscopy detects the fluorescent compounds present in the media or incorporated into the cells or recombinant product. These fluorescent compounds are mostly metabolic-related: amino acids, metabolic co-factors and vitamins (Teixeira et al., 2009). **In Chapter II**, we identified fluorescence regions corresponding to NAD(P)H, riboflavin, tryptophan and tyrosine as being possibly correlated with metabolic pathways for rAAV production or amino acid incorporation into viral particles. To further elucidate the metabolic pathways relevant for rAAV production, fluorescence spectroscopy can be combined with deeper metabolic studies, using carbon tracers and metabolic flux analysis. Importantly, the influence of the baculovirus in infected cell metabolism, extensively studied by our group (Bernal et al., 2009; Carinhas et al., 2010; Monteiro et al., 2016, 2014), needs to be considered in the experimental design to decouple metabolic signatures from rAAV production from the ones caused by baculovirus replication.

Although direct detection of cell and product concentration is possible, for bioprocessing monitoring most authors use fluorescence spectroscopy as a soft sensor, relying in chemometric analysis for correlating fluorescence spectra dynamics with the critical process variables (Bayer et al., 2019; Chopda et al., 2017; Faassen and Hitzmann, 2015; Kroll et al., 2017; Zabadaj et al., 2017). Consequently, the choice and application of the right spectra pre-treatment is critical (Glassey, 2013), as demonstrated in **Chapter II**.

Digital differential holographic microscopy (**Chapter III**) relies on cell detection and quantification, followed by calculation of the light phase characteristics for every cell. These quantitative parameters can then be correlated with the desired critical process variables and product characteristics using data analysis techniques. Compared with traditional soft

sensors, DDHM models have the advantage of providing important biologic insights regarding the changes induced by the recombinant product formation. However, in contrast with spectroscopic techniques, DHM does not allow metabolite quantification, and consequently it cannot be used to find metabolic correlations.

Dielectric spectroscopy (**Chapter IV**) is the technique explored in this thesis that provides more information regarding the cell physiological state, although with less interpretability than DDHM. The main advantage of the probe used is the ability to measure permittivity at 18 different frequencies, which can be used to calculate the beta-dispersion curve parameters and infer information regarding the cell state throughout the infection process.

Throughout the thesis we demonstrate that the techniques utilized in each chapter can work independently as a PAT tool. Still, combination of at least two probes would significantly increase the process information obtained and improve the model-prediction capabilities, as well as reducing the pre-processing and modeling necessary. Since viral vector production induces metabolic and physiological alterations in the producer cells (Monteiro et al., 2012), a good two-probe approach should combine these two types of information. Metabolic insights could be obtained using fluorescence, Raman or MIR/NIR, while digital holographic microscopy or dielectric spectroscopy could provide the information regarding the cell physiological state. This is even more useful if metabolic or cell-related viral-induced changes are known, such as the high alanine secretion of infected Sf9 cells (Bernal et al., 2009) or the increase of the cell diameter upon baculovirus infection (Palomares et al., 2001).

When calibrating prediction models for real-time monitoring, one important consideration is the choice of the calibration dataset. The experiment design space needs to include a considerable distribution of the range of the process

variables, to assure variations in the process variable and product attribute can be detected using the real-time monitoring tool. This was done in **Chapter II** by building a dataset with fluorescence data from two spectrofluorometers and from bioreactors infected at different MOIs; in **Chapter III** using one infected and one uninfected batch; and in **Chapter IV** with the addition of perturbation batches to decouple physiological parameters associated with rAAV production from the ones associated with baculovirus infection or cell growth.

The predictive power of the data-driven models developed in this thesis can be improved by adding data from the process controllers, since the controller inputs and outputs are recorded throughout the culture. This improvement in model predictions by adding process data such as accumulated added compounds, temperature data or total inlet air is demonstrated in other works (Bayer et al., 2019; Guerra et al., 2019). In the case of the insect cell-baculovirus system, in which the O₂ uptake increases significantly during baculovirus infection, oxygen uptake rate calculations have been applied for process improvement (Hidalgo et al., 2017; Kioukia et al., 1995; Lecina et al., 2006). Finally, the available biological process knowledge, such as rAAV metabolic requirements or degradation kinetics can be combined with the real-time probe outputs to yield hybrid models with improved prediction accuracy (Bayer et al., 2019; von Stosch et al., 2016).

1.2. Manufacturing challenges for rAAV production in the insect cell system

In rAAV manufacturing, the critical quality attributes more important are the vector transducing potential and the ratio of empty to full capsids (Merten, 2016). This is especially relevant in the IC-BEVS, with low vector infectivity being the most important issue reported (Kondratov et al., 2017; Le et al., 2019; Merten, 2016; Wang et al., 2011). The low infectivity is mostly due to the release of intracellular proteases upon baculovirus-induced cell lysis

(Berry and Asokan, 2017; Horowitz et al., 2013; Nam et al., 2011; Rayaprolu et al., 2013) and due to pH alterations during the manufacturing and purification process (Mitchell and Samulski, 2013; Salganik et al., 2012), which can affect rAAV specific domains. Recombinant AAV infectivity is mostly related with the phospholipase A2 domain in the VP1 N-terminus (Brown et al., 2017; Galibert and Merten, 2011; Kondratov et al., 2017).

Online monitoring of the highly variable and process dependent quality characteristics of these vectors is one of the challenges ahead for the field. One possible approach is to find surrogate markers that correlate well with the desired quality characteristics, an approach that would even deepen the interplay between vector quality and the measured surrogate (Zhang et al., 2015). Consequently, the phospholipase A2 domain could work as the surrogate marker for detecting rAAV infectivity, for instance by fusing a fluorescence marker to the VP1 protein, similar to the SpyTag approach (Hatlem et al., 2019), and using fluorescence spectroscopy to measure the presence of those proteins during culture time. A similar approach has already been used for monitoring intracellular AAV trafficking (Zhang et al., 2018).

The empty to full rAAV particle ratio is dependent on the expression system (Merten and Gaillet, 2016) and it can be affected by process conditions, such as temperature modulation after infection (Aucoin et al., 2007). To monitor this CQA, DHM would probably be the chosen technique. A possible strategy is to build a dataset consisting of reactors infected only with *repcap* baculovirus and reactors infected with the dual baculovirus strategy, together with blend batches as exemplified in **Chapter IV**. This approach can be further explored by adding to the dataset bioreactor runs using other production systems known by their high full particle ratio, as the herpes simplex production system (Merten and Gaillet, 2016). After identification of the relevant attributes, it would be interesting to assess how those attributes

would change for other production systems, rAAV serotypes or packaged transgenes.

The quality of rAAV vectors is a highly debatable concern in the industry. Although the titer of infectious vectors is universally accepted as a critical quality attribute, the mindset towards the presence of empty capsids in the final product is switching. Initially, the presence of empty capsids was considered detrimental, due to their possible immunogenic potential (Wright, 2014; Schnödt and Büning, 2017) and evidence of reduced inflammation when total capsid content was reduced by empty capsid removal (Timmers et al., 2019). However, some authors consider the presence of empty capsids as desirable, since empty capsids may work as a decoy for the presence of rAAV neutralizing antibodies in the patient (Flotte, 2017; Wright, 2014; Mingozi and High, 2013). Moreover, the administration route and site also has relevance when deciding the presence of empty capsids or not, since immune privileged sites such as the retina benefit from an increase in genome-containing particles, while systemic administration may benefit from the presence of empty capsids (Flotte, 2017). As such, after identification of the process parameters affecting the empty to full ratio, we envision rAAV production processes to tailor the ratio of full and empty capsids as desired, through the implementation of real-time monitoring and control systems.

Still, more importantly than the discussion over rAAV quality is the ability to detect such quality attributes. The lack of standardized methods in academia and industry is a concern, which led to a consortium taking action to develop rAAV reference standard materials (Ayuso et al., 2014; Lock et al., 2010; Penaud-Budloo et al., 2019). The physical and biological properties of the reference material were measured in different labs using standardized protocols, but the standard deviation of the measured quality characteristics among the different lab consortiums clearly shows the lack of standardization in this field.

As such, the development of real-time monitoring methods to track rAAV quality characteristics is hindered not only because of the difficulty and time-consuming nature of the current quality characterization methods, but also because of the lack of standardization, which may prevent models developed in one lab to be used in another lab. Still, we strongly believe on the potential for monitoring rAAV quality attributes of some of the approaches developed in this thesis, in particular DHM (**Chapter III**), as referred above. Real-time monitoring of the infectious vectors is, to the best of our knowledge, the more challenging approach, also because rAAV potency is largely dependent on the cell type and rAAV serotype used (Ellis et al., 2013) and the “definition” of potency is dependent on the therapeutic application and mechanism of action (protein expression or gene knockdown).

Another concern on the use of the IC-BEVS for rAAV production is the fact that baculovirus induces cell growth arrest and ultimately cell apoptosis, and consequently rAAV production is limited in time. Strategies to prevent generation of contaminating baculovirus virions (Marek et al., 2017) or increase the time viable insect cells are expressing the recombinant product (Fath-goodin et al., 2009; Steele et al., 2017; Weidner et al., 2017) are a possible way to increase the rAAV-production time of insect cells, while keeping the high volumetric productivities achieved with this system.

In line with the PAT initiative, after establishing tools for real-time monitoring of rAAV quality attributes, the implementation of real-time control systems for keeping the CQAs in the desired range would follow. Although there are feeding schemes that increase the viral vector production titers (Carinhas et al., 2010; Huang et al., 2014; Lee et al., 2003; Liu et al., 2010; Mena et al., 2010; Monteiro et al., 2016), a *de facto* control mechanism that would act upon the process when the viral titers detour from the desired profile is, to our knowledge, not available. However, when therapeutic monoclonal antibody research started, the scientific community was far from imagining that it would

be possible to tailor the glycosylation profile of the produced antibodies (reviewed in Sha et al., 2016). With the current rAAV research focused on understanding metabolic and process limitations to increase rAAV titers, it is certain that AAV future use as gene therapy vector is “bright and impacting” (Hastie and Samulski, 2015).

2. Contributions to the field and future directions

This PhD thesis main contribution is to the field of bioprocess engineering, with the development and implementation of real-time monitoring tools for rAAV production in the insect cell system, and the data analysis and modeling tools used. The genetic algorithm-based “toolbox” for fluorescence spectra pre-processing presented in **Chapter II** can be applied to any spectroscopic technique, by adjusting the available pre-processing and multivariate data analysis methods. This is critical since spectroscopic tools always require spectra pre-processing before data analysis, and the spectra pre-processing step has a strong influence in the final data analysis interpretation and model development (Bayer et al., 2019; Glassey, 2013). Additionally, we demonstrated the applicability of stepwise forward/backward attribute selection combined with multiple linear regression as a simple yet powerful way to develop interpretable and robust predictive models (**Chapters III and IV**).

The tools and strategies developed in this thesis were developed with the aim of being as universal as possible and can be applied to other biopharmaceuticals produced in the IC-BEVS, such as virus-like particles and vaccines, and possibly to other viral vector production systems as well. Specifically, the methods developed can be readily applied for following the baculovirus infection progress. Although in low MOI infections multiple baculovirus replication cycles take place, with consequent several phases of

baculovirus entry and release from the host cells, in general the progress of baculovirus infection can be estimated through the increase in the mean cell diameter of the population. This was briefly addressed in **Chapter IV**, relying on the correlation between culture permittivity and cell biovolume, and it is reported in other works using either dielectric spectroscopy (Ansorge et al., 2007; Negrete et al., 2007; Petiot et al., 2016; Zeiser et al., 2000, 1999) and imaging microscopy (Janakiraman et al., 2006; Laasfeld et al., 2017; Palomares et al., 2001).

The other main contribution of this thesis is the improvement of the understanding of rAAV production kinetics. In all chapters, intracellular rAAV titer was quantified and the rAAV production kinetics described. This knowledge is important in order to improve the production process by determining the time when intracellular rAAV concentration is maximized. Moreover, the identification of possibly rAAV-related signals is translational to other AAV research topics. These signals include the DDHM attribute known as “phase skewness” (**Chapter III**) or the fluorescence region between 270-300 nm excitation and 310-370 nm emission (**Chapter II**), validated in the work of Fu and coworkers (Fu et al., 2019).

The work developed in this thesis, in particular the models for viable cell concentration, viability and the “process-to-target” script, can be used for developing predictive models of infection timing and harvest and feed starting times, as well as to develop feedback control mechanisms to keep the cell concentration and viability at the desired setpoints. Once other process parameters impacting rAAV quality attributes are known, the same models can be used to develop feedback control mechanisms to keep the desired product profile and minimize the global production costs.

Overall, this thesis will contribute to the advance of Process Analytical Technology implementation in the IC-BEVS.

3. References

- Ansonge, S., Esteban, G., Schmid, G., 2007. On-line monitoring of infected Sf-9 insect cell cultures by scanning permittivity measurements and comparison with off-line biovolume measurements. *Cytotechnology* 55, 115–24. <https://doi.org/10.1007/s10616-007-9093-0>
- Aucoin, M.G., Perrier, M., Kamen, A.A., 2007. Improving AAV vector yield in insect cells by modulating the temperature after infection. *Biotechnol. Bioeng.* 97, 1501–1509. <https://doi.org/10.1002/bit.21364>
- Ayuso, E., Blouin, V., Lock, M., McGorray, S., Leon, X., Alvira, M.R., Auricchio, A., Bucher, S., Chtarto, A., Clark, K.R., Darmon, C., Doria, M., Fountain, W., Gao, G., Gao, K., Giacca, M., Kleinschmidt, J., Leuchs, B., Melas, C., Mizukami, H., Müller, M., Noordman, Y., Bockstael, O., Ozawa, K., Pythoud, C., Sumaroka, M., Surosky, R., Tenenbaum, L., van der Linden, I., Weins, B., Wright, J.F., Zhang, X., Zentilin, L., Bosch, F., Snyder, R.O., Moullier, P., 2014. Manufacturing and characterization of a recombinant adeno-associated virus type 8 reference standard material. *Hum. Gene Ther.* 25, 977–87. <https://doi.org/10.1089/hum.2014.057>
- Bayer, B., von Stosch, M., Melcher, M., Duerkop, M., Striedner, G., 2019. Soft sensor based on 2D-fluorescence and process data enabling real-time estimation of biomass in *Escherichia coli* cultivations. *Eng. Life Sci.* <https://doi.org/10.1002/elsc.201900076>
- Bernal, V., Carinhas, N., Yokomizo, A.Y., Carrondo, M.J.T., Alves, P.M., 2009. Cell density effect in the baculovirus-insect cells system: A quantitative analysis of energetic metabolism. *Biotechnol. Bioeng.* 104, 162–180. <https://doi.org/10.1002/bit.22364>
- Berry, G., Asokan, A., 2017. Cellular transduction mechanisms of adeno-associated viral vectors 54–60. <https://doi.org/10.1016/j.coviro.2016.08.001>.
- Brown, N., Song, L., Kollu, N.R., Hirsch, M., 2017. AAV Vectors and Stem Cells – Friends or Foes? *Hum. Gene Ther.* 27517, hum.2017.038. <https://doi.org/10.1089/hum.2017.038>
- Carinhas, N., Bernal, V., Monteiro, F., Carrondo, M.J.T., Oliveira, R., Alves, P.M., 2010. Improving baculovirus production at high cell density through manipulation of energy metabolism. *Metab. Eng.* 12, 39–52. <https://doi.org/10.1016/j.ymben.2009.08.008>
- Chopda, V.R., Pathak, M., Batra, J., Gomes, J., Rathore, A.S., 2017. Enabler for process analytical technology implementation in *Pichia pastoris* fermentation: Fluorescence-based soft sensors for rapid quantitation of product titer. *Eng. Life Sci.* 17, 448–457. <https://doi.org/10.1002/elsc.201600155>
- Ellis, B.L., Hirsch, M.L., Barker, J.C., Connelly, J.P., Steininger, R.J., Porteus, M.H., 2013. A survey of ex vivo/in vitro transduction efficiency of mammalian primary cells and cell lines with Nine natural adeno-associated virus (AAV1-9) and one engineered adeno-associated virus serotype. *Virology* 10, 1–10. <https://doi.org/10.1186/1743-422X-10-74>
- Faassen, S.M., Hitzmann, B., 2015. Fluorescence spectroscopy and chemometric modeling for bioprocess monitoring. *Sensors (Basel)*. 15, 10271–10291. <https://doi.org/10.3390/s150510271>
- Fath-goodin, A., Kroemer, J., Webb, B.A., 2009. The Campoletis sonorensis ichnovirus vankyrin protein P-vank-1 inhibits apoptosis in insect Sf9 cells 18, 497–506. <https://doi.org/10.1111/j.1365-2583.2009.00892.x>
- Flotte, T.R., 2017. Empty Adeno-Associated Virus Capsids: Contaminant or Natural Decoy? *Hum. Gene Ther.* 28, 147–148. <https://doi.org/10.1089/hum.2017.29039.trf>
- Fu, X., Chen, W.-C., Argento, C., Clarner, P., Bhatt, V., Dickerson, R., Bou-Assaf, G., Bakhshayeshi, M., Lu, X., Bergelson, S., Pieracci, J., 2019. Analytical Strategies for Quantification of Adeno-Associated Virus Empty Capsids to Support Process Development. *Hum. Gene Ther. Methods* 30, 144–152. <https://doi.org/10.1089/hgtb.2019.088>
- Galibert, L., Merten, O.-W., 2011. Latest developments in the large-scale production of adeno-associated virus vectors in insect cells toward the treatment of neuromuscular diseases. *J. Invertebr. Pathol.* 107 Suppl, S80–S93. <https://doi.org/10.1016/j.jip.2011.05.008>
- Glasse, J., 2013. *Multivariate Data Analysis for Advancing the Interpretation of Bioprocess Measurement and Monitoring*

- Data, in: *Adv Biochem Eng Biotechnol* Vol. 132. pp. 167–191. https://doi.org/10.1007/10_2012_171
- Grein, T.A., Loewe, D., Dieken, H., Salzig, D., Weidner, T., Czermak, P., 2018. High titer oncolytic measles virus production process by integration of dielectric spectroscopy as online monitoring system. *Biotechnol. Bioeng.* 115, 1186–1194. <https://doi.org/10.1002/bit.26538>
- Guerra, A., von Stosch, M., Glassey, J., 2019. Toward biotherapeutic product real-time quality monitoring. *Crit. Rev. Biotechnol.* 39, 289–305. <https://doi.org/10.1080/07388551.2018.1524362>
- Hastie, E., Samulski, R.J., 2015. AAV at 50: A golden anniversary of discovery, research, and gene therapy success, a personal perspective. *Hum. Gene Ther.* 265, 1–24. <https://doi.org/10.1089/hum.2015.025>
- Hatlem, D., Trunk, T., Linke, D., Leo, J.C., 2019. Catching a SPY: Using the SpyCatcher-SpyTag and Related Systems for Labeling and Localizing Bacterial Proteins. *Int. J. Mol. Sci.* 20, 2129. <https://doi.org/10.3390/ijms20092129>
- Hidalgo, D., Paz, E., Palomares, L.A., Ramírez, O.T., 2017. Real-time imaging reveals unique heterogeneous population features in insect cell cultures. *J. Biotechnol.* 259, 56–62. <https://doi.org/10.1016/j.jbiotec.2017.08.019>
- Horowitz, E.D., Rahman, K.S., Bower, B.D., Dismuke, D.J., Falvo, M.R., Griffith, J.D., Harvey, S.C., Asokan, A., 2013. Biophysical and Ultrastructural Characterization of Adeno-Associated Virus Capsid Uncoating and Genome Release. *J. Virol.* 87, 2994–3002. <https://doi.org/10.1128/JVI.03017-12>
- Huang, D., Xia-Hou, K., Liu, X.-P., Zhao, L., Fan, L., Ye, Z., Tan, W.-S., Luo, J., Chen, Z., 2014. Rational design of medium supplementation strategy for improved influenza viruses production based on analyzing nutritional requirements of MDCK Cells. *Vaccine* 32, 7091–7097. <https://doi.org/10.1016/j.vaccine.2014.10.067>
- Janakiraman, V., Forrest, W.F., Chow, B., Seshagiri, S., 2006. A rapid method for estimation of baculovirus titer based on viable cell size. *J. Virol. Methods* 132, 48–58. <https://doi.org/10.1016/j.jviromet.2005.08.021>
- Joshi, P.R.H., Cervera, L., Ahmed, I., Kondratov, O., Zolotukhin, S., Schrag, J., Chahal, P.S., Kamen, A.A., 2019. Achieving High-Yield Production of Functional AAV5 Gene Delivery Vectors via Fedbatch in an Insect Cell-One Baculovirus System. *Mol. Ther. - Methods Clin. Dev.* 13, 279–289. <https://doi.org/10.1016/j.omtm.2019.02.003>
- Kioukia, N., Nienow, A.W., Emery, A.N., Al-rubeai, M., 1995. Physiological and environmental factors affecting the growth of insect cells and infection with baculovirus. *J. Biotechnol.* 38, 243–251. [https://doi.org/10.1016/0168-1656\(94\)00128-Y](https://doi.org/10.1016/0168-1656(94)00128-Y)
- Kondratov, O., Marsic, D., Crosson, S.M., Mendez-Gomez, H.R., Moskalenko, O., Mietzsch, M., Heilbronn, R., Allison, J.R., Green, K.B., Agbandje-McKenna, M., Zolotukhin, S., 2017. Direct Head-to-Head Evaluation of Recombinant Adeno-associated Viral Vectors Manufactured in Human versus Insect Cells. *Mol. Ther.* 25, 2661–2675. <https://doi.org/10.1016/j.ymthe.2017.08.003>
- Kroll, P., Stelzer, I. V., Herwig, C., 2017. Soft sensor for monitoring biomass subpopulations in mammalian cell culture processes. *Biotechnol. Lett.* 39, 1667–1673. <https://doi.org/10.1007/s10529-017-2408-0>
- Laasfeld, T., Kopanchuk, S., Rinken, A., 2017. Image-based cell-size estimation for baculovirus quantification. *Biotechniques* 63, 161–168. <https://doi.org/10.2144/000114595>
- Le, D.T., Radukic, M.T., Müller, K.M., 2019. Adeno-associated virus capsid protein expression in *Escherichia coli* and chemically defined capsid assembly. *Sci. Rep.* 9, 18631. <https://doi.org/10.1038/s41598-019-54928-y>
- Lecina, M., Soley, A., Gràcia, J., Espunya, E., Lázaro, B., Cairó, J.J., Gòdia, F., Gòdia, F., 2006. Application of on-line OUR measurements to detect actions points to improve baculovirus-insect cell cultures in bioreactors. *J. Biotechnol.* 125, 385–394. <https://doi.org/10.1016/j.jbiotec.2006.03.014>
- Lee, Y.Y., Yap, M.G.S., Hu, W.-S., Wong, K.T.K., 2003. Low-Glutamine Fed-Batch Cultures of 293-HEK Serum-Free Suspension Cells for Adenovirus Production. *Biotechnol. Prog.* 19, 501–509. <https://doi.org/10.1021/bp025638o>
- Liu, Y.-K., Yang, C.-J., Liu, C.-L., Shen, C.-R., Shiau, L.-D., 2010. Using a fed-batch culture strategy to enhance rAAV production in the baculovirus/insect cell system. *J. Biosci. Bioeng.* 110, 187–193. <https://doi.org/10.1016/j.jbiosc.2010.02.004>
- Lock, M., McGorray, S., Auricchio, A., Ayuso, E., Beecham, E.J., Blouin-Tavel, V., Bosch, F., Bose, M., Byrne, B.J., Caton, T., Chiorini, J.A., Chtarto, A., Clark, K.R., Conlon, T., Darmon, C., Doria, M., Douar, A., Flotte, T.R., Francis, J.D., Francois, A., Giacca, M., Korn, M.T., Korytov, I., Leon, X., Leuchs, B., Lux, G., Melas, C., Mizukami, H., Moullier,

- P., Müller, M., Ozawa, K., Philipsberg, T., Poulard, K., Raupp, C., Rivière, C., Roosendaal, S.D., Samulski, R.J., Soltys, S.M., Surosky, R., Tenenbaum, L., Thomas, D.L., van Montfort, B., Veres, G., Wright, J.F., Xu, Y., Zelenia, O., Zentilin, L., Snyder, R.O., 2010. Characterization of a recombinant adeno-associated virus type 2 Reference Standard Material. *Hum. Gene Ther.* 21, 1273–1285. <https://doi.org/10.1089/hum.2009.223>
- Marek, M., van Oers, M.M., Merten, O.-W., 2017. Baculovirus-based production of biopharmaceuticals free of contaminating baculoviral virions. *US10428315B2*.
- Martin, J., Frederick, A., Luo, Y., Jackson, R., Joubert, M., Sol, B., Poulin, F., Pastor, E., Armentano, D., Wadsworth, S., Vincent, K., 2013. Generation and characterization of adeno-associated virus producer cell lines for research and preclinical vector production. *Hum. Gene Ther. Methods* 24, 253–69. <https://doi.org/10.1089/hgtb.2013.046>
- Mena, J., Aucoin, M., Montes, J., Chahal, P., Kamen, A., 2010. Improving adeno-associated vector yield in high density insect cell cultures. *J. Gene Med.* 157–167. <https://doi.org/10.1002/jgm>
- Merten, O., 2016. AAV vector production : state of the art developments and remaining challenges. *Cell Gene Ther.* 521–551. <https://doi.org/10.18609/cgti.2016.067>
- Merten, O., Gaillet, B., 2016. Viral vectors for gene therapy and gene modification approaches. *Biochem. Eng. J.* 108, 98–115. <https://doi.org/10.1016/j.bej.2015.09.005>
- Mingozzi, F., High, K.A., 2013. Immune responses to AAV vectors: Overcoming barriers to successful gene therapy. *Blood* 122, 23–36. <https://doi.org/10.1182/blood-2013-01-306647>
- Mitchell, A.M., Samulski, R.J., 2013. Mechanistic Insights into the Enhancement of Adeno-Associated Virus Transduction by Proteasome Inhibitors. *J. Virol.* 87, 13035–13041. <https://doi.org/10.1128/JVI.01826-13>
- Monteiro, F., Bernal, V., Chaillet, M., Berger, I., Alves, P.M., 2016. Targeted supplementation design for improved production and quality of enveloped viral particles in insect cell-baculovirus expression system. *J. Biotechnol.* 233, 34–41. <https://doi.org/10.1016/j.jbiotec.2016.06.029>
- Monteiro, F., Bernal, V., Saelens, X., Lozano, A.B., Bernal, C., Sevilla, A., Carrondo, M.J.T., Alves, P.M., 2014. Metabolic profiling of insect cell lines: Unveiling cell line determinants behind system's productivity. *Biotechnol. Bioeng.* 111, 816–828. <https://doi.org/10.1002/bit.25142>
- Monteiro, F., Carinhas, N., Carrondo, M.J.T., Bernal, V., Alves, P.M., 2012. Toward system-level understanding of baculovirus-host cell interactions: From molecular fundamental studies to large-scale proteomics approaches. *Front. Microbiol.* 3, 1–16. <https://doi.org/10.3389/fmicb.2012.00391>
- Nam, H.-J., Gurda, B.L., McKenna, R., Potter, M., Byrne, B., Salganik, M., Muzyczka, N., Agbandje-McKenna, M., 2011. Structural Studies of Adeno-Associated Virus Serotype 8 Capsid Transitions Associated with Endosomal Trafficking. *J. Virol.* 85, 11791–11799. <https://doi.org/10.1128/jvi.05305-11>
- Negrete, A., Esteban, G., Kotin, R.M., 2007. Process optimization of large-scale production of recombinant adeno-associated vectors using dielectric spectroscopy. *Appl. Microbiol. Biotechnol.* 76, 761–72. <https://doi.org/10.1007/s00253-007-1030-9>
- Palomares, L.A., Pedroza, J.C., Ramirez, O.T., 2001. Cell size as a tool to predict the production of recombinant protein by the insect-cell baculovirus expression system. *Biotechnol. Lett.* 23, 359–364. <https://doi.org/10.1023/A:1005688417525>
- Penaud-Budloo, M., Broucque, F., Harrouet, K., Bouzelha, M., Saleun, S., Douthe, S., D'Costa, S., Ogram, S., Adjali, O., Blouin, V., Lock, M., Snyder, R.O., Ayuso, E., 2019. Stability of the adeno-associated virus 8 reference standard material. *Gene Ther.* 1. <https://doi.org/10.1038/s41434-019-0072-9>
- Petiot, E., Ansoorge, S., Rosa-Calatrava, M., Kamen, A., 2016. Critical phases of viral production processes monitored by capacitance. *J. Biotechnol.* 242, 19–29. <https://doi.org/10.1016/j.jbiotec.2016.11.010>
- Puri, R., 2019. FDA Regulation of Cell and Gene Therapies: Facilitating Advanced Manufacturing. Presented at the American Society for Cell and Gene Therapy (ASGCT) 22nd meeting.
- Qu, W., Wang, M., Wu, Y., Xu, R., 2015. Scalable Downstream Strategies for Purification of Recombinant Adeno- Associated Virus Vectors in Light of the Properties. *Curr. Pharm. Biotechnol.* 16, 684–95.
- Rayaprolu, V., Kruse, S., Kant, R., Venkatakrishnan, B., Movahed, N., Brooke, D., Lins, B., Bennett, A., Potter, T.,

- McKenna, R., Agbandje-McKenna, M., Bothner, B., 2013. Comparative Analysis of Adeno-Associated Virus Capsid Stability and Dynamics. *J. Virol.* 87, 13150–13160. <https://doi.org/10.1128/JVI.01415-13>
- Rininger, J., Fennell, A., Schoukroun-Barnes, L., Peterson, C., Speidel, J., 2019. Capacity Analysis for Viral Vector Manufacturing: Is There Enough? [WWW Document]. *Bioprocess Int.* URL <https://bioprocessintl.com/manufacturing/emerging-therapeutics-manufacturing/capacity-analysis-for-viral-vector-manufacturing-is-there-enough/>
- Salganik, M., Venkatakrisnan, B., Bennett, a., Lins, B., Yarbrough, J., Muzyczka, N., Agbandje-McKenna, M., McKenna, R., 2012. Evidence for pH-Dependent Protease Activity in the Adeno-Associated Virus Capsid. *J. Virol.* 86, 11877–11885. <https://doi.org/10.1128/JVI.01717-12>
- Schnödt, M., Büning, H., 2017. Improving the Quality of Adeno-Associated Viral Vector Preparations: The Challenge of Product-Related Impurities. *Hum. Gene Ther. Methods* 28, 101–108. <https://doi.org/10.1089/hgtb.2016.188>
- Sha, S., Agarabi, C., Brorson, K., Lee, D.-Y., Yoon, S., 2016. N-Glycosylation Design and Control of Therapeutic Monoclonal Antibodies. *Trends Biotechnol.* 34, 835–846. <https://doi.org/10.1016/j.tibtech.2016.02.013>
- Shahryari, A., Jazi, M.S., Mohammadi, S., Nikoo, H.R., Nazari, Z., Hosseini, E.S., Burtscher, I., Mowla, S.J., Lickert, H., 2019. Development and clinical translation of approved gene therapy products for genetic disorders. *Front. Genet.* 10. <https://doi.org/10.3389/fgene.2019.00868>
- Steele, K.H., Stone, B.J., Franklin, K.M., Fath-goodin, A., Zhang, X., Webb, B.A., Geisler, C., 2017. Improving the Baculovirus Expression Vector System with Vankyrin-enhanced Technology. <https://doi.org/10.1002/btpr.2516>
- Teixeira, A.P., Portugal, C.A.M., Carinhas, N., Dias, J.M.L., Crespo, J.P., Alves, P.M., Carrondo, M.J.T., Oliveira, R., 2009. In situ 2D fluorometry and chemometric monitoring of mammalian cell cultures. *Biotechnol. Bioeng.* 102, 1098–1106. <https://doi.org/10.1002/bit.22125>
- Timmers, A., Newmark, J., Turunen, H.T., Farivar, T., Liu, J., Song, C., Ye, G., Pennock, S., Gaskin, C., Knop, D.R., Shearman, M.S., 2019. Ocular inflammatory response to intravitreal injection of AAV vector: relative contribution of genome and capsid. *Hum. Gene Ther.* 1–45. <https://doi.org/10.1089/hum.2019.144>
- von Stosch, M., Hamelink, J.-M., Oliveira, R., 2016. Hybrid modeling as a QbD/PAT tool in process development: an industrial *E. coli* case study. *Bioprocess Biosyst. Eng.* 39, 773–84. <https://doi.org/10.1007/s00449-016-1557-1>
- Wang, L., Blouin, V., Brument, N., Bello-roufai, M., Francois, A., 2011. Adeno-Associated Virus. <https://doi.org/10.1007/978-1-61779-370-7>
- Weidner, T., Druzinec, D., Mühlmann, M., Buchholz, R., Czermak, P., 2017. The components of shear stress affecting insect cells used with the baculovirus expression vector system. *Zeitschrift für Naturforsch. C* 72, 429–439. <https://doi.org/10.1515/znc-2017-0066>
- Wright, J.F., 2014. AAV Empty Capsids: For Better or for Worse? *Mol. Ther.* 22, 2013–2014. <https://doi.org/10.1038/mt.2013.268>
- Zabadaj, M., Chreptowicz, K., Mierzejewska, J., Ciosek, P., 2017. Two-Dimensional Fluorescence as Soft Sensor in the Monitoring of Biotransformation Performed by Yeast. *Biotechnol. Prog.* 33, 299–307. <https://doi.org/10.1002/btpr.2381>
- Zeiser, A., Bédard, C., Voyer, R., Jardin, B., Tom, R., Kamen, a, 1999. On-line monitoring of the progress of infection in Sf-9 insect cell cultures using relative permittivity measurements. *Biotechnol. Bioeng.* 63, 122–6. [https://doi.org/10.1002/\(SICI\)1097-0290\(19990405\)63:1<122::AID-BIT13>3.0.CO;2-I](https://doi.org/10.1002/(SICI)1097-0290(19990405)63:1<122::AID-BIT13>3.0.CO;2-I)
- Zeiser, A., Elias, C.B., Voyer, R., Jardin, B., Kamen, A.A., 2000. On-line monitoring of physiological parameters of insect cell cultures during the growth and infection process. *Biotechnol. Prog.* 16, 803–808. <https://doi.org/10.1021/bp000092w>
- Zhang, A., Tsang, V.L., Moore, B., Shen, V., Huang, Y.M., Kshirsagar, R., Ryll, T., 2015. Advanced process monitoring and feedback control to enhance cell culture process production and robustness. *Biotechnol. Bioeng.* 112, 2495–2504. <https://doi.org/10.1002/bit.25684>
- Zhang, C., Zhou, X., Yao, T., Tian, Z., Zhou, D., 2018. Precision Fluorescent Labeling of an Adeno-Associated Virus Vector to Monitor the Viral Infection Pathway. *Biotechnol. J.* 1700374, 1–11. <https://doi.org/10.1002/biot.201700374>

ITQB-UNL | Av. da República, 2780-157 Oeiras, Portugal
Tel (+351) 214 469 100 | Fax (+351) 214 411 277

www.itqb.unl.pt

Oeiras, April, 2020

Development of advanced monitoring and control tools for rAAV production in the insect cell system

Daniel A. Marques Pais

